TECHNISCHE UNIVERSITÄT MÜNCHEN
Lehrstuhl für Vegetationsökologie

Grass-tree interactions and the ecology of African savannas under current and future climates

Simon Scheiter

Vollständiger Abdruck der von der Fakultät Wissenschaftszentrum Weihenstephan für Ernährung, Landnutzung und Umwelt der Technischen Universität München zur Erlangung des akademischen Grades eines

Doktors der Naturwissenschaften

genehmigten Dissertation.

Vorsitzender:		Univ.-Prof. Dr. H. Pretzsch
Prüfer der Dissertation:	1.	Univ.-Prof. Dr. St. I. Higgins, Ph.D. (Goethe-Universität Frankfurt am Main)
	2.	Univ.-Prof. Dr. J. Pfadenhauer
	3.	Univ.-Prof. Dr. J. Schnyder

Die Dissertation wurde am 1.12.2008 bei der Technischen Universität München eingereicht und durch die Fakultät Wissenschaftszentrum Weihenstephan für Ernährung, Landnutzung und Umwelt am 14.05.2009 angenommen.

Abstract. Tropical savannas are generally defined by the co-dominance of a homogeneous understorey of C_4-grasses and a discontinuous tree layer. Savannas are primarily determined by competition for resources, by seasonal drought and by disturbances such as herbivory and fire. The nature of grass-tree interactions, and thereby the grass-tree ratio and fire regimes strongly vary over environmental gradients. Despite intense savanna research during the last decades, important questions have not been answered conclusively. Two specific questions are (1) how do grasses and trees manage to coexist in savannas while excluding each other in grasslands or rainforests and (2) how do savannas respond to anticipated climate change.

This thesis presents two different savanna models to explore these questions. The first model gives a heuristic representation of savannas and it is based on the partitioning between aboveground and belowground biomass of grasses and trees. This partitioning allows us to simulate that fire and herbivory only consume aboveground biomass while belowground biomass provides a buffer from which vegetation can recover from fire and herbivory. The model predicts that when competition is balanced and low that grass-tree coexistence is stable and fire is not necessary for coexistence. Fire only changes the dynamics from a stable equilibrium to stable limit-cycles. When light competition is intense and trees potentially out-compete grasses, then fire might reduce competition sufficiently to allow coexistence. An indirect parametrization of the model with empirical data shows that fire is not necessary for coexistence at a rainfall gradient between 200 mm and 1200 mm mean annual precipitation.

The second model, the adaptive dynamic vegetation model (aDGVM) is a process and individual-based simulation model that imitates biophysical, physiological and ecological processes. The model combines generally accepted model components with novel and flexible sub-models for phenology, carbon allocation and fire. The model allows us to simulate the response of vegetation to fire and climate change at the plant level. The sensitivity analysis shows high responses of the simulation results to the parameters describing vegetation characteristics and we conclude that vegetation models should be more flexible and adaptive in the sense that plant characteristics can change in response to the environmental conditions instead of being constant as it is assumed in most existing vegetation models. We used the model to simulate current and future vegetation in Africa in presence and absence of fire. The model correctly predicts the current distribution of major biomes. Fire suppression experiments indicate high fire impacts on regional scale and a 13% increase of biomass for Africa. Simulations under IPCC climate change scenarios predict strong increases in tree biomass and a significant shift towards tree dominated biomes, indicating a huge potential of savannas to store carbon. The carbon storage potential is not saturated at ambient conditions and will further increase in response to future climate change.

This thesis contributes to the current savanna and climate change research as it presents the first deterministic grass-tree coexistence model that can simulate coexistence on a broad environmental gradient and as it presents a dynamic savanna vegetation model that allows one to explore how grass-tree systems respond to climate change. We conclude that future research should focus on including adaptive mechanisms into vegetation models, coupling climate and vegetation models and investigating impacts of landuse in savannas.

Contents

1 Introduction **7**

I Heuristic grass-tree coexistence models 15

2 Partitioning of root and shoot competition and the stability of savannas 17
2.1 Introduction 18
2.2 Model description 20
2.3 General model behavior 25
2.4 Analysis of the simplified model 29
2.5 Discussion 41
2.6 Appendix: Isoclines of the grass shoot-woody shoot system 45
2.7 Appendix: Fixed points 46

3 The stability of African savannas 49
3.1 Introduction 50
3.2 Model description 51
3.3 Model fitting 53
3.4 Results and Discussion 57
3.5 Conclusions 64
3.6 Appendix: Isoclines and fixed-points 66

II Dynamic vegetation modelling and the future vegetation of savannas 69

4 aDGVM: An adaptive dynamic global vegetation model 71
4.1 Introduction 72
4.2 Modelling concepts 73
4.3 Input data 76
4.4 Leaf photosynthesis 76
4.5 Individual plant model 81
4.6 Stand scale dynamics 92
4.7 Synthesis of sub-models 99
4.8 Sensitivity analysis 101
4.9 Perspectives – adaptive vegetation modelling 112

4.10 Programming 116
4.11 Model parameters 118

5 Climate change in Africa: a modelling study **131**
5.1 Introduction 132
5.2 Materials and Methods 135
5.3 Results 147
5.4 Discussion 157

6 Discussion and conclusions **165**
6.1 Summary of the main results 165
6.2 Fire effects 167
6.3 Model selection 169
6.4 Model parametrization and validation 170
6.5 Model uniqueness 173
6.6 Land use 174
6.7 Coupling of vegetation and climate models 175
6.8 Conclusions 176

Zusammenfassung **179**

Acknowledgements **183**

Bibliography **185**

Electronic Appendix: Source code of the aDGVM **205**

1 Introduction

Tropical savannas are generally characterized as ecosystems with a continuous understorey of C_4 grasses and a more or less discontinuous tree layer, that is by the co-dominance of grasses and trees (Huntley and Walker 1982; Scholes and Walker 1993). The savanna ecosystem covers about 12% of the earth's surface and it is distributed over large areas of Africa, South America, Australia and Asia (Huntley and Walker 1982, Figure 1.1). In Africa, savannas cover about 65% of the Sub-Saharan land surface and are thus the dominant ecosystem (Huntley and Walker 1982). As a consequence, savannas significantly contribute to the world's carbon cycle. Savannas are responsible for about 30% of the world's net primary production (Grace *et al.* 2006) and African

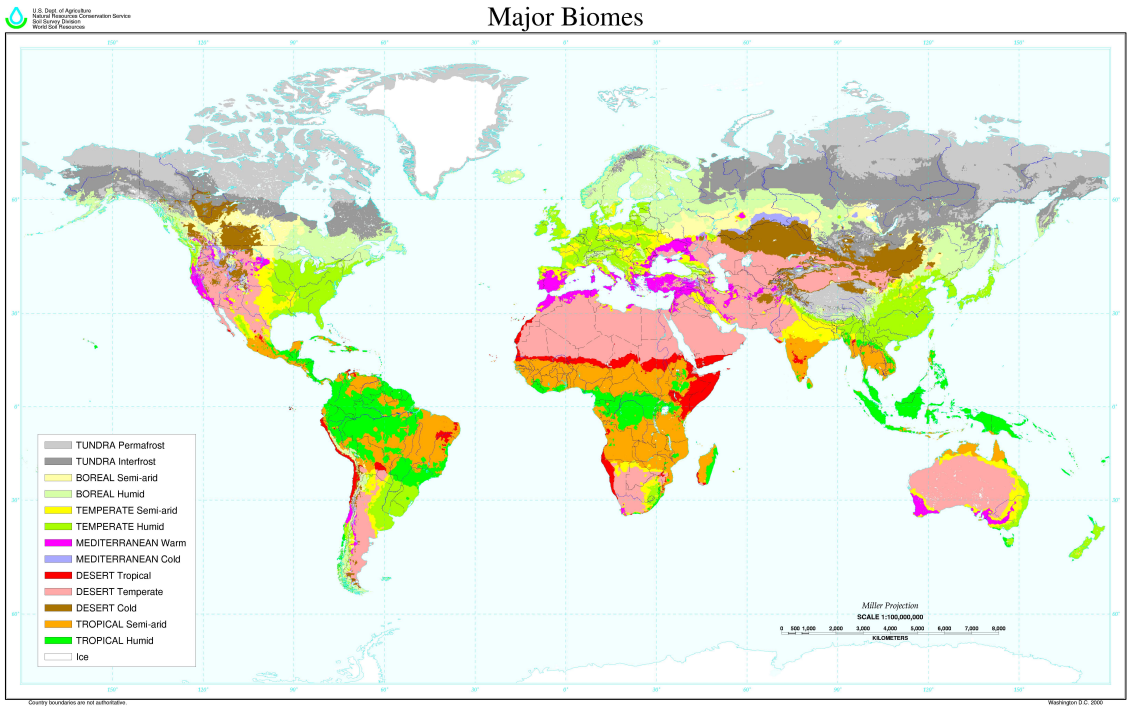

Figure 1.1: The distribution of major biomes of the world. Source: http://soils.usda.gov/use/worldsoils/mapindex/biomes.html.

savannas are responsible for about 6% (Williams *et al.* 2007) of the world's net primary production. Apart from their significance for the carbon cycle, savannas are also socio-economically important, particularly in Africa where large areas face increasing pressure of human landuse such as livestock production, deforestation and crop production (Scholes and Archer 1997; Williams *et al.* 2007).

Most authors would agree that savannas are controlled by resource availability, competition for these resources, seasonal drought as well as by disturbances (Sankaran *et al.* 2004). A major disturbance that shapes savannas are grass fires (Scholes and Walker 1993). Grass fires act as a demographic bottleneck in the tree establishment phase since the aboveground biomass of small trees (typically <2m) is often completely consumed by fire, and even by fires with low intensities. Tall trees (>2m) might only be affected by intense fires (Higgins *et al.* 2000). Thus, on an ecosystem level, fire prevents trees from reaching the potential tree biomass defined by environmental conditions (Sankaran *et al.* 2005). In turn, grass biomass might be promoted by fire, as reduced tree biomass implies a reduction of the competitive effects exerted by trees on grasses (Scholes and Hall 1996).

Seasonality, manifest in distinct wet and dry seasons regulates the time point of bud burst and leaf abscission and thereby the length of the growing season. The length of the growing season, in turn, determines the efficiency of the plant as it controls the cost-benefit relation between photosynthesis, leaf construction cost and leaf maintenance cost (Givnish 2002). At the ecosystem level, phenology thus controls the net primary production and the total biomass that accumulates in savannas. Further, seasonality is a major determinant of fire regimes. When grass moves from the metabolically active to the dormant state, biomass dries out quickly and provides fuel for fire, while in the wet season, grass biomass is generally too wet for fire ignition (Cheney and Sullivan 1997).

Savannas are distributed over a large gradient of environmental conditions and differ largely in the relative abundance of grasses and trees, fire regimes and the nature of grass-tree interactions (Scholes and Walker 1993; Sankaran *et al.* 2005). At high rainfall sites such as the borders to the tropical rainforests of central Africa, savannas are dominated by woody vegetation and might almost have a closed tree cover (Figure 1.2). At these sites, trees exert intense light competition on grasses, such that grasses are strongly suppressed or even out-competed (Scholes and Walker 1993). It has been argued, that mesic savannas are unstable as fire is necessary to establish grass-tree coexistence (Sankaran *et al.* 2005). At drier sites, the woody component is generally low

and grasses are the dominant vegetation type (Figure 1.2). In arid savannas grass-tree interactions are predominantly influenced by water competition, while light competition only plays a minor role. Hence, Sankaran *et al.* (2005) argued that arid savannas are stable in the sense that they are limited by resources and fire is not necessary for grass-tree coexistence.

Figure 1.2: Gradient from grass dominated savannas to tree dominated savannas; from left to right: Etosha National Park (350 mm MAP), Kruger National Park (550 mm MAP) and Gile Reserve, Mozambique (1000 mm MAP). Pictures taken by Steven Higgins.

Although savannas worldwide face increasing pressure from landuse and climate change and have been subjected to intense research during the last decades, our understanding of the functioning of savannas is relatively poor compared to boreal or temperate ecosystems (House *et al.* 2003; Sankaran *et al.* 2004; Bond and Keeley 2005). Thus, fundamental questions on savannas have not been conclusively answered. Two specific questions are (1) how do grasses and trees manage to coexist in savannas while excluding each other in grasslands or rainforests (Sarmiento 1984) and (2) how might future climates influence grass-tree interactions, fire regimes and the vegetation of savannas (Bond *et al.* 2005). The question of grass-tree coexistence is a classical problem in (theoretical) population ecology and, more generally, in coexistence theory. Many authors have developed models that provide coexistence mechanism for savannas, however, there exists no simple deterministic model that integrates resource and disturbance based aspects of savannas and that can describe savannas on the entire gradient

of environmental conditions where they have been observed (Sankaran *et al.* 2004). The most prominent and accepted deterministic savanna model is the rooting-niche separation model (Walter 1971). This model assumes that grasses use upper soil layers for water supply, while trees have exclusive access to deeper soil layers. Hence, grasses and trees use different rooting niches to maintain their water supply, allowing them to coexist. However, as has been repeatedly reviewed (Scholes and Archer 1997; Higgins *et al.* 2000; House *et al.* 2003; Sankaran *et al.* 2004), the rooting niche assumption cannot explain grass-tree coexistence on the whole gradient of environmental conditions where savannas have been empirically observed. Hence, the rooting niche hypothesis cannot be considered as a general model to explain savannas. Alternative savanna models use temporal (Higgins *et al.* 2000; Gardner 2006) or spatial (Jeltsch *et al.* 1996, 1998) variation in environmental conditions to explain grass-tree coexistence and can thus be thought of as stochastic models. However, these stochastic coexistence models often rely on specific details of savanna dynamics and it remains to be tested whether the mechanisms proposed by Jeltsch *et al.* (1996, 1998), Higgins *et al.* (2000) and Gardner (2006), although theoretically plausible, are empirically valid and general.

The understanding of grass-tree interactions and the role of competition and disturbance is pre-requisite to explore the second question, that is the question of how savannas might respond to future climates. This question is, due to significant changes in the climate, induced by anthropogenic CO_2 and other green house gas emissions, currently the focus of many studies (IPCC 2007). Recent climate projections suggest that Africa will be subjected to particularly severe changes in climatic conditions (IPCC 2007). Yet, most existing studies that analyze carbon cycles and vegetation shifts under climate change focus on global processes while Africa and the grassland-savanna-rainforest complex have rarely been explicitly investigated (Cao *et al.* 2001; Grace *et al.* 2006; Hély *et al.* 2006; Williams *et al.* 2007). It has been argued that the response of savannas to climate change is a significant uncertainty in projections of the future carbon cycle due to the complexity of grass-tree interactions and the tension between observed biomass and climatically-defined potential biomass (Hély *et al.* 2006; IPCC 2007). Thus, there is empirical evidence that increasing atmospheric CO_2 concentrations stimulate C_3 photosynthesis (Drake *et al.* 1997; Ehleringer *et al.* 1997), which may favor trees over grasses due to potentially larger benefit that C_3 plants would gain over C_4 plants. By contrast, increases in temperature would increase rates of C_4 photosynthesis (Collatz *et al.* 1992; Ehleringer *et al.* 1997), C_3 photo-respiration (Tjoelker *et al.* 2001; Arora 2003) and evaporative demand (Jones 1992; Allen *et al.*

1998) and may provide C_4 plants an advantage over C_3 plants (Collatz *et al.* 1992; Ehleringer *et al.* 1997).

The most powerful tool ecologists use to explore questions of how vegetation and carbon dynamics behave under future climates are dynamic global vegetation models (DGVMs). Such models simulate the dynamics of different simplified and representative functional types at a given study site in response to environmental conditions such as climate and soil and allow the exploration of the influence of disturbances such as fire, drought or climate change on the relative abundance of different functional types. However, although many DGVMs have been developed and successfully employed in many studies (e.g. Cramer *et al.* 2001; Sitch *et al.* 2003; Woodward *et al.* 2004; Bond and Keeley 2005; Hély *et al.* 2006; Hickler *et al.* 2006; Schaphoff *et al.* 2006; Sato *et al.* 2007), existing DGVMs have not been developed specifically for tropical grass-tree systems and hence, do often not describe the complex grass-tree interactions and fire effects adequately (House *et al.* 2003). As a consequence, existing DGVMs underestimate the extent of savannas and predict either grasslands or tropical rainforests in savanna regions (Cao *et al.* 2001; Grace *et al.* 2006; Hély *et al.* 2006; Schaphoff *et al.* 2006; Sato *et al.* 2007). Further, it has been argued that to understand the effects of climate change on vegetation it is necessary to understand how single individuals are influenced by climate change (McGill *et al.* 2006), yet, most existing DGVMs are not individual-based. These observations cast doubt that existing models can reliably simulate vegetation changes in savannas under future atmospheric conditions.

This thesis presents and uses different modeling approaches to explore the questions discussed in the previous paragraphs, that is, the question of grass-tree coexistence and the question of how grass-tree systems respond to climate change. The presented models integrate aspects of demographic or disturbance based theories with competition or resource based explanations of savannas. It has been argued, that such integrative models are a pre-requisite for significant progress in the understanding of savannas (Sankaran *et al.* 2004). The first model used to investigate grass-tree coexistence is a simple and heuristic model (Chapter 2). The model consists of a system of four differential equations describing biomass and inter- and intraspecific competition of aboveground and belowground compartments of grasses and trees as well as the effect of fire and herbivory on aboveground biomass. The model provides novel insights into grass-tree interactions and it suggests that grass-tree coexistence is determined by the interplay of competition and fire. The presented approach is the first deterministic model of grass-tree coexistence that does not rely on stochastic mechanisms and/or on

the restrictive assumption of rooting niche separation.

In Chapter 3 the grass-tree model from Chapter 2 is indirectly parameterized with basal area data of trees in African savannas (Sankaran *et al.* 2005) by using Markov chain Monte Carlo methods. The parametrized version of the model serves as model validation as it allows to test whether the model is capable of describing African savannas and thus, whether the model can predict grass-tree coexistence over a broader range of environmental conditions than alternative coexistence mechanisms do. Further, the parametrized model is used to explore Sankaran *et al.* (2005)'s hypothesis that savannas are stable when mean annual precipitation (MAP) is lower than 650mm while savannas are instable when MAP is higher than 650mm.

Although the grass-tree coexistence model is usefull in a heuristic sense, this model is not explicitly based on bio-physical mechanisms, with the consequence that it cannot predict vegetation states as a function of climatic and soil conditions. The second model presented in this thesis (the adaptive dynamic global vegetation model, aDGVM) is a complex process- and individual-based simulation model that imitates bio-physical, physiological and ecological mechanisms observed in savannas. The model combines established modules for leaf physiology, canopy scaling, reproduction and mortality with novel concepts for phenology, carbon allocation and fire within an individual-based framework. The model was specifically developed for tropical ecosystems and it incorporates competition and disturbance based mechanisms that are generally assumed to shape grass-tree dynamics. The model simulates fire, different rooting depth of grasses and trees as well as inter- and intra-specific light and water competition (Scholes and Walker 1993). A novel aspect of the model is that it uses flexible and adaptive rules for phenology and allocation, hence, the model is not based on bioclimatic limits or predefined phenological strategies as it is the case in many existing DGVMs (Cramer *et al.* 2001). The model simulates the biomass of grasses and trees, tree population structure and how fire regimes respond to soil and climate variables. Due to the flexible sub-models for leaf physiology, carbon allocation and leaf phenology, the model allows us to simulate the response of vegetation to disturbances such as fire and climate change on an individual-based level. Chapter 4 provides a general motivation for the development of a novel vegetation model. Then, our implementation of the aDGVM is explained in detail. To explore the model uncertainties we conducted a sensitivity analysis that shows how variations in the model parametrization influence the simulation results. Further, we outline future perspectives of vegetation modelling by proposing a shift towards a more adaptive vegetation modelling. Specifically, we call for the inclusion

of processes that allow the simulation of how traits of single individuals are modified by changing environmental conditions and how the plant community at a study site is assembled from a large species pool by simulating analogies of selection, inheritance, mutation and cross-over.

In Chapter 5, the aDGVM is evaluated. Specifically, it is shown that the model can correctly project the distribution of major vegetation formations of Africa. We use the model to explore how fire suppression would modify vegetation patterns in Africa and how the vegetation in Africa may respond to anticipated changes in the atmospheric CO_2 concentration, precipitation and temperature, defined by the (IPCC 2007) SRES scenario A1B. This analysis shows how the extent of different biomes in Africa changes in response to climate change and in addition, it provides insights to how plant physiology and the tree population structure are modified by climate change.

Chapter 6 summarizes the main results from the different chapters and shows that all ecological modeling work is challenged with the same difficulties: model selection, parametrization and validation. Further, future perspectives within the framework of the proposed models are presented.

This thesis is written in a cumulative style. Each chapter of the thesis can be read independently from the others as no chapter presumes the knowledge of the other chapters. However, Chapters 2 and 3 and Chapters 4 and 5 can be seen as an entity, as the same model is used. All Chapters have been submitted or published (eventually in a slightly modified version) together with Steven Higgins who is also the first author of Chapter 3. Mahesh Sankaran has contributed to Chapter 3.

Part I

Heuristic grass-tree coexistence models

2 Partitioning of root and shoot competition and the stability of savannas

Abstract. A classic problem in coexistence theory is how do grasses and trees coexist in savannas. A popular deterministic model of savannas, the rooting niche separation model, is based on an assumption that is not empirically supported in many savannas. Alternative models that do not rely on the rooting niche assumption invoke intricate stochastic mechanisms that limit their attractiveness as general models of savannas. In this paper we develop an alternative deterministic model of grass-tree interactions and use it to analyze the conditions under which grass-tree coexistence is possible. The novel feature of this model is that it partitions aboveground and belowground competition and simulates the fact that fire and herbivory only remove aboveground biomass. The model predicts that stable coexistence of grasses and trees is possible, even when grasses and trees do not have separate rooting niches. We show that when aboveground competition is intense, grasses can be excluded by trees; under such conditions, fire can prevent grasses from exclusion and induce a stable savanna state. The model provides a general framework for exploring the interactive effects of competition, herbivory and fire on savanna systems.

Key words: deterministic model, coexistence, competition, rooting niche separation, Savanna, fire

2.1 Introduction

Coexistence theory seeks to understand how species avoid competitive exclusion. One explanation, known as niche partitioning theory (Gause 1934), is that species coexist because they use different resources and therefore avoid competitive interactions. However, many species appear to share a common niche, yet avoid competitive exclusion (Hutchinson 1961). A classic example of this paradox from biogeography is the coexistence of grasses and trees over large proportions of tropical regions (Sarmiento 1984). Grasses and trees appear to use the same resources and competitive exclusion, manifest by forests or grasslands, is the outcome of grass-tree interactions in other regions, yet it is not clear what characteristic of savanna regions allows grasses and trees to coexist.

Early biogeographers proposed that trees and grasses can coexist when edaphic conditions are such that grasses and trees can occupy different rooting niches (Walter 1971). This rooting niche separation model was formalized by Walker and Noy-Meir (1982), who used it to explore the effects of rainfall, soils, fire, browsing and grazing on the stability of savannas. More recently, van Langevelde *et al.* (2003) performed a more detailed analysis of a modified version of the Walker and Noy-Meir (1982) model. The insights from these studies remain true to Walter's (1971) hypothesis, that is, grasses and trees can only coexist when intra-specific competition for soil resources is stronger than inter-specific competition for soil resources. In these variants of the rooting niche model grazing, browsing and fire are not responsible for coexistence but rather serve to modify the relative abundance of grasses and trees.

However, as has been repeatedly reviewed (Scholes and Archer 1997; Higgins *et al.* 2000; House *et al.* 2003; Sankaran *et al.* 2004) the rooting niche assumption is not empirically supported in many savannas, yet grasses and trees coexist in these systems. This observation suggests that the rooting niche hypothesis cannot be a general explanation for grass–tree coexistence. As reviewed in Sankaran *et al.* (2004), a number of alternative mechanisms, have been explored. Notable here are models that propose that temporal (Higgins *et al.* 2000; Gardner 2006) and/or spatial variation (Jeltsch *et al.* 1996, 1998) in environmental conditions prevent grasses from excluding trees or trees from excluding grasses. These models can be thought of as stochastic models, because they explicitly consider variance in demographic rates. For example, Jeltsch *et al.* (1996, 1998) invoked small mammal disturbances while Higgins *et al.* (2000) and Gardner (2006) invoked fire and drought as sources of variance in recruitment rates. The authors of these papers have argued that particular kinds of stochastic processes,

such as ecological buffering mechanisms (Jeltsch *et al.* 2000) or storage mechanisms (Chesson and Warner 1981) prevent the system from being dominated by either grasses or trees.

Although the proposed stochastic mechanisms seem reasonable and can explain grass-tree coexistence, there are two arguments against the stochastic models reviewed in the previous paragraphs. First, whether the conditions for the stochastic mechanisms proposed by Jeltsch *et al.* (1996, 1998), Higgins *et al.* (2000) and Gardner (2006) operate in all savannas remains to be tested. For instance, the storage mechanism of Higgins *et al.* (2000) functions only when trees have high levels of persistence and high levels of variance in recruitment rates. Second, since stochastic models do not need to be invoked to explain the existence of other biomes, one might expect that they should not be necessary to explain savannas. On the other hand, available deterministic models for savannas such as the rooting niche model are based on assumptions that cannot be observed in many savannas (Scholes and Archer 1997; Higgins *et al.* 2000; Sankaran *et al.* 2004). This means that it may be worthwile searching for alternative deterministic mechanisms of grass-tree coexistence. The aims of this paper are to propose a deterministic model of grass-tree coexistence that does not rely on root niche separation and to analyze the conditions under which grass-tree coexistence is possible.

Existing models have ignored how the interplay between aboveground biomass and belowground biomass influences savanna dynamics. The central concept of the proposed model is to separate aboveground and belowground biomasses of both grasses and trees. This allows the model to reflect the different functions fulfilled by the different plant compartments. Specifically, partitioning of aboveground and belowground compartments allows the model to partition aboveground and belowground competition and to simulate the fact that fire and herbivory only remove aboveground biomass. The model analysis shows the following results. (1) Grasses and trees can coexist in a stable equilibrium without explicitly assuming rooting niche separation and without invoking stochastic mechanisms. This result is not qualitatively influenced by alternative ways of linking aboveground and belowground growth. (2) Fire can alter the grass-tree dynamics, but it is only necessary for coexistence, when competition for aboveground and belowground resources is intense. (3) Below a threshold level, herbivory can only modify the parameter ranges for which (1) and (2) hold, but it does not invalidate (1) or (2).

This paper is structured as follows. We first provide a very general representation of grass-tree interactions that partitions aboveground form belowground compartments

and hence, aboveground from belowground competition. We then derive a simplified version of this model and show that this simplified model is an adequate representation of the general model. In the remaining sections of the paper we analyze the simplified model more formally with respect to the interactions between competition, fire and herbivory.

2.2 Model description

The model that we present here distinguishes between grasses and woody vegetation (trees and shrubs). Each vegetation type is separated into an aboveground and a belowground biomass compartment, that is, into shoots and roots. The model thus describes the four state variables grass shoots GS, grass roots GR, woody shoots WS and woody roots WR. State variables are assumed to be abundances bounded between zero and one. Figure 2.1 shows a conceptual representation of the state variables and the interactions operating between the state variables. If $\mathbf{V} = (GS, GR, WS, WR)$ is the vector of state variables, then the components of the model's growth functions $f(\mathbf{V}, t) = (f_{GS}, f_{GR}, f_{WS}, f_{WR})$ are

$$f_{GS}(\mathbf{V},t) = g_{GS}\,\mathcal{G}(GS,GR)\,(1-GS-\mathcal{L}(WS)) - d_{GS}\,GS - Z_G, \tag{2.1}$$

$$f_{GR}(\mathbf{V},t) = g_{GR}\,\mathcal{G}(GR,GS)\,(1-GR-\mathcal{R}(WR)) - d_{GR}\,GR, \tag{2.2}$$

$$f_{WS}(\mathbf{V},t) = g_{WS}\,\mathcal{G}(WS,WR)\,(1-WS) - d_{WS}\,WS - Z_W, \tag{2.3}$$

$$f_{WR}(\mathbf{V},t) = g_{WR}\,\mathcal{G}(WR,WS)\,(1-WR-\mathcal{R}(GR)) - d_{WR}\,WR. \tag{2.4}$$

If t denotes the time, the trajectory is defined by the system of differential equations $df(\mathbf{V},t)/dt = f(\mathbf{V},t)$ given initial values $\mathbf{V}_0 \neq (0,0,0,0)$ at $t = 0$. The constant growth rates are denoted by g_{GS}, g_{GR}, g_{WS} and g_{WR}. The aggregated effect of decomposition, mortality and respiration is given by rates d_{GS}, d_{GR}, d_{WS} and d_{WR}. The function $\mathcal{G}$ describes how shoots and roots contribute to the growth of a biomass compartment and the functions $\mathcal{L}$ and $\mathcal{R}$ describe aboveground and belowground competition. The parameters Z_G and Z_W describe the effects of grazing and browsing respectively. For the model to be biologically reasonable, all parameters must be greater than zero and growth parameters must be greater than decomposition parameters. In the following paragraphs we justify the model given in equations (2.1) to (2.4) and specify the functions $\mathcal{G}$, $\mathcal{L}$ and $\mathcal{R}$ as well as the impact of fire on the system.

We split biomass into aboveground and belowground compartments for three reasons.

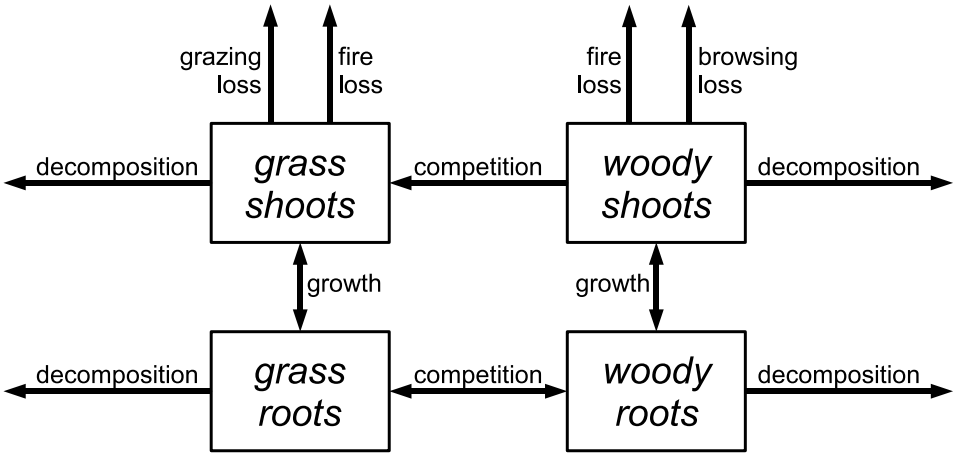

Figure 2.1: Conceptual representation of the grass-tree model. Aboveground and belowground compartments of grasses and trees are coupled by growth, grasses and trees are coupled by aboveground competition (light competition) and belowground competition (water and nutrient competition). Decomposition removes biomass from all compartments, fire removes aboveground biomass, grazing removes exclusively grass shoot biomass and browsing removes exclusively woody shoot biomass.

First, aboveground and belowground biomass fulfill different functions. Belowground biomass is responsible for water and nutrient acquisition. In turn, shoot biomass harvests light energy which is used to produce carbon by photosynthesis. There is empirical evidence for high transfer rates between shoots and roots, thus, over 60% of the carbon fixed by photosynthesis can be allocated to roots (Law *et al.* 1999) while 75% of the N acquired by roots can be allocated to shoots (Poorter *et al.* 1990). In the growth functions, this inter-dependence between aboveground and belowground biomass compartments is simulated by making the growth of shoot biomass a function of root biomass, and the growth of root biomass a function of shoot biomass:

$$\mathcal{G}(M, N) = \phi M + (1 - \phi)N. \tag{2.5}$$

Here, M is the abundance of the target biomass compartment and N is the abundance of the other biomass compartment; ϕ is a parameter between zero and one that describes how growth of biomass M is influenced by the biomasses M and N and it can be different for all four biomass compartments.

All biomass compartments are influenced by competition and the second reason for separating biomass into shoots and roots is to better account for different forms of

competition. The effects of intra-specific competition are often linear functions of density (Bond *et al.* 1995; Case 2000) and we also assume this here. Inter-specific competition is treated more flexibly, allowing aboveground and belowground competitive responses $\mathcal{L}$ and $\mathcal{R}$ to be a linear, convex or concave function of competitor density.

In this model we interpret aboveground competition as light competition, which we assume to take the general form

$$\mathcal{L}(M) = \omega\, M^{\theta}, \tag{2.6}$$

where $\omega \geq 0$ describes the strength of light competition and $\theta > 0$ describes the non-linearity of light competition (Figure 2.2A). For $0 < \theta < 1$, the light available to grasses decreases similar to an exponential function of tree cover, as implied by Beer's law (Jones 1992). However, Beer's law presumes a homogeneous tree cover that does not exist in savannas, moreover, the low leaf area indices common to savannas mean that light is in general not limiting in savannas. Yet, the definition of $\mathcal{L}$ is flexible enough to represent a situation where light competition is absent at low tree abundances but present at high tree abundances (Scholes and Walker 1993). Specifically, when $\theta > 1$, then grasses and trees grow in the same light environment when the tree abundance is low; however, once the tree abundance is high, light competition is intense and asymmetric in favor of trees. Hence, this light competition model can be thought of as an approximation of the complex shading processes found in inhomogeneous canopy structures (e.g. Shabanov *et al.* 2000).

The belowground competition function describes the aggregated effects of competition for water, rooting space and nutrients on root growth. Nutrient acquisition by roots is a complex process, that is influenced by resource depletion, root architecture, neighboring plants and chemical interactions within and between root systems (de Kroon *et al.* 2003) and models that attempt to describe these processes must solve the partial differential equations that govern resource availabilities in the soil layer (Rodriguez-Iturbe *et al.* 1999, 2001). Heuristic models of root competition use non-linear functions to describe competition (e.g. Walker and Noy-Meir 1982; McMurtrie and Wolf 1983; van Langevelde *et al.* 2003; Stigter and van Langevelde 2004). We use a heuristic approach which is motivated by Cahill and Casper (2000)'s observation that belowground competition is size symmetric, that is, individuals compete in proportion to their size. Hence, we describe the effect exerted by competitor root biomass M by the general

function

$$\mathcal{R}(M) = \alpha\, M^{\sigma}, \tag{2.7}$$

where $\alpha \geq 0$ and $\sigma > 0$ describe the strength and non-linearity of root competition. This simplified model allows to simulate a realistic response of root competition to the competitor root biomass when $\sigma < 1$ (Figure 2.2B). In the model, the parameters α and σ are allowed to differ for grasses and trees.

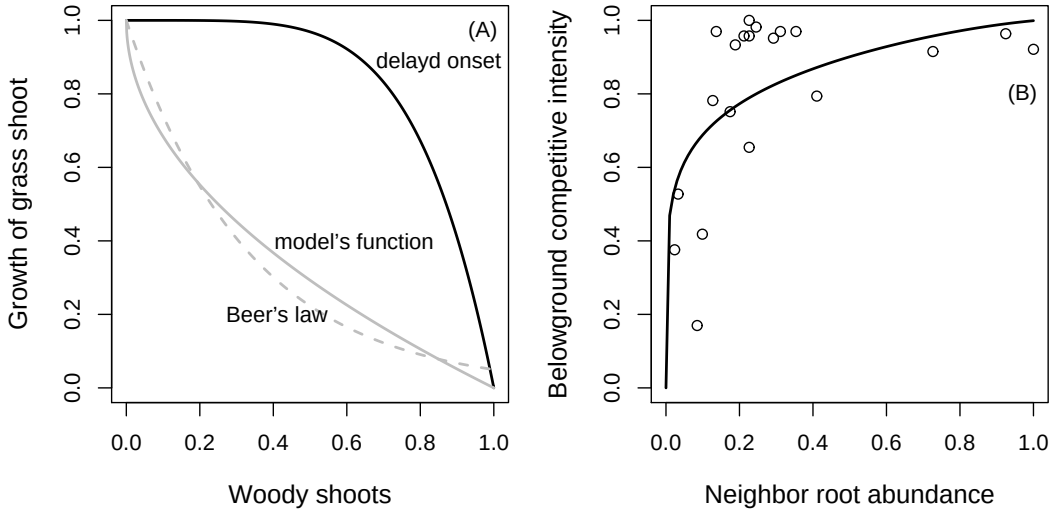

Figure 2.2: Panel (A) depicts different functional responses of grass shoot growth to inter-specific light competition exerted by woody shoots. When grasses are shaded by a homogeneous canopy cover of trees, Beer's law is often used to describe light availability (dashed gray line). The model presented here can represent Beer's law when $\theta < 1$ (gray line) and can simulate the delayed onset of light competition effects when $\theta > 1$ (black line). Panel (B) depicts the relationship between competitor root biomass and root competition intensity. Points indicate measurements conducted by Cahill and Casper (2000), the line depicts modelled results when the root competition parameter σ is less then one.

The third reason for splitting biomass into roots and shoots is to account for the fact that fire and herbivory only remove aboveground biomass. It is known that root growth slows down or stops after shoot removal (Crider 1955; Wolfson 1999) and that root biomass allows plants to resprout when aboveground biomass is damaged (Bond and Midgley 2001). During this phase carbon is allocated from roots to shoots, allowing a balanced shoot-root ratio to be restored. Because the model separates root and shoot biomass compartments, it can simulate this response to defoliation.

We model fire as a discontinuous event that reduces biomass instantaneously when

conditions for fire ignition are fulfilled. Such models are often called impulsive differential equations (Ballinger and Liu 1997) or impact models (Dercole and Maggi 2005). Fire occurs when grass shoot biomass GS (the fuel biomass) exceeds a threshold value δ. Empirical evidence (Higgins *et al.* 2000; Hoffmann and Solbrig 2003) suggests that fire damage is a sigmoidal function of the fire intensity F, which is in turn linearly related to fuel biomass, $F = \gamma GS$. For this reason we describe the grass shoot biomass immediately after a fire by the sigmoidal function

$$GS^+ = \left(1 - \frac{F^b}{F^b + a^b}\right) GS, \tag{2.8}$$

and the woody shoot biomass immediately after a fire as

$$WS^+ = \left(1 - \frac{F^d}{F^d + c^d}\right) WS. \tag{2.9}$$

Here, a, b, c and d are model parameters that describe the from of the sigmoidal functions.

Finally, grazing and browsing reduce grass and woody shoots by values Z_G and Z_W, which can depend on the shoot biomass. We consider a herbivory model where the grazing rate Z_G is $u_G GS$ and the browsing rate Z_W is $u_W WS$ (van Langevelde *et al.* 2003). Herbivory models of this kind assume that the herbivore density is perfectly adjusted to the shoot biomass, such that at any time a constant proportion u_G or u_W of the shoot biomass is consumed. Of course, this is only a caricature; in reality a farmer or natural production and mortality processes cannot perfectly adjust the herbivore density to the shoot biomass. Although we do not consider alternative herbivory strategies, we wish to point out that the choice of the herbivory strategy strongly influences the system dynamics and the asymptotic behavior. For instance, should the stocking rate not be adjusted to the shoot biomass, then herbivory is simply a constant u_G or u_W; this would lead to instability in the grass-tree system as grass or tree biomass could easily be driven to extinction by overgrazing or overbrowsing.

As it is beyond the scope of this paper to analyze grazing and fire management strategies we refer to Higgins *et al.* (2007b) who used this model to find optimal grazing and fire management strategies for savanna rangelands and to Noy-Meir (1978), Woodward (1997) and Xu *et al.* (2005) who all investigated different grazing strategies.

2.3 General model behavior

In this section we show that (1) the model system is an adequate representation of grass-tree dynamics and shoot-root dynamics and that (2) grass-tree coexistence depends on the partitioning between shoots and roots and not on the details of the formulation of the growth and competition functions $\mathcal{G}$, $\mathcal{L}$ and $\mathcal{R}$. This finding justifies the derivation of a simplified version of the model. This simplified model preserves the dynamic properties of Equations (2.1) to (2.4) but is mathematically more tractable.

To demonstrate that the model adequately represents the system's dynamics we analyze how fire and different parameter values of ϕ in Equation (2.5), influence the trajectories of the system defined in Equations (2.1) to (2.4). We explore the sensitivity of the model's dynamics to the form of the competition functions, Equations (2.6) and (2.7), by analyzing the sensitivity of the isoclines of the model to variation in the shape parameters θ and σ. We consider isoclines in the two-dimensional phase space, defined by the root biomasses GR and WR (or the shoot biomasses GS and WS) while the shoot biomasses (root biomasses) are in equilibrium. Both the analysis of trajectories and the analysis of isoclines allow a graphical representation of the asymptotic properties of the system.

2.3.1 The growth function $\mathcal{G}$ and the impact of fire

The parameter ϕ in function $\mathcal{G}$ (Equation 2.5) determines the contribution of aboveground and belowground biomass on the growth of either the aboveground or belowground biomass compartments. For instance, when $\phi = 1$, then growth of the one compartment is not influenced by the other compartment. Such a description of shoot-root dynamics is obviously inadequate because it allows shoots or roots to persist in the absence of the other compartment. At the other extreme, when $\phi = 0$, the compartments are tightly coupled and growth of one compartment is solely determined by the other compartment. That is, the growth rate of shoots is influenced by root biomass, but not by shoot biomass. It follows that, some intermediate value of ϕ seems biologically most reasonable (Figure 2.3).

By analyzing the effect of fire, the buffering effects between shoots and roots can be observed. Assume that shoots and roots are strongly coupeled (ϕ is positive and close to zero) and that a fire has reduced shoot biomass to zero. From equations (2.2) and (2.4) it is clear that in this situation the growth of roots becomes negative as it is determined solely by decomposition. Hence, roots react instantaneously to a shoot

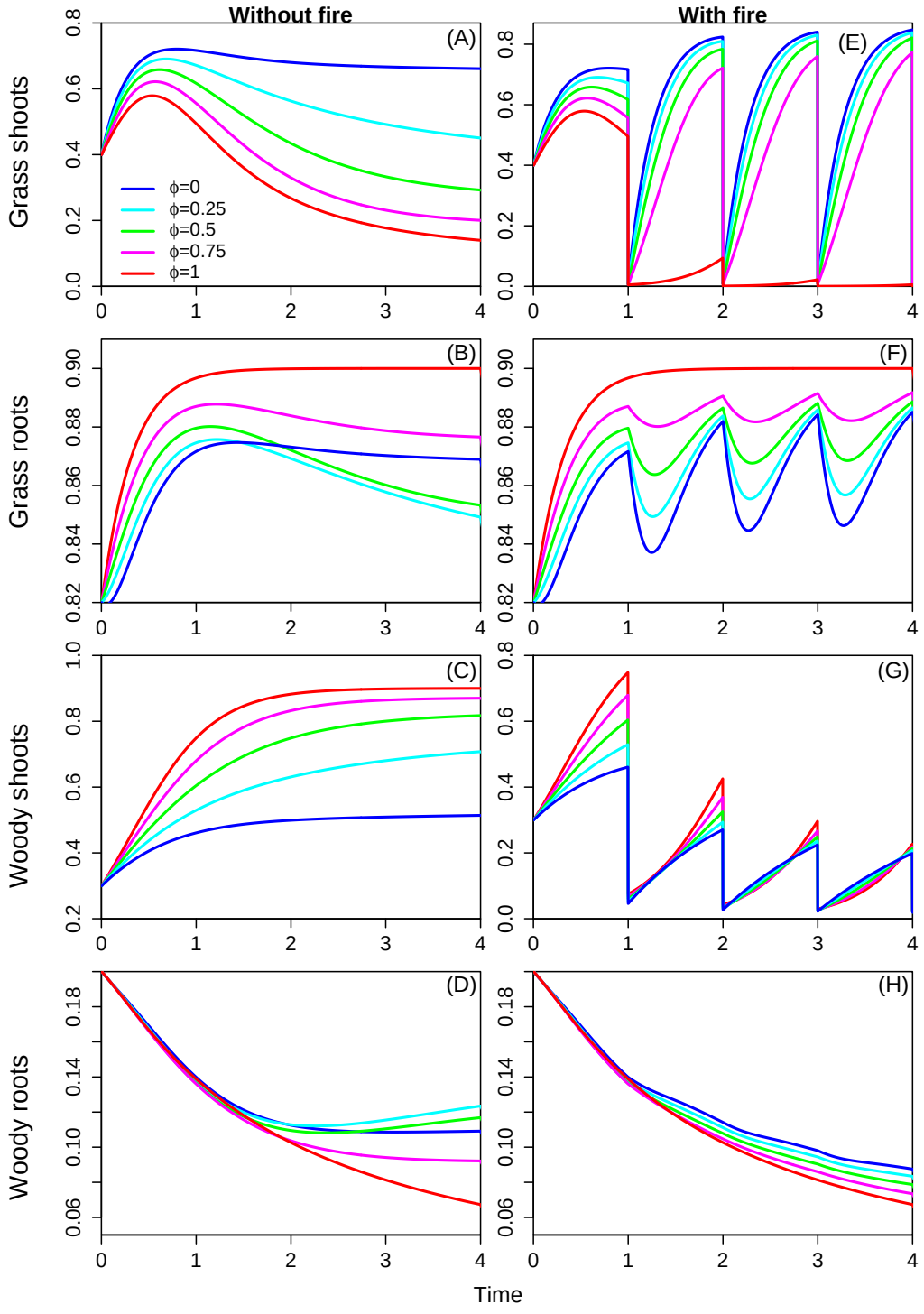

Figure 2.3: Trajectories of the system defined in Equations (2.1) to (2.4) when grass roots exert strong competition on woody roots and woody shoots exert strong competition on grass shoots. Panels (A) to (D) depict trajectories without fire, panels (E) to (H) depict trajectories with fire. Different colors depict different values of the coupling parameter ϕ in the function $\mathcal{G}$.

removal (Figures 2.3E and 2.3F). However, as long as root biomass remains greater than zero, the shoot biomass will have a positive growth rate and can therefore recover from disturbance. After some time, the plant will reach a stable shoot-root ratio again. Hence, roots subsidize shoot regrowth at the cost of a decrease in root biomass. When shoots and roots are not coupled ($\phi = 1$), roots cannot buffer the regrowth of shoots, hence shoots tend to zero after repeated fires (Figures 2.3E).

The important finding here is that as long as there is some coupling between roots and shoots, then the dynamics of the system are qualitatively not influenced by the level of coupling between shoots and roots. For instance, the trajectories for GS, GR, WS and WR simulated in Figure 2.3 show that grass and tree compartments can coexist when $0 \leq \phi < 1$ and in this situation they represent the response of the system to fire adequately.

2.3.2 The competition functions $\mathcal{L}$ and $\mathcal{R}$

To explore how inter-specific shoot and root competition $\mathcal{L}$ and $\mathcal{R}$ influences the system dynamics we parametrized the model such that it provides a system state where grasses and trees coexist and then analyzed the response of the isoclines in the shoot and root phase planes to variable shape parameters θ and σ in Equations (2.6) and (2.7). This analysis shows that while the equilibrium biomasses are sensitive to θ and σ, the values of θ and σ do basically not influence whether coexistence occurs or not.

The equilibrial grass shoot biomass increases with the non-linearity parameter of light competition θ, because when θ is higher, the competitive pressure exerted by woody shoots is only felt at high woody shoot biomasses hence, grass growth is facilitated (Figure 2.4A). The effect of variable θ on the equilibrial grass root biomass is almost negligible (Figure 2.4B). Hence, whether light competition is modelled as delayed onset ($\theta > 1$) or according to Beer's law ($\theta < 1$) only determines whether the grass isocline is convex or concave (Figure 2.4A) and thereby modifies the equilibrial grass shoot biomass while preserving the system behavior. Sensitivity of the grass isoclines to variation in the parameters θ and σ, which respectively describe the non-linearity in (inter-specific) light competition and root competition. Panels (A) and (B) depict variable shoot competition (variable θ), panels (C) and (D) depict variable root competition (variable σ). The intersection points between the tree isocline and the different grass isoclines are asymptotically stable points of the different cases.

The non-linearity parameter of root competition σ has an effect analogous to that of θ

(Figures 2.4C and 2.4D). In this case, σ does not influence the equilibrial shoot biomass and only slightly modifies the equilibrial root biomass, while the system behavior is preserved.

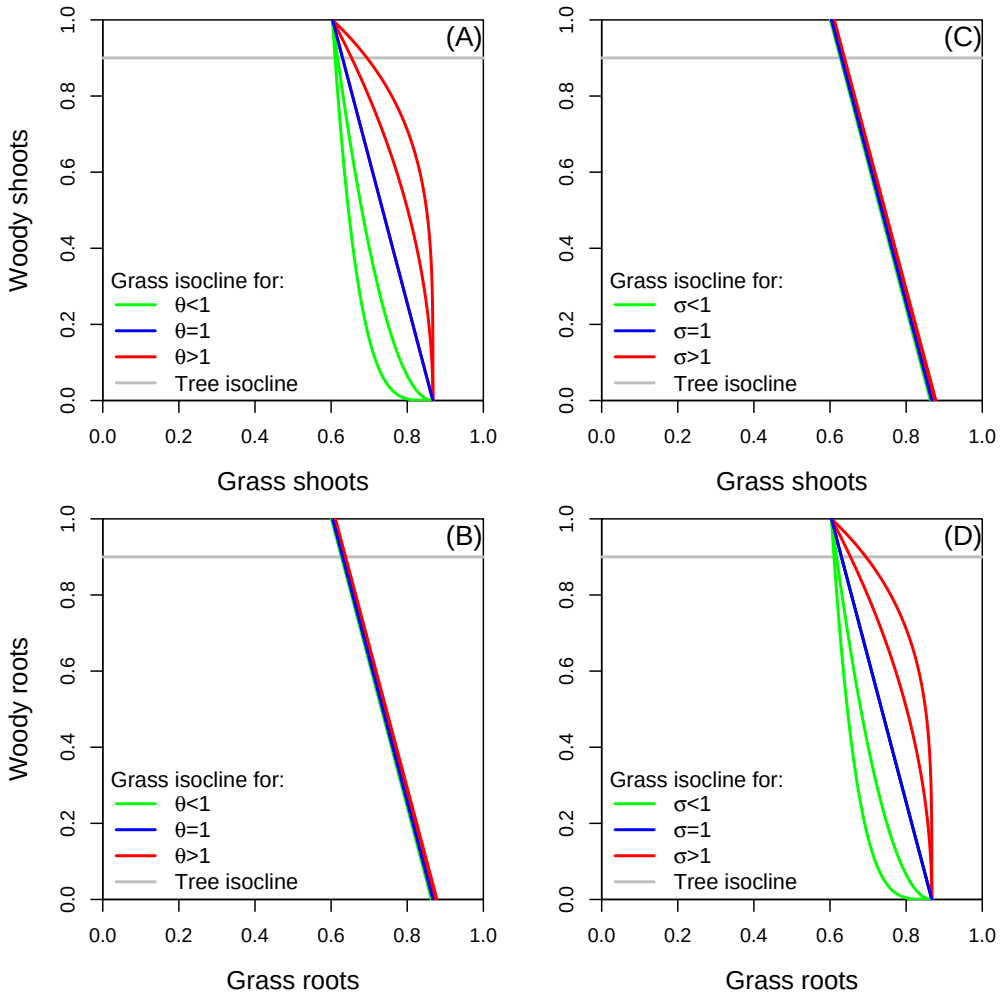

Figure 2.4: Sensitivity of the grass isoclines to variation in the parameters θ and σ, which respectively describe the non-linearity in (inter-specific) light competition and root competition. Panels (A) and (B) depict variable shoot competition (variable θ), panels (C) and (D) depict variable root competition (variable σ). The intersection points between the tree isocline and the different grass isoclines are asymptotically stable points of the different cases.

2.4 Analysis of the simplified model

The previous paragraphs illustrate that as long as aboveground and belowground compartments are coupled ($\phi \neq 1$) the conditions required for coexistence are insensitive to the values of ϕ, θ and σ. To simplify the further analysis of the model we therefore assume $\phi = 0$ and $\sigma = 1$, that is, coupling between shoot and roots is strong and root competition is linear. All analyses that follow use this simplified model:

$$\begin{aligned} f_{GS}(\mathbf{V}) &= g_{GS}\, GR\, \left(1 - GS - \omega_{WG} WS^{\theta}\right) - d_{GS}\, GS - Z_G, && (2.10)\\ f_{GR}(\mathbf{V}) &= g_{GR}\, GS\, (1 - GR - \alpha_{WG} WR) - d_{GR}\, GR, && (2.11)\\ f_{WS}(\mathbf{V}) &= g_{WS}\, WR\, (1 - WS) - d_{WS}\, WS - Z_W, && (2.12)\\ f_{WR}(\mathbf{V}) &= g_{WR}\, WS\, (1 - WR - \alpha_{GW} GR) - d_{WR}\, WR. && (2.13) \end{aligned}$$

Here, α_{GW} and α_{GW} describe the effect of root competition and ω_{WG} describes the effect of light competition. To explore how the nature and intensity of inter-specific competitive interactions determine whether coexistence is possible or not, we conducted an isocline analysis in the two-dimensional phase space, defined by the root biomasses GR and WR. To do this we assume that fire and herbivory are absent and that grass shoots and woody shoots are in equilibrium. Here, we present the analysis of the root biomasses rather then the shoot biomasses because the equations governing their behavior are simpler to solve. However, an analogous analysis for shoot biomasses GS and WS, that yields the same results as described below, is provided in Appendix 2.6. The grass and tree root isoclines when grass and tree shoots are in equilibrium are given as

$$\begin{aligned} \mathcal{I}_{GR}(WR) &= \frac{g_{GR} P_{\omega}(WR)}{g_{GR} P_{\omega}(WR) + d_{GR}} \left(1 - \frac{d_{GR} d_{GS}}{g_{GR} g_{GS} P_{\omega}(WR)} - \alpha_{WG} WR\right), && (2.14)\\ \mathcal{I}_{WR}(GR) &= \frac{g_{WR}}{g_{WR} + d_{WR}} \left(1 - \frac{d_{WR} d_{WS}}{g_{WR} g_{WS}} - \alpha_{GW} GR\right), && (2.15) \end{aligned}$$

where

$$P_{\omega}(WR) = 1 - \omega_{WG} \left(\frac{g_{WS} WR}{g_{WS} WR + d_{WS}}\right)^{\theta}. \qquad (2.16)$$

The function $P_{\omega}(WR)$ acts as a scaling factor that reduces the effective growth rate between 0 and g_{GR}. The maximum equilibrial biomass values that GR and WR can take are denoted as K_{GR} and K_{WR} (Table 2.1) where $K_{GR} = \mathcal{I}_{GR}(0)$ is defined as the

intercept between the grass isocline and the GR-axis and $K_{WR} = \mathcal{I}_{WR}(0)$ is defined as the intercept between the tree isocline and the WR-axis. The intercept of the grass isocline and the WR-axis is denoted as $H_{GR} = \mathcal{I}_{GR}^{-1}(0)$, the intercept of the tree isocline and the GR-axis is denoted as $H_{WR} = \mathcal{I}_{WR}^{-1}(0)$ (Table 2.1).

Table 2.1: Characteristics of the isoclines and maximum competition parameters.

Variable name	Grass roots	Tree roots
	Without light competition	
Maximum biomass	$K_{GR} = \frac{g_{GR}g_{GS} - d_{GR}d_{GS}}{g_{GR}g_{GS} + d_{GR}g_{GS}}$	$K_{WR} = \frac{g_{WR}g_{WS} - d_{WR}d_{WS}}{g_{WR}g_{WS} + d_{WR}g_{WS}}$
	$K_{GS} = \frac{g_{GS}g_{GR} - d_{GS}d_{GR}}{g_{GS}g_{GR} + d_{GS}g_{GR}}$	$K_{WS} = \frac{g_{WS}g_{WR} - d_{WS}d_{WR}}{g_{WS}g_{WR} + d_{WS}g_{WR}}$
Axis intercepts	$H_{GR} = \frac{1}{\alpha_{WG}}\left(1 - \frac{d_{GR}d_{GS}}{g_{GR}g_{GS}}\right)$	$H_{WR} = \frac{1}{\alpha_{GW}}\left(1 - \frac{d_{WR}d_{WS}}{g_{WR}g_{WS}}\right)$
Slope of isocline	$S_{GR} = -\alpha_{WG}\,\frac{g_{GR}}{g_{GR} + d_{GR}}$	$S_{WR} = -\alpha_{GW}\,\frac{g_{WR}}{g_{WR} + d_{WR}}$
Max. root competition	$\alpha_{WG}^{max} = \frac{1}{K_{WR}}\left(1 - \frac{d_{GR}d_{GS}}{g_{GR}g_{GS}}\right)$	$\alpha_{GW}^{max} = \frac{1}{K_{GR}}\left(1 - \frac{d_{WR}d_{WS}}{g_{WR}g_{WS}}\right)$
	With light competition	
Max. root competition	$\alpha_{WG}^{max}(\omega) = \frac{1}{K_{WR}}\left(1 - \frac{d_{GR}d_{GS}}{g_{GR}g_{GS}P_{\omega}(K_{WR})}\right)$	$\alpha_{GW}^{max} = \frac{1}{K_{GR}}\left(1 - \frac{d_{WR}d_{WS}}{g_{WR}g_{WS}}\right)$

2.4.1 Effect of root competition

To analyze how root competition, defined by the parameters α_{GW}, α_{WG} in Equations (2.11) and (2.13), influences coexistence in the absence of light competition, we set $\omega_{WG} = 0$ in Equation (2.10). In this case the isocline $\mathcal{I}_{GR}$ is, analogous to $\mathcal{I}_{WR}$, a linear function with slope and axis intercepts as given in Table 2.1.

The fixed points of the dynamic system defined in Equations (2.10) to (2.13) are the origin of the coordinate system, the maximum biomasses K_{GR} and K_{WR} (Table 2.1), and (if it exists) the intersection point of both isoclines (see Appendix 2.7). The maximum biomasses are constants, as they are independent of the competition parameters α_{GW},

α_{WG} and ω_{WG} and are fully determined by the growth and decomposition parameters (which are assumed to be constant). Hence, the asymptotic behavior of the fixed-points depends on the relation between the maximum biomasses K_{GR} and K_{WR} and the values H_{WR} and H_{GR} or equivalently on the slopes of the isoclines (Table 2.1), which are linear functions of the root competition parameters α_{GW} and α_{WG}.

Figure 2.5 (see page 32): Grass root and tree root isoclines and the corresponding conditions that define stability. Panels (A) and (E) depict stable grass-tree coexistence, panels (B) and (F) the unstable case, panels (C) and (G) the grass dominated case and panels (D) and (H) the tree dominated state. Panels (A) to (D) show the isoclines in absence of light competition, panels (E) to (H) show the influence of light competition. Tree isoclines are solid black, grass isoclines are solid gray. The dashed gray lines in panels (E) to (H) are grass isoclines in absence of light competition, the dotted gray lines in panels (E) and (G) show situations where light competition changes the system state. Each panel includes two black dashed lines which show how the system's state converges, from different initial conditions, to the asymptotically stable points. Circles indicate asymptotically stable points, rectangles indicate unstable nodes and triangles indicate the axis intercepts H_{GR} and H_{WR}. The right column gives the corresponding conditions for the competition parameters (see Table 2.1 for a definition of the notation and Figure 2.6 for the isoclines in the shoot system).

Figure 2.6 (see page 33): Grass and tree isoclines and the corresponding conditions that define stability in the aboveground phase plane (GS-WS-system). The figure is structured in the same way as Figure 2.5; see the caption of Figure 2.5 for details.

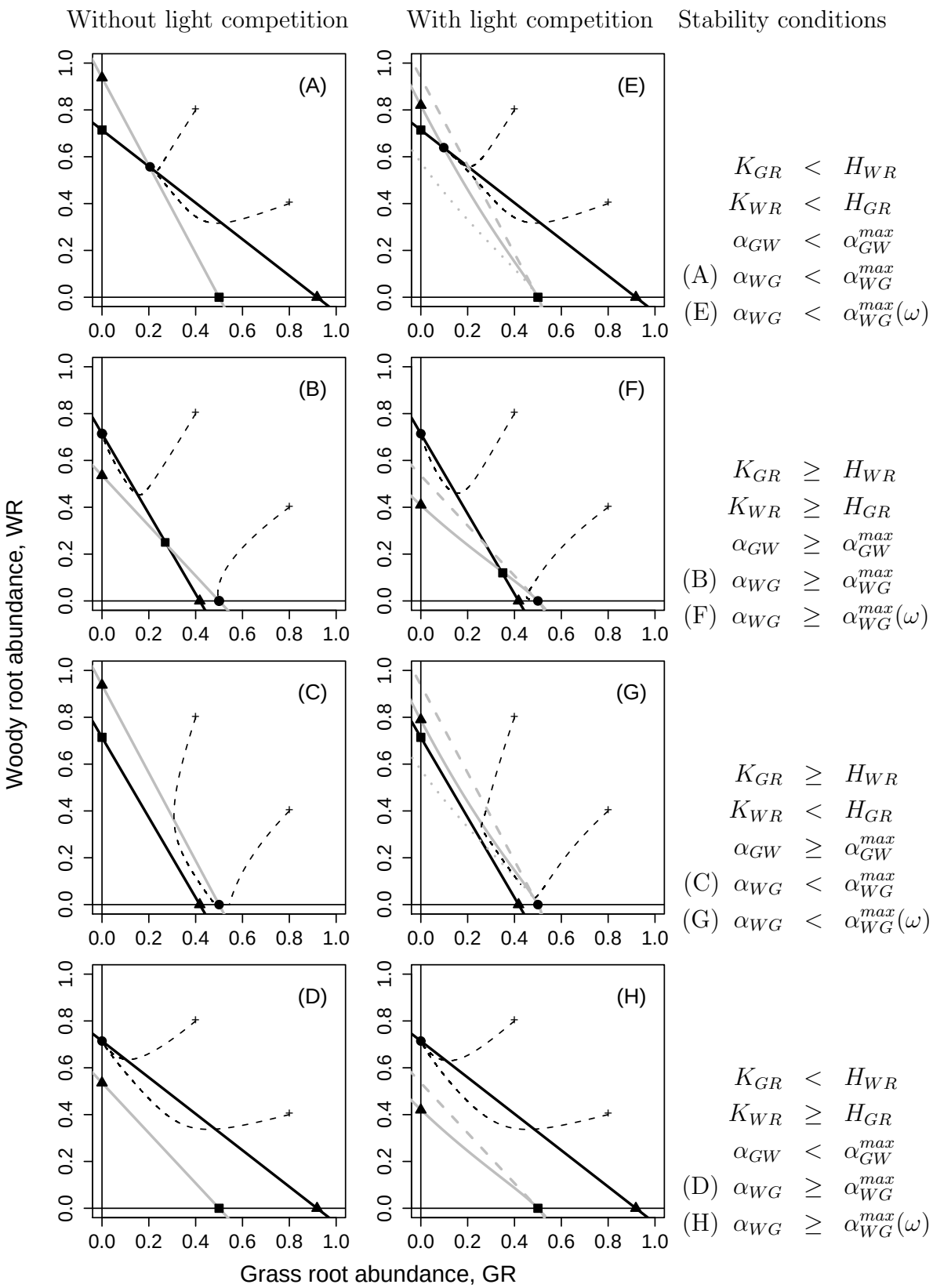

Figure 2.5: See page 31 for figure captions.

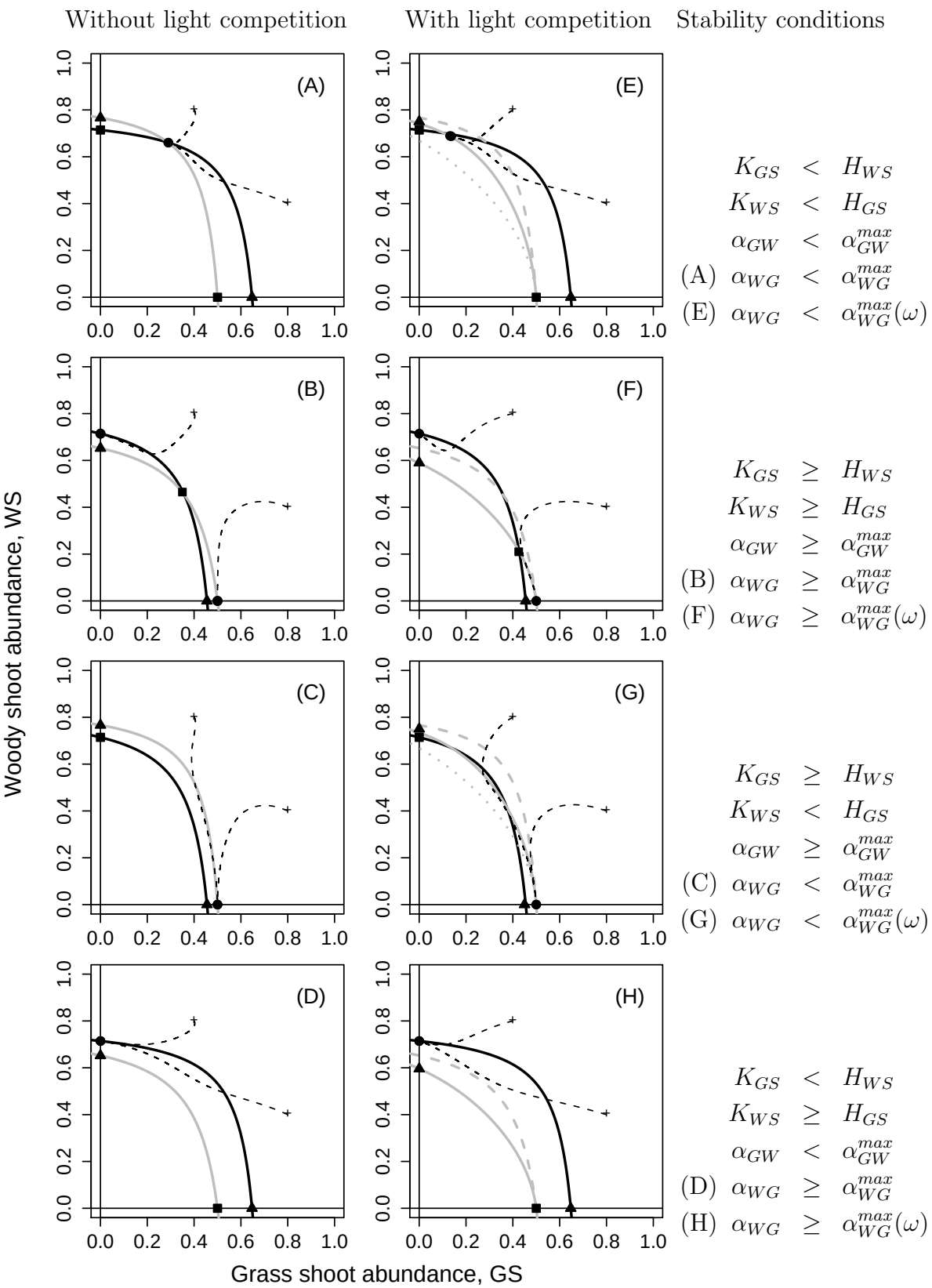

Figure 2.6: See page 31 for figure captions.

If both α_{GW} and α_{WG} are equal to zero, the dynamics of grasses and woody vegetation are decoupled and both vegetation types reach their maximum biomass. If the competition parameters are greater than zero, the competition parameters determine which of the following four qualitatively different system states emerges (Figure 2.5 provides a summary for the root system, Figure 2.6 provides a summary for the shoot system).

When $H_{GR} > K_{WR}$ and $H_{WR} > K_{GR}$, there exists an asymptotically stable intersection point between the isoclines and the intercepts K_{WR} and K_{GR} are unstable (Figure 2.5A). Hence, grasses and trees coexist and all trajectories converge towards the intersection point between the isoclines. The model thus predicts that stable coexistence of grasses and trees is possible when light competition is absent and competition between the root systems is balanced. Root competition is balanced, as long as $\alpha_{GW} < \alpha_{GW}^{max}$ and $\alpha_{WG} < \alpha_{WG}^{max}$, where α_{GW}^{max} and α_{WG}^{max} describe the maximum level of competition that can be sustained by trees and grasses. These parameters are completely defined by the growth and decomposition parameters (Table 2.1). Note that both α_{GW}^{max} and α_{WG}^{max} can be greater than one. This result means that a rooting niche is not necessary for grass-tree coexistence.

When $H_{GR} \leq K_{WR}$ and $H_{WR} \leq K_{GR}$, then the intersection point between the isoclines is an unstable node, and the maximum biomasses K_{GR} and K_{WR} are asymptotically stable (Figure 2.5B). The trajectory may tend towards the unstable node, suggesting a stable savanna state, however, it eventually converges towards one of the asymptotically stable points K_{GR} or K_{WR}, that is to a grassland or to a woodland. Whether it tends to a grassland or a woodland depends on the initial conditions. Unstable coexistence emerges when both root competition parameters α_{GW} and α_{WG} exceed the maximum values α_{GW}^{max} and α_{WG}^{max} (Table 2.1). The vegetation type with the superior initial conditions out-competes the other vegetation type. Small differences in the initial conditions can lead to different outcomes.

When $H_{GR} > K_{WR}$ and $H_{WR} \leq K_{GR}$, then there is no intersection point between the isoclines and the grass isocline lies above the tree isocline. The maximum biomass K_{GR} is asymptotically stable, whereas K_{WR} is unstable (Figure 2.5C), hence the system tends to a grass dominated state. Analogously, there is no intersection point between the isoclines when $H_{GR} \leq K_{WR}$ and $H_{WR} > K_{GR}$. In this case, the tree isocline lies above the grass isocline and K_{WR} is asymptotically stable, whereas K_{GR} is unstable (Figure 2.5D); hence, the system converges towards a tree dominated state. The tree or grass dominated states occur when one root competition parameter exceeds the cor-

responding maximum value α_{GW}^{max} or α_{WG}^{max} (Table 2.1) and the other root competition parameter lies below this maximum. Under these conditions the root competition abilities of one vegetation type are strong enough to limit growth of the other vegetation type to such an extent that it is out-competed.

2.4.2 Effect of root and light competition

Under light competition ($\omega_{WG} > 0$ in Equation 2.10) the shape of the tree isocline (Equation 2.15) remains unchanged, whereas the grass isocline (Equation 2.14) becomes non-linear. Increasing ω_{WG} decreases the maximum root competition parameter $\alpha_{WG}^{max}(\omega)$ (Table 2.1) and thereby decreases the axis intercept H_{GR}. As consequence, by the introduction of light competition the stability conditions identified by the isoclines (Figure 2.5) might be modified. The stable points can be influenced in two ways: (1) the asymptotic behavior remains unchanged, but the values of the fixed-points are eventually modified and (2) the asymptotic behavior changes and the system shifts into another state.

The asymptotic behavior remains unchanged by the introduction of weak light competition when growth parameters and root competition parameters define a stable savanna state as in Figure 2.5A. Should we increase the light competition parameter ω_{WG}, we find that the intersection point between the isoclines moves along the isocline $\mathcal{I}_{WR}$ towards a lower equilibrium grass biomass and a higher equilibrium tree biomass (Figure 2.5E). If light competition is so intense that H_{GR} falls below K_{WR}, then the system flips into the tree dominated state (dotted line in Figure 2.5E and Figure 2.5H), where the isoclines do not intersect. In the tree dominated state variation of the light competition parameter has no effect on the system dynamics (Figure 2.5H).

In the grass dominated state where the isoclines do not intersect, low values of light competition might slightly influence the trajectories but do not influence the system state (Figure 2.5G). However, if light competition is intense (ω_{WG} is large), then H_{GR} eventually falls below K_{WR} and the isoclines intersect. The system changes into the unstable savanna state as depicted in Figure 2.5F and by the dotted line in Figure 2.5G. In the unstable savanna state increasing light competition only acts to reduce the domain of attraction of the grass dominated state while the system state cannot be changed.

2.4.3 Effect of fire

Now we discuss how fire influences grass-tree coexistence. First, we examine the case of fire in a stable savanna system where the stability conditions $H_{GR} > K_{WR}$ and $H_{WR} > K_{GR}$ are fulfilled (Table 2.1, Figures 2.5A and 2.5E). In this case, fire spreads regularly when grass shoot biomass exceeds the threshold δ and thereby reduces shoot biomasses GS and WS (Equations 2.8 and 2.9). After fire induced biomass reduction, the system begins moving towards the asymptotically stable savanna state, only to be drawn away from this point when the next fire occurs. Such a system behavior can be described as truncated event-to-event dynamics (Ives *et al.* 2000). Although fire imposes periodicity on the state variables, the dynamics of system remain unchanged in the sense that fire is no prerequisite for coexistence. Fire only reduces the total long-term mean biomass and is thus merely a modifier of the savanna.

In the case where the competition parameters define unstable coexistence (Figure 2.5B and 2.5F) the fire parameters determine the domain of attraction in which the trajectory is located after a fire. The domain of attraction, in turn, determines whether the system converges towards a grass dominated state or towards a tree dominated state.

In the case where the competition parameters define a grass dominated state (Figure 2.5C and 2.5G), fire cannot prevent woody biomass from extinction, because the competitive intensity and the growth rate of grasses are too high relative to the regrowth capabilities of woody vegetation.

The ecologically most interesting situation is the case where the competition parameters define a system state where trees dominate due to high levels of light competition ω_{WG} (Figure 2.5H). In this case, the reduced woody shoot biomass after a fire gives grasses the chance to grow under lowered competitive pressure, thereby allowing grass persistence and grass-tree coexistence (Figure 2.7A). Fire changes the system state and is a prerequisite for coexistence.

Whether fire can facilitate coexistence is significantly influenced by the amount of fuel biomass at ignition. Frequent fires do not allow enough time for the accumulation of the fuel-loads required to sufficiently damage tree biomass and reduce light competition, whereas infrequent fires allow tree biomass to accumulate to levels required to suppress grass biomass. It follows that intermediate fire frequencies are needed if fire is to facilitate grass-tree coexistence.

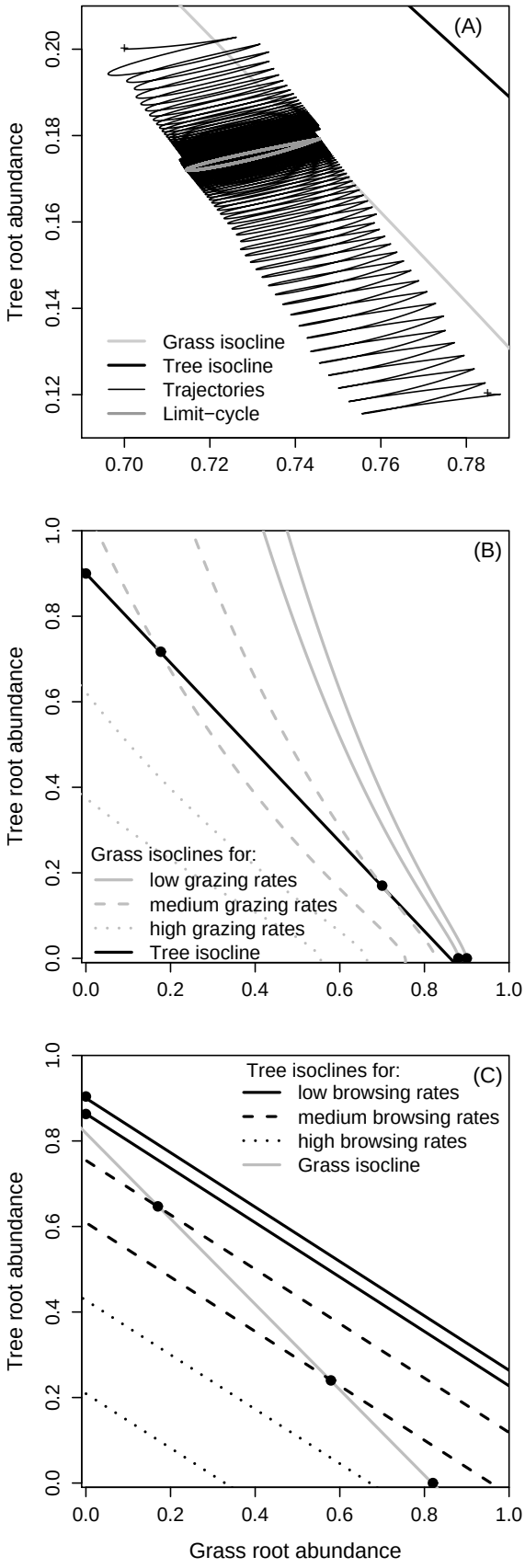

Figure 2.7: Panel (A) depicts a case where light and root competition are too intense to allow coexistence, hence the isoclines do not meet. The introduction of fire in this system allows the system to converge to a stable limit-cycle characterized by grass-tree coexistence. Note that only a small section of the phase plane is illustrated. Panel (B) shows the tree isocline, the grass isoclines and the corresponding asymptotically stable points (circles) for increasing (from right to left) grazing intensities. In the grass dominated state, low grazing rates only reduce the equilibrial grass biomass. Medium grazing rates push the system from the grass dominated state into a stable savanna state. High grazing rates push the system into the tree dominated state where grasses are excluded. Analogously, panel (C) shows the isoclines and the asymptotically stable points for increasing browsing pressure (from top down). Low browsing rates only reduce the equilibrial tree biomass, medium browsing rates push the system from the tree dominated state into a stable savanna state and high browsing rates push the stable savanna state into a grass dominated state.

2.4.4 Effect of herbivory

The previous sections have ignored herbivory and while the insights gained might be relevant for savannas where herbivore biomass is low, e.g. in the South American savannas described by Sarmiento (1984), we now explore how herbivory influences grass-tree coexistence. Our examination of herbivory effects focuses on the effects of grazing and browsing on coexistence and we define in both cases the maximum grazing/browsing rate under which the stable savanna state can persist.

We first examine grazing. The grazing function $Z_G = u_G GS$ can be interpreted exactly as decomposition is interpreted since growth function for grass shoots (Equation 2.10) under grazing is

$$f_{GS}(\mathbf{V}) = g_{GS} GR \left(1 - GS - \omega_{WG} WS^{\theta}\right) - (d_{GS} + u_G) GS. \tag{2.17}$$

Hence, grazing merely reparametrizes the "decomposition" term from d_{GS} to $d_{GS} + u_G$.

In the grass dominated state (Figures 2.5C and 2.5G and Figure 2.7B), low grazing pressure reduces the grass biomass but does not change the asymptotic behavior of the system. However, grazing reduces the maximum grass biomass K_{GR} (Table 2.1). At high grazing pressure, K_{GR} falls below H_{WR}, the isoclines intersect and a stable savanna state is established (Figure 2.7B). If the grazing pressure is further increased and exceeds the maximum grazing pressure

$$u_G^{max} = \frac{1}{d_{GR}} \left(g_{GR} g_{GS} P_{\omega}(K_{WR}) \left(1 - \alpha_{WG} K_{WR}\right) - d_{GR} d_{GS}\right), \tag{2.18}$$

then the intersection point between the isoclines vanishes and the system is driven from the stable savanna state into the tree dominated state (Figure 2.7B).

Analogously, browsing can be understood as a reparametrization of the decomposition term of woody shoots from d_{WS} to $d_{WS} + u_W$ and it can influence the asymptotic behavior of the system the opposite way to grazing (Figure 2.7C): browsing can shift a tree dominated state (Figures 2.5D and 2.5H) into a stable savanna state (Figures 2.5A and 2.5E), which can be driven to a state of tree absence (Figures 2.5C and 2.5G) when the browsing pressure exceeds the maximum browsing pressure, which is defined as

$$u_W^{max} = \frac{1}{d_{WR}} \left(g_{WR} g_{WS} \left(1 - \alpha_{GW} K_{GR}\right) - d_{WR} d_{WS}\right). \tag{2.19}$$

When both grazing and browsing are strong, a stable savanna state might be established,

however, the total biomass of the system is reduced in contrast to the situation without herbivory.

2.4.5 Effect of fire and grazing

Many savannas are used as grazing lands. For this reason we now turn our attention to grazing systems and analyze how grazing and fire interact. We implicitly assume that any residual browsing effects are included by simply reparametrizing d_{WS}. We first calculate the maximum yield Z^* without fire (Figures 2.8A to 2.8C) analytically by expressing Z^* as a function of the model parameters (specifically, of the competition parameters α_{GW}, α_{WG} and ω_{WG}) and the maximum yield with fire by maximizing the outcome of simulation results using numerical optimization. Then we explore the interactive effect of fire and grazing by examining the difference between the maximum yields obtained with and without fire (Figures 2.8D to 2.8F).

The sensitivity of the maximum yield Z^* to variation of the competition parameters α_{GW}, α_{WG} and ω_{WG} in the case without fire is shown in Figures 2.8A to 2.8C. The maximum yield Z^* is equal to zero if woody root competition exceeds the threshold value α_{WG}^{max} (Table 2.1), independent of the light competition parameter. Above α_{WG}^{max}, the system is in the tree dominated state and grass biomass is driven to extinction; grazing only acts to accelerate this process. When woody root competition is less than α_{WG}^{max} and light competition is absent, Z^* decreases linearly with woody root competition and grass root competition has no effect on Z^* (Figure 2.8A). In contrast, grass root competition α_{GW} influences the maximum yield at higher levels of light competition (Figures 2.8B and 2.8C). When $\omega_{WG} > 0$ and the system is in the savanna state, Z^* is increased with increasing α_{GW}. When $\alpha_{GW} > \alpha_{GW}^{max}$ (Table 2.1) and the system is in the grass dominated state, Z^* is only weakly affected by light competition. These results simply mean that Z^* is higher in the absence of trees and the associated competitive pressure.

Fire can change the maximum yield; however, its effect is contingent on grazing and competition. Fire has a negative effect on the maximum yield Z^* if light competition is absent and woody root competition is low (Figure 2.8D). In such cases the system is in a stable savanna state and fire removes grass biomass and therefore reduces the maximum yield. Fire also has a negative effect on Z^* when grass root competition exceeds the threshold α_{GW}^{max}, irrespective of light competition (Figures 2.8D to 2.8F). In such cases the system is in the grass dominated state and grass growth is not affected

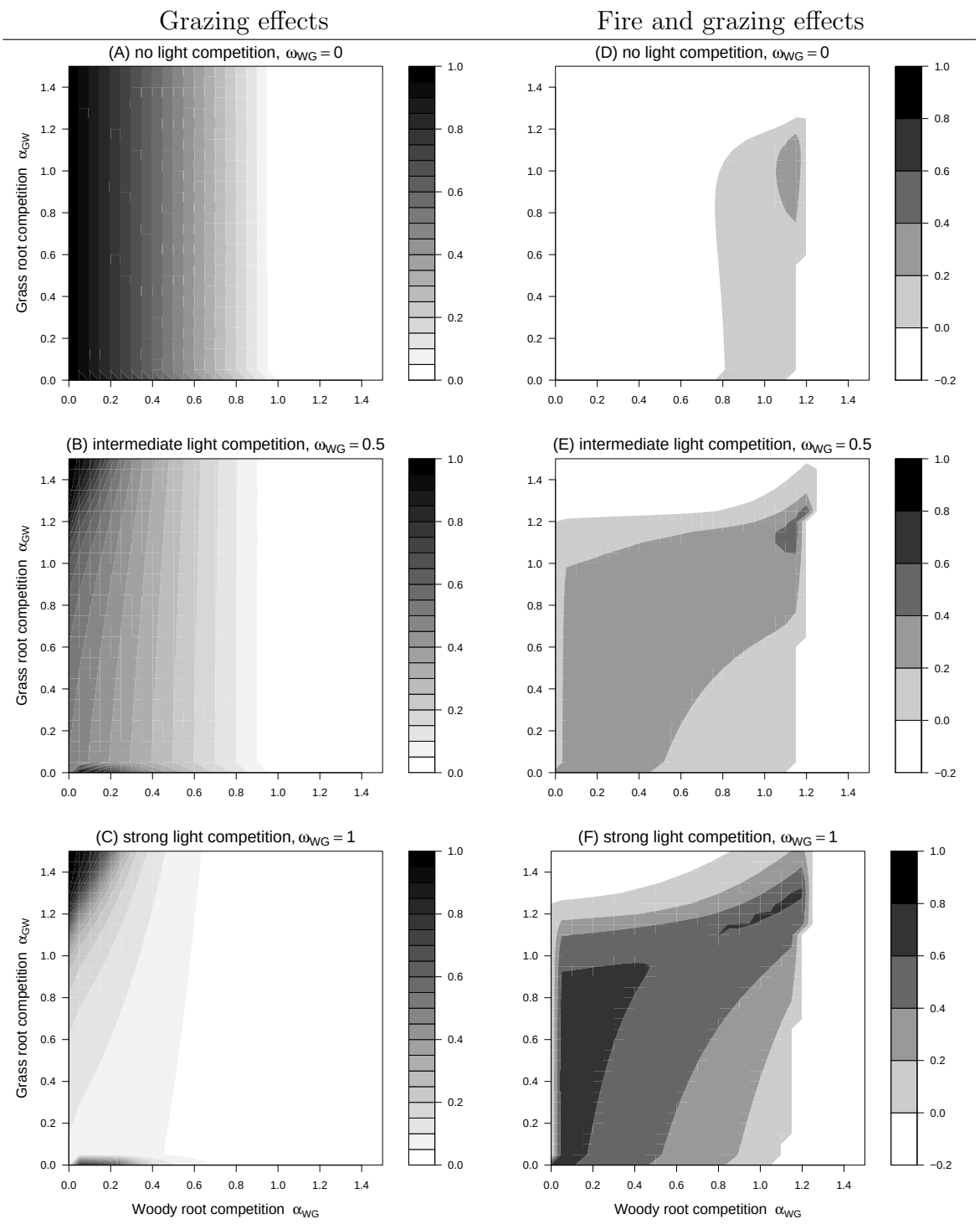

Figure 2.8: The effect of fire on the maximum grazing yield of the system. Panels (A), (B) and (C) show the sensitivity of the maximum yield to the root competition parameters in the case without fire. Panels (D), (E) and (F) show the difference between the maximum yields with fire and without fire. In each row, light competition is constant. In all cases the maximum root competition parameters are $\alpha_{GW}^{max} = \alpha_{WG}^{max} = 1.1$.

by competition from trees. Fire merely acts to delay the eventual extinction of trees.

Fire has a positive effect on Z^* when light competition is strong enough to limit grass growth (Figures 2.8E and 2.8F). In such cases fire regularly reduces woody shoot biomass, and hence the competitive pressure on grasses. Fire therefore allows grass biomass to reach higher levels and as consequence, the maximum yield is higher. This effect is most pronounced at high levels of light competition, low levels of woody root competition and moderate values of grass root competition (Figure 2.8F). Fire has also a weak positive effect on Z^* when light competition is absent and woody root competition is strong (Figure 2.8D). In such cases fire prevents root biomasses from reaching high levels and thereby reduces the competitive pressure that tree roots exert on grass growth.

Note, that the outcome of the simulations that we described in this section can significantly depend on the fire parameter δ and on the choice of the fire response parameters a, b, c and d from Equations (2.8) and (2.9). A different set of parameter values might define a system where the effects described above are not observable.

2.5 Discussion

This study shows how root and shoot competition between grasses and trees interact with fire and herbivory to define the conditions under which grasses and trees coexist. The novel feature of our model is that it separates aboveground and belowground processes, thus allowing a more realistic representation of competitive interactions and the response of plants to disturbances such as fire and herbivory. The model therefore achieves some level of integration of resource and disturbance based perspectives of savannas as called for by Sankaran *et al.* (2004, 2005). We show in the absence of fire, herbivory and light competition that coexistence is possible and solely determined by the strength of competition for soil resources. Coexistence is possible when root interactions are balanced (House *et al.* 2003), in the sense that the intensities of root competition for both competitors must remain below thresholds, which are defined by the growth and mortality rates of grass and trees. In the model, the maximum levels of root competition are such that a rooting niche (Walter 1971) is not needed for grass-tree coexistence, while many existing deterministic models for grass-tree coexistence rely on a rooting niche (Walker and Noy-Meir 1982; van Langevelde *et al.* 2003). However, when light competition is intense, a niche separation is necessary for grass-tree coexistence.

Fire is necessary for grass-tree coexistence when light competition is strong enough to force competitive exclusion (Murray 2002; House *et al.* 2003) of grasses. Fire can reduce woody shoot biomass and the associated light competition exerted by woody shoots on grass shoots sufficiently to allow grasses to persist. Several existing studies have similarly shown that abrupt mortality events, as imposed by fire, or other periodic events might induce complex system dynamics (e.g. Rinaldi *et al.* 1993; Gragnani and Rinaldi 1995; Ives *et al.* 2000) that enable coexistence even in situations where the non-periodic system does not allow coexistence (Koch 1974; Cushing 1980). Yet, in the savanna models of Walker and Noy-Meir (1982) and van Langevelde *et al.* (2003), fire was modelled as a process that continuously removes a moderate proportion of biomass. Hence, in these models, fire acts exactly as grazing or browsing act. While this approach can be justified by casting fire as an unselective herbivore (Bond and Keeley 2005), this analogy is not completely appropriate in savannas as it ignores the fact that fire consumes biomass in a punctuated event. Modeling fire as an acute impact rather than a chronic process can change the criteria for grass-tree coexistence in savannas and thereby our interpretation of the role of fire in structuring savannas.

Herbivory can fundamentally change the system's characteristics and the model allows us to understand the conditions under which herbivory can facilitate or prevent grass-tree coexistence. Grazing acts to promote woody vegetation by reducing the competitive pressure exerted by grasses on trees. Grazing can establish stable coexistence in situations where grasses would otherwise dominate, while high levels of grazing can push the system into tree dominated state. Analogously, browsing promotes grass vegetation by reducing the competitive pressure experienced by grasses. Hence, both fire and grazing can establish coexistence but can also push the system towards a tree dominated or "bush-encroached" state (Smit *et al.* 1999; Bond and Keeley 2005). Such "bush-encroached" systems are from a perspective of livestock production considered as degraded (Vetter 2005). In such situations, the model and empirical studies (Prins and Van der Jeugd 1993; Roques *et al.* 2001) suggest that browsing and management fires can prevent bush-encroachment.

Our model is a phenomenological representation of the processes that shape grass-tree interactions. The advantage of such an approach is that the model is simple enough to analyze while a more realistic representation of the processes might not yield to mathematical analysis. However, we justify our phenomenological approach by showing that the details of how aboveground and belowground processes are linked and how root and shoot competition are modelled does not influence our main findings. The fundamental

model assumption that provides an adequate representation of grass-tree dynamics is the partitioning of roots and shoots and the resulting partitioning of aboveground and belowground processes.

The disadvantage of the phenomenological approach is that the highly aggregated and compact formulation of the system's dynamics makes parameter estimation difficult. Studies that estimate the parameters of Volterra-Lotka type models from field data are rare (Pascual and Kareiva 1996; Freckleton and Watkinson 2000). However, model parameters can be estimated by (1) fitting the model to field data using indirect statistical methods and (2) by field or green house experiments that directly estimate model parameters. Despite the intuitive appeal of directly estimating model parameters (Connell 1983; Gurevitch *et al.* 1992; Cahill and Casper 2000) Freckleton and Watkinson (2000, 2001) showed that indirect fitting techniques provide better results than direct methods for parameter estimation.

Indirect methods include fitting model parameters to field data using non-linear regression techniques (Rees and Bergelson 1997) and maximum likelihood techniques (Rees and Bergelson 1997; Law and Watkinson 1987). For the presented model, we indirectly estimated parameters by fitting the model to a tree abundance data set from Africa (Sankaran *et al.* 2005, Chapter 3). This analysis shows, that the model can predict patterns of tree abundance over a rainfall gradient from about 200 to 1200 mm mean annual precipitation. Moreover, the parameter estimates were consistent with the expectation that root competition is intense and that there is a delayed onset of the effect of light competition.

An alternative way to verify the model is to derive qualitative, yet testable hypothese. For instance, the model predicts that in arid savannas where tree leaf areas are low, light competition experienced by grasses would be low and grasses and trees can coexist even when fire and herbivory are absent and when soil conditions preclude rooting niche separation. At the other extreme the model predicts that fire is essential for grass-tree coexistence when light competition is strong enough to force competitive exclusion (Murray 2002; House *et al.* 2003), e.g. at sites where the climate potential is sufficient for trees to develop high leaf areas (and hence exert high levels of light competition) and where soils are shallow enough to preclude the possibility of rooting niche separation. Should, in such a situation, fire be lost from the system, it is inevitable that grasses are excluded and trees dominate. This result agrees with the findings of fire exclusion experiments in savannas that show that fire exclusion induces a shift to woodland or forest states (Bond and Keeley 2005). However, in a tree dominated savanna when

trees are sufficiently damaged by management fires, then the model predicts that coexistence might be re-established. These model predictions broadly agree with Sankaran *et al.* (2005)'s interpretation of empirical data from Africa, which suggested that fire is necessary for grass-tree coexistence at higher rainfall sites.

The failure of existing deterministic models of savannas (Walker and Noy-Meir 1982; van Langevelde *et al.* 2003) to predict grass-tree coexistence in the range of ecological situations, in which grass-tree coexistence is empirically observed and the weak empirical support of the rooting niche assumption (Scholes and Archer 1997; Higgins *et al.* 2000; Sankaran *et al.* 2004) have been interpreted as evidence that savannas are fundamentally determined by a variety of stochastic mechanisms (Jeltsch *et al.* 1996, 1998; Higgins *et al.* 2000; Gardner 2006; D'Odorico *et al.* 2006). While savannas are undoubtedly influenced by many sources of stochasticity, we show that deterministic processes can explain grass-tree coexistence in savannas under a broad range of ecological conditions. Hence, the model presented here is the first deterministic model of grass-tree coexistence that does not rely on stochastic mechanisms and/or on the restrictive assumption of rooting niche separation.

2.6 Appendix: Isoclines of the grass shoot-woody shoot system

This appendix provides the isoclines of Equations (2.10) to (2.13) in the grass shoot-woody shoot system (GS-WS system). We assume that grass roots and woody roots are in equilibrium and solve the fixed-point equations for grass shoots and woody shoots. The grass shoot isocline is given as

$$\begin{aligned}\mathcal{I}_{GS}(WS) = & \\ & \frac{-g_G^2\alpha_{WG}d_W WS + g_G^2\alpha_{WG}d_W WS\omega_{WG}WS^\theta - d_G^2 g_W + d_G^2 g_W WS}{g_G(-g_G g_W + g_G g_W WS + g_G\alpha_{WG}d_W WS + d_G g_W WS - d_G g_W)} \\ + & \frac{-g_G^2 g_W - g_G^2 g_W\omega_{WG}WS^\theta - g_G^2 g_W WS + g_G^2 g_W WS\omega_{WG}WS^\theta}{g_G(-g_G g_W + g_G g_W WS + g_G\alpha_{WG}d_W WS + d_G g_W WS - d_G g_W)},\end{aligned}$$

the (inverse of the) woody shoot isoclines is given as

$$\begin{aligned}\mathcal{I}_{WS}^{-1}(WS) = & \\ & \frac{g_G(-d_W^2 + d_W g_W WS\omega_{WG}WS^\theta + d_W^2\omega_{WG}WS^\theta)}{-g_W^2 g_G + g_W^2 g_G WS - g_W^2\alpha_{GW}d_G + g_W^2\alpha_{GW}d_G WS + d_W g_G g_W WS + d_W^2 g_G} \\ + & \frac{g_G(g_W^2 - g_W^2 WS - g_W^2\omega_{WG}WS^\theta + g_W^2 WS\omega_{WG}WS^\theta - d_W g_W WS)}{-g_W^2 g_G + g_W^2 g_G WS - g_W^2\alpha_{GW}d_G + g_W^2\alpha_{GW}d_G WS + d_W g_G g_W WS + d_W^2 g_G}.\end{aligned}$$

The isoclines are non-linear, however, the conditions for the different system states (stable savanna, unstable savanna, grass dominated and tree dominated) in the shoot system are analogous to the conditions identified for the root system (Figure 2.5). The grass isoclines that corresponds to the panels in Figure 2.5 are depicted in Figure 2.6.

We do not provide isoclines for the general system (2.1) to (2.4) here (see Figure 2.4), although they can be evaluated using a computer algebra system; the resulting analytic solutions of those isoclines would not aid our understanding of the model.

2.7 Appendix: Fixed points

This appendix provides to the fixed-points of the system (2.10) to (2.13). These results were obtained using a computer algebra program. For simplicity, we assumed $g_{GS} = g_{GR} = g_G$, where g_{GS} and g_{GR} are constant growth rates of grass shoots and grass roots and g_S is a simplified notation (and analogously defined d_G, g_W and d_W where d_G and d_W are decomposition rates of grasses and trees, respectively). When light competition is absent ($\omega_{WG} = 0$), then the system possesses the fixed points

$$\begin{aligned} M_1 &= (0,0,0,0) \\ M_2 &= \left(1-\frac{d_G}{g_G}, 1-\frac{d_G}{g_G}, 0, 0\right) \\ M_3 &= \left(0, 0, 1-\frac{d_W}{g_W}, 1-\frac{d_W}{g_W}\right) \end{aligned}$$

and a fixed-point M_4 where grasses and trees coexist. The components of M_4 are

$$GS_4 = \frac{g_W^2 d_G^2 + d_W d_G^2 g_W - d_W g_G^2 g_W - g_W^2 g_G^2 + g_G^2 \alpha_{WG} g_W^2 - g_G^2 \alpha_{WG} d_W^2}{g_G(-g_W^2 d_G + g_W^2 d_G \alpha_{GW} \alpha_{WG} - d_W g_W d_G - d_W g_G g_W - g_W^2 g_G + g_G \alpha_{WG} g_W^2 - g_G \alpha_{WG} d_W^2)}$$

$$GR_4 = -\frac{g_W^2 d_G^2 + d_W d_G^2 g_W - d_W g_G^2 g_W - g_W^2 g_G^2 + g_G^2 \alpha_{WG} g_W^2 - g_G^2 \alpha_{WG} d_W^2}{g_G(g_W d_G + g_W g_G - g_W \alpha_{GW} g_G \alpha_{WG} + d_W g_G + d_W d_G) g_W}$$

$$WS_4 = \frac{g_W^2 g_G d_G + g_W^2 \alpha_{GW} d_G^2 + g_W^2 g_G^2 - d_W^2 g_G^2 - d_W^2 g_G d_G - g_W^2 \alpha_{GW} g_G^2}{g_W(d_G g_G g_W + g_W \alpha_{GW} d_G^2 + d_W g_G d_G + g_G^2 g_W - g_W \alpha_{GW} g_G^2 + g_G^2 dW - \alpha_{GW} g_G^2 \alpha_{WG} d_W)}$$

$$WR_4 = \frac{g_W^2 g_G d_G + g_W^2 \alpha_{GW} d_G^2 + g_W^2 g_G^2 - d_W^2 g_G^2 - d_W^2 g_G d_G - g_W^2 \alpha_{GW} g_G^2}{g_W(g_W d_G + g_W g_G - g_W \alpha_{GW} g_G \alpha_{WG} + d_W g_G + d_W d_G) g_G}.$$

Clearly, the components of the fixed-points M_2 and M_3 are equal to the maximum biomasses K_{GS}, K_{GR}, K_{WS} and K_{WR} (Table 2.1).

When light competition is present ($\omega_{WG} > 0$), then there might exist more than four fixed-points, however, we do not provide them here. The number of fixed points

depends on the exponent θ. When $\theta = 2$, then there exist five fixed-points: zero, a grass dominated state, a tree dominated state, a savanna state and a state with negative biomass, which can be neglected. When θ is greater than two, then complex solutions might occur, which are not relevant for our analysis. The same situation might appear, when θ is less than one. An eigenvalue analysis that analytically shows conditions for asymptotic stability of fixed-points is not provided; however, it is possible to conduct a numerical eigenvalue analysis for a fixed set of parameters to obtain the domains of attraction of the fixed-points.

3 The stability of African savannas: Insights from the indirect estimation of the parameters of a dynamic model

Abstract. Savannas are characterised by a competitive tension between grasses and trees and theoretical models illustrate how this competitive tension is influenced by resource availability, competition for these resources and disturbances. How this universe of theoretical possibilities translates into the real world is, however, poorly understood. In this paper we indirectly parametrise a theoretical model of savanna dynamics with the aim of gaining insights as to how the grass-tree balance changes across a broad biogeographical gradient. We use data on the abundance of trees in African savannas and Markov chain Monte Carlo methods to estimate the model parameters. The analysis shows that grasses and trees can coexist over a broad range of rainfall regimes. We further found that, irrespective of rainfall levels, savannas may be regulated by either asymptotically stable dynamics (in the absence of fire) or by stable limit cycles (in the presence of fire). Hence, the stability of savannas may not be influenced by rainfall levels. We conclude that even though fire might not be necessary for grass-tree coexistence it nonetheless is an important important modifier of grass-tree ratios.

Key words: savanna, indirect parameter estimation, coexistence, biogeographical patterns, resource gradient, disturbance gradient

3.1 Introduction

The relative abundance of grasses and trees strongly defines the structure and function of tropical savannas. Although the factors that influence this balance are well known, consensus on the details of how these factors shape savannas remains elusive (House *et al.* 2003; Sankaran *et al.* 2004). A recent contribution to this debate was provided by Sankaran *et al.* (2005) who investigated the factors that determine tree cover observed at 854 savanna sites in Africa. Sankaran and colleagues statistically examined these data and showed that (1) tree cover is not simply related to resource availability, and (2) that at sites that receive less than 650 mm MAP, tree cover is constrained linearly with moisture availability; while sites that receive more than 650 mm MAP canopy closure is possible, but disturbances such as fire can prevent canopy closure and are therefore necessary to prevent the exclusion of grasses. Sankaran *et al.* (2005) interpreted these data to mean that arid ($<$ 650 mm MAP) savannas are stable in the sense that fire is not necessary for grass-tree coexistence and that mesic savannas ($>$ 650 mm MAP) are unstable in that fire is needed for grass-tree coexistence.

This interpretation of the empirical data was influenced by the state of existing theoretical models. Two kinds of theoretical models, resource and disturbance based models, have been influential in shaping thinking about savannas. Resource based models show that when the effects of grass-tree competition are strong (when the product of the per capita effect of competition and competitor density is high) that competitive exclusion is possible (Walker and Noy-Meir 1982; van Langevelde *et al.* 2003). Disturbance based models show that the disturbance regimes common to savanna regions can prevent competitive exclusion even when grass-tree competition is strong (Higgins *et al.* 2000; Gardner 2006). Sankaran *et al.* (2005) argued that the data on tree cover in Africa could be explained by assuming that when resource levels are low that grasses and trees can coexist because both are below critical densities. However, when resource levels are high, tree leaf area index can be high enough to exert a highly asymmetric light competitive effect on grasses. The consequence of this is that grasses are excluded at resource rich sites unless fire can prevent trees from reaching the critical densities beyond which competitive exclusion is inevitable. While this argument appears plausible, it is something that existing theoretical models of savannas (e.g. Higgins *et al.* 2000; van Langevelde *et al.* 2003) do not predict.

Sankaran *et al.* (2005)'s data analysis and discussion calls for a formal integration of resource and disturbance based theories of savannas. A recently developed model

of savanna dynamics integrates resource and disturbance based theories (Higgins *et al.* 2007b, Chapter 2) and thereby shows that coexistence between grasses and trees is possible under a broad range of conditions. Specifically, coexistence in the model does not rely on a rooting niche separation mechanism as assumed by e.g. Walker and Noy-Meir (1982), Anderies *et al.* (2002) and van Langevelde *et al.* (2003), nor does it rely on the demographic bottlenecks invoked by Higgins *et al.* (2000).

The aim of this paper is to use tree abundance data from Africa to indirectly parametrise this model and thereby to test whether the model is capable of describing empirical observations from African savannas. Secondly we use the parametrised model to explore Sankaran *et al.* (2005)'s suggestions that fire is essential for grass-tree coexistence at sites that receive more than 650 mm MAP and that arid and mesic savannas differ in their stability.

3.2 Model description

We use a simplified version of the model proposed by Higgins *et al.* (2007b) and analysed in Chapter 2. The model simulates, for both grasses and trees, two biomass compartments, roots and shoots. This allows us to simulate the fact that fire cannot consume roots, and allows a separation of belowground and aboveground competition (Figure 3.1). In the paragraphs that follow we describe growth functions for the grass and tree biomass components of the model.

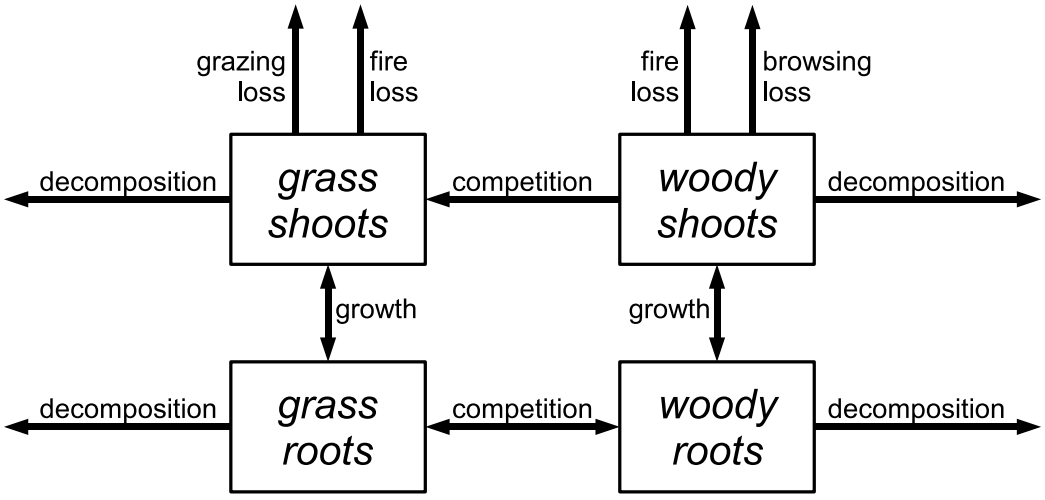

Figure 3.1: Conceptual illustration of the model's structure emphasising the separation of above and belowground biomass of grasses and trees.

The grass shoot biomass in the next time step (GS_{t+1}) is determined by a growth rate parameter (g_G) and grass root biomass (GR_t). Growth is negatively influenced by competition from grass shoot biomass and woody shoot biomass. The parameter ω_{WG} describes the intensity of the competitive effect of woody shoots on grass shoot growth. Grass shoot biomass can be reduced by decomposition at rate d_G, consumed by grazing at rate z and consumed by fire. We assume that fires are periodic, that the return interval of fires is defined by the integer parameter F and that when a fire occurs that all grass shoot biomass is consumed. The proportion of grass shoot biomass consumed by fire is then,

$$c_t = \begin{cases} 1 & \text{for } t \mod F = 0 \\ 0 & \text{for } t \mod F \neq 0. \end{cases} \tag{3.1}$$

The equation for shoot biomass growth at time $t+1$ is then,

$$GS_{t+1} = GS_t + g_G GR_t(1 - GS_t - \omega_{WG} WS_t) - c_t GS_t - d_G GS_t - zGS_t. \tag{3.2}$$

The grass root biomass in the next time step, GR_{t+1}, is influenced by a growth rate parameter (g_G), grass shoot biomass, and negatively by grass root biomass and tree root biomass (WR_t). The effect of tree biomass is included to simulate competition between grasses and trees for soil water (Walter 1971). The intensity of tree on grass root competition is described by the parameter α_{WG}. Grass root biomass decomposes at a constant rate (d_G). These assumptions yield the root growth equation,

$$GR_{t+1} = GR_t + g_G GS_t(1 - GR_t - \alpha_{WG} WR_t) - d_G GR_t. \tag{3.3}$$

The tree shoot biomass in the next time step, WS_{t+1}, is determined by a growth rate parameter g_W, tree root biomass (WR_t) and is negatively influenced by the density of tree shoot biomass. Tree shoots decompose at rate d_W and can be consumed by fire. For simplicity we assume that all tree shoot biomass is consumed by fire. The woody shoot growth equation is thus,

$$WS_{t+1} = WS_t + g_W WR_t(1 - WS_t) - c_t WS_t - d_W WS_t. \tag{3.4}$$

The tree root biomass in the next time step, WR_{t+1}, is determined by a growth rate parameter g_W, tree shoot biomass, and is negatively influenced by tree root biomass, as well as by grass root biomass. The intensity of grass on tree root competition is

described by the parameter α_{GW}. Tree root biomass decomposes at a constant rate (d_W). These assumptions yield the root growth equation,

$$WR_{t+1} = WR_t + g_W WS_t(1 - WR_t - \alpha_{GW} GR_t) - d_W WR_t. \tag{3.5}$$

We assume that rainfall influences plant growth rates. We define $\hat{g}$, the rainfall dependent versions of the growth parameters used in Equations (3.2)-(3.5), as sigmoidal functions of a site's mean annual precipitation (R),

$$\hat{g} = \frac{1}{1 + (\tilde{g}/R)} \tag{3.6}$$

where $\tilde{g}$ is a coefficient that describes a sigmoidal relationship between rainfall and growth. It is assumed that $\tilde{g}$ differs for grasses and trees.

Analyses of the model show that stable coexistence, unstable coexistence or competitive exclusion of either grasses or trees are possible outcomes of this model system (Chapter 2, Appendix 3.6). Which outcome is realised is determined by the competition and fire parameters. A unique feature of the model is that it is not reliant on a rooting niche mechanism for grass-tree coexistence and that the inclusion of fire allows coexistence even when both belowground (α_{WG} and α_{GW}) and aboveground (ω) competition are intense.

3.3 Model fitting

Each model parameter summarises the outcome of several aggregated ecological processes. The parameters describing such aggregated processes are difficult or even impossible to directly estimate from field measurements. This is a general problem, encountered by many types of ecological models. One solution to this problem is indirect parameter estimation (Freckleton and Watkinson 2000; Wiegand *et al.* 2003; Nelson *et al.* 2004). Here, a process-based model is used to find the combination of model parameters that best match some or several observed patterns from the system. A lack of fit between model and data would suggest that the system is not well described by the model. A good fit between the model and data suggests that the model can describe the system. However, a good fit is only useful if the solution is unique: many indirect estimation procedures are plagued by the problem that more than one parameter combination might fit the data equally well. This problem of "non-uniqueness" in the

parameter estimates can be addressed by using ecological understanding to constrain the values that the parameters can assume (Nelson *et al.* 2004). In the paragraphs below we describe the data used for the indirect fitting, the mechanics of the fitting processes and how we constrain the problem to ensure that the solutions are unique.

We use data from 197 sites scattered across Africa. This data-set is a subset of the data-set used by Sankaran *et al.* (2005) where aboveground tree biomass estimates can, on the basis of basal area measurements, be made. We restrict ourselves to these data because they provide a better description of abundance than does canopy-cover. The data covers a rainfall gradient from 200 to 1200 mm MAP.

The model is forced with R_i the mean annual precipitation of each site i. For the entire data set we estimate values of the growth ($\tilde{g}_G$, $\tilde{g}_W$), decomposition (d_G, d_W) and the competition (ω_{WG}, α_{WG}, α_{GW}) parameters. In addition, for each site i we wish to estimate F_i the site specific fire return interval.

We use a Bayesian approach to estimate the parameters and to assess parameter uncertainty. Specifically we use a Markov chain Monte Carlo (MCMC) algorithm to estimate the parameters. Using MCMC has the advantage that it allows uncertainty (in Bayesian terminology the credible intervals) of the parameter estimates to be assessed. Alternatives for estimating parameter uncertainty such as gradient methods or non-parametric bootstrap are precluded due to the dimension and non-linearity of the problem which ensure that the likelihood profile is not a smooth function of the parameters. A second advantage of the Bayesian approach is that it allows one to combine prior knowledge of where the parameters are thought to lie (the prior densities, $\text{pr}(\phi)$) and the information contained in the data (the likelihood $\text{pr}(\text{data}|\phi)$), to estimate posterior densities of the parameters ($\text{pr}(\phi|\text{data})$). We used informed Gaussian priors for all parameters (Table 3.1 lists the mean and standard deviations of the Gaussian priors). The priors for the competition parameters (ω_{WG}, α_{WG}, α_{GW}) describe our expectation that the competition parameters are approximately 1, whereas priors for the growth and decomposition parameters are based on numerical considerations (explained in the next paragraph). The likelihood of the data is estimated by assuming the errors in the tree abundance data are normally distributed.

To avoid the effects of transient dynamics and initial conditions on the solutions we randomly selected the initial abundances of GS, GR, WS and WR for each simulation, and defined the priors for the growth and decomposition so as to ensure that the systems dynamics are fast enough that a stable state is achieved after 2000 time steps. We assume that each time step represents two months, this allows several time steps

Table 3.1: Parameter ranges used to define the Gaussian prior distributions.

Parameter name	Symbol	mean	s.d.	Main text equation
Growth coefficient grass	$\tilde{g_G}$	1.0	0.25	3.6
Ratio grass to tree growth	$\beta_1 = \tilde{g}_G/\tilde{g}_W$	1.0	0.10	3.6
Decomposition rate grass	d_G	0.075	0.01	3.2,3.3
Ratio grass to tree decomposition	$\beta_2 = d_G/d_W$	1.0	0.10	3.4,3.5
Intensity light competition	ω_{WG}	1.0	0.25	3.2
Tree on grass root competition	α_{WG}	1.0	0.25	3.3
Grass on tree root competition	α_{GW}	1.0	0.25	3.5

per year without unduly increasing the computation cost of model runs. Note that the length of the time steps is, for this study, of minor importance because we compare the model's asymptotic state to the empirical abundance data. The length of the time steps is, however, useful for interpreting the fire return intervals and allows us to constrain fire frequency to be the integer part of $t/6$ (i.e. to be {annual, biennial, triennial,...}). The model predicts relative abundance in the interval 0-1. For comparison to data and to facilitate the interpretation of model output we transform these values using separate linear scaling factor for trees and grasses (1 unit of tree abundance = 120 t.Ha^{-1}; 1 unit of grass abundance = 12 t.Ha^{-1}). These scaling factors are consistent with aboveground biomass data presented in Higgins *et al.* (1999, 2000, 2007a) and Grace *et al.* (2006).

The model was implemented in C. We use our own R (R Development Core Team 2005) implementation of the Delayed Rejection Adaptive Metropolis algorithm (DRAM, Haario *et al.* 2006) for running the MCMCs. To improve convergence of the chains we express all parameters on a log scale and we define $\tilde{g}_W = \beta_1 \tilde{g}_G$ and estimate β_1 and $\tilde{g}_G$. Similarly we define $d_W = \beta_2 d_G$ and estimate β_2 and d_G.

There is no accepted diagnostic that can prove that a chain has converged to the posterior distribution (Geyer 1992). We tested convergence by confirming that replicate chains initiated with different starting values all converged to the same region in parameter space and by confirming that the correlation structure in the estimated parameters was weak (analyses not shown). For the estimation of the posterior distributions of the parameters we ran one long (1.5e5) chain. Figure 3.2 illustrates that this chain is well mixed.

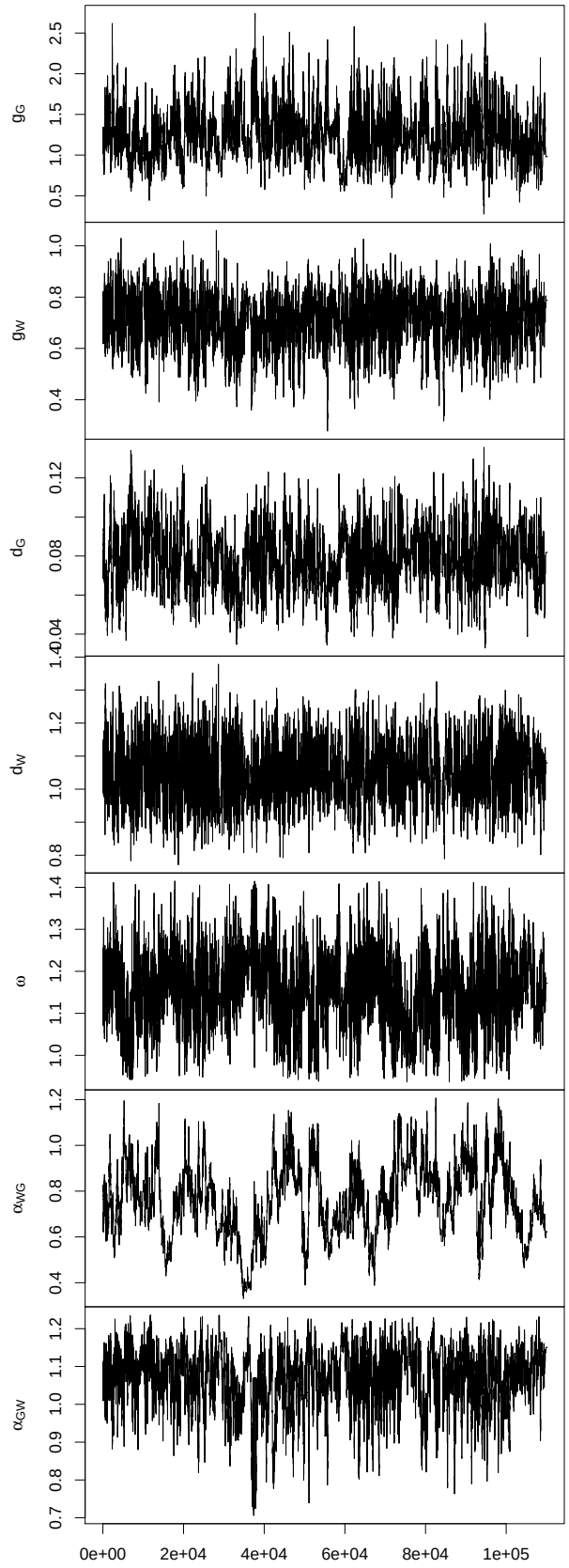

Figure 3.2: The Markov chain used for estimating the posterior distributions. The burn-in phase is not shown.

3.4 Results and Discussion

3.4.1 Parameter estimates

The model is flexible enough to almost perfectly replicate the empirically estimated biomass at the majority of the sampled sites (solid points in Figure 3.3). Several sites (open symbols in Figure 3.3) have higher estimated biomass than the model parametrisation is capable of predicting. These data points could be outliers or could be explained by high grazing levels (see Figure 3.7 and the discussion of grazing effects below). When fire is excluded, the model predicts a rainfall-defined upper limit of tree biomass (dotted line in Figure 3.3).

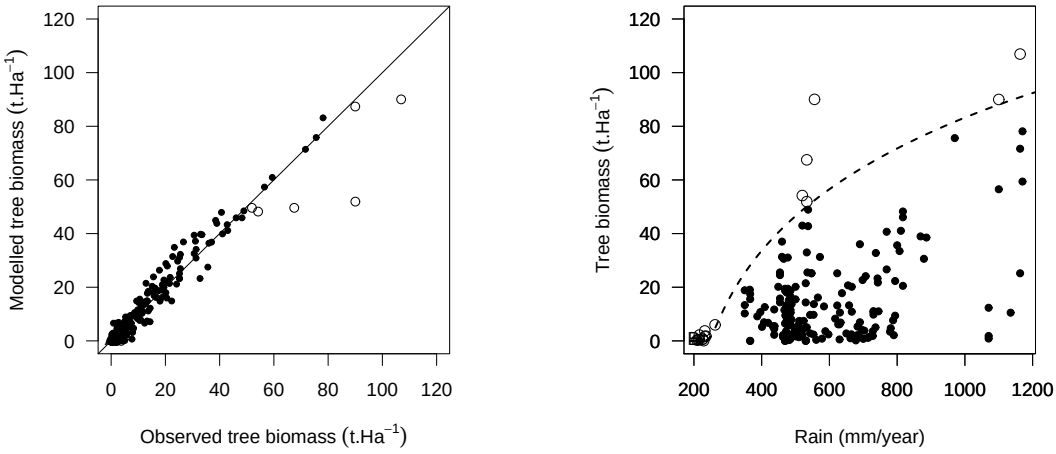

Figure 3.3: Modelled versus observed aboveground tree biomass for 197 sites scattered across Africa (left panel). The empirical data is plotted against rainfall in the right panel. The dotted line is the model's predicted tree biomass in the absence of fire across the rainfall gradient. Open circles in both panels indicate data points where the model parametrisation, in the absence of fire, under-predicts the empirically estimated tree biomass.

The posterior distributions of the parameter estimates are shown in Figure 3.4. These distributions show that all parameters are well defined. Particularly well defined are the light competition parameter (ω) and the grass on tree root competition parameter (α_{GW}), whereas the tree on grass root competition (α_{WG}) has relatively wide credible intervals.

The parameter estimates suggest that grass growth rates (Figure 3.5A) are higher than tree rates. The growth rate parameters ($\tilde{g}_G$ and $g_{\tilde{W}}$, Equation 3.6) for grasses

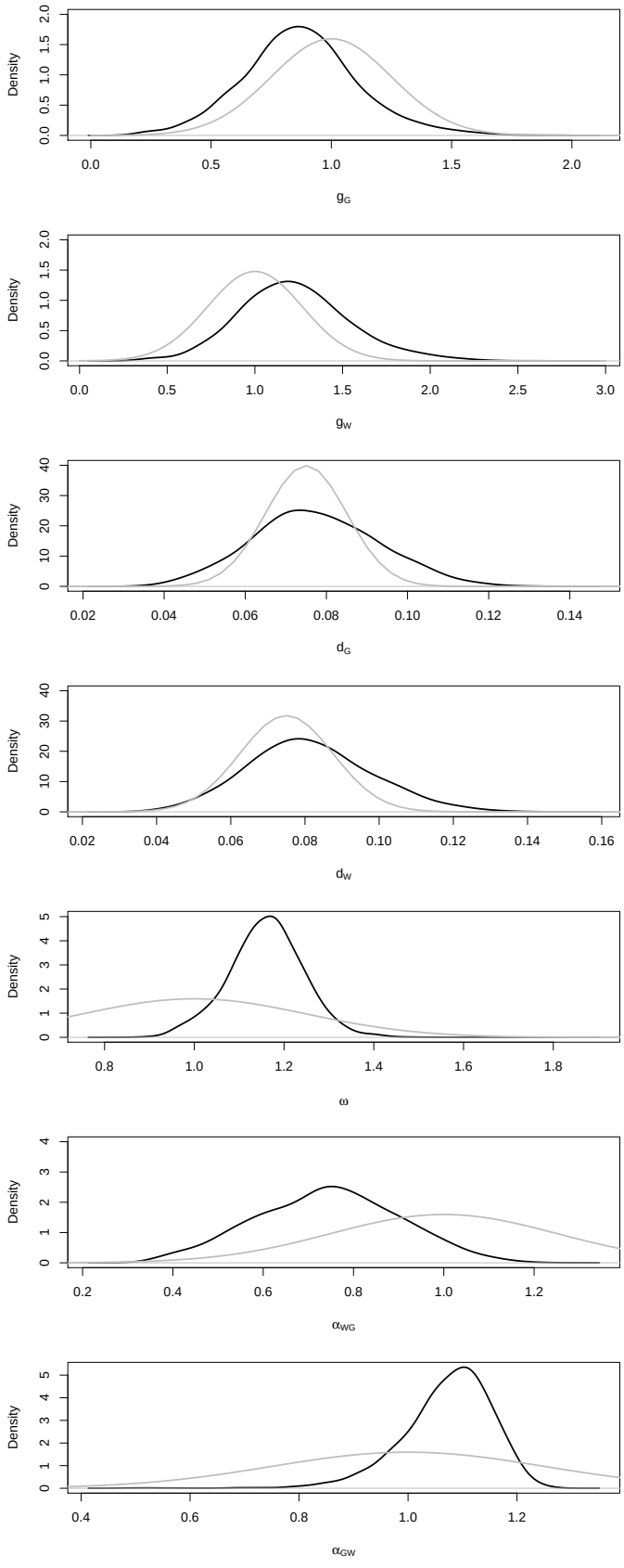

Figure 3.4: Prior (gray) and posterior (black) distributions of the parameter estimates.

and trees were respectively 0.87 (CI = [0.49, 1.29]) and 1.23 (CI = [0.74, 1.80]). The decomposition rates of grasses and trees were similar (d_G= 0.077, CI = [0.055, 0.10]; d_W= 0.081, CI = [0.055, 0.011]). The parameter estimates suggest that grass growth is more responsive to rainfall. This is qualitatively consistent with empirical knowledge from savannas (Scholes and Walker 1993) and other ecosystems (Shipley 2006) and can be understood as being a consequence of architectural differences between trees and grasses.

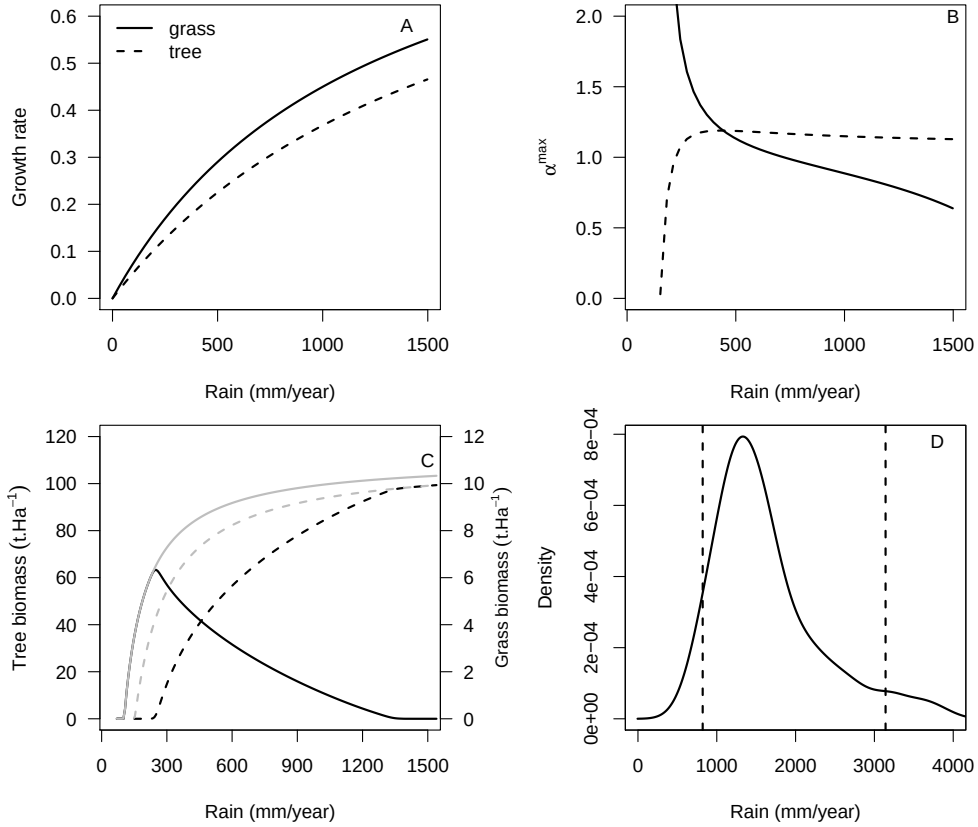

Figure 3.5: The growth rate function (Equation 3.6) selected by the MCMC procedure for grasses and trees (A). The maximum root competition coefficient that grasses and trees can tolerate as a function of rainfall (panel B). The calculation of the maximum root competition levels are described in Chapter 2 and Appendix 3.6. Panel C shows the predicted tree and grass abundance as a function of rainfall in the absence of fire. Black lines depict the predicted biomass in the presence of competitors, gray lines in the absence of competitors. The uncertainty in the estimate of the maximum rainfall level at which grass-tree coexistence is possible in the absence of fire (D) is estimated by using the MCMC to propagate error in the estimate of the maximum rainfall for which $\alpha_{WG}^{max} < \alpha_{WG}$. The vertical lines indicate the credible intervals in this rainfall threshold.

Root competition was found to be asymmetrical, with grass root biomass having a stronger effect on tree root biomass growth ($\alpha_{GW} = 1.07$, CI = [0.92, 1.19]) than tree root biomass has on grass root biomass growth ($\alpha_{WG} = 0.74$, CI = [0.48, 1.00]). This is consistent with the empirical studies which have shown that grasses are more effective competitors for soil water than trees, although other empirical studies suggest that $\alpha_{WG} \approx \alpha_{GW} \approx 1$ (see Scholes and Archer 1997, for a review). Light competition was predicted to be intense ($\omega = 1.16$, CI = [1.02, 1.29]).

The maximum level of competition that a competitor can tolerate varies across the rainfall gradient (Figure 3.5B; the definition of the maximum competition levels is described in Appendix 3.6). Trees cannot persist in the presence of grasses at rainfall levels much below 200 mm MAP; however, above this rainfall threshold the level of competition trees can tolerate is not influenced by rainfall (Figure 3.5B). Grasses, by contrast, can tolerate high levels of tree competition at rainfall levels below 200 mm MAP, but the level of competition they can tolerate decreases gradually as rainfall increases. Above a threshold of 1200 mm MAP the parameter estimates suggest that grasses can, in the absence of fire, no longer persist (Figure 3.5C). Our confidence in the position of this threshold is, however, low. We assess the confidence by using the MCMC to propagate the error in the maximum rainfall level for which $\alpha_{WG}^{max} < \alpha_{WG}$. The credible intervals of this rainfall threshold are 821 and 3142 mm (Figure 3.5D). Hence we are uncertain where this threshold level lies, but certain that the threshold lies above 821 mm MAP.

3.4.2 The nature of grass-tree interactions

Chapter 2 defines the zero-growth isoclines for the model for the case without fire (the equations defining these isoclines are described in Appendix 3.6). Plotting these isoclines using the Bayesian parameter estimates shows that, in the absence of fire the dynamics are characterised by a stable equilibrium point at what we have termed arid and semi-arid sites (Figure 3.6). At what we term mesic sites (1400 mm MAP; see Figure 3.5D for a description of the uncertainty in this MAP threshold) the model predicts that, in the absence of fire, trees exclude grasses (Figure 3.6). When fire is introduced the solution is, in all cases, a stable oscillator (Figure 3.6). Fire prevents the tree abundance from reaching its rainfall-defined equilibrium point (open points in Figure 3.6), instead the system trajectory oscillates around a stable point of lower tree abundance and higher grass abundance. In the case of the mesic site in Figure 3.6, fire allows grasses to persist

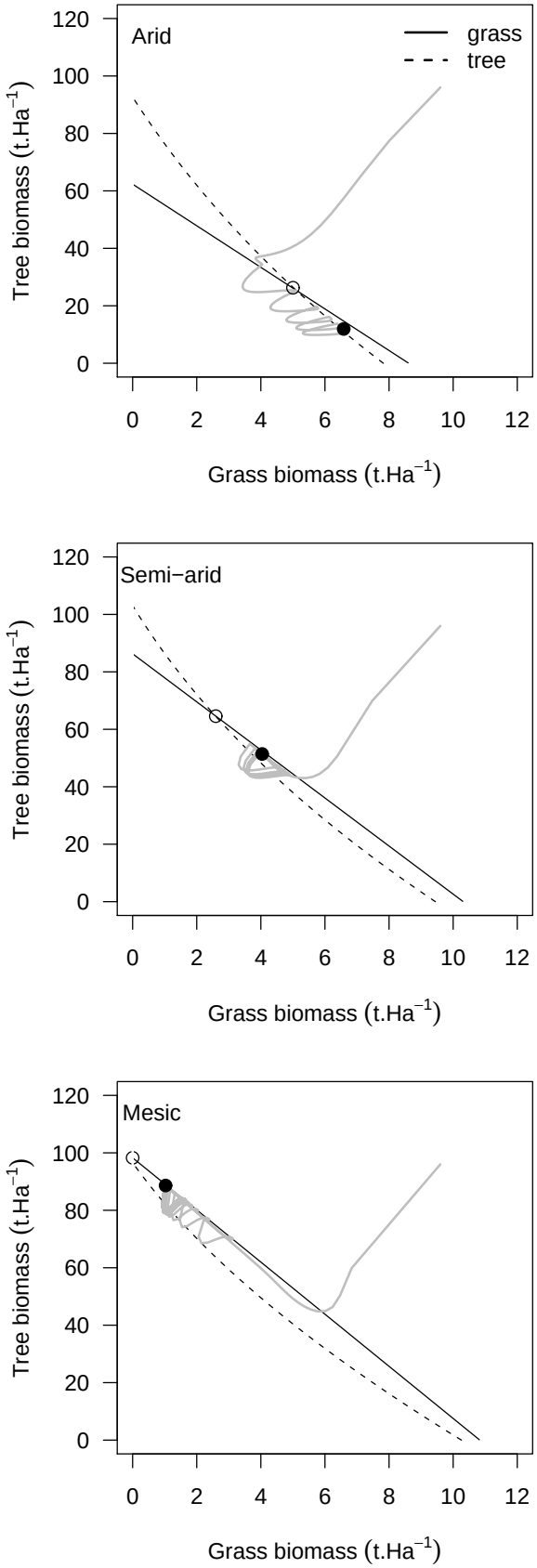

Figure 3.6: Phase planes of the model's dynamics in arid (350 mm MAP), semi-arid (700 mm MAP) and mesic (1400 mm MAP) sites in the presence and absence of fire. The isoclines are for the case without fire and the trajectory (gray line) is for the case with fire. The open symbol is the stable point for the system without fire and the closed symbol is a point within the stable limit cycle that occurs in the presence of fire. Note that at the mesic site the isoclines do not intersect and the stable point (in the absence of fire) is at zero grass biomass.

in the system by reducing trees to abundances below which they can exert a critical competitive effect on grasses. Hence in mesic systems fire does not, as is the case in arid and semi-arid systems, merely modify the position of the equilibrium point, but it qualitatively changes the outcome from competitive exclusion to coexistence and this coexistence is characterised by a stable-limit cycle.

This result shows that at more mesic sites that the role of fire shifts from being a modifier of the structure of savannas to being a factor that allows the savanna state to exist. Sankaran *et al.* (2005) interpret tree cover data from Africa to suggest that fire is needed for grass-tree coexistence at sites receiving more than 650 mm MAP. Our model and parameter estimates suggests that fire is only needed for grass-tree coexistence at sites receiving more than 1200 mm MAP. Although, as discussed in the previous section, our confidence in the position of this threshold is low, the credible intervals suggest that it lies above 821 mm MAP.

The maximum mean annual precipitation at the sites investigated was 1200 mm MAP. Within this domain all our solutions were, irrespective of rainfall, characterised by the same qualitative dynamics. That is, the model parametrisation predicts that fire does not play a fundamentally different role in African savannas receiving between 200 and 1200 mm MAP. This is well illustrated by plotting the relative deviation of observed biomass data from the tree abundance predicted in the absence of fire (Figure 3.7A). This plot suggests that the relative effect of fire in drawing tree abundance away from the rainfall defined tree abundance does not change across the rainfall gradient. The caveats are that as rainfall increases more frequent fires are required to draw tree abundance away from the rainfall defined tree abundance (Figure 3.7B) and that fire is necessary for grass persistence above some threshold in precipitation (Figures 3.5C and 3.5D). Our analysis is therefore consistent with the view that fire is not necessary for grass-tree coexistence over a broad range of conditions. This does, however, not mean that fire is not important. Fire can draw savanna tree biomass away from the climate potential (Figure 3.7B). Taken together our findings support the view promoted by Frost *et al.* (1986) that rainfall and nutrients are the primary drivers of savannas, but that fire and herbivory are secondary drivers.

To explore the role of herbivory we ran simulations which include grazing ($z > 0$; Equation 3.2). These simulations show that grazing favours trees and generates a "bush-encroached" savanna (Figure 3.7C). This observation suggests a functional definition of bush encroachment in savannas: Savannas are bush encroached if the observed tree biomass is higher than the tree biomass that is defined by resource levels. Under this

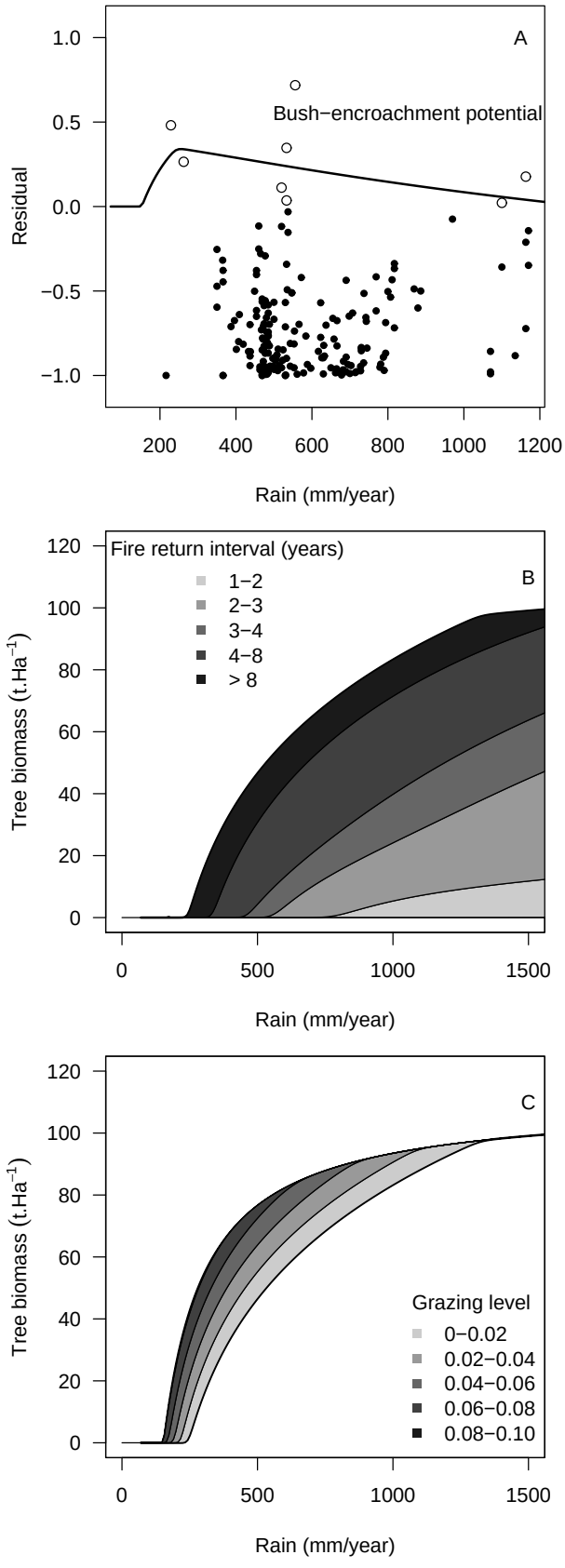

Figure 3.7: The relative deviation between the model's rainfall determined tree abundance and empirically estimated tree abundance as a function of rainfall (panel A). Open circles indicate data points where the model parametrisation, in the absence of fire, under-predicts the empirically estimated tree abundance. Panel B illustrates the effect of different fire return intervals on tree abundance along a rainfall gradient and Panel C illustrates the effect of different levels of grazing (parameter z, Equation 3.2) on tree abundance, in the absence of fire. The bush encroachment potential line in Panel A is the deviation between the rainfall defined tree abundance the the tree abundance predicted under high grazing levels.

definition, savannas which are tree dominated due to fire suppression would not be erroneously described as being bush-encroached. Using this definition, we describe the potential for grazing induced bush-encroachment as the deviation between the rainfall defined tree abundance and the tree abundance predicted under high grazing levels. This bush encroachment potential line (plotted in Figure 3.7A) shows that the potential for bush-encroachment is highest at intermediate rainfall sites. Consistent with this prediction is the observation that the sites with positive deviations from the rainfall-defined tree abundance (open circles in Figures 3.3 and 3.7A) are at intermediate rainfall levels.

3.5 Conclusions

This study used a heuristic model of savanna dynamics to explain the biogeographic patterns of tree abundance observed in African savannas. The fitted model shows that grass-tree coexistence, and hence the savanna vegetation state, is possible across the entire (200-1200 mm MAP) rainfall gradient investigated. This is true even in the absence of fire. At sites receiving higher levels of rainfall, fire is needed for grass-tree coexistence. The model additionally shows that fire can reduce tree biomass across the entire gradient and while the absolute effect of fire is greater at mesic sites, the relative effect of fire does not change across the gradient. Finally, the solutions generated by the model are stable points for solutions without fire and stable oscillators for solutions with fire. That is, whether the solution is a stable oscillator or stable point is influenced solely by the presence or absence of fire. Hence our results imply that there is no fundamental difference in the stability of arid and mesic savannas.

Several data points in the empirical data had higher tree abundance than the model could predict. We can explain these points by showing that grazing can lead to tree abundances higher than the rainfall-defined tree abundance. This in turn suggests a new functional definition of grazing-induced bush-encroachment as tree biomass above the rainfall-defined tree biomass. Adopting this definition yields the prediction that the potential for bush-encroachment is highest at sites receiving intermediate levels of rainfall.

Our analysis is based on indirect parameter estimation. This means that our interpretation is influenced by a combination of the information in the empirical data, the information contained in the model structure and our prior estimates of parameters. Additional data interpreted with this model might yield different insights. We expect that

these additional analyses will contradict details of the quantitative predictions made by this analysis. The real test of the utility of this analysis is whether the following predictions are true (1) fire is not needed for grass-tree coexistence at sites receiving between 200 and 1200 mm (the precipitation range examined here) but can substantially modify the relative abundance of grasses and trees, (2) the relative importance of fire in savannas is not influenced by rainfall, and (3) fire determines whether the asymptotic dynamics of savannas are described by a fixed point or by a stable oscillator.

3.6 Appendix: Isoclines and fixed-points

This appendix describes the zero growth isoclines for the model system (Figure 3.6) as well as the maximum levels of root competition grasses and trees can tolerate (Figure 3.5). A more detailed derivation of these results can be found in Chapter 2. The notation follows the notation used in the main text's model description.

The isocline analysis can be used to explore how the nature and intensity of interspecific competitive interactions determine whether coexistence is possible or not. In Chapter 2 we conducted an isocline analysis of the model system in the two-dimensional phase space, defined by the root biomasses GR and WR and by the shoot biomasses GS and WS. Here we describe only the results for the root phase plane. For the analysis of the root biomasses, we assume that fire and herbivory are absent and that grass shoots and woody shoots are in equilibrium. The grass and tree root isoclines are given as

$$\mathcal{I}_{GR}(WR) = \frac{g_G P_\omega(WR)}{g_G P_\omega(WR) + d_G}\left(1 - \frac{d_G^2}{g_G^2 P_\omega(WR)} - \alpha_{WG} WR\right), \tag{3.7}$$

$$\mathcal{I}_{WR}(GR) = \frac{g_W}{g_W + d_W}\left(1 - \frac{d_W^2}{g_W^2} - \alpha_{GW} GR\right), \tag{3.8}$$

where

$$P_\omega(WR) = 1 - \omega_{WG}\left(\frac{g_W WR}{g_W WR + d_W}\right)^\theta. \tag{3.9}$$

The function $P_\omega(WR)$ acts as a scaling factor that reduces the effective growth rate between 0 and g_G. The tree isocline $\mathcal{I}_{WR}(GR)$ is a linear function of GR while the grass isocline $\mathcal{I}_{GR}(WR)$ is only linear in absence of light competition (when $\omega_{WG} = 0$); in presence of light competition it is a non-linear function. The maximum equilibrial root biomass values that GR and WR can take are

$$K_{GR} = \mathcal{I}_{GR}(0) = 1 - \frac{d_G}{g_G} \quad \text{and} \tag{3.10}$$

$$K_{WR} = \mathcal{I}_{WR}(0) = 1 - \frac{d_W}{g_W}. \tag{3.11}$$

The maximum biomass K_{GR} is defined as the intersection point of the grass isocline and the GR-axis and K_{WR} is defined at the intersection point of the tree isocline and the WR-axis. The intersection point of the grass isocline and the WR-axis and the

intersection point of the tree isocline and the GR-axis are given as

$$H_{GR} = \mathcal{I}_{GR}^{-1}(0) = \frac{1}{\alpha_{WG}} \left(1 - \frac{d_G^2}{g_G^2}\right) \quad \text{and} \tag{3.12}$$

$$H_{WR} = \mathcal{I}_{WR}^{-1}(0) = \frac{1}{\alpha_{GW}} \left(1 - \frac{d_W^2}{g_W^2}\right). \tag{3.13}$$

Here, it is assumed that light competition is absent. In presence of light competition, H_{GR} would be a non-linear expression.

Using the intersection points K_{GR}, K_{WR}, H_{GR} and H_{WR} we can identify four different system states. When $H_{GR} > K_{WR}$ and $H_{WR} > K_{GR}$, there exists an asymptotically stable intersection point between the isoclines and the intercepts K_{WR} and K_{GR} are unstable. Hence, grasses and trees coexist in a stable equilibrium (savanna state). In this situation, competition between grasses and trees is balanced, which means that grass competition α_{GW} remains below some maximum value α_{GW}^{max} that can be sustained by trees and tree root competition α_{WG} remains below some value $\alpha_{WG}^{max}(\omega)$ that can be sustained by grasses. The maximum tree root competition is also a function of light competition, exerted by trees on grasses. The maximum root competition parameters are defined as

$$\alpha_{WG}^{max}(\omega) = \frac{1}{K_{WR}} \left(1 - \frac{d_G^2}{g_G^2 P_\omega(K_{WR})}\right) \quad \text{and} \tag{3.14}$$

$$\alpha_{GW}^{max} = \frac{1}{K_{GR}} \left(1 - \frac{d_W^2}{g_W^2}\right). \tag{3.15}$$

In absence of light competition, the maximum woody root competition parameter is given as

$$\alpha_{WG}^{max} = \frac{1}{K_{WR}} \left(1 - \frac{d_G^2}{g_G^2}\right). \tag{3.16}$$

When $H_{GR} \leq K_{WR}$ and $H_{WR} \leq K_{GR}$, then the intersection point between the isoclines is an unstable node, and the maximum biomasses K_{GR} and K_{WR} are asymptotically stable. Hence, trajectories tend towards a grassland or woodland, depending on the initial conditions. Such a situation occurs, when both root competition parameters α_{GW} and α_{WG} exceed the maximum values α_{GW}^{max} and $\alpha_{WG}^{max}(\omega)$.

When $H_{GR} > K_{WR}$ and $H_{WR} \leq K_{GR}$, then there is no intersection point between the isoclines and the grass isocline lies above the tree isocline. The maximum biomass

K_{GR} is asymptotically stable, whereas K_{WR} is unstable, hence the system tends to a grass dominated state. Analogously, when $H_{GR} \leq K_{WR}$ and $H_{WR} > K_{GR}$, then there is no intersection point between the isoclines and the tree isocline lies above the grass isocline. The maximum biomass K_{WR} is asymptotically stable and K_{GR} is unstable; the system converges towards a tree dominated state. The tree or grass dominated states occur when one root competition parameter exceeds the corresponding maximum value α_{GW}^{max} or $\alpha_{WG}^{max}(\omega)$ and the other root competition parameter lies below this maximum.

Table 3.2: Characteristics of the root phase plane isoclines and the maximum competition parameters.

Variable name	Grass Roots	Tree Roots
	Without light competition	
Maximum biomass	$K_{GR} = 1 - \frac{d_G}{g_G}$	$K_{WR} = 1 - \frac{d_W}{g_W}$
Isocline intercepts	$H_{GR} = \frac{1}{\alpha_{WG}} \left(1 - \frac{d_G^2}{g_G^2}\right)$	$H_{WR} = \frac{1}{\alpha_{GW}} \left(1 - \frac{d_W^2}{g_W^2}\right)$
Isocline slope	$S_{GR} = -\alpha_{WG} \frac{g_G}{g_G + d_G}$	$S_{WR} = -\alpha_{GW} \frac{g_W}{g_W + d_W}$
Max. root competition	$\alpha_{WG}^{max} = \frac{1}{K_{WR}} \left(1 - \frac{d_G^2}{g_G^2}\right)$	$\alpha_{GW}^{max} = \frac{1}{K_{GR}} \left(1 - \frac{d_W^2}{g_W^2}\right)$
	With light competition	
Max. root competition	$\alpha_{WG}^{max}(\omega) = \frac{1}{K_{WR}} \left(1 - \frac{d_G^2}{g_G^2 P_\omega(K_{WR})}\right)$	$\alpha_{GW}^{max} = \frac{1}{K_{GR}} \left(1 - \frac{d_W^2}{g_W^2}\right)$

Part II

Dynamic vegetation modelling and the future vegetation of savannas

4 aDGVM: An adaptive dynamic global vegetation model for tropical ecosystems.

Abstract. This Chapter provides a description of the aDGVM, the adaptive dynamic global vegetation model which has been specifically devoloped for tropical grass-tree systems. First, we motivate the devellopment of the model, then we outline the basic model concepts included in the model and then we give a detailed explanation the different sub-models. We provide a sensitivity analysis of the model to quantify how different model parameters influence the simulation results and to explore the major uncertainties of the model. Finaly, we propose that vegetation models could be improved by allowing plants to modify their traits in response to climate and by implementing community assembly within an dynamic vegetation model.

Key words: DGVM, savanna, dynamic vegetation model, process-based model, fire, adaptive vegetation model, demographic model, sensitivity analysis, grass-tree interactions

4.1 Introduction

Tropical regions are dominated by grasslands, savannas and forests. The factors that determine whether savannas, forests or grasslands dominate a given location have long intrigued ecologists and biogeographers (Sarmiento 1984; Scholes and Archer 1997; Higgins *et al.* 2000; House *et al.* 2003; Sankaran *et al.* 2004). Recent studies have argued that progress can be made by integrating demographic or disturbance based theories of savanna dynamics with resource or competition based theories (Sankaran *et al.* 2005). For instance models have been developed (Chapter 2) that allow one to understand, in a theoretical sense, the conditions under which grasslands, forests or savannas exist. Although useful in a heuristic sense this model and other similar models are not explicitly based on bio-physical mechanisms, with the consequence that they cannot predict vegetation states as a function of climatic and edaphic conditions.

How climate influences vegetation, can in principle, be addressed by a class of models called dynamic global vegetation models (DGVMs, Figure 4.1). Several models of this class have been proposed and used (e.g. Lüdeke *et al.* 1994; Cramer *et al.* 2001; Moorcroft *et al.* 2001; Arora 2003; Bonan *et al.* 2003; Sitch *et al.* 2003; Hély *et al.* 2006; Hickler *et al.* 2006; Schaphoff *et al.* 2006; Sato *et al.* 2007) to simulate the response of vegetation to environmental conditions by simulating bio-physical, physiological and demographic mechanisms. However, these models have not been developed and tested in tropical regions (House *et al.* 2003, but see Moocroft *et al.* 2001 for an exception) and therefore poorly represent processes that are known to be important in these systems. Thus, transitional zones such as savannas have been identified as being subjected to high uncertainties (Hickler *et al.* 2006). For instance, existing DGVMs often describe fire by simply correlating litter to a fire frequency and by assuming that fire removes a constant fraction of standing biomass (Thonicke *et al.* 2001; Venevsky *et al.* 2002). One consequence of such fire models is that existing DGVMs underestimate the extent of savannas and often predict grasslands or forests in regions where savannas are observed (Cramer *et al.* 2001). Further, most existing DGVMs are not individual-based which means that those models cannot explicitly simulate the effect of fire on the horizontal structure of tree populations and the impact of climate change on a plant level.

In the following we present an individual-based vegetation model that is based on the bio-physical, physiological and demographic processes that are assumed to determine tropical vegetation. The model only needs general soil and climate data as input and thus, the model allows us to predict, using readily available environmental data, whether

the environmental conditions at a study site define a savanna, grassland, deciduous woodland or an evergreen forest.

This manuscript is structured as follows. First, we outline the basic model structure. Then we provide a detailed description of the input data and the different sub-models. Finally, we describe how the sub-models are linked together in our model implementation.

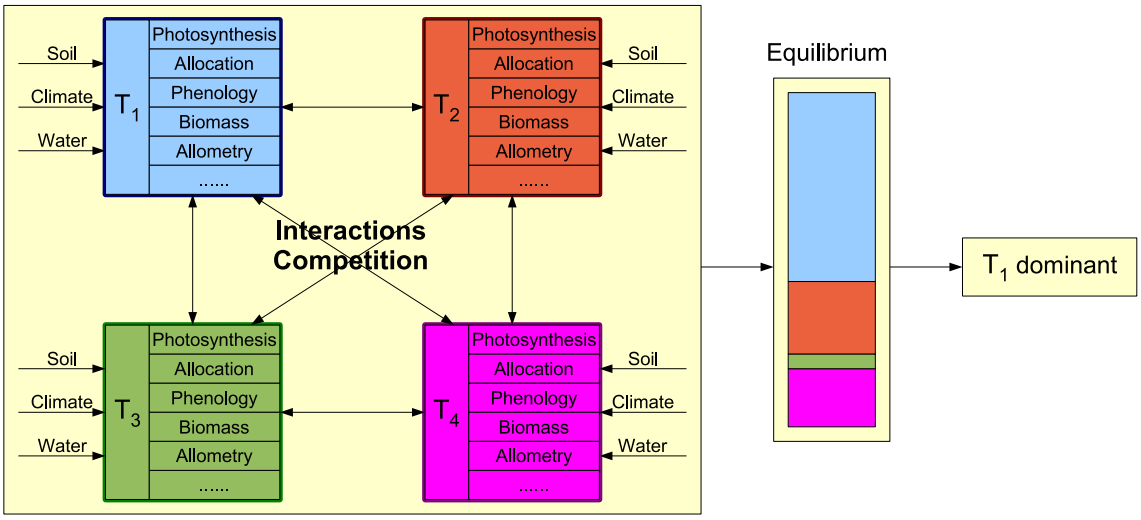

Figure 4.1: Basic structure of a DGVM. The models define different vegetation types which are characterized by different model parameters and by their response to environmental variables. Depending on inter- and intra-specific compatition and interactions, the model converges towards an equilibrium state, characterized by the relative abundance of different vegetation types. Potentially, one of them is dominant and suppresses the others.

4.2 Modelling concepts

The sections that follow provide detailed descriptions of the sub-models while this section outlines the basic features of the model's structure. The model simulates biophysical, physiological and demographic processes at the leaf, canopy, plant, population and ecosystem level (Figure 4.2). The model includes several sub-models that represent plant growth and inter- and intra-specific competition for light and moisture. The model also considers how demographic processes and disturbance may influence vegetation development. The model strives to represent these processes in a mechanistic way. However, we wish to emphasize the semantic point that few models are truly mechanistic. For

instance, the rates of many processes in the model are temperature dependent and we represent these temperature dependencies using statistically estimated functions.

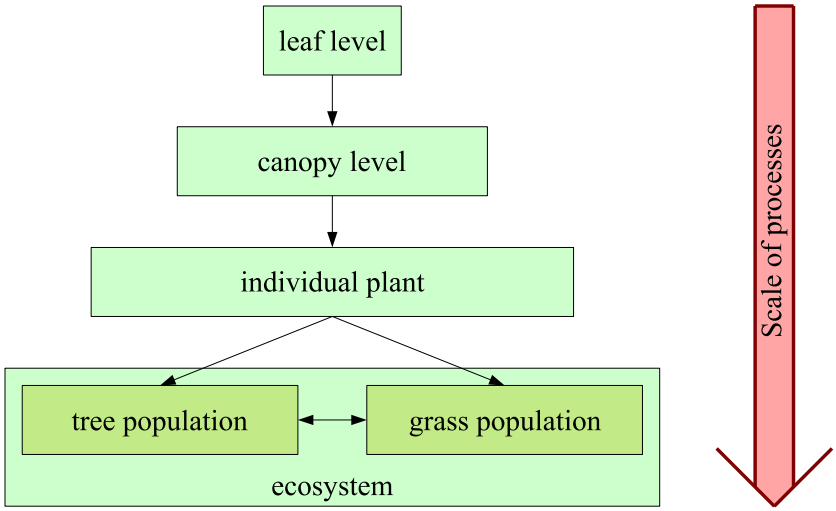

Figure 4.2: The different process levels of the model.

The model simulates two life forms, grasses and trees. Apart from the fact that we simulate grasses as using the C_4 photosynthetic pathway and trees as using the C_3 pathway, we assume that both are regulated by the same biophysical processes. The rates of the biophysical processes are determined by generally available soil and climate data (Global Soil Data Task Group 2000; New *et al.* 2002).

At the leaf level the model simulates photosynthetic and respiration rates by linking sub-models for photosynthesis and stomatal conductance. For photosynthesis, we follow Collatz *et al.* (1991, 1992)'s implementation of the Farquhar *et al.* (1980) photosynthesis model for C_3 and C_4 plants. We use the stomatal conductance sub-model proposed by Ball *et al.* (1987) and link it to photosynthesis using a diffusion gradient definition of photosynthesis.

The leaf level processes are scaled to the whole plant level. A plant is defined by its different biomass pools and by allometric equations that relate biomass in these pools to height, basal area, canopy area, leaf area index and rooting depth. Using light availability (which is influenced by the leaf area index) and water availability (determined by rooting depth and soil water content) we scale the leaf level photosynthetic rate to the canopy level photosynthetic rate (Schulze *et al.* 1994; Ronda *et al.* 2001; Arora 2002). Photosynthetic carbon gain is reduced by growth respiration, while all living biomass pools are affected by maintenance respiration (Arora 2003). Hence, canopy photosyn-

thesis and respiration together define the net carbon gain of the plant. Carbon gain is allocated to living biomass compartments of the plant, following the allocation concept of Tilman (1988) and Friedlingstein *et al.* (1999), which assumes that the carbon gain is preferentially allocated to the compartment that most limits growth. A plant has two phenological states, active and dormant. We use a simplified version of the phenology models proposed by Lüdeke *et al.* (1994) and Givnish (2002) to simulate the transitions between these two states. Transitions between dormant and active state occur when the potential carbon gain exceeds or falls below the costs of photosynthesis. Plant material is lost due the senescence of leaf and root material.

The next level is the population level. The population structure we consider includes a continuous layer of grass and a more or less discontinuous layer of trees. We do not simulate different species; we assume that the biomass is adequately described by a "typical" tree and by a "typical" grass species. We simulate a grass population consisting of two super-individuals representing grass below and between tree canopies. For the grass population we ignore population structure and demography and assume that grasses are adequately described by these two immortal super-individuals. In contrast, the tree population is individual-based and we keep track of attributes of each individual tree. For trees, we explicitly simulate reproduction and mortality of each individual. Reproduction is controlled by temperature, soil moisture and the carbon status, while mortality is controlled by the tree's carbon status. Intra-specific (grass-grass and tree-tree) interactions are influenced by light and water competition. Inter-specific (grass-tree) interactions are mediated by shading effects and competition for water in different soil layers (Walter 1971). Finally, fire shapes both the grass biomass and the tree population and hence inter-specific interactions. We use a semi-empirical fire model proposed by Higgins *et al.* (2008) that estimates the fire intensity as a function of available fuel biomass, moisture content and windspeed and that explicitly simulates the fire damage suffered by individual trees (Higgins *et al.* 2000).

The grass and tree populations are embedded in a sub-model that describes micro-climatic conditions and soil moisture availability. The soil moisture levels are determined by rainfall and evapotranspiration. We simulate stochastic sequences of daily rainfall using the mean and variance of observed rain, following New *et al.* (2002). Evapotranspiration is calculated following Jones (1992) and Allen *et al.* (1998). Radiation is computed using Allen *et al.* (1998)'s guidelines.

The model provides output data from each process levels. Specifically, the model calculates the biomasses of grasses and trees, treecover, number of trees and the size

structure of the tree population. The fire sub-model reports the frequency, intensity and timing of fire and data on the effect of fire on the vegetation.

4.3 Input data

For the model to be flexible enough to simulate vegetation at arbitrary locations, we use only generally available site specific soil and climate data as input data. Soil data were obtained from a global 5×5 minute data set of selected soil characteristics (Global Soil Data Task Group 2000). We used the soil nitrogen S_N, soil carbon S_C, wilting point θ_{wp} and field capacity θ_{fc} from this data set. Climate data were obtained from New *et al.* (2002)'s global 10×10 minute data set of mean monthly surface climate data. We used precipitation (given by the mean value r_m and the coefficient of variance r_{cv}), wet-day frequency w_f, days with frost d_f, mean temperature $\bar{T}$, diurnal temperature range T_Δ, relative humidity h_s, sunshine percentage p_s, wind speed u_{ref} and elevation Z from this data set (Table 4.1).

These input data are used to calculate secondary atmospheric characteristics of the study site, needed to calculate radiation, photosynthesis and evapotranspiration. We use Allen *et al.* (1998)'s guidelines to calculate atmospheric pressure P, minimum and maximum temperature T_{min} and T_{max}, day temperature T, average saturation vapor pressure e^A, saturation vapor pressure e^S, slope of the vapor pressure curve s, vapor pressure deficit h_{vpd}, psychrometric constant γ, density of air ρ_{air}, photosynthetic active radiation Q_p and the net radiation Q_0 (Table 4.1). The rainfall algorithm (New *et al.* 2002) generates a time series of daily rainfall F_i for each year from the parameters r_m and r_{cv} (section *"Total evapotranspiration and soil water balance"*).

Characteristics of the input data from the database and other variables characterizing the environment are summarized in Table 4.1. Should alternative soil or climate datasets for specific study sites be available, e.g. the IPCC (2007) SRES climate projections, they can be used as an alternative input data source.

4.4 Leaf photosynthesis

The following sections describe how we estimate the monthly leaf-level photosynthetic and respiration rates of the study site from temperature, relative humidity, atmospheric pressure, wind speed, soil nitrogen, soil carbon and photosynthetic active radiation. We link sub-models for photosynthesis and for stomatal conductance.

4.4.1 Photosynthesis sub-model

In principle we follow Collatz *et al.* (1991, 1992)'s implementation of the Farquhar *et al.* (1980) model of leaf photosynthesis to generate the (bio-physical) gross and net photosynthetic rates A_0^b and A_n^b (units μmol m^{-2}s^{-1}). An empirical function derived by Woodward *et al.* (1995) from data presented by Woodward and Smith (1994b, a) allows the estimation of the maximum light saturated rate of photosynthesis A_{max} from the soil carbon content S_C (g m^{-2}) and the soil nitrogen content S_N (g m^{-2}) as

$$A_{max} = \begin{cases} 50 \cdot 0.999927^{S_C} & \text{when} \quad S_N > 600 \\ 50 \cdot 0.999927^{S_C} \cdot 0.00166 \cdot S_N & \text{when} \quad S_N < 600. \end{cases} \tag{4.1}$$

Equation (4.1) is valid for soil carbon content $S_C \leq 30000$ g m^{-2}. We assume that A_{max} for C_4 plants relates to S_N and S_C in the same way as A_{max} for C_3 plants does. However, following Collatz *et al.* (1992) we assume that A_{max} for C_4 photosynthesis is only a fraction $A_R = 0.435$ of A_{max} for C_3 photosynthesis.

The maximum light saturated rate of photosynthesis A_{max} is used to estimate the maximum carboxylation rate V_{max} (μmol m^{-2}s^{-1}) as

$$V_{max} = 2^{0.1(T-25)} A_{max} A_S \frac{1}{\left(1 + e^{0.3(13-T)}\right)\left(1 + e^{0.3(T-36)}\right)}, \tag{4.2}$$

where T is the (leaf) temperature (Collatz *et al.* 1992) and A_S is a global scaling factor for both C_3 and C_4 photosynthesis (Collatz *et al.* 1992).

The internal CO_2 partial pressure is defined as c_i. For C_3 plants, c_i is taken to be 70% of its atmospheric partial pressure (Woodward *et al.* 1995). For C_4 plants, c_i represents the bundle sheath value. There is no consensus on how to chose c_i and we estimated c_i to be eight times the atmospheric partial pressure of CO_2 even though in our simulations, photosynthesis is not sensitive to the bundle sheath value as photosynthesis is not CO_2 limited. The CO_2 compensation point is defined as

$$\Gamma_* = \frac{O_i}{2\tau}, \tag{4.3}$$

where τ describes the partitioning of RuBP to the carboxylase or oxygenase reactions of Rubisco and O_i is the intercellular partial pressure of oxygen (assumed to be 21 kPa). Further, K_c is the Michaelis constant for CO_2 and K_o is the O_2 inhibition constant. We

use the function

$$f_{25}(T) = K_{25} Q_{10}^{\frac{T-25}{10}} \tag{4.4}$$

to describe the response of K_c, K_o and τ to temperature T. Here, K_{25} and Q_{10} are empirically determined parameters specific for K_c, K_o and τ (see Table 4.2).

The gross rate of photosynthesis A_0 is calculated, following Collatz *et al.* (1991) for C_3 plants and Collatz *et al.* (1992) for C_4 plants, as the minimum of three potentially limiting assimilation rates. The Rubisco limited assimilation rate J_c is defined as

$$J_c = \frac{V_{max}(c_i - \Gamma_*)}{c_i + K_c(1 + O_i/K_o)} \tag{4.5}$$

$$J_c = V_{max} \tag{4.6}$$

for C_3 and C_4 respectively. When light is limiting, the efficiency of CO_2 fixation is limited by the quantum yield. The light limited assimilation rate J_e is defined as

$$J_e = a\alpha Q_0 \frac{c_i - \Gamma_*}{c_i + 2\Gamma_*} \tag{4.7}$$

$$J_e = a\alpha Q_0 \tag{4.8}$$

for C_3 and C_4 respectively. Here Q_0 is the incident quantum flux density (μmol $m^{-2}s^{-1}$) that a leaf receives, a is the leaf absorptance and α is the intrinsic quantum yield of photosynthesis (see Table 4.2). When light and Rubisco do not limit the assimilation rate, then it is assumed that the capacity for the export of the products of photosynthesis is limiting for C_3 plants. This transport limited assimilation rate J_s is approximated as

$$J_s = \frac{V_{max}}{2}. \tag{4.9}$$

For C_4 plants, when light and Rubisco are not limiting it is assumed that CO_2 concentrations limit the assimilation rate. This CO_2 limited rate J_p is approximated as

$$J_p = \frac{\kappa c_i}{P} \tag{4.10}$$

(Woodward and Smith 1994b). The term κ is the empirically defined initial slope of the response of CO_2 to photosynthesis (units μmol m^{-2} s^{-1}) and P is the atmospheric

pressure (Pa). In summary, the gross rate of (bio-physical) photosynthesis A_0^b is

$$A_0^b = \min(J_c, J_e, J_s) \tag{4.11}$$

$$A_0^b = \min(J_c, J_e, J_p) \tag{4.12}$$

for C_3 plants and for C_4 plants. The net rate of (bio-physical) photosynthesis A_n^b is

$$A_n^b = A_0^b - R_{mLs}, \tag{4.13}$$

where

$$R_{mLs} = rV_{max} \tag{4.14}$$

is the single leaf maintenance respiration rate. Here, r is a proportion assumed to be 0.015 for C_3-photosynthesis and 0.025 for C_4-photosynthesis (Collatz *et al.* 1991, 1992) and V_{max} is the maximum carboxylation rate from Equation (4.2). All parameters and variables for this section are summarized in Table 4.2.

4.4.2 Stomatal conductance sub-model

The CO_2 assimilation rate is coupled to stomatal conductance using Ball *et al.* (1987)'s empirical model. The model relates the response of stomatal conductance g_s (μmol $m^{-2}s^{-1}$) to the net rate of CO_2 uptake A_n:

$$g_s = m\frac{A_n h_s P}{c_s} + b. \tag{4.15}$$

The terms m and b are empirically derived parameters (see Table 4.3), h_s is the relative humidity (expressed as unitless ratio), P is the atmospheric pressure (Pa) and c_s is the partial pressure of CO_2 at the leaf surface, calculated as

$$c_s = c_a - \frac{1.4A_n P}{g_b}. \tag{4.16}$$

Here, c_a is the atmospheric partial pressure of CO_2 (Pa) and g_b is the leaf boundary layer conductance, estimated as

$$g_b = 0.271 \cdot 10^6 \sqrt{\frac{u(z)}{D_L}}, \tag{4.17}$$

where, $u(z)$ is the wind speed (ms^{-1}) at height z (m) above the ground and D_L is the characteristic leaf dimension (Jones 1992). We calculate the windspeed $u(z)$ from the reference windspeed u_{ref} (m s^{-1}), measured at height z_{ref} (m) above the ground as

$$u(z) = u_{ref} \frac{\ln(z - z_d) - \ln(z_0)}{\ln(z_{ref} - z_d) - \ln(z_0)}. \tag{4.18}$$

Here, z_d is the displacement height (m) and z_0 is the roughness length (m) (Jones 1992). Both z_0 and z_d are functions of the aerodynamic properties of the vegetation and following Jones (1992) we simply assume $z_d = 0.86\bar{H}$ and $z_0 = 0.06\bar{H}$. For these purposes we assume mean vegetation height $\bar{H}$ is 1.5m. The reference height z_{ref} is 10 m and the windspeed u_{ref} is read from a database. Variables of this section are summarized in Table 4.3.

4.4.3 Linking photosynthesis and stomatal conductance

The leaf photosynthetis and conductance sub-models are interdependent. The photosynthesis model requires estimates of c_i, which is determined by stomatal conductance. The stomatal model, in turn requires estimates of A_n, which also depends on c_i. The system of equations is closed by noting that A_n can also be defined in terms of the CO_2 diffusion gradient

$$A_n^d = \frac{g_s(c_s - c_i)}{1.6P}. \tag{4.19}$$

When solving for A_n we iteratively seek the value of c_i that satisfies both Equation (4.19) and the equations

$$A_n^b = \min(J_c, J_e, J_s) - R_{mLs}, \tag{4.20}$$

$$A_n^b = \min(J_c, J_e, J_p) - R_{mLs}, \tag{4.21}$$

for C_3 and C_4 plants given by Equations (4.11) or (4.12) and (4.13), hence, we solve the equation

$$c_i^* = \min_{c_i > 0} \left| A_n^b - A_n^d \right|. \tag{4.22}$$

4.5 Individual plant model

In this section we describe how we model individual plants. Here, we do not differentiate between trees and grasses and we assume that apart from differences in the photosynthetic pathways and plant specific parameters, grasses and tree have the same physiological properties and are influences by the same biophysical processes.

4.5.1 Biomass pools of a plant

Each individual consists of eight different biomass pools. The biomass pools are divided into living and dead biomass pools. The living biomass pools are root biomass B_R, stem biomass B_S and leaf biomass B_L. The dead biomass pools are standing dead stem and leaf biomass B_{Ss} and B_{Ls}, stem and leaf litter B_{Sd} and B_{Ld} and dead root biomass B_{Rd}. Figure 4.3 illustrates the geometry of a plant in its environment and Table 4.4 provides a summary of the biomass compartments.

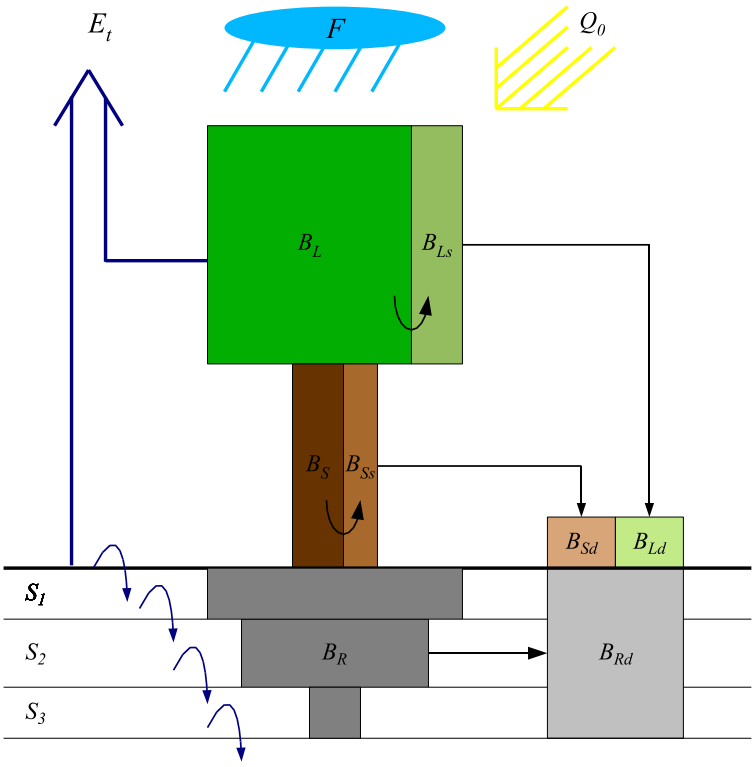

Figure 4.3: The figure depicts the different biomass pools and allometric properties of a single individual in its environment.

We motivate this biomass partitioning as follows. The living biomass pools differ in their functions. Leaf biomass is responsible for photosynthesis and carbon gain, root

biomass is responsible for water and nutrient uptake, stem biomass creates the infrastructure needed for leaves to capture light effectively. Roots and stems store resources of the plant, especially for re-allocation of leaf biomass after dormancy or after fire (Wolfson 1999; Higgins *et al.* 2000; Hoffmann and Solbrig 2003) and act to buffer the plant against disturbance. The splitting of biomass also allows the simulation of how competition for water and light, herbivory or fire can influence the plant (Section 2). The differentiation of dead biomass pools is important for light competition, fire and for the carbon accounting of the ecosystem.

4.5.2 Plant allometry

Stem biomass B_S and leaf biomass B_L (kg/plant for trees and kg/m^2 for grasses) are translated into height H (m) using the relationships

$$H = H_1 \cdot (B_S + B_L)^{H_2} \tag{4.23}$$

$$H = H_1 \cdot B_L^{H_2} \tag{4.24}$$

for trees (Equation 4.23) and grasses (Equation 4.24). The parameters H_1 and H_2 for trees (Equation 4.23) were taken from Higgins *et al.* (2007a) and the parameters for grasses (Equation 4.24) were taken from Arora and Boer (2005). For trees, we follow Higgins *et al.* (2007a) to calculate the stem diameter d_s (cm) from height H (m) as

$$d_s = \frac{d_{s1}}{d_{s2}} H. \tag{4.25}$$

The canopy area of a plant is given by

$$\mathcal{C} = \pi(H\gamma_c)^2, \tag{4.26}$$

where γ_c is the ratio of stem height to canopy radius. We estimated $\gamma_c = 0.37$ for trees and $\gamma_c = 0.4$ for grasses. The leaf area index L is defined as

$$L = \frac{B_L A_{SL}}{\mathcal{C}}. \tag{4.27}$$

Here, A_{SL} is the specific leaf area and we use A_{SL}=10.9 m^2 kg^{-1} for grass and A_{SL}=10 m^2 kg^{-1} for trees (Scholes and Walker 1993). The rooting depth D_{root} is assumed to be defined by the biomass needed to construct a narrow cylinder with radius r_r (0.5cm for

grasses and 1.5cm for trees) and assuming the density of root biomass is $\rho_r = 10^2$ kg m^{-3},

$$D_{cyl} = \frac{B_R}{\rho_r r_r^2 \pi}. \tag{4.28}$$

Rooting depth is limited by the maximum rooting depth of the plant D_{mrd} and by the soil depth D_{soil}, hence

$$D_{root} = \min\left(D_{mrd}, D_{soil}, D_{cyl}\right). \tag{4.29}$$

Variables and constants of this section are listed in Table 4.5.

4.5.3 Canopy photosynthesis and stomatal conductance

To estimate the whole plant's carbon gain, the leaf level estimates of A_0 and g_s generated in section 4.4 (*"Leaf photosynthesis"*) need to be scaled up to the canopy scale. We assume that the quantum flux density Q in the canopy exponentially decays with leaf layer l following Beer's law (Jones 1992)

$$Q(l) = Q_0 e^{-kl}. \tag{4.30}$$

Here, Q_0 is the quantum flux density incident on the canopy and k is the canopy extinction coefficient ($k = 0.5$). Hence, the light received by an unshaded plant (Q_{sum}) is given by the integral

$$Q_{sum} = Q_0 \int_0^L e^{-kl}\, dl, \tag{4.31}$$

where L is the leaf area index of the canopy, Equation (4.27). We follow Sellers *et al.* (1992) in assuming that light is the primary determinant of how photosynthesis scales through the canopy. This assumption implies that light limited canopy photosynthesis A_c can be defined as

$$A_c = A_0 Q_i \int_0^L e^{-kl}\, dl. \tag{4.32}$$

Here, Q_i is an additional factor that describes the potential light availability of the plant. For a single unshaded plant, Q_i is equal to one, however, in presence of other competitor plants, Q_i can be less than one, as the light environment of the target plant might be modified by competitor plants (see section 4.6.2, *"Light competition"*).

Canopy photosynthesis and stomatal conductance are limited by the soil moisture content (Schulze *et al.* 1994). To simulate this effect, we first define a soil moisture

index $G(\theta_i)$ for each soil layer i as

$$G(\theta_i) \quad = \quad 2\beta(\theta_i) - \beta^2(\theta_i), \tag{4.33}$$

where

$$\beta(\theta_i) \quad = \quad \max\left(0, \min\left(1, \frac{\theta_i - \theta_{wp}}{\theta_{fc} - \theta_{wp}}\right)\right). \tag{4.34}$$

Here, θ_i is the soil moisture content of soil layer i and θ_{wp} and θ_{fc} are wilting point and field capacity (Ronda *et al.* 2001). We assume that water availability G_w of a plant is given as the weightened mean value of the soil moisture indexes $G(\theta_i)$ of all soil layers where the plant has roots,

$$G_w = \frac{1}{D_{root}} \sum_i d_i G(\theta_i), \tag{4.35}$$

Here, d_i is the thickness of soil layer i. The light and water limited rate of canopy photosynthesis A_{cs} is then defined as

$$A_{cs} = A_0 Q_i G_w \int_0^L e^{-kl}\, dl. \tag{4.36}$$

Canopy stomatal conductance g_s^c is calculated using the Ball-Berry equation (Ball *et al.* 1987)

$$g_s^c = m\frac{(A_{cs} - R_{mL})h_s P}{c_s^c} + b, \tag{4.37}$$

where b, m and h_s are defined as in Equation (4.15) and Table 4.3. The partial pressure of CO_2 of the canopy is given as

$$c_s^c = c_a - \frac{1.4 A_{cs} P}{g_b^c} \tag{4.38}$$

as in Equation (4.16) except that the canopy boundary layer conductance g_b^c (m s^{-1}) is used,

$$g_b^c = \frac{u_{ref} K^2}{\ln^2\left(\frac{z_{ref} - z_d}{z_0}\right)}. \tag{4.39}$$

Here, K is the von Karman constant ($K = 0.41$) while u_{ref}, z_{ref}, z_d and z_0 are defined as in Equation (4.18). To compute z_0 and z_d we use the plant height H. The canopy

maintenance respiration R_{mL} in Equation (4.37) is defined as

$$R_{mL} = rA_{cs}, \tag{4.40}$$

where r is a constant defined in Equation (4.14) and Table 4.2. Maintenance respiration is determined by canopy light extinction and it is also influenced by soil moisture conditions, since there is evidence that maintenance respiration rates are closely related to carbon assimilation rates (Thornley and Cannell 2000). See Table 4.6 for a summary of variables and constants used in this section.

4.5.4 Respiration sub-model

Respiration is poorly understood and there is no consensus on how it should be modeled (Thornley and Cannell 2000). We distinguish between growth respiration R_g and maintenance respiration R_m. Growth respiration R_g, which we define as the cost of producing new tissue, is calculated as

$$R_g = \sigma A_{cs} \mathcal{C}, \tag{4.41}$$

where σ is a constant proportion, assumed to be 0.35 (Arora 2003), and $\mathcal{C}$ is the canopy area of the plant as defined in Equation (4.26). The leaf level photosynthetic rate A_{cs} and the leaf level respiration rate R_{mL} are transformed from μmol $\mathrm{m}^{-2}\mathrm{s}^{-1}$ to kg/day/plant by multiplication of leaf level rates with $44\mathrm{e}^{-9} \cdot (12/44) \cdot 3600 \cdot p_s \cdot 24$, where p_s is the percentage of sunshine per day.

Maintenance respiration R_m is the cost of keeping live tissue functional and is estimated as the sum of leaf respiration R_{mL}, stem respiration R_{mS} and root respiration R_{mR}, hence, $R_m = R_{mL} + R_{mS} + R_{mR}$. We assume that the total leaf biomass is alive and canopy maintenance respiration is given by $R_{mL} = rA_{cs}$, as defined in Equation (4.40). For stem biomass we assume that a fraction β_S is living sapwood and subjected to maintenance respiration. The remaining biomass is dead heartwood, that does not respire. We assume that roots consist of fine roots, sapwood and heartwood. Fine roots are most active and hence, are the most important source of respiration. Since we know little about fine root dynamics, we simply assume that fine root respiration can be estimated as a function of leaf respiration (Thornley and Cannell 2000). More specifically, we assume that fine root respiration is equal to leaf maintenance respiration R_{mL}. From the root biomass which is not in fine roots, a fraction β_R is sapwood and subjected to

maintenance respiration. The remaining root biomass is heartwood and not subjected to respiration. The parameters β_S and β_R effectively scale the total respiration $R_m + R_g$ and hence, the ratio between respiration and photosynthesis (carbon use efficiency). Empirical estimates suggest that carbon use efficiency in tropical vegetation lies between 0.35 and 0.6 (Scholes and Walker 1993; Thornley and Cannell 2000; DeLucia *et al.* 2007).

Stem and root maintenance respiration R_{mS} and R_{mR} (kg d^{-1}) are calculated as a function of the carbon content and carbon to nitrogen ratios of roots or stem (Arora 2003):

$$R_{mS} = \beta_N \frac{\beta_R B_S}{\upsilon_S} f(T) \tag{4.42}$$

$$R_{mR} = \beta_N \frac{\beta_S (B_R - B_L)}{\upsilon_R} f(T) + R_{mL}. \tag{4.43}$$

Here, β_N is a constant respiration rate, B_L, B_S and B_R are the leaf, stem and root biomasses (kg) and υ_S and υ_R are the C:N ratios of the stems and roots (see Table 4.7). The function

$$f(T) = (3.22 - 0.046T)^{\frac{T-20}{10}} \tag{4.44}$$

allows us to simulate that respiration rates depend on temperature (Tjoelker *et al.* 2001). Table 4.7 summarizes parameters and variables of this section.

4.5.5 Carbon balance and allocation

The difference between canopy photosynthesis and respiration rates from the above sections defines the net carbon gain C_Δ (kg per day) of the plant,

$$C_\Delta = A_{cs}\mathcal{C} - R_g. \tag{4.45}$$

Vegetation models differ greatly in how they simulate carbon allocation to living biomass pools, probably because no allocation sub-model provides a generally applicable abstraction of this complex process. We follow the allocation concepts of Tilman (1988) and Friedlingstein *et al.* (1999). The allocation model assumes that the greatest part of the carbon gain is directed to the compartment that most limits growth. That is, if light is limiting growth, then allocation is directed towards stems. If water is limiting, allocation is directed towards roots. When photosynthesis is limiting after the plant has

moved from the dormant to the active state or after a fire, then allocation is directed to leaf biomass. The realized proportions of carbon gain directed to roots, shoots and leaves a_R, a_S and a_L are given as

$$a_R = \frac{1 + a_{0R} - G_w}{3 + a_{0R} + a_{0S} - Q_i - G_w - Ci}, \tag{4.46}$$

$$a_S = \frac{1 + a_{0S} - Q_i}{3 + a_{0R} + a_{0S} - Q_i - G_w - Ci}, \tag{4.47}$$

$$a_L = \frac{1 - C_i}{3 + a_{0R} + a_{0S} - Q_i - G_w - Ci}. \tag{4.48}$$

The parameters a_{0R}, a_{0S} and a_{0L} describe the proportional allocation to roots, shoots and leaves when resources are not limiting, G_w and Q_i describe water and light availability (Equations 4.32 and 4.35) and

$$C_i = \frac{B_L}{a_{0L}(B_R + B_S + B_L)} \tag{4.49}$$

describes the deviance of leaf biomass from the fraction of leaf biomass in the non-limiting case, a_{0L}. Figure 4.4 depicts how the allocation model behaves in different situations and Table 4.8 summarizes the variables and parameters used in this section.

4.5.6 Leaf phenology

As it is the case for respiration and allocation, ignorance of the underlying processes means that there is no consensus on how leaf phenology (hereafter simply refered to as phenology) should be modeled. In existing DGVMs it is typically assumed that phenology is controlled by temperature or soil moisture (Cramer *et al.* 2001). However, phenology has a large impact on the global carbon cycle as the growing season length is a major determinant of a plant's water uptake and carbon gain (Jolly and Running 2004). We use a simplified version of Lüdeke *et al.* (1994)'s and Givnish (2002)'s phenological model. The phenology model is resource based which means that the model allows the simulation of transitions between a dormant and an active state in response to resource availability and environmental conditions. The model assumes that switches between dormant and active states are determined by photosynthetic carbon gain and

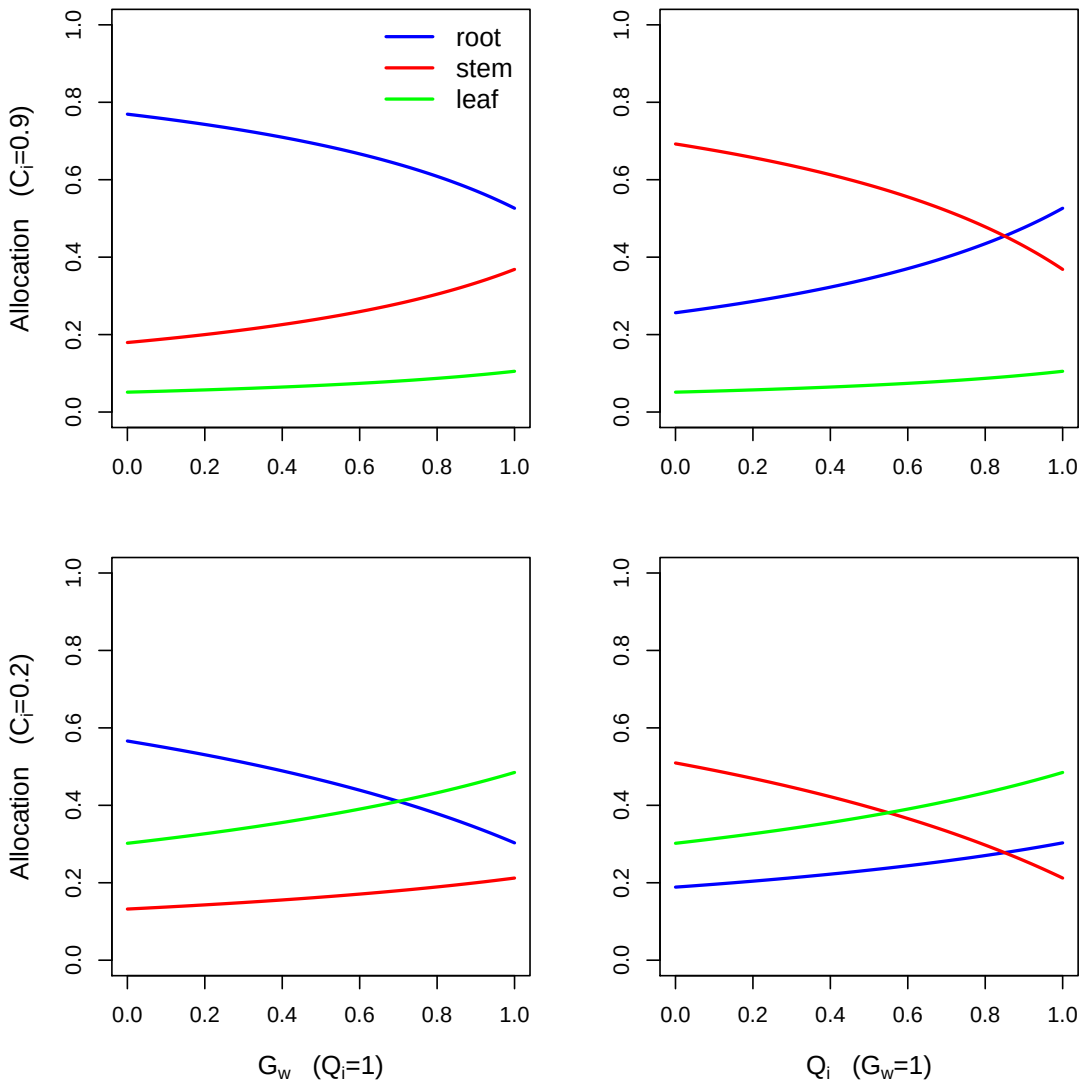

Figure 4.4: The panels depict how the plant's carbon gain C_Δ is allocated to different plant compartments, when light is highly available ($Q_i = 1$, left column) or when water is highly available ($G_w = 1$, right column) in response to light or water availability (variable G_w or Q_i). Further, the panels depict differences in allocation when leaf biomass is high ($C_i = 0.9$) or when leaf biomass is low ($C_i = 0.2$).

the respirative costs of carbon gain. These costs and benefits are indexed as

$$A_{index} = A_0 \left(G_i + T_i\right) - R_{mL}. \tag{4.50}$$

The benefits are a function of A_0 and the costs are a function of leaf level maintenance respiration R_{mL}. A soil moisture index defined as

$$G_i = \frac{2}{3}\theta_4 + \frac{1}{3}G_w \tag{4.51}$$

is used to weight A_0. Here, θ_4 is the water content of the fouth soil layer (20cm to 30cm) and G_w is the average water available to plants, defined by the water content of all soil layers in which the plant has roots (Equation 4.35). By using this definition of G_i we can assume that the phenology is primarily determined by water and that single precipitation events, which strongly influence the water content of the upper soil layer, are less likely to influence phenology than deeper soil layers (Jolly and Running 2004). Additionally, the index G_i allows plants with different rooting depth to respond differently to soil moisture availability. Plants with shallow roots use only water in the highly variable upper soil layers, and sensitivity analyses (not shown) indicate that the dynamics of the upper soil layers are best represented by the fourth soil layer (20cm to 30cm). Plants with deep roots have access to the less dynamic deeper soil layers, which are adequately described by the mean soil water content G_w. It should be noted that the definition of G_i is dependent on the number and depth of soil layers included and would require a re-calibration should the number of soil layers be changed.

Phenology is also controled by temperature as photosynthesis A_0 and respiration R_{mL} respond to temperature. Further, T_i is a temperature index, defined as $T_i = 0$ when the minimum monthly temperature T_{min} is above a threshold T_* and as

$$T_i = 2.5 \left(\frac{T_{min}}{T_*} - 1\right) \tag{4.52}$$

when T_{min} is below T_* (Table 4.9). In tropical regions, phenology is generally not influenced by temperature, however, at high altitudes T_i might play a role.

The A_{index} controls leaf phenology by determining when a plant shifts the phenological state. When A_{index} becomes negative a plant moves from the growing phase into a standby phase. After d_{neg} successive days of negative A_{index}, the plant moves into a phase of leaf abscission and dormancy. A return to the growing phase occurs after d_{pos}

successive days of positive A_{index}. Both the transition from the growing phase to the dormancy phase and the transition from the dormancy phase to the growing phase take place instantaneously but they affect the biomass pools in different ways. While moving from the growing phase to the dormant phase, photosynthesis is not possible and only a proportion ζ_L of leaf biomass remains alive. The rest accumulates in the dead biomass pools (Table 4.9 defines the constants). When a plant turns from the dormant into the growing phase, photosynthesis is possible again, allowing carbon gain (see Figure 4.5). We assume that the phenological sequence is influenced by frost. On days with frost, the counter d_{neg} is advanced by one which means that given the same distribution of G_i, the plants at sites with frost have a shorter growing season length.

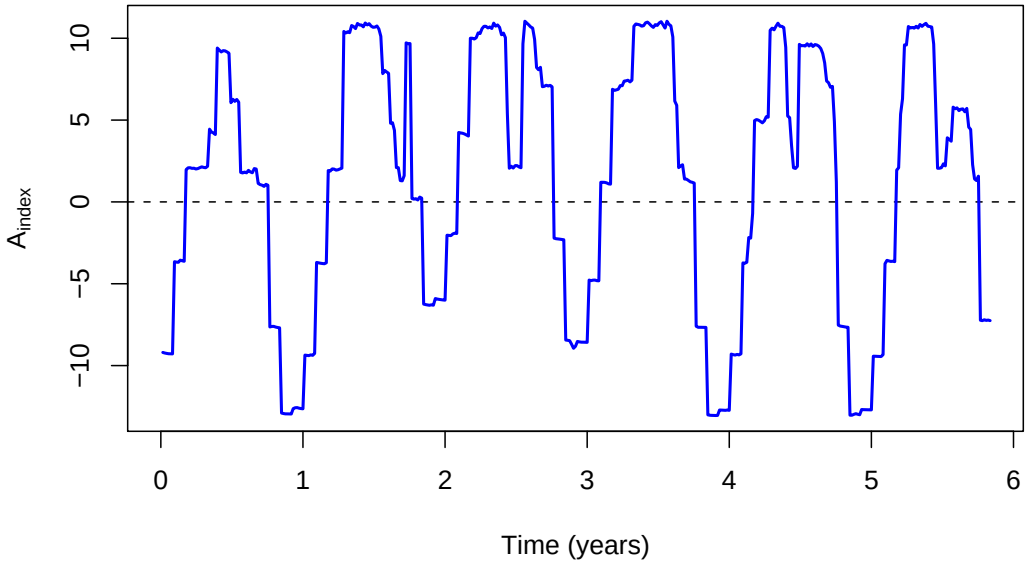

Figure 4.5: The cost-benefit index of photosynthesis, A_{index}, defines the phenological state of the plant: the plant moves to the active state after d_{pos} successive days of positive A_{index} and it moves to the dormant state after d_{deg} successive days of negative A_{index}.

4.5.7 Biomass turnover and decomposition

The living plant compartments (leaf, stem and root biomass) are affected by turnover, that is the continuous death of living biomass. The turnover rates are determinded by longevities ω_L, ω_S and ω_R of leaf, stem and root biomass. The biomass removed by turnover accumulates in the standing dead biomass compartments.

Dead biomass is continuously influenced by the transition from standing to lying

dead biomass and by decomposition. During the transition, proportions ξ_L and ξ_S of standing dead leaf and stem biomass permanently turn into litter and accumulate to the lying dead biomass compartments. Decomposition removes a fraction defined by the longevity ω_D of dead material. The decomposed biomass is lost for the system. The turnover and decomposition parameters we used (Table 4.10) are taken from Scholes and Walker (1993) and Gill and Jackson (2000). Figure 4.6 summarizes the biomass accounting of plants.

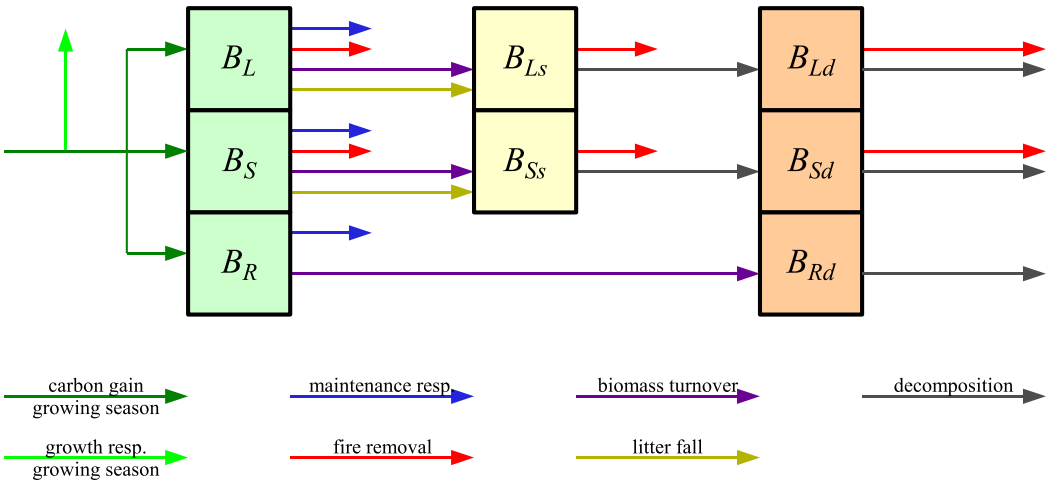

Figure 4.6: The diagram depicts the biomass pools of a plant and the processes that modify biomass: carbon gain, respiration, decomposition, turnover, litter fall and fire.

4.5.8 Evapotranspiration

The plant's evapotranspiration is calculated using the Penman-Monteith equation (Jones 1992; Allen *et al.* 1998),

$$E_t^p = \frac{sQ_0 + 86400\rho_{air}c_p h_{vpd} g_b^c}{\lambda\left(s + \gamma\left(1 + \frac{g_b^c}{g_s^c}\right)\right)}. \tag{4.53}$$

Here s is the slope of vapor pressure curve, Q_0 is the net radiation, ρ_{air} is the density of air, c_p is the specific heat of moist air, h_{vpd} is the saturation vapor pressure deficit, g_b^c is the canopy boundary layer conductance from Equation (4.39), λ is the latent heat of air, γ is the psychrometric constant and g_s^c is the canopy stomatal conductance from Equation (4.37). We use Allen *et al.* (1998)'s detailed guide to the computation of the components of E_t^p.

4.6 Stand scale dynamics

The stand structure we consider follows the definition of a savanna, that is a continuous layer of grasses and a discontinuous layer of trees (Huntley and Walker 1982; Scholes and Walker 1993). The tree population is described using an individual-based structure that allows us to simulate reproduction, establishment and mortality of single trees. The population structure of the grass layer is ignored and we consider only biomass of two super-individuals (Scheffer *et al.* 1995) representing grass under and grass between the canopies of trees. Hence, we assume that the grass layer is adequately described by biomass and that vegetative reproduction buffers the biomass dynamics from demographic events.

Variables describing the tree population are the number of trees n_t, the size S of the study site and the proportional tree cover Υ, defined as the sum of the canopy areas of all trees taller than half a meter without competitor, divided by the size of the study site, S (Table 4.11).

4.6.1 Total evapotranspiration and soil water balance

Vegetation and soil characteristics, are used to calculate the total evapotranspiration rate E_t (m s^{-1} m^{-2}) of the system. Total evapotranspiration is given as the sum of soil evaporation E_t^s, grass evapotranspiration E_t^g and tree evapotranspiration E_t^t. Soil evaporation is given as

$$E_t^s = \frac{0.0864}{2.45}\frac{1}{g_b^s}\exp(-4.28 + 11.97\min(0.35, \theta_1))h_{vpd}, \tag{4.54}$$

where g_b^c is the boundary layer conductance of the soil (Equation 4.39) and θ_1 is the water content of the upper soil layer. Grass evapotranspiration E_t^g is defined as the weighted mean value of evapotranspiration rates of grass between and grass under the canopies of trees, calculated with Equation (4.53). Tree evapotranspiration E_t^t is given as the mean value of evapotranspiration of all trees,

$$E_t^t = \frac{1}{S}\sum_{i=1}^{n_t} E_i^p. \tag{4.55}$$

The rainfall algorithm (New *et al.* 2002) generates a time series of daily rainfall F_i for each year of the simulation. It assumes that monthly rainfall is a gamma-distributed

random variable and that the mean rainfall event size is monthly rainfall r_m divided by the mean number of rain days per month w_f. Monthly parameters for the gamma distribution and for rainy days per month are provided by New *et al.* (2002). We assume that daily rainfall is an exponentially distributed random number with mean equalling the mean event size.

Rainfall and evapotranspiration are used to drive a multi-layer, tipping bucket model of soil moisture content. All soil layers are assumed to have the same wilting point θ_{wp} and field capacity θ_{fc}, while they may differ in thickness d_i. Rainfall is tipped from one layer into a lower layer when the soil moisture content of a soil layer exceeds its field capacity θ_{fc}. Evapotranspiration causes moisture to move from deeper soil layers to higher soil layers and finally from the top-soil into the atmosphere. Upper soil layers are assumed to dry out first, and we assume that a soil layer cannot be dried beyond its wilting point θ_{wp}.

4.6.2 Light competition

The light competition algorithm estimates the relative light availability Q_i (Equation 4.32) of a single grass or tree individual (which we call the target plant and index with "t"), depending on its neighbor plants (competitors, indexed with "c"). Light competition occurs within and between the grass and the tree populations. Unshaded plants receive the incident photosynthetically active radiation ($Q_i = 1$). If a plant is shaded by a competitor (either another tree or grass) then light availability Q_i and as consequence the photosynthetic rate A_{cs} are reduced. Light competition is often described by using a linear function of competitor abundance (Bond *et al.* 1995; Case 2000). We follow this approach and simply assume that light availability of the target plant is reduced as a linear function of the competitor height. The light competition model is only a coarse approximation of the real situation, as we assume that a tree has either no competitor tree or exactly one competitor tree. Of course, this is an over-simplification of the reality, but light models that consider shading effects of several trees in a three-dimensional environment (e.g. Chave 1999; Shabanov *et al.* 2000) are computionally expensive.

The light environment of trees is influenced by grasses and by a competitor tree. Whether a tree has a competitor tree or not is assigned at the beginning of a tree's life by randomly assigning a neighbor contingent on the treecover and the number of trees. More explicitly, a tree has a competitor with probability $e_1 - e_2\Upsilon - n_t/e_3$. This ensures, that in sparse populations, most of the trees do not have a competitor while in a dense

tree population, there is a high probability that trees have a competitor. Should a tree have a competitor, the identity of the competitor is randomly drawn from the current tree population.

Whether the light availability of the target tree is influenced by the competitor tree or not depends on the tree heights of the target tree, H_t, and its competitor tree, H_c. If the target tree is taller than the competitor, then the target tree has full light availability and $Q_i = 1$. When the target tree is smaller than the competitor, then Q_i is scaled by the linear function

$$Q_{comp} = \mu_c \frac{H_t}{H_c} + (1 - \mu_c) \qquad (H_t < H_c) \tag{4.56}$$

where μ_c is a parameter that measures the maximum influence of the competitor on the light environment of the target tree. Analogously, we use a factor

$$Q_{grass} = \mu_g \frac{H_t}{H_g} + (1 - \mu_g) \qquad (H_t < H_g) \tag{4.57}$$

to simulate the influence of the grasses on trees (this only applies when $H_t < H_g$, i.e. in the tree seedling phase). Here, μ_g measures the maximum influence of grasses on trees and H_g is the height of grass between tree canopies. For grass on tree competition, we use grass between tree canopies as the competitor. The light availability of trees is then given by

$$Q_i = Q_{comp}\, Q_{grass}. \tag{4.58}$$

The light environment of grasses is assumed to be influenced by two factors: by the shading effects of trees (only for sub-canopy grass) and by shading of dead grass biomass. The shading effect of trees is given by

$$Q_{tree} = \mu_t \frac{H_g}{H_t} + (1 - \mu_t) \qquad (H_g < H_t) \tag{4.59}$$

and the shading effect of dead biomass is

$$Q_{dead} = \mu_d \frac{B_L}{B_{Ls}} + (1 - \mu_d) \qquad (B_L < B_{Ls}). \tag{4.60}$$

Here, μ_t and μ_d meassure the maximum influence of trees and dead grass biomass on the light environment of grasses, H_t and H_g are the mean tree height and the grass height and B_L and B_{Ls} are live and standing dead grass leaf biomasses. The light availability

of grasses is given by

$$Q_i = Q_{tree}\, Q_{dead}. \tag{4.61}$$

Table 4.12 defines the constants of this section.

4.6.3 Tree population dynamics

The sections 4.5 (*"Individual plant model"*) and 4.6.2 (*"Light competition"*) described the processes that influence the growth of single individuals. In this section we discuss birth and death processes that change the size n_t of the tree population (Table 4.13 summarizes the constants).

Reproduction and seed bank model

To simulate seed production and germination, we simulate a seed bank. The seed bank accumulates the seed production of all trees. The number of seeds produced by each tree depends on environmental conditions as well as on the plants carbon balance. We assume that to be able to produce seeds, a tree must have a positive carbon balance C_Δ and it must be adult, which means older than A_a years (we assume $A_a = 10$ years). Then, the number of seeds produced by a tree is given by

$$\phi_i = \left\lfloor \frac{C_\Delta}{B_{seed}} \right\rfloor. \tag{4.62}$$

Here, $B_{seed} = 1\text{g}$ (Hovestadt *et al.* 1999) is the seed weight and C_Δ is the carbon gain (Equation 4.45). Equation (4.62) implies, that trees with low net carbon gain only produce few seed while adult trees with high carbon gain produce many seeds. To mimic the fact that seed production is variable and linked to environmental conditions, we assume that C_Δ in Equation (4.62) is the total carbon gain on the first day of the month with the highest potential photosynthetic rate A_0. The total number Φ of seeds in the seed bank is given by summing over the seed production ϕ_i of all trees. Hence, no dispersal process is simulated. Trial simulations suggest that the seed production rate does not limit reproduction and population growth in this model. Seeds are assumed to have short survival times, specifically we assume that the annual mortality rate ϕ_{mort} of seeds is 70% (Higgins *et al.* 2000).

Seeds cannot germinate until the next wet season, thus the seed bank buffers the population dynamics. We assume, that seeds can germinate when the counter of wet

days d_{wet} reaches 3 days. Here, a wet day is defined as a day without frost where the soil moisture of the upper soil layer θ_1 reaches the field capacity θ_{fc}. When the soil moisture of the upper soil layer does not reach the field capacity then the counter d_{wet} is reduced by one. On each day fulfilling the condition $d_{wet} = 3$, a proportion ϕ_{sprout} of the seeds Φ are available for germination but the germination probability of these seeds is only ϕ_{germ}. This mechanism prevents all seeds from germinating at once and introduces a stochastic element to the timing and number of germinations.

Death process

Grasses are assumed to be immortal. We consider three additive factors that determine the probability that a tree dies. (1) When a tree is in the active state and the carbon balance of a tree is negative ($C_\Delta < 0$), then the death probability is increased by P_{carb}. (2) When a tree has a competitor tree then the death probability is increased by P_{comp}. (3) On days with frost, the probability for tree mortality is increased by P_{frost}. Each day, the probabilities of the three mortality processes are used to determine the total mortality probability P_{death} of the tree. When a uniformly distributed random number between zero and one is less than P_{death}, then the tree is deleted from the population and the biomass is added to the dead biomass pools.

4.6.4 Grass fires and tree topkill

Grass fires are a characteristic feature of savannas. Fires remove grass biomass and also induce topkill (stem mortality) in trees. The potential fire intensity I (kJ $s^{-1}m^{-1}$) is predicted using Higgins *et al.* (2008)'s semi-empirical model of grass fire intensity,

$$I(B_F, \theta_F) = hB_F \frac{\arctan(u_{ref}) c f(B_F, a_w)}{Q_m \theta_F + Q_v(1 - \theta_F)}. \tag{4.63}$$

Here, B_F is the average fuel biomass (kg m^{-2}), θ_F is the fuel moisture, Q_m and Q_v are heats of preignition of moisture and fuel, c is regression parameter, u_{ref} is the wind speed (m s^{-1}) and h is the heat yield of fuel consumed (typically 16890 kJ kg^{-1}). Further,

$$f(B_F, a_w) = \frac{B_F}{B_F + a_w} \tag{4.64}$$

is a sigmoidal function of fuel biomass and a_w is a regression parameter estimated from data on fire behavior. To estimate the fuel biomass B_F and the moisture content θ_F,

we divide the biomass into live biomass B_{live} which is moist and dead biomass B_{dead} which is dry. Live fuel biomass B_{live} is given by the grass leaf biomass B_L^g and by one half of the grass standing dead biomass B_{Ls}^g,

$$B_{live} = B_L^g + \frac{1}{2} B_{Ls}^g. \tag{4.65}$$

Live tree biomass does not contribute to B_{live}. Dead fuel biomass B_{dead} is given by the leaf litter of all trees, B_{Ld}^t, as well as by grass lying dead biomass B_{Ld}^g and one half of the grass standing dead biomass B_{Ls}^g,

$$B_{dead} = B_{Ld}^g + \frac{1}{2} B_{Ls}^g + B_{Ld}^t. \tag{4.66}$$

The moisture content of live fuel is assumed to equal the air humidity h_s that is, $\theta_{live} = h_s$. For dead biomass the moisture content quickly decreases by an exponential function (Cheney and Sullivan 1997)

$$\theta_{dead} = h_s \cdot \theta_r^T, \tag{4.67}$$

where θ_r (=0.95) describes how fast biomass dries out and T is the number of days since litter fall, that is the last transition from the active to the dormant state. Total fuel biomass is given as

$$B_F = B_{live} + B_{dead} \tag{4.68}$$

and fuel moisture is given as the mean value

$$\theta_F = \frac{B_{live}\theta_{live} + B_{dead}\theta_{dead}}{B_{live} + B_{dead}}. \tag{4.69}$$

For a fire to spread, two conditions must be fulfilled; first, an ignition must take place and second, the potential fire intensity I must exceed a minimum intensity of 300 kJ $s^{-1}m^{-1}$ (van Wilgen and Scholes 1997). An annual stochastic ignition sequence is generated in the beginning of each year. The number of ignitions is limited by the random variable $i_1\Upsilon - i_2$ which imitates that fuel biomass in tree stands with high canopy cover is shaded and dries out slower. The probability that a fire spreads in case of an ignition event and an appropriate fire intensity is $p_{fire} = 1.5\%$.

Fire consumes the total grass and tree litter as well as all standing dead grass biomass. Fire removes most of the live aboveground grass biomass compartments B_S^g and B_L^g,

$$B_S^{g'} = \psi_g B_S^g \tag{4.70}$$

$$B_L^{g'} = \psi_g B_L^g. \tag{4.71}$$

Here ψ_g is the proportion of grass biomass that survives a fire. Fire might induce topkill of trees. Following Higgins *et al.* (2000) the probability of topkill is an empirically derived function of fire intensity I and tree height H (Figure 4.7),

$$P_{topkill}(H, I) = \frac{\exp(D_1 - D_2 \ln(H) + D_3\sqrt{I})}{1 + \exp(D_1 - D_2 \ln(H) + D_3\sqrt{I})}. \tag{4.72}$$

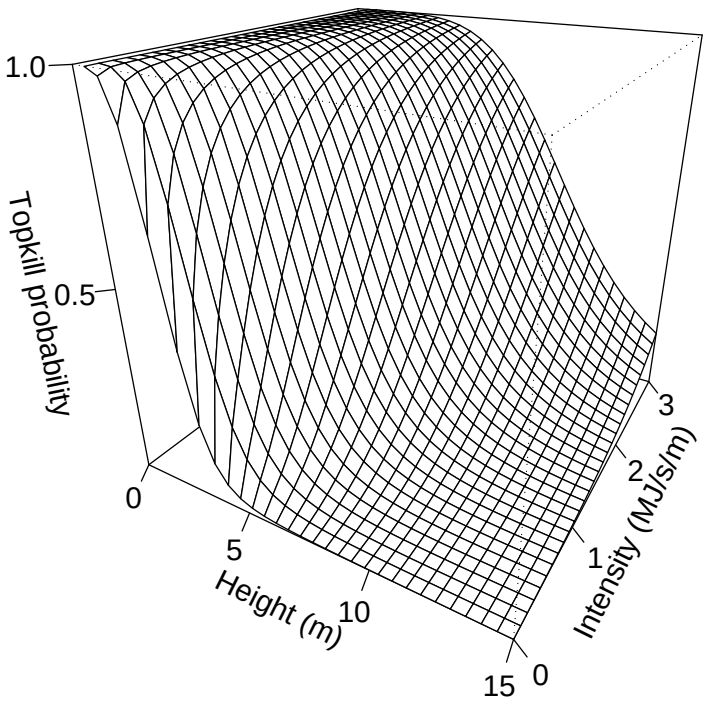

Figure 4.7: The figure depicts the topkill probability of a single tree as a function of tree height and fire intensity. Small trees have a high topkill probability while tall trees might only be topkilled by intense fires.

A tree is subjected to topkill when a uniformly distributed random number between zero and one is less than the tree's topkill probability $P_{topkill}(H, I)$. Topkilled trees

retain only a proportions ψ_{ts} and ψ_{tl} of their stem and leaf biomass:

$$B_S^{t'} = \psi_{ts} B_S^t, \tag{4.73}$$

$$B_L^{t'} = \psi_{tl} B_S^t. \tag{4.74}$$

Topkilled tree stems usually resprout from rootstocks (Hoffmann and Solbrig 2003). For savanna trees the probability of resprouting is high (Higgins *et al.* 2000). Fire mostly affects the trees in the juvenile state and prevents them from reaching the adult state. Adults are unaffected by fire, because they are, according to Equation (4.72) too large to be topkilled. Table 4.14 provides a summary of the parameters and variables of the fire model.

4.7 Synthesis of sub-models

Figure 4.8 depicts a flow diagram for the model. First, environmental data of the defined study site are read from data bases and site characteristics, such as radiation, potential leaf level photosynthesis and respiration are calculated. Further, the grass and tree populations are initialized. At the beginning of each simulation year, we generate a stochastic rain sequence and a stochastic fire ignition sequence for the year. For each day in the year, we first calculate the net radiation. Then we run the death process for trees and eventually remove dead trees. Then, we calculate the components of evapotranspiration (trees, grasses and soil) and update the soil water content of the different layers using precipitation and evapotranspiration. The next step is to run the grass and tree physiology. We first calculate the carbon balance and the potential carbon gain using light and water availability. The carbon balance defines whether the plant is in the active or in the dormant state. In the active state, carbon gain is allocated to the live plant compartments using the allocation sub-model. Finally, we remove biomass by decomposition, respiration and turnover. For trees, we run the reproduction process, that is, we determine the seed production and eventually add individuals into the tree population, when environmental conditions allow germination. At the end of each simulation day, we check if a fire spreads and if yes, we remove aboveground grass biomass and, in the case of topkill, aboveground biomass of selected trees. Finally, the model writes the desired output data to a file.

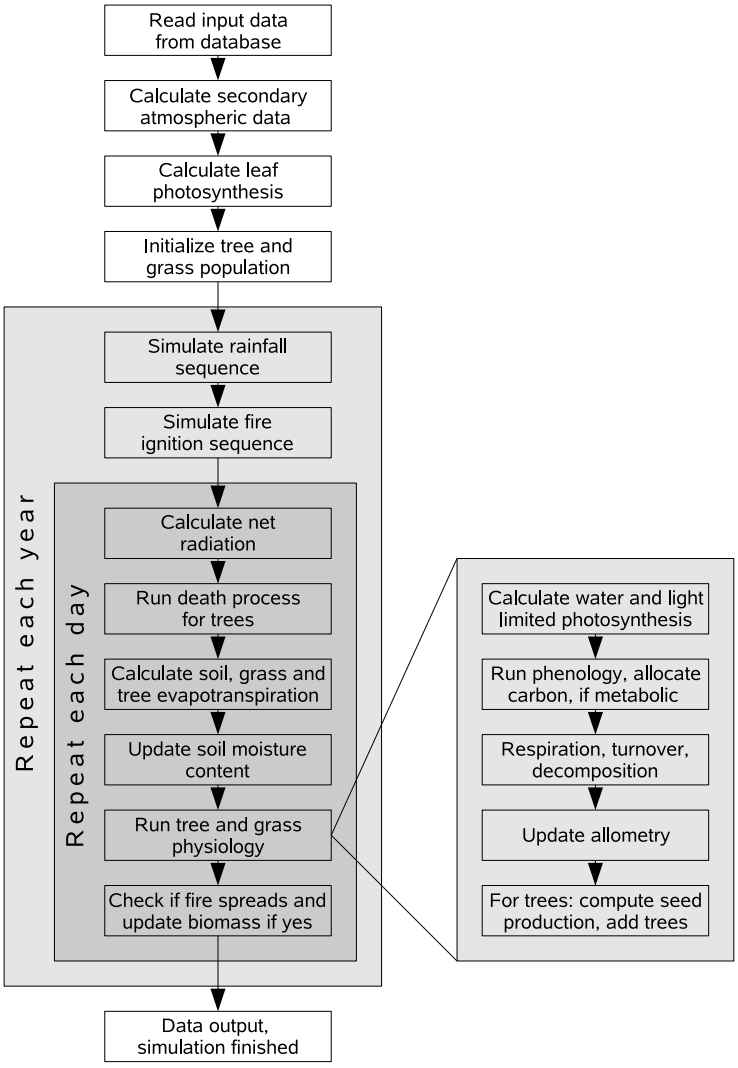

Figure 4.8: The figure depicts a flow diagram of the different components used in the model.

4.8 Sensitivity analysis

We conducted a sensitivity analysis to evaluate the uncertainty of model results when model parameters and input variables are modified. We tested 151 parameters and constants listed in Tables 4.1 to 4.14. To conduct the sensitivity analysis we follow the procedure previously applied to ecological models (Perry and Enright 2002; Popp *et al.* 2007): the parameter values listed in Tables 4.1 to 4.14 were scaled between -10% and +10% by steps of 1.25%, relative to the values given in Tables 4.1 to 4.14. Each parameter was varied individually while the other parameters were held constant. Hence, we ignored uncertainties provided by interactions of two or more parameters. An exception are the allocation parameters a_{0R}, a_{0S} and a_{0L} for both grasses and trees which were scaled such that the sum $a_{0R} + a_{0S} + a_{0L}$ is always equal to one. Simulations were conducted in absence fire, as fire potentially hides the uncertainty of the target parameter. To examine the sensitivity of the variables defining the fire sub-model, simulations were conducted in presence of fire. For each parameter and each step between -10% and +10%, the simulations were repeated ten times to account for the stochasticity of the model, hence, we conducted 170 simulations per parameter. For parameters describing the fire sub-model we conducted 100 simulations per step between -10% and +10%, hence we conducted 1700 simulations per parameter. The sensitivity analysis was conducted at Pretoriuskop (25°10' S and 31°16' E), which is a savanna site in the Kruger National Park, South Africa, that receives about 650 mm MAP. We used the same rainfall sequence for all simulations to reduce the uncertainty added by the stochastic rainfall generator. Simulations were conducted for 150 years.

The response variables of the sensitivity analysis were mean tree biomass and mean grass biomass, that is, we explored how mean tree and grass biomass change when a parameter is changed. To quantify the sensitivity of the model results to variations in the parameters, we conducted a linear regression by using the 170 data points (1700 data points for parameters of the fire sub-model) for both grass and tree biomass. For the regression analysis, we normalized grass and tree biomasses by dividing grass and tree biomasses by the mean grass and tree biomass of the simulations when the target parameter is not changed, hence, the mean biomass of simulations without changes in the target parameter is equal to one. The slope of the regression line is used as a linear approximation of the slope of the response curve of biomass to parameter variations and hence, an approximation of the sensitivity. Due to the normalization of biomasses, the slopes of the response curves of different parameters can be compared, as they represent

the relative change in the mean grass and tree biomass in response to a relative change in the target parameter. When sensitivities are expressed in this way, they are often referred to as elasticities (de Kroon *et al.* 2000).

The tested parameters can be grouped into three classes. (1) Parameters that we used for the model parametrization and which are potentially specific for certain study sites or functional types. These parameters might be chosen differently at different study sites or for different functional types. Most of these parameters describe plant traits such as plant allometry, leaf characteristics, mortality or reproduction rates. (2) Parameters and constants of different sub-models that were taken from the literature, for instance parameters of the leaf level photosynthesis model, the respiration model, the radiation model or the fire model. We assume that these parameters are estimates close to the real values. (3) Input data that define soil and climate at the study site and that were taken from global databases. The sensitivities of all parameters are given in Tables 4.16 to 4.19, the following paragraphs discuss the most important parameters of the three groups in more detail.

(1) The results of the sensitivity analysis for the parameters of the first group are depicted in Figures 4.9 to 4.12. The most sensitive parameters are H_1, H_2 and γ_c for trees (HEIGHT_C1_TREE, HEIGHT_C1_TREE, GAMMA_CANOPY_TREE), describing how biomass is translated into tree height (H_1 and H_2) and the ratio between canopy diameter and tree height (γ_c, Figure 4.9). The slope of the tree response curves for these parameters is between 0.78 and 1.76 which means that an increase of the target parameter by 1% increases the tree biomass by values between 0.78% and 1.76%. Thereby, grass-tree interactions reduce grass biomass as an increase in these parameters indicates and increase in tree height and tree canopy area which results in a competitive advantage of trees over grasses. The sensitivity of grass biomass lies between -1.18 and -2.85. The sensitivity analysis of these parameters implies, that good estimates for the allometry of the simulated vegetation might significantly improve the simulation results and decrease uncertainty. Whenever better parameters or site specific parameters are available, for instance for a case study, then they should be used.

Other parameters that strongly influence the simulation results are the parameters of the carbon allocation model, particularly a_{0S} and a_{0R} of trees (A0_STEM_TREE, A0_ROOT_TREE, Figure 4.9). These parameters define how the carbon gain is allocated root, stem and leaf biomass. This result suggests, that the flexible allocation scheme used in the aDGVM has substantial impacts on the simulation results.

Reproduction and mortality parameters also influence the system dynamics, however,

the relative impact is low (between -0.55 and 0.74, Figure 4.10). An exception is the parameter SEED_DECAY_RATE which describes the decay rate of seeds in the soil. The response curve is non-linear and biomass is highly sensitive to parameter changes.

Biomass is highly sensitive to the parameters STRESS_INDEX_TREE and STRESS_INDEX_GRASS used in the leaf phenology sub-model (Figure 4.12). These parameters define the threshold of A_{index} where plants move between the dormant and the metabolic states, and hence these parameters control the growing season length. This result agrees with previous studies that showed the importance of feedbacks between the growing season length and biomass production (Jolly *et al.* 2005).

(2) Figures 4.13 to 4.15 depict the model sensitivity to variation in parameters of the second class, that is parameters of different sub-models taken from the literature. Some of the parameters strongly influence the outcome of the simulations, however, these parameters are based on excellent estimates and we assume that estimates are close to their true values. Sensitive parameters are for instance the ratio σ between photosynthesis and respiration (SIGMA_GROW_RESP_TREE and SIGMA_GROW_RESP_GRASS, Figure 4.13) and the relation $f(T)$ between temperature and respiration (defined by MAIN_RESP_CARB_PROPORT and MAIN_RESP_TEMP_TRANS, Figure 4.13). Other sensitive parameters are the latent heat of air (LAMBDA), the specific heat of moist air (SP_HEAT) and the specific gas constant (SGC) which are required to calculate the evapotranspiration (Equation 4.53, Figure 4.14).

Figure 4.15 shows that fire generally increases the variability of the simulation results which means that it increases the model uncertainty. Model results are most sensitive to parameters of the topkill probability function $P_{topkill}$ (TOP_KILL_CONST, TOP_KILL_H, TOP_KILL_I, Equation 4.72) while the impact of the other parameters is, in average, relatively low.

(3) The model is highly sensitive to most of the climate and soil input data which means, that input data add significant uncertainty to the model results (Figure 4.16). The strongest responses are observed for the atmospheric CO_2 concentration (CA_PAR_PREASSURE), temperature (TEMPERATURE, TMP_MIN, TMP_MAX) and precipitation (PRECIPITATION). The effects of changes in these parameters are explored in detail in Chapter 5. These responses indicate that the uncertainty of model results can be decreased by using better input datasets, e.g. with higher spatial resolution or by using climate data generated by a climate model.

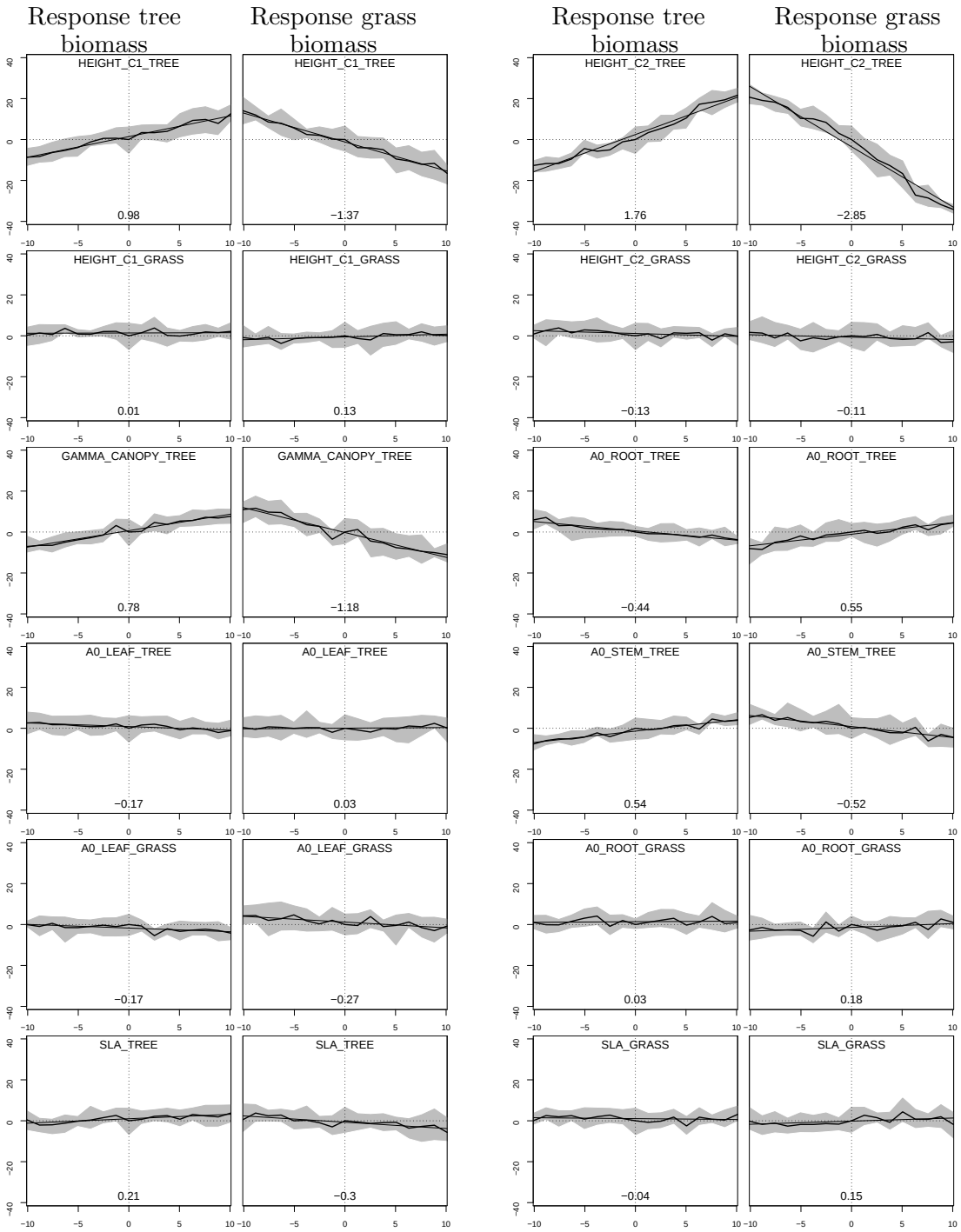

Figure 4.9: Model sensitivity to plant specific parameters. The x-axis gives the variation of the target parameter (in %), the y-axis gives the relative change of tree and grass biomass (in %). In each panel, the left diagram depicts the tree biomass and the right diagram depicts the grass biomass. The bold lines depict the mean of ten simulations, the shaded area describes ±10% quantiles and the dotted lines identify the situation without variation of the target parameter. The number in each panel is the slope of the sensitivity curve.

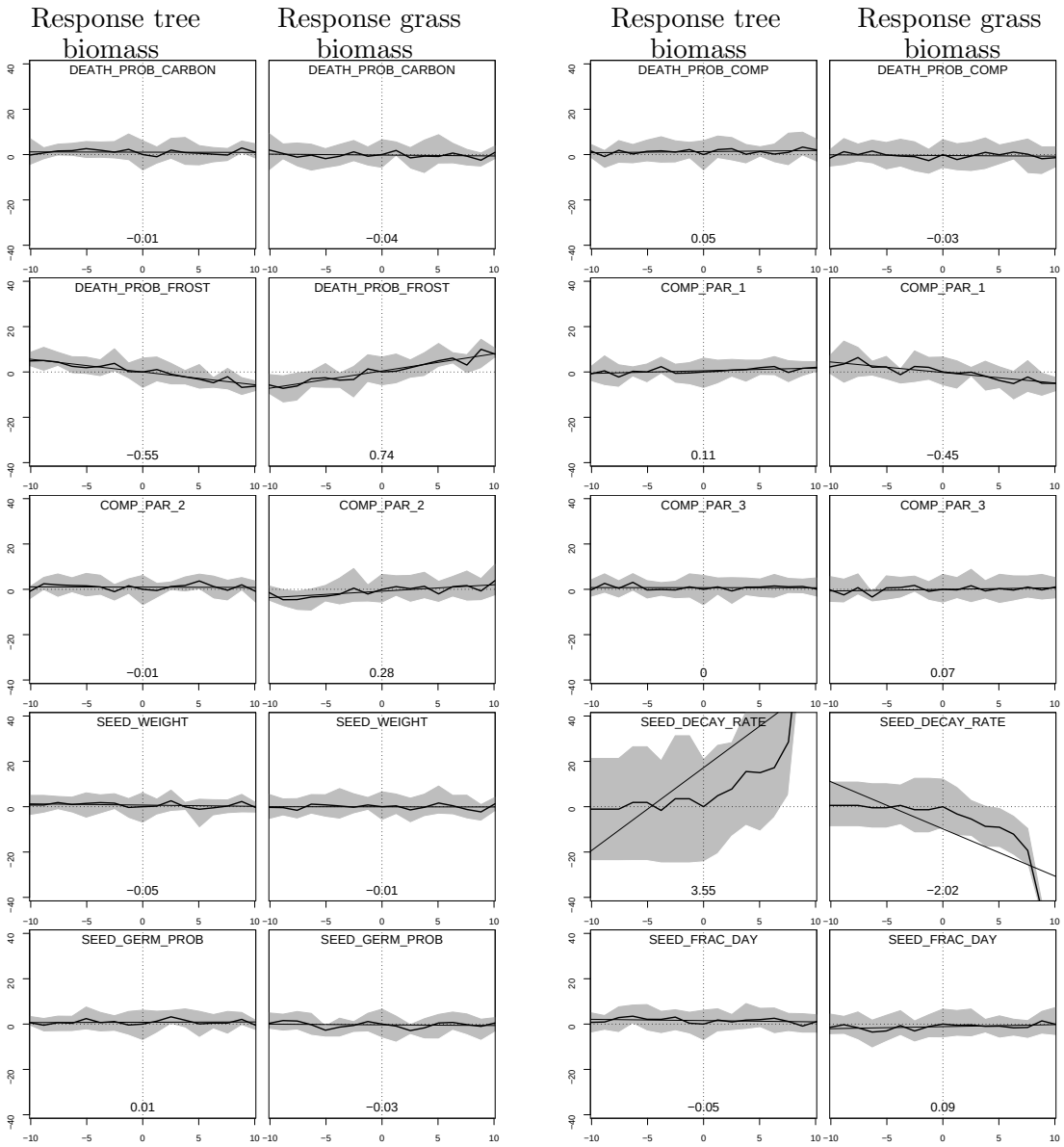

Figure 4.10: Sensitivity to reproduction and mortality parameters. See caption for Figure 4.9 for details.

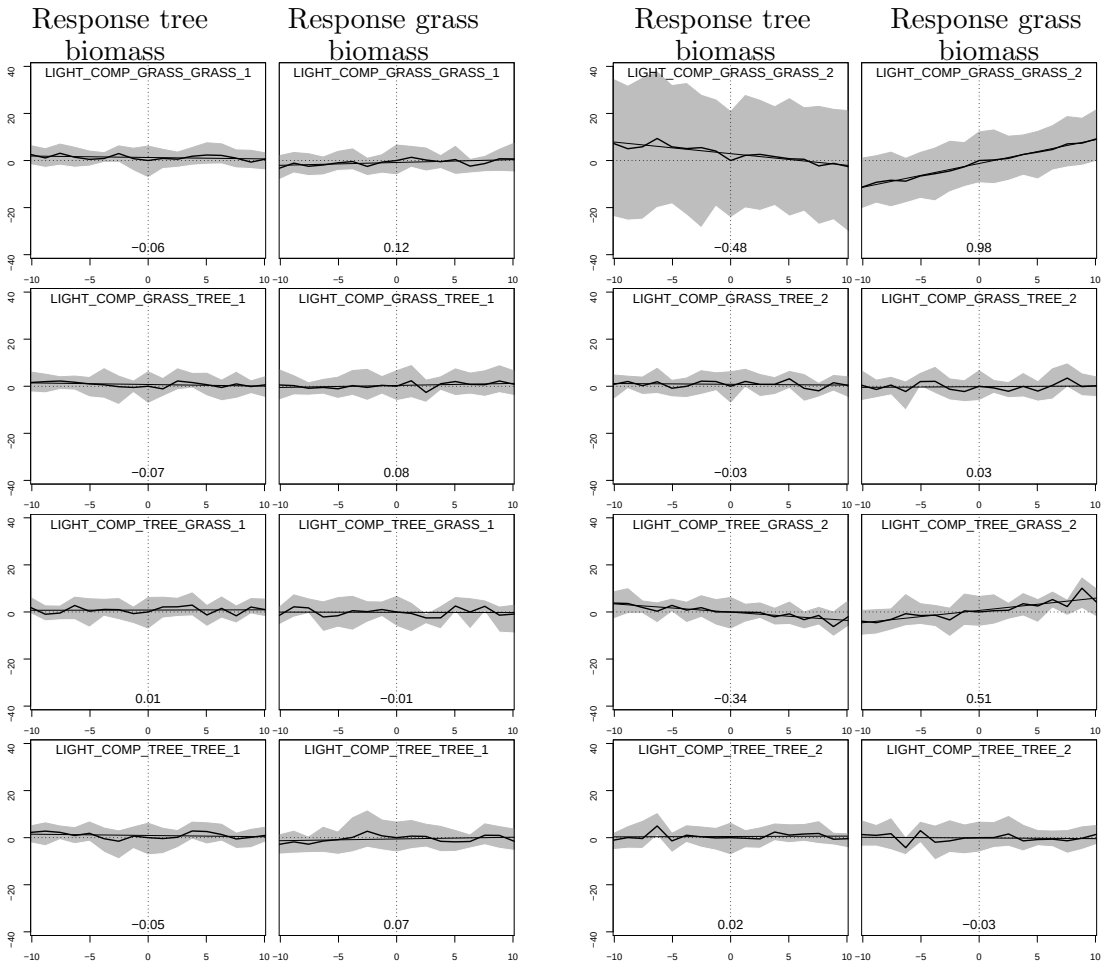

Figure 4.11: Sensitivity to parameters describing inter- and intraspecific light competition. See caption for Figure 4.9 for details.

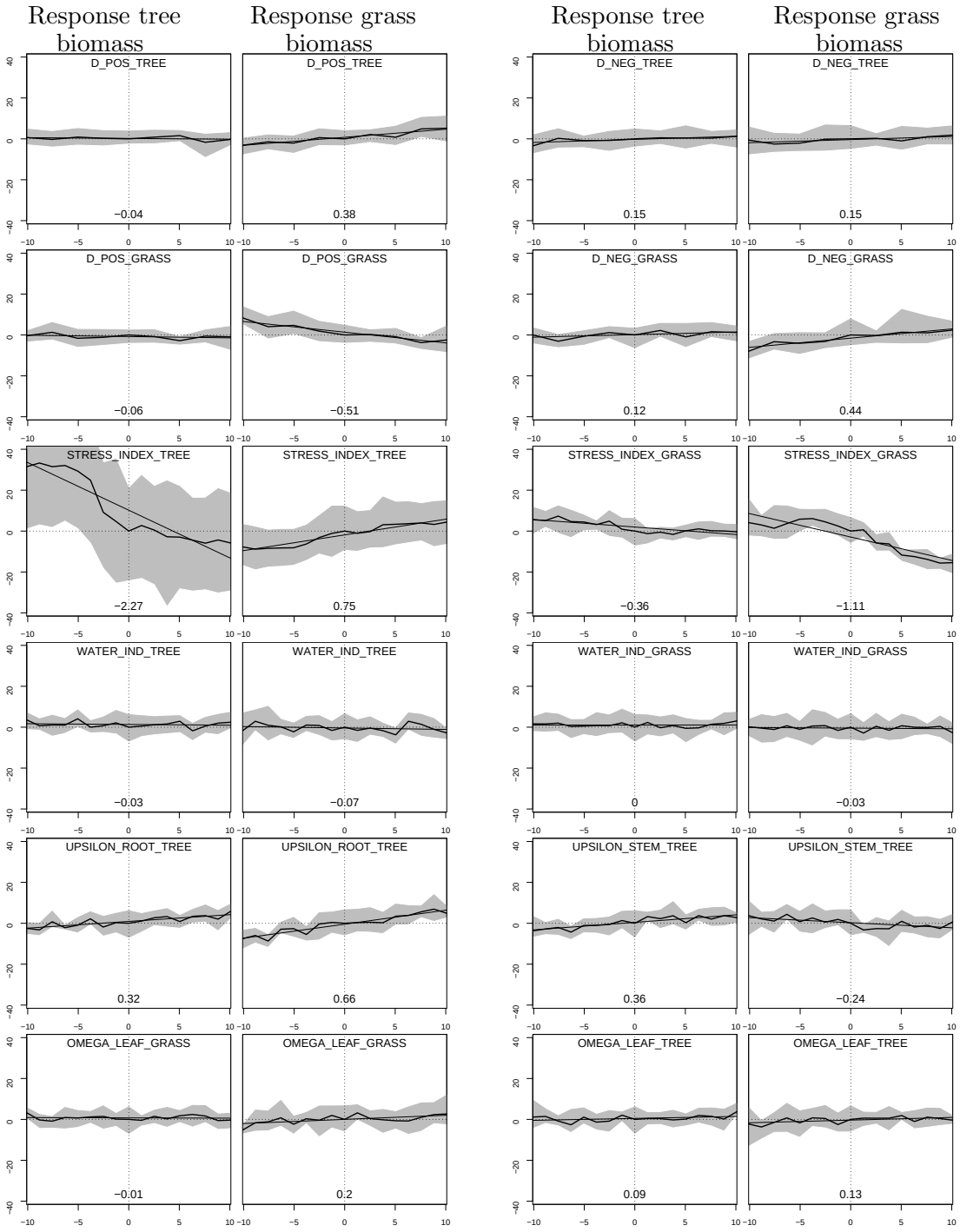

Figure 4.12: Sensitivity to parameters used in the phenology sub-model, C:N ratios and leaf longevity. See caption for Figure 4.9 for details.

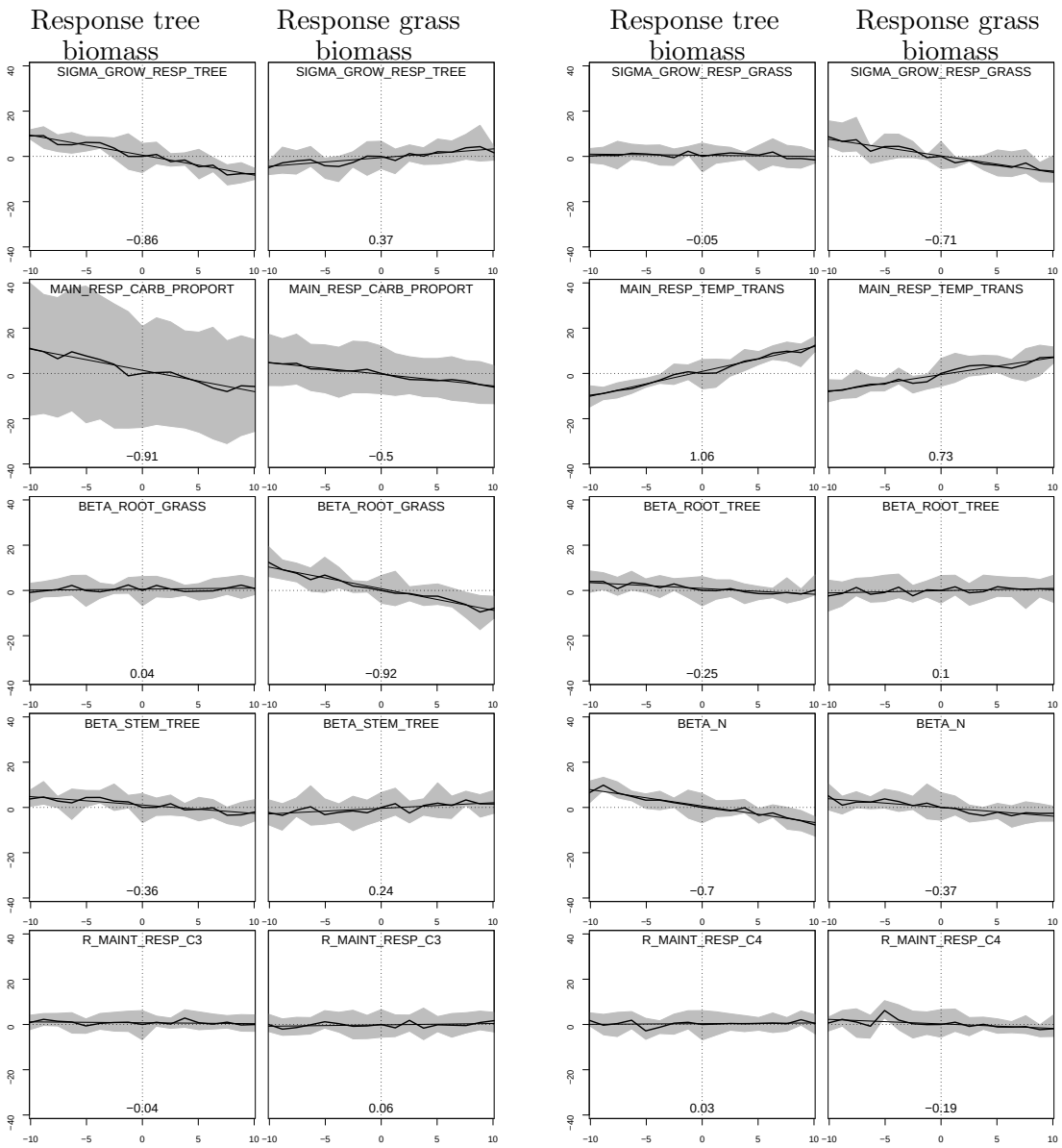

Figure 4.13: Sensitivity to parameters used in the respiration sub-model. See caption for Figure 4.9 for details.

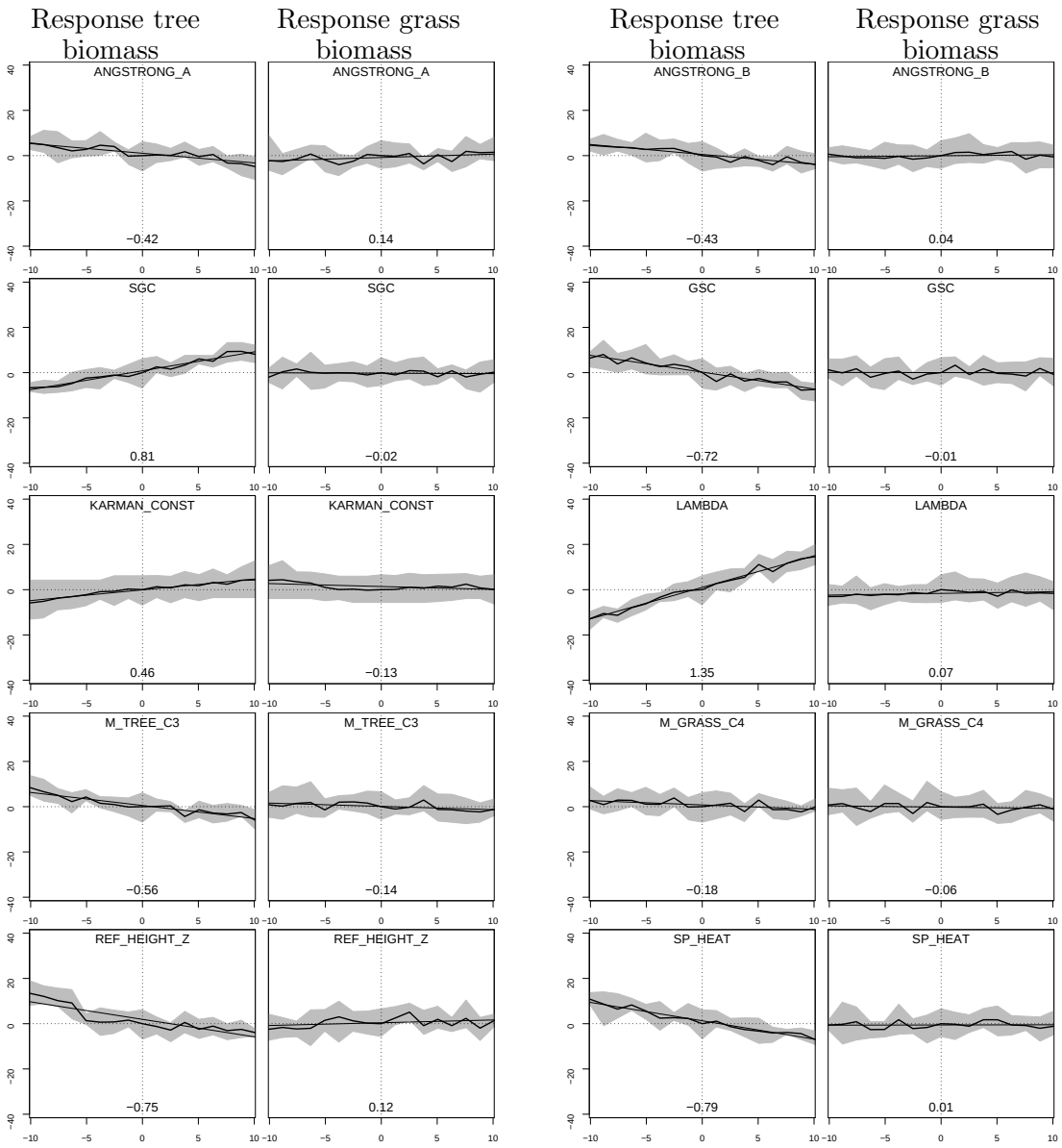

Figure 4.14: Sensitivity to constants of different sub-models (leaf physiology, radiation, stomatal conductance). See caption for Figure 4.9 for details.

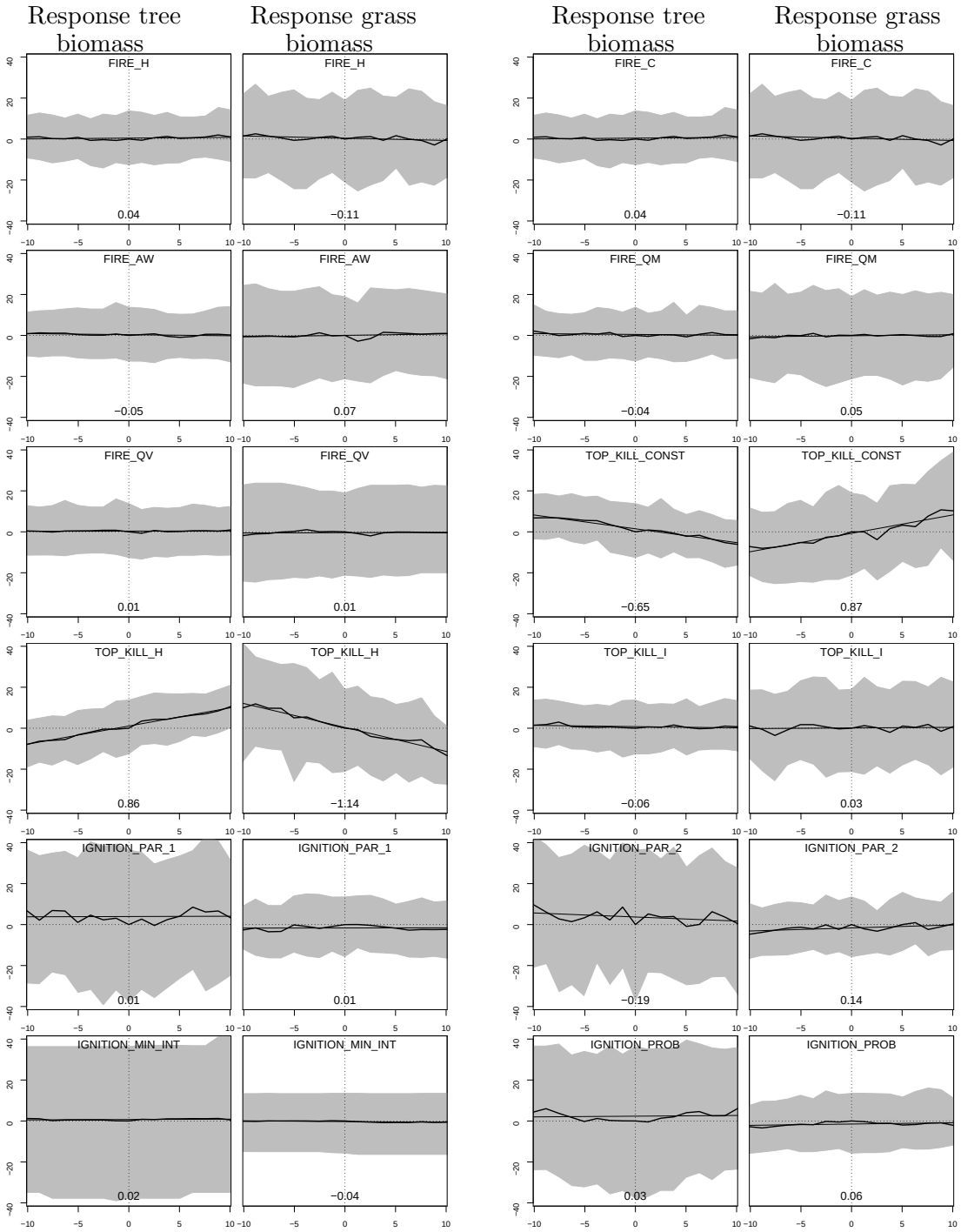

Figure 4.15: Model sensitivity to parameters used in the fire model. See caption for Figure 4.9 for details.

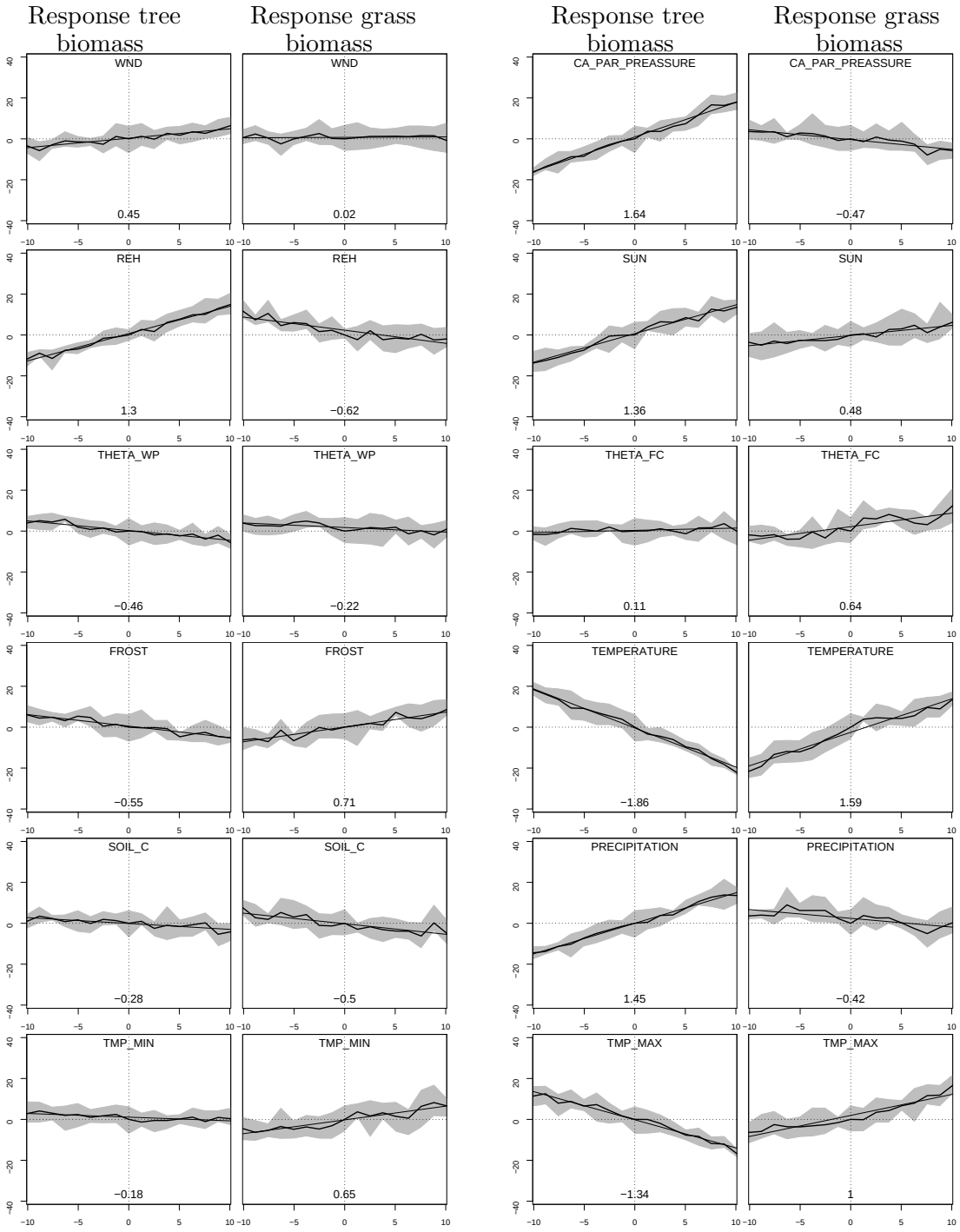

Figure 4.16: Model sensitivity to different climate variables taken from global databases. See caption for Figure 4.9 for details.

4.9 Perspectives – adaptive vegetation modelling

DGVMs are a powerful tool to explore vegetation dynamics and the global carbon cycle and they have been successfully employed in many studies (e.g. Cramer *et al.* 2001; Sitch *et al.* 2003; Woodward *et al.* 2004; Bond and Keeley 2005; Hély *et al.* 2006; Hickler *et al.* 2006; Schaphoff *et al.* 2006; Sato *et al.* 2007). However, a major weakness of existing DGVMs (including the aDGVM) is that they typically ignore variability in traits within one functional type or species and the potential of plants to adapt to environmental conditions or to climate change. The assumption of such models is, that the parameters used to simulate the current vegetation are still valid under future conditions (Clark *et al.* 2001). However, it has been observed that plants have a high potential to adapt to the environmental conditions by the modification of traits such as the growing season length or allocation patterns. Such adaptions allow plants to improve their performance and functionality under given and eventually changing environmental conditions (Novoplansky 2002). Since single species are defined by a continuum of trait combinations instead of a single and fixed trait combination, we might expect that the traits of single species might strongly differ on environmental gradients.

Existing vegetation models generally simulate a fixed number of different functional types where each type is characterized by a fixed trait combination. However, in reality the process of community assembly selects a community of species from a large pool of species, that performs best under given environmental conditions (Keddy 1992). Thereby, each species or functional type is defined by a spectrum of trait combinations. Community assembly implies that inefficient trait combinations are outcompeted. When environmental conditions change, then it is expected that the species composition at a site might change due to changes in the relative performance of different species. Hence, trait combinations that are efficient under current conditions might be inefficient under future conditions and the process of community assembly might allow other trait combinations to invade into the system and to establish. These dynamic processes are not simulated in existing vegetation models. In existing models, changing environmental conditions modify the equilibrial abundances of different functional types while the traits of the functional types, the plant community assembled at a site and the number of functional types are not influenced.

Existing vegetation modelling approaches simulate biodiversity as a discrete variable as each functional type is defined by only one point in the trait space and the number of functional types is fixed. This major weakness of existing vegetation models casts doubt

that they can reliably simulate how vegetation and vegetation dynamics respond along environmental gradients and to climate change. We argue that to improve DGVMs and their predictions, more general and adaptive vegetation models should be developed, that are not limited by the weaknesses of simulating biodiversity as a discrete variable as described in the previous paragraphs. Such models should (1) be individual-based, (2) allow plant populations or even single plants to adapt to the environment by allowing the dynamic adaption of selected plant traits and (3) aim to mimic the assembly of a community at a site from an infinite pool of species (Keddy 1992) by simulating mechanistic analogies of the processes of selection, mutation, inheritance and crossover. The inclusion of such processes would allow models to simulate biodiversity as a continuous variable in the sense that plants can potentially take arbitrary trait combinations and that depending on the environmental conditions of the specific study site, only a certain subset of the total pool of trait combinations can establish while inefficient trait combinations are outcompeted. In such a modelling framework, functional types are defined by a spectrum of trait combinations rather than by fixed traits. Such a modelling approach would allow to simulate effects of climate change on single individuals which has been argued to be necessary to understand how climate change modifies vegetation (Chuine and Beaubien 2001; McGill *et al.* 2006). A schematic representation of different vegetation modelling approaches and there dynamics under climate change is depicted in Figure 4.17.

One examples for a plant trait which should be considered in an adaptive vegetation model is phenology, which is tightly coupeled to SLA, leaf nitrogen and longevity. There is empirical evidence that the growing season length of vegetation is controlled by climatic conditions such as soil water dynamics or atmospheric CO_2 concentrations (Taylor *et al.* 2008) and longer growing seasons potentially indicate higher carbon gain. To a certain degree, the current version of the aDGVM allows the adaption of phenology to environmental conditions as phenology is controlled by a cost-benefit relation defined by photosynthesis and respiration. However, leaf phenology is, in the current model version, not linked to leaf longevity, leaf nitrogen content or to the SLA.

A second candidate for adaptive modelling is the carbon allocation scheme which is influenced by environmental conditions. For instance, in water limited systems, vegetation might build large root systems to maintain water supply. In dense systems, vegetation might invest much carbon to height growth to escape light competition. The carbon allocation model used in the aDGVM allows carbon gain of single plants to be allocated in response to environmental conditions as carbon is allocated to the biomass

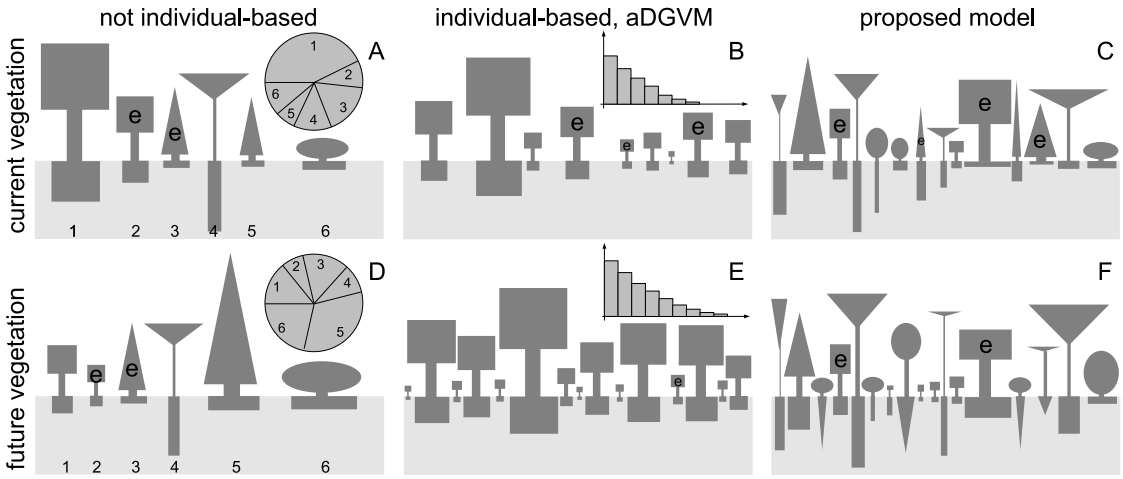

Figure 4.17: The panels depict how vegetation is represented in different vegetation models. (A) The model simulates six individuals where each individual represents a functional type. The "e" indicates an evergreen functional type. The number of individuals and their parameters are fixed. The dominant vegetation is defined by the relative abundance of the functional types (indicated by the pie chart). Here, functional type 1 is dominant. (B) The model is individual-based and each individual can differ in size or biomass (indicated by the histogram) while all individuals of one functional type have a fixed trait combination. The number of individuals is controlled by reproduction and mortality. The dominant vegetation is defined by biomass and density of different functional types. (C) The model is individual-based and each individual has a unique trait combination. Individuals can differ both in size or biomass and in allometric parameters. The number of individuals is controlled by reproduction and mortality. The dominant vegetation is defined by the relative abundance of individuals with a certain trait combination. Panels (D), (E) and (F) depict how climate change influences vegetation. (D) The relative abundances of the functional types change (depicted by the pie chart) while the number of functional types and their characteristics are not modified. (E) The number of trees, biomasses and the height structure (indicated by the histogram) are modified. The trait combination of individuals is not modified. (F) Tree number, tree community and traits of individuals can be modified. Some functional types were out-competed while other new functional types (indicated by triangular roots) could establish.

compartment that most limits the plants growth. However, due to the high plasticity of plants, changes in the allocation pattern might also modify the allometry of the plant, such as the ratios between stem height and stem diameter or between stem height and canopy radius. For instance, tall trees with thin stems might be superior competitors in dense tree stands as they can capture more light, while at sites with intense fires, trees with thick stems and barks might be me more efficient as they are more fire resistant. Such adaption processes are not possible in the aDGVM as allometric parameters are assumed to be constant.

The process of community assembly at a site from an infinite pool of species (Keddy 1992) can be realized in a vegetation model by simulating processes that mimic mutation, selection, crossover and inheritance. Mutation means that plant characteristics are subjected to random changes. Selection means that inefficient trait combinations cannot reproduce sufficiently to establish in the population and are outcompeted. Crossover and inheritance allow new individuals to obtain traits from some combination of traits of parent individuals. Hence, starting with a plant population where each plant is defined by its individual, eventually randomly chosen trait combination, an adaptive vegetation model iteratively assembles a plant community that performs best under the given environmental conditions while inefficient trait combinations cannot establish and are outcompeted. The community that can permanently establish defines the biome type at a site. In this model, each individual can be defined by a unique trait combination such that a functional type is defined by a spectrum of trait combinations rather than by a fixed trait combination. For instance, at sites where water supply and temperature are high throughout the whole year, plant performance might be maximized by an evergreen phenology and the majority of simulated individuals would be expected to be evergreen. At sites characterized by seasonality, plants must, when the environmental conditions are appropriate, quickly produce a high amount of leaf biomass to allow sufficient carbon gain. Hence, leaf construction cost should be low to optimize the plant's carbon efficiency (Wright *et al.* 2004). Under changing environmental conditions, the dominant functional type might change as the performance of a given trait combination might, although optimal under current conditions, be sub-optimal under future conditions.

The importance of the adaptive modelling approach is also supported by the sensitivity analysis (Section 4.8). Thus, variations in allocation parameters (a_{0R}, a_{0S} and a_{0L}) and allometry parameters (γ_c, H_1 and H_2) strongly modify the total grass and tree biomass which indicates that these parameters should be used within an adaptive model.

Other candidate traits for adaptive modeling are reproduction and mortality traits, although the sensitivity analysis showed that the impact of these processes is relatively low, compared to parameters describing allometry and allocation (Figure 4.10).

A related weakness of the current version of the aDGVM is, that it simulates tropical trees and C_4-grasses while ignoring other vegetation forms such as C_3-grasses, conifers or shrubs. These functional types cover great parts of the earth's surface and are major contributors to the global carbon cycle. To be able to simulate the global carbon cycle the aDGVM needs to be extended by these additional functional types. This extension should happen by applying the adaptive modelling paradigm. Additional traits for the photosynthetic pathway (C_3 or C_4) and for the leaf type (needle leaved or broad leaved) need to be included in the representation of individual plant. Further, a differentiation between forest tree species and savanna tree species is necessary. Major differences between these species are allometry and fire resistance (Hoffmann and Solbrig 2003; Hoffmann *et al.* 2003). In the extended model, it is again community assembly which determines the dominant functional type and hence which biome dominates. For instance, in boreal regions broad leaved trees are expected to be outcompeted by needle leaved trees due to low temperatures and short growing seasons. In arid regions, C_4-grasses might dominate over C_3-vegetation as they are better adapted to high temperatures.

4.10 Programming

The aDGVM is implemented in C++ and has been compiled on the Linux operating system using both the GNU-compiler (http://gcc.gnu.org) and the Intel compiler (http://www.intel.com). The Intel compiler was available on the Linux cluster of the Leibnitz Rechenzentrum (LRZ) in Munich/Garching (http://www.lrz-muenchen.de) that we used to conduct our simulations (see Chapter 5). Literature on C and C++ programming predominantly used for the model development was Kernighan and Ritchie (1990), Lowes and Paulik (1995), Schmaranz (2001) and Schmaranz (2003) as well as the C/C++ reference (http://www.cppreference.com). For the analysis of output data and for data plots (Chapter 5) we used the R package (R Development Core Team 2005). Please visit the website of our working group (http://www.geo.uni-frankfurt.de/ipg/ag/hi/index.html) or contact the authors (scheiter@em.uni-frankfurt.de, higgins@em.uni-frankfurt.de) for more details on the model.

The infrastructure necessary to conduct high resolution simulations (Chap-

ter 5) was provided by the LRZ. We had access to the Linux cluster (www.lrz-muenchen.de/services/compute) and used the 32 bit cluster as well as the 64 bit cluster for serial jobs and the 64 bit Altix system to run parallel jobs. For the Altix, we used MPI (Message Passing Interface) to parallelize the simulations. Parallelization was necessary as simulations are numerically expensive and would not be possible using a single desktop computer.

The LRZ porting initiative and in particular Iris Christadler supported us with using the LRZ Linux cluster and helped us to profile, optimize and parallelize the code. The code was optimized by compiler optimization and by profiling the code using the open source profiler kprof (http://kprof.sourceforge.net). Further, we used the memory checker valgrind (http://valgrind.org) and the GNU debugger (http://sourceware.org/gdb). Goedecker and Hoisie (2001) give an overview over principles and techniques of optimizing source code. The LRZ also offers courses on High Performance Computing (HPC) and parallel programming that were helpfull for the model development.

4.11 Model parameters

Table 4.1: Input data from databases, secondary environmental variables and constants. In Tables 4.1-4.14 the notation "prop" indicates a value between zero and one and "variable" indicates that this parameter is a modelled variable.

Name	Description	Value	Units
T_Δ	Daily temperature range	database	°C
$\bar{T}$	Mean day temperature	database	°C
w_f	Wet day frequency	database	frequency
r_m	Mean value of rain	database	$^{mm}/_{month}$
r_{cv}	Coefficient of variance of rain	database	%
p_s	Percentage of sunshine per day	database	%
h_s	Relative humidity	database	%
d_f	Frost days per month	database	$^{days}/_{month}$
u_{ref}	Reference wind speed	database	$^{m}/_{s}$
Z	Elevation	database	m
S_N	Soil nitrogen content	database	$^{g}/_{m^2}$
S_C	Soil carbon content	database	$^{g}/_{m^2}$
θ_{fc}	Field capacity	database	mm
θ_{wp}	Wilting point	database	mm
P	Atmospheric partial pressure	variable	Pa
T	Day temperature	variable	°C
T_{min}	Minimum temperature	variable	°C
T_{max}	Maximum temperature	variable	°C
s	Slope of vapor pressure curve	variable	$^{kPa}/_{C}$
γ	Psychrometric constant	variable	$^{kPa}/_{C}$
e^A	Actual vapor pressure	variable	kPa
e^S	Saturation vapor pressure	variable	kPa
ρ_{air}	Density of air	variable	$^{g}/_{m^3}$
h_{vpd}	Saturation vapor pressure deficit	variable	kPa
Q_p	Photosynthetically active radiation	variable	$^{\mu mol}/_{m^2 s}$
Q_0	Net radiation	variable	$^{\mu mol}/_{m^2 s}$
F_i	Simulated precipitation at day i	variable	mm

Table 4.2: Photosynthesis sub-model.

Name	Description	Value C_3	Value C_4	Units
A_{max}	Maximum light saturated photosynthesis	variable	variable	$\mu mol/m^2s$
A_0	Gross photosynthetic rate	variable	variable	$\mu mol/m^2s$
A_n	Net photosynthetic rate	variable	variable	$\mu mol/m^2s$
A_0^b	Gross photosynthesis (bio-physical)	variable	variable	$\mu mol/m^2s$
A_n^b	Net photosynthesis (bio-physical)	variable	variable	$\mu mol/m^2s$
A_n^d	Net photosynthesis (diffusion)	variable	variable	$\mu mol/m^2s$
V_{max}	Maximum carboxylation rate	variable	variable	$\mu mol/m^2s$
A_R	Scaling factor for C_4 photosynthesis	1	39/90	unitless
A_S	Scaling factor for V_{max}	2	2	unitless
R_{mLs}	Constant leaf level respiration rate	0.82	1.36	$\mu mol/m^2s$
c_a	Atmospheric partial pressure of CO_2	38.1	38.1	Pa
c_i	Internal CO_2 pressure (C_3 only)	$0.7c_a$	—	Pa
c_i	Bundle sheath value (C_4 only)	—	$8c_a$	Pa
K_c	Michaelis constant for CO_2	variable	variable	Pa
K_o	O_2 inhibition constant	variable	variable	Pa
τ	Fraction of RuBP to reaction of rubisco	variable	variable	prop
$f_{25}(T)$	Temperature function for K_c, K_o, τ	variable	variable	unitless
K_{25,K_c}	Constant for f_{25} for K_c	30	140	Pa
Q_{10,K_c}	Constant for f_{25} for K_c	2.1	2.1	Pa
K_{25,K_o}	Constant for f_{25} for K_o	30	34	Pa
Q_{10,K_o}	Constant for f_{25} for K_o	1.2	1.2	Pa
$K_{25,\tau}$	Constant for f_{25} for τ	2600	2600	Pa
$Q_{10,\tau}$	Constant for f_{25} for τ	0.57	0.67	Pa
O_i	Intercellular partial pressure of oxygen	21	21	kPa
Γ_*	CO_2 compensation point	variable	variable	Pa
J_c	Rubisco limited assimilation rate	variable	variable	$\mu mol/m^2s$
J_e	Light limited assimilation rate	variable	variable	$\mu mol/m^2s$
J_s	Transport limited assimilation rate for C_3	variable	—	$\mu mol/m^2s$
J_p	CO_2 limited assimilation rate for C_4	—	variable	$\mu mol/m^2s$
a	Leaf absorbtance of incident flux	0.86	0.80	unitless
α	Intrinsic quantum yield of photosynthesis	0.08	0.067	unitless
κ	Initial slope of response of CO_2	—	$0.7{\cdot}10^6$	$\mu mol/m^2s$
V_{max}^c	Initial estimation for V_{max}	0.8	0.4	$\mu mol/m^2s$
r	Respiration as fraction of V_{max}	0.015	0.025	prop
c_p	Specific heat of moist air	$1.013{\cdot}10^{-3}$	$1.013{\cdot}10^{-3}$	$MJ/kgdegC$
λ	Latent heat of air	2.45	2.45	MJ/kg

Table 4.3: Stomatal conductance sub-model.

Name	Description	Value C_3	Value C_4	Units
g_s	Leaf level stomatal conductance	variable	variable	$^{\mu mol}/_{m^2 s}$
m	Empirical parameter for g_s	9	4	unitless
b	Empirical parameter for g_s	0.01	0.04	$^{\mu mol}/_{m^2 s}$
g_b	Leaf level boundary layer conductance	variable	variable	m
c_s	Partial pressure of CO_2 at leaf surface	variable	variable	Pa
D_L	Characteristic leaf dimension	0.02	0.005	m
$\bar{H}$	Mean vegetation height	1.5	1.5	m
$u(z)$	Wind at height z from ground level	variable	variable	$^{m}/_{s}$
z_d	Displacement height	$0.86\bar{H}$	$0.86\bar{H}$	m
z_0	Roughness length	$0.06\bar{H}$	$0.06\bar{H}$	m
z_{ref}	Reference height	10	10	m

Table 4.4: Biomass pools of a plant.

Name	Description	Value	Units
B_R	Live root biomass	variable	$^{kg}/_{plant}$
B_S	Live stem biomass	variable	$^{kg}/_{plant}$
B_L	Live leaf biomass	variable	$^{kg}/_{plant}$
B_{Ss}	Standing dead stem biomass	variable	$^{kg}/_{plant}$
B_{Ls}	Standing dead leaf biomass	variable	$^{kg}/_{plant}$
B_{Rd}	Dead root biomass	variable	$^{kg}/_{plant}$
B_{Sd}	Lying dead stem biomass	variable	$^{kg}/_{plant}$
B_{Ld}	Lying dead leaf biomass	variable	$^{kg}/_{plant}$

Table 4.5: Allometric constants and variables.

Name	Description	Value C_3	Value C_4	Units
H	Height of plant	variable	variable	m
H_1	Linear factor for height calculation	1.3	3.5	unitless
H_2	Exponent for height calculation	0.392	0.5	unitless
d_s	Stem diameter	variable	variable	cm
d_{s1}	Parameter to calculate stem diameter	2.797	—	unitless
d_{s2}	Parameter to calculate stem diameter	200	—	unitless
$\mathcal{C}$	Canopy area of plant	variable	variable	m^2
γ_c	Ratio of canopy radius to height	0.37	0.4	prop
L	Leaf area index	variable	variable	unitless
A_{SL}	Specific leaf area	10	10.9	$^{m^2}/_{kg}$
D_{root}	Rooting depth	variable	variable	m
D_{mrd}	Maximum rooting depth	2	0.3	m
D_{soil}	Soil depth	2	2	m
D_{cyl}	Depth of cylindrical root	variable	variable	m
ρ_r	Density of root biomass	100	100	$^{kg}/_{m^3}$
r_r	Minimum root radius	0.015	0.005	m

Table 4.6: Canopy scaling.

Name	Description	Value	Units
Q_{sum}	Light received by a plant	variable	$^{\mu mol}/_{m^2 s}$
$Q(l)$	Light distribution in canopy	variable	$^{\mu mol}/_{m^2 s}$
Q_i	Light availability index of plants	variable	prop
k	Canopy extinction coefficient	0.5	unitless
θ_i	Soil moisture content in layer i	variable	mm
$G(\theta_i)$	Soil water availability in layer i	variable	%
$\beta(\theta_i)$	Soil moisture function for G_i	variable	%
d_i	Thickness of soil layer i	defined	m
G_w	Water availability index of plants	variable	%
A_c	Light stressed canopy photosynthesis	variable	$^{\mu mol}/_{m^2 s}$
A_{cs}	Water and light stressed canopy photosynthesis	variable	$^{\mu mol}/_{m^2 s}$
g_s^c	Canopy level stomatal conductance	variable	$^{\mu mol}/_{m^2 s}$
g_b^c	Canopy boundary layer conductance	variable	$^{\mu mol}/_{m^2 s}$
c_s^c	Canopy partial pressure of CO_2	variable	Pa
K	Von Karman constant	0.41	unitless

Table 4.7: Respiration sub-model.

Name	Description	Value C_3	Value C_4	Units
β_N	Respiration rate for roots and stems	0.218	0.218	$^{\mathrm{kg\,C}}/_{\mathrm{kg\,N}}$
β_S	Fraction of sapwood in stems	2.5	15	%
β_R	Fraction of sapwood in roots	2.5	15	%
v_S	C to N ratio for stems	150	120	prop
v_R	C to N ratio for roots	60	120	prop
$f(T)$	Temperature function for respiration	variable	variable	unitless
σ	Growth respiration constant	0.35	0.35	prop
R_g	Growth respiration	variable	variable	$^{\mu\mathrm{mol}}/_{\mathrm{m^2 s}}$
R_m	Total maintenance respiration	variable	variable	$^{\mathrm{kg}}/_{\mathrm{d\,plant}}$
R_{mL}	Leaf maintenance respiration	variable	variable	$^{\mathrm{kg}}/_{\mathrm{d\,plant}}$
R_{mS}	Stem maintenance respiration	variable	variable	$^{\mathrm{kg}}/_{\mathrm{d\,plant}}$
R_{mR}	Root maintenance respiration	variable	variable	$^{\mathrm{kg}}/_{\mathrm{d\,plant}}$

Table 4.8: Carbon allocation sub-model.

Name	Description	Value C_3	Value C_4	Units
C_Δ	Net carbon gain of plant	variable	variable	$^{\mathrm{kg}}/_{\mathrm{d\,plant}}$
a_R	Proportion of carbon allocated to roots	variable	variable	%
a_S	Proportion of carbon allocated to stem	variable	variable	%
a_L	Proportion of carbon allocated to leaf	variable	variable	%
a_{0R}	Not-limited carbon gain allocated to roots	0.35	0.4	%
a_{0S}	Not-limited carbon gain allocated to stem	0.35	0	%
a_{0L}	Not-limited carbon gain allocated to leaf	0.3	0.6	%
C_i	Limitation factor of photosynthesis	variable	variable	prop

Table 4.9: Phenology sub-model.

Name	Description	Value C_3	Value C_4	Units
A_{index}	Stress index controlling phenology	variable	variable	unitless
G_i	Water availability index for phenology	variable	variable	prop
T_i	Temperature index for phenology	variable	variable	prop
T_*	Threshold temperature for phenology	15	15	°C
d_{neg}	Counter for days with negative C balance	7	5	d
d_{pos}	Counter for days with positive C balance	10	7	d
ζ_L	Remaining leaf biomass after litter fall	0.1	0.1	prop

Table 4.10: Decomposition and mass turnover.

Name	Description	Value C_3	Value C_4	Units
ω_R	Longevity of root biomass	9125	384	d
ω_S	Longevity of stem biomass	9125	384	d
ω_L	Longevity of leaf biomass	451	417	d
ω_D	Longevity of dead biomass	1408	577	d
ξ_L	Standing to lying dead grass biomass	0	$7.5{\cdot}10^{-2}$	%

Table 4.11: Evapotranspiration and population properties.

Name	Description	Units
Υ	Treecover	prop
n_t	Number of trees	number
S	Size of study site	m^2
E_t	Total evapotranspiration	$^{mm}/_{day}$
E_t^s	Soil evapotranspiration	$^{mm}/_{day}$
E_t^p	Single plant evapotranspiration	$^{mm}/_{day}$
E_t^g	Total grass evapotranspiration	$^{mm}/_{day}$
E_t^t	Total tree evapotranspiration	$^{mm}/_{day}$

Table 4.12: Light competition.

Name	Description	variable	Units
e_1	Probability function for competitor tree	1.1	unitless
e_2	Probability function for competitor tree	1.5	unitless
e_3	Probability function for competitor tree	1000	unitless
Q_{comp}	Shading effect of competitor tree	variable	prop
Q_{grass}	Shading effect of grasses on trees	variable	prop
Q_{tree}	Shading effect of trees on grasses	variable	prop
Q_{dead}	Shading effect of dead grass	variable	prop
μ_c	Maximum effect of Q_{comp}	0.35	prop
μ_g	Maximum effect of Q_{grass}	0.25	prop
μ_t	Maximum effect of Q_{tree}	0.4	prop
μ_d	Maximum effect of Q_{dead}	0.5	prop
H_t	Height of target tree	variable	m
H_c	Height of competitor tree	variable	m
H_g	Height of grasses	variable	m

Table 4.13: Reproduction and mortality sub-model.

Name	Description	Value	Units
B_{seed}	Weight of tree seed	1	g
A_a	Minimum age of trees for seed production	10	years
ϕ_i	Seed production of tree i	variable	seeds
Φ	Seed production of all trees	variable	seeds
ϕ_{mort}	Mortality rate of seed per year	70	%
ϕ_{sprout}	Proportion of seed that sprouts per day	10	%
ϕ_{germ}	Germination probability of seed	25	%
d_{wet}	Number of wet days needed for germination	3	days
P_{carb}	Mortality rate: carbon deficiency	0.1	%
P_{comp}	Mortality rate: competitor	0.1	%
P_{frost}	Mortality rate: frost	0.1	%
P_{death}	Total mortality rate of trees	variable	%

Table 4.14: Fire sub-model.

Name	Description	Value	Units
I	Fire intensity	variable	$^{kJ}/_{s\,m}$
h	Heat yield of grass	16890	$^{kJ}/_{kg}$
c	Regression parameter	301	unitless
a_w	Regression parameter	119.7	unitless
Q_m	Heat of preignition	$2.6{\cdot}10^6$	$^{J}/_{g}$
Q_v	Heat of preignition	160749	$^{J}/_{g}$
B_F	Fuel biomass	variable	$^{kg}/_{m^2}$
B_{live}	Living fuel biomass	variable	kg
B_{dead}	Dead fuel biomass	variable	kg
θ_F	Fuel moisture	variable	%
θ_{live}	Moisture of living fuel biomass	variable	%
θ_{dead}	Moisture of dead fuel biomass	variable	%
θ_r	Drying of dead fuel biomass	0.95	prop
T	Days since litter fall	variable	days
i_1	Fire ignition probability function	0.08333	unitless
i_2	Fire ignition probability function	0.1	unitless
p_{fire}	Fire probability	1	%
$P_{topkill}$	Topkill probability of trees	variable	%
D_1	Regression parameter for topkill	4.3	unitless
D_2	Regression parameter for topkill	5.003	unitless
D_3	Regression parameter for topkill	0.004408	unitless
ψ_g	Grass survival after fire	0.1	%
ψ_{ts}	Tree stem survival after fire	1	%
ψ_{tl}	Tree leaf survival after fire	0.1	%

Table 4.15: Size of soil layers.

Name	Description	Value	Cumul.	Units
d_1	Layer S_1	5	5	cm
d_2	Layer S_2	5	10	cm
d_3	Layer S_3	10	20	cm
d_4	Layer S_4	10	30	cm
d_5	Layer S_5	10	40	cm
d_6	Layer S_6	20	60	cm
d_7	Layer S_7	20	80	cm
d_8	Layer S_8	20	100	cm
d_9	Layer S_9	25	125	cm
d_{10}	Layer S_{10}	25	150	cm
d_{11}	Layer S_{11}	25	175	cm
d_{12}	Layer S_{12}	25	200	cm

Table 4.16: The table summarizes the results from the sensitivity analysis. The columns ΔB_T and ΔB_G give the relative change of tree and grass biomass (in %) when the target parameter (given in the first column) is varied by 1%. The value represents the slope of a linear approximation of the sensitivity curve.

Variable	ΔB_T	ΔB_G
ZZ_A0_LEAF_GRASS	-0.17	-0.27
ZZ_A0_LEAF_TREE	-0.17	0.03
ZZ_A0_ROOT_GRASS	0.03	0.18
ZZ_A0_ROOT_TREE	-0.44	0.55
ZZ_A0_STEM_TREE	0.54	-0.52
ZZ_ABS_PHOTONS_C3	0	0
ZZ_ABS_PHOTONS_C4	0	0
ZZ_ALBEDO	0.25	0.05
ZZ_ALPHA_C3	0	0
ZZ_ALPHAR_F_C4	0	0
ZZ_ANGSTRONG_A	-0.42	0.14
ZZ_ANGSTRONG_B	-0.43	0.04
ZZ_BETA_N	-0.7	-0.37
ZZ_BETA_ROOT_GRASS	0.04	-0.92
ZZ_BETA_ROOT_TREE	-0.25	0.1
ZZ_BETA_STEM_TREE	-0.36	0.24
ZZ_B_GRASS_C4	0	0
ZZ_B_TREE_C3	0	0
ZZ_BULK_DENS	0	0
ZZ_CA_PAR_PREASSURE	1.64	-0.47
ZZ_CLD_GRASS	0	0
ZZ_CLD_TREE	-0.03	0.03
ZZ_COMP_PAR_1	0.11	-0.45
ZZ_COMP_PAR_2	-0.01	0.28
ZZ_COMP_PAR_3	0	0.07
ZZ_CS_FACTOR	-0.01	-0.01
ZZ_DEATH_PROB_CARBON	-0.01	-0.04
ZZ_DEATH_PROB_COMP	0.05	-0.03
ZZ_DEATH_PROB_FROST	-0.55	0.74
ZZ_D_NEG_GRASS	0.12	0.44
ZZ_D_NEG_TREE	0.15	0.15
ZZ_D_POS_GRASS	-0.06	-0.51
ZZ_D_POS_TREE	-0.04	0.38
ZZ_ELEVATION	0.09	0.04
ZZ_EXTINC_EXP_GRASS	0.02	-0.99
ZZ_EXTINC_EXP_TREE	-0.49	-0.4
ZZ_EXTINC_FAC_GRASS	-0.01	0.2
ZZ_EXTINC_FAC_TREE	0.16	0.1

Table 4.17: Continuation of Table 4.17.

Variable	ΔB_T	ΔB_G
ZZ_FIRE_AW	-0.05	0.07
ZZ_FIRE_C	0.04	-0.11
ZZ_FIRE_H	0.04	-0.11
ZZ_FIRE_QM	-0.04	0.05
ZZ_FIRE_QV	0.01	0.01
ZZ_FROST	-0.55	0.71
ZZ_GAMMA_CANOPY_GRASS	0	0
ZZ_GAMMA_CANOPY_TREE	0.78	-1.18
ZZ_GSC	-0.72	-0.01
ZZ_HEIGHT_C1_GRASS	0.01	0.13
ZZ_HEIGHT_C1_TREE	0.98	-1.37
ZZ_HEIGHT_C2_GRASS	-0.13	-0.11
ZZ_HEIGHT_C2_TREE	1.76	-2.85
ZZ_IGNITION_MIN_INT	0.02	-0.04
ZZ_IGNITION_PAR_1	0.01	0.01
ZZ_IGNITION_PAR_2	-0.19	0.14
ZZ_IGNITION_PROB	0.03	0.06
ZZ_KAPPA_C4	0	0
ZZ_KARMAN_CONST	0.46	-0.13
ZZ_K_CAN_EXT	-0.14	-0.2
ZZ_KC_K25_C3	-0.58	0.49
ZZ_KC_K25_C4	0	0
ZZ_KC_Q10_C3	-0.09	0.01
ZZ_KC_Q10_C4	0	0
ZZ_KO_K25_C3	0.29	-0.24
ZZ_KO_K25_C4	0	0
ZZ_KO_Q10_C3	0.09	-0.07
ZZ_KO_Q10_C4	0	0
ZZ_LAMBDA	1.35	0.07
ZZ_LIGHT_COMP_GRASS_GRASS_1	-0.06	0.12
ZZ_LIGHT_COMP_GRASS_GRASS_2	-0.29	1.1
ZZ_LIGHT_COMP_GRASS_TREE_1	-0.07	0.08
ZZ_LIGHT_COMP_GRASS_TREE_2	-0.03	0.03
ZZ_LIGHT_COMP_TREE_GRASS_1	0.01	-0.01
ZZ_LIGHT_COMP_TREE_GRASS_2	-0.34	0.51
ZZ_LIGHT_COMP_TREE_TREE_1	-0.05	0.07
ZZ_LIGHT_COMP_TREE_TREE_2	0.02	-0.03
ZZ_MAIN_RESP_CARB_PROPORT	-0.91	-0.5
ZZ_MAIN_RESP_FAC	0	0
ZZ_MAIN_RESP_TEMP_FAC	0	0
ZZ_MAIN_RESP_TEMP_TRANS	1.06	0.73
ZZ_MAIN_RESP_TRANS	0	0
ZZ_MAX_ROOT_DEP_GRASS	-0.07	1.11
ZZ_MAX_ROOT_DEP_TREE	-7.05	20.35

Table 4.18: Continuation of Table 4.17.

Variable	ΔB_T	ΔB_G
ZZ_M_GRASS_C4	-0.18	-0.06
ZZ_MIN_ROOT_RAD_TREE	0.04	-0.04
ZZ_MOIST_CONST_A	0	0
ZZ_MOIST_CONST_B	0	0
ZZ_MOIST_CONST_C	0	0
ZZ_MOIST_CONST_D	0	0
ZZ_M_TREE_C3	-0.56	-0.14
ZZ_OI_PAR_PREASSURE	-0.19	0.07
ZZ_OMEGA_DEAD_GRASS	0	0
ZZ_OMEGA_DEAD_TREE	0	0
ZZ_OMEGA_LEAF_GRASS	-0.01	0.2
ZZ_OMEGA_LEAF_TREE	0.09	0.13
ZZ_OMEGA_ROOT_GRASS	0	0
ZZ_OMEGA_ROOT_TREE	0	0
ZZ_OMEGA_STEM_GRASS	0	0
ZZ_OMEGA_STEM_TREE	0	0
ZZ_OMEGA_TRANS	-0.07	0.23
ZZ_PRECIPITATION	1.45	-0.42
ZZ_REF_HEIGHT_Z	-0.75	0.12
ZZ_REH	1.3	-0.62
ZZ_REM_BM_GRASS	0.02	0.02
ZZ_REM_BM_TREE	0.02	-0.08
ZZ_R_MAINT_RESP_C3	-0.04	0.06
ZZ_R_MAINT_RESP_C4	0.03	-0.19
ZZ_ROOT_DENSITY_GRASS	-0.05	0.06
ZZ_ROOT_DENSITY_TREE	-0.03	0.05
ZZ_SBC	0.18	-0.02
ZZ_SEED_DECAY_RATE	3.55	-2.02
ZZ_SEED_FRAC_DAY	-0.05	0.09
ZZ_SEED_GERM_PROB	0.01	-0.03
ZZ_SEED_WEIGHT	-0.05	-0.01
ZZ_SGC	0.81	-0.02
ZZ_SIGMA_GROW_RESP_GRASS	-0.05	-0.71
ZZ_SIGMA_GROW_RESP_TREE	-0.86	0.37
ZZ_SLA_GRASS	-0.04	0.15
ZZ_SLA_TREE	0.21	-0.3
ZZ_SOIL_C	-0.28	-0.5
ZZ_SOIL_N	0	0
ZZ_SP_HEAT	-0.79	0.01
ZZ_STEM_AREA_C1	0.11	-0.32
ZZ_STEM_AREA_C2	-0.05	0.24
ZZ_STRESS_INDEX_GRASS	-0.36	-1.11
ZZ_STRESS_INDEX_TREE	-2.27	0.75

Table 4.19: Continuation of Table 4.17.

Variable	ΔB_T	ΔB_G
ZZ_SUN	1.36	0.48
ZZ_TAU_K25_C3	-0.08	0.12
ZZ_TAU_K25_C4	0	0
ZZ_TAU_Q10_C3	-0.06	0.04
ZZ_TAU_Q10_C4	0	0
ZZ_TEMPERATURE	-1.86	1.59
ZZ_THETA_FC	0.11	0.64
ZZ_THETA_WP	-0.46	-0.22
ZZ_TMP	-0.42	0.64
ZZ_TMP_MAX	-1.34	1
ZZ_TMP_MIN	-0.18	0.65
ZZ_TOP_KILL_CONST	-0.65	0.87
ZZ_TOP_KILL_H	0.86	-1.14
ZZ_TOP_KILL_I	-0.06	0.03
ZZ_UPSILON_ROOT_GRASS	0	0
ZZ_UPSILON_ROOT_TREE	0.32	0.66
ZZ_UPSILON_STEM_GRASS	-0.01	0.01
ZZ_UPSILON_STEM_TREE	0.36	-0.24
ZZ_VEGETATION_HEIGHT	-0.01	0.06
ZZ_WATER_IND_GRASS	0	-0.03
ZZ_WATER_IND_TREE	-0.03	-0.07
ZZ_WND	0.45	0.02
ZZ_Z0_CONST	0.21	0.03
ZZ_ZD_CONST	-1.23	-1.42
ZZ_Z_WIND	0	0

5 Impacts of climate change on the vegetation of Africa: an adaptive dynamic vegetation modelling approach

Abstract. Recent IPCC projections suggest that Africa will be subject to particularly severe changes in atmospheric conditions. How the vegetation of Africa and particularly the grassland-savanna-forest complex will respond to these changes has rarely been investigated. Most studies on global carbon cycles use vegetation models that do not adequately account for the complexity of the interactions that shape the distribution of tropical grasslands, savannas and forests. This casts doubt on their ability to reliably simulate the future vegetation of Africa. We present a new vegetation model, the aDGVM, that was specifically developed for tropical vegetation. The aDGVM combines established components from existing DGVMs with novel process-based and adaptive modules for phenology, carbon allocation and fire within an individual-based framework. Thus, the model allows vegetation to adapt phenology, allocation and physiology to changing environmental conditions and disturbances in a way not possible in models based on fixed functional types. We used the model to simulate the current vegetation patterns of Africa and found good agreement between model projections and vegetation maps. We simulated vegetation in absence of fire and found that fire suppression strongly influences tree dominance at the regional scale while at a continental scale fire suppression increases biomass in vegetation by a more modest 13%. Simulations under elevated temperature and atmospheric CO_2 concentrations predicted longer growing periods, higher allocation to roots, higher fecundity, more biomass and a dramatic shift towards tree dominated biomes. Our analyses suggest that the CO_2 fertilisation effect is not saturated at ambient CO_2 levels and will strongly increase in response to further increases in CO_2 levels. The model provides a general and flexible framework for describing vegetation response to the interactive effects of climate and disturbances.

Key words: Savanna, Africa, climate change, DGVM, process-based model, fire, demographic model, adaptive vegetation modelling, vegetation distribution, aDGVM

5.1 Introduction

Many studies have shown that the climatic conditions under which plants grow are changing (IPCC 2007). Three major determinants of plant growth, the atmospheric CO_2 concentration, rainfall and temperature have changed significantly since the pre-industrial time and current projections obtained from simulation models predict further changes in these climate variables (IPCC 2007). It is well established that the nutrient and water use efficiency of vegetation responds to changes in the climate and the atmospheric CO_2 concentrations (Drake *et al.* 1997; Ehleringer *et al.* 1997). In African savannas, which are characterized by the co-dominance of C_4-grasses and C_3-trees (Sarmiento 1984), paleo-ecological studies have correlated increasing CO_2 with an increasing abundance of savanna trees (Scott 1999; Bond *et al.* 2003). Hence, an increase in CO_2 might favor trees over grasses due to potentially larger benefit that C_3-plants would gain over C_4-plants. On the other hand, an increase in temperature would increase rates of C_4-photosynthesis (Collatz *et al.* 1992; Ehleringer *et al.* 1997), C_3-photo-respiration (Tjoelker *et al.* 2001; Arora 2003) and evaporative demand (Jones 1992; Allen *et al.* 1998). Each of these temperature driven factors might directly as well as indirectly by favoring fire, favor grasses. This tension between stimulation of grasses and/or trees under projected atmospheric changes makes the projection of the relative abundances of trees and grasses and thereby the amount of carbon stored in vegetation challenging. Yet, even though it is anticipated that tropical regions in general and Africa in particular will be subjected to significant atmospheric changes (Hély *et al.* 2006; IPCC 2007), the impacts of atmospheric changes in these regions have rarely been specifically considered (Cao *et al.* 2001; Grace *et al.* 2006; Hély *et al.* 2006; Williams *et al.* 2007).

Studies that address how the carbon cycle and carbon storage are modified in response to elevated climates typically use dynamic global vegetation models (DGVMs). For instance, Cramer *et al.* (2001) conducted a global analysis of effects of climate change on future vegetation and carbon storage using six different DGVMs. However, most of the DGVMs used in Cramer *et al.* (2001)'s study predicted either grasslands or tropical forests in the savanna regions. More recent studies, the majority of which use further developed versions of the models used in Cramer *et al.* (2001)'s study, also underestimate the extent of savannas (Bonan *et al.* 2003; Hély *et al.* 2006; Hickler *et al.* 2006; Schaphoff *et al.* 2006; Sato *et al.* 2007). For Africa, the best agreement between simulated and observed functional types was obtained with the SDGVM (Cramer

et al. 2001; Woodward and Lomas 2004; Bond *et al.* 2005). One reason for the underestimation of the extent of savannas is that existing DGVMs were not specifically designed and tested for tropical grass-tree systems (House *et al.* 2003). Thus, existing DGVMs do not simulate or do not adequately describe the complex web of ecological processes such as competition and fire that shape the relative abundance of grasses and trees in the tropics (Scholes and Archer 1997; Higgins *et al.* 2000; Sankaran *et al.* 2004). However, the inability of many DGVMs to correctly simulate the contemporary distribution of savannas casts doubt on their ability to reliably simulate how vegetation in the tropics might respond to future climate change.

One particular weakness of existing DGVMs is their poor representation of fire and the effects of fire on vegetation (Thonicke *et al.* 2001). Fire has been shown to be a major determinant of the structure and dynamics of savannas (Scholes and Archer 1997; Higgins *et al.* 2000; Sankaran *et al.* 2004; Bond *et al.* 2005; Sankaran *et al.* 2005; Higgins *et al.* 2007a). Thus, fire has been shown to modify the demography of trees and fire is often invoked to explain the substantial discrepancies between observed biomass and potential biomass (Bond *et al.* 2005; Sankaran *et al.* 2005; Higgins *et al.* 2007a). Despite its importance, fire is treated simplistically in DGVMs. For instance, the LPJ, the SDGVM and the SEIB-DGVM (Sato *et al.* 2007) use fire models that assume that fire frequency is determined purely by the moisture content of litter and that fires remove a pre-defined fraction of biomass (Thonicke *et al.* 2001; Venevsky *et al.* 2002). However, the response of trees to fire is more complex since the aboveground biomass of small (<2m height) trees is often completely consumed by fire, while large (>2m height) trees are generally unaffected by fire (Higgins *et al.* 2000). For an adequate representation of this *topkill* effect it is necessary to use an individual-based model that can simulate growth and fire effects for individual trees. Further, topkill and survival rates are influenced by traits such as bark thickness or stem diameter (Hoffmann and Solbrig 2003; Hoffmann *et al.* 2003), properties that can only be represented in an individual-based approach. Although an individual-based approach has been adopted in Hybrid3 (Friend *et al.* 1997), ED (Moorcroft *et al.* 2001) and SEIB-DGVM (Sato *et al.* 2007), the response of vegetation to fire in these models has not be treated in an individual-based manner.

Another limitation of existing models relates to how they treat leaf phenology and carbon allocation. Savannas are seasonal environments and the length of the growing season is a crucial determinant of savanna productivity. Yet, most existing DGVMs assume fixed temperature or soil moisture thresholds to define the growing season length

of each functional type (Cramer *et al.* 2001) which means that functional types cannot dynamically adapt their growing season length to changing rainfall and temperature regimes. Similarly, in most DGVMs the allocation of carbon gain to leaves, stems or roots is typically defined by fixed allocation rules (Cramer *et al.* 2001). In such models, there is no possibility for plants to dynamically adapt the allocation ratios to resource availability. The model we develop allows leaf phenology and allocation to be functions of resource availability by using allocation concepts developed by Tilman (1988) and Friedlingstein *et al.* (1999) and leaf phenology concepts developed by Lüdeke *et al.* (1994) and Givnish (2002). The allocation model allows carbon to be preferentially allocated to roots when water is limiting, hence allowing the plant to improve its water uptake. Similarly, when light is limiting or when fire removes aboveground biomass, carbon is allocated to stems to create the infrastructure needed to escape light competition.

Our phenology model differs from the phenology models common to existing DGVMs as it allows photosynthesis, respiration, temperature and moisture availability to define when leaf abscission and leaf bud burst occur. Hence, whether a plant is deciduous or evergreen is defined by resource availability and not by a predefined temperature or soil moisture threshold as is the case in most existing DGVMs. This phenology model assumes that deciduousness is a facultative plant trait (Givnish 2002; Bowman and Prior 2005) allowing individuals to be deciduous in seasonal environments and evergreen in less variable environments.

Existing DGVMs define 3 (VECODE) to 18 (LPJ, Hickler *et al.* 2006) functional types with predefined phenology and allocation strategies. These models represent the vegetation cover in a grid cell as a fractional composition of different competing functional types. The fractional composition and other parameters (e.g. the leaf area index in the LPJ and SEIB-DGVM) are then used to classify the biome type. This biome classification is, however not appropriate for tropical biomes which are largely defined by the relative abundance of grasses and trees.

In this paper we present a new vegetation model (the adaptive dynamic global vegetation model, aDGVM) that was specifically developed for tropical vegetation. The model combines established elements of existing DGVMs within an individual-based framework. Established elements are sub-models for photosynthesis and respiration (Farquhar *et al.* 1980; Ball *et al.* 1987; Collatz *et al.* 1991, 1992), canopy scaling (Schulze *et al.* 1994; Ronda *et al.* 2001; Arora 2002), water and light competition (Walter 1971; Scholes and Archer 1997), reproduction and mortality (Higgins *et al.*

2000). Novel elements are dynamic carbon allocation (based on Friedlingstein *et al.* 1999) and phenology (based on Lüdeke *et al.* 1994; Givnish 2002) functions and a fire model that estimates fire intensity as a function of fuel biomass, fuel moisture and wind speed (Higgins *et al.* 2008) and simulates topkill (stem mortality) as a function of individual tree size and fire intensity (Higgins *et al.* 2000). The individual-based nature of the model allows us to simulate growth, establishment, reproduction and mortality of individual plants as a function of the plant's physiological state and environmental conditions. The model only requires site specific soil and climate conditions as input data and is hence capable of simulating the distribution and physiology of savanna vegetation under current and future environmental conditions.

The aims of this paper are (1) to describe the aDGVM, (2) to show that it can predict the major vegetation formations of Africa and (3) to explore how future temperature, rainfall and CO_2 anticipated by the IPCC (2007) SRES scenario A1B will influence the extent and attributes of the grasslands, savannas and woodlands of Africa.

5.2 Materials and Methods

5.2.1 Model description

We present an individual-based ecosystem model that explicitly simulates the key processes that drive the dynamics of tropical ecosystems. The model simulates how physiological and biogeochemical rates respond to the physical environment and how plant level processes like resource allocation respond to disturbances and competition and influence ecosystem structure. The model combines well established routines for simulating photosynthesis, respiration and evapotranspiration with novel models for fire, phenology and allocation within an individual-based framework. In the model plant growth is based on Collatz *et al.* (1991, 1992)'s implementations of the Farquhar *et al.* (1980) photosynthesis model, which is linked to the Ball *et al.* (1987) stomatal conductance model. Leaf level photosynthetic and respiration rates are scaled to the canopy level by using standard methods to describe the plant's water and light availability (Schulze *et al.* 1994; Ronda *et al.* 2001; Arora 2002). Canopy level photosynthesis, growth and maintenance respiration define the whole plant's net carbon balance. Canopy level photosynthesis, stomatal conductance, plant water uptake and evapotranspiration are modelled on a daily time step. The amount of carbon fixed by each individual each day is influenced by temperature, atmospheric CO_2, absorbed photosynthetically active ra-

diation, stomatal conductance and inter- and intra-specific competition for light and water. Leaf phenology is sensitive to the leaf level photosynthetic rate, water availability and temperature. Biomass of different biomass compartments is regulated by carbon allocation, which is influenced by photosynthesis, water and light availability.

The model simulates grasses and trees, where grasses are simulated as super-individuals (Scheffer *et al.* 1995) that represent grass under and grass between tree canopies. Trees are simulated individually. Apart from differences in photosynthetic pathways and allometry it is assumed that grasses and trees are regulated by the same biophysical processes. We do not simulate different species, we rather assume that the dynamics are adequately described by a "typical" tree and a "typical" grass type (see Table 5.1 for important attributes of plants and Chapter 4 for all details). Note, however, that because individuals of these "typical" types allocate carbon and develop leaves as a function of local environmental conditions these "typical" types are highly plastic and through this plasticity are capable of representing the important tropical plant functional types. Litter fall, biomass turnover and plant mortality replenish the litter pool and litter is subjected to decomposition. Establishment, mortality and disturbance influence vegetation composition and dynamics. Disturbance by fire is modelled using a semi-empirical fire model (Higgins *et al.* 2000, 2008) that allows the model to simulate the effect of fire on single trees. Fire frequency and intensity are defined by fuel biomass, fuel moisture and wind speed. Climate influences plant growth via temperature effects on leaf level photosynthesis, maintenance respiration and phenology. Atmospheric CO_2 influences photosynthetic rates, water use efficiency and indirectly, the growing season length and reproduction.

The driving variables for the model are temperature, rainfall, wind speed, atmospheric pressure (in this study taken from New *et al.* 2002), soil carbon, soil nitrogen, wilting point and field capacity (in this study taken from the Global Soil Data Task Group 2000). These parameters are used to describe a study site. Within a site, it is assumed that the environment is homogeneous and we typically simulate a one hectare stand. Within a stand, vegetation is described by grass and tree biomass, tree cover, tree number and by a set of parameters describing allometry, physiology and phenology of each tree and the two grass super-individuals. A full description of the model and details of our implementation can be found in the Chapter 4. In the following paragraphs we provide an overview of novel aspects that distinguish this model from existing models. These novel aspects are (1) the individual-based approach for trees, (2) the phenology model, (3) the carbon allocation model and (4) the fire model.

Table 5.1: The table provides parameters and constants used in the sub-models for phenology, allocation and fire as well as important allometric constants that characterize the simulated C_3-trees and C_4-grasses. The notation "prop" indicates a value between zero and one and "variable" indicates that this parameter is a modelled variable. A full list of parameters and constants is given in Chapter 4.

Symbol	Description	Value C_3	Value C_4	Units
B_L	Leaf biomass of single plant	variable	variable	kg
B_S	Stem biomass of single plant	variable	variable	kg
B_R	Root biomass of single plant	variable	variable	kg
H	Plant height	$1.3B_S^{0.392}$	$3.5B_L^{0.5}$	m
d_s	Stem diameter	$2.797H/200$	—	cm
$\mathcal{C}$	Canopy area of plant	$\pi(H\gamma_c)^2$	$\pi(H\gamma_c)^2$	m^2
γ_c	Ratio of canopy radius to height	0.37	0.4	ratio
A_{SL}	Specific leaf area	10	10.9	m^2/kg
A_{index}	Cost-benefit index controlling phenology	variable	variable	unitless
A_0	Leaf level photosynthetic rate	variable	variable	$\mu mol/m^2 s$
R	Leaf level respiration rate	variable	variable	$\mu mol/m^2 s$
G_i	Water availability index for phenology	variable	variable	prop
T_i	Temperature index for phenology	variable	variable	prop
d_{neg}	Successive days with negative A_{index}	7	5	days
d_{pos}	Successive days with positive A_{index}	10	7	days
a_R	Proportion of carbon allocated to roots	variable	variable	prop
a_S	Proportion of carbon allocated to stem	variable	variable	prop
a_L	Proportion of carbon allocated to leaf	variable	variable	prop
a_{0R}	Not-limited carbon allocation to roots	0.5	0.4	prop
a_{0S}	Not-limited carbon allocation to stem	0.2	0	prop
a_{0L}	Not-limited carbon allocation to leaf	0.3	0.6	prop
Q_i	Light availability index of plants	variable	variable	prop
C_i	Leaf abundance index of plants	variable	variable	prop
I	Fire intensity	—	variable	$kJ/s\,m$
h	Heat yield of grass	—	16890	kJ/kg
c	Regression parameter	—	301	unitless
a_w	Regression parameter	—	119.7	unitless
Q_m	Heat of preignition	—	$2.6{\cdot}10^{-6}$	J/g
Q_v	Heat of preignition	—	160749	J/g
B_F	Fuel biomass	—	variable	kg/m^2
θ_F	Fuel moisture	—	variable	prop
H	Individual tree height	variable	—	m
$P_{topkill}$	Topkill probability of individual trees	variable	—	prop

Individual-based tree population. We model trees using an individual-based approach which allows us to simulate a heterogeneous tree population. The model keeps track of the biomass in roots, stems and leaves and simulates the carbon status, phenology and fire response of each tree. In addition, the individual-based approach allows us to simulate reproduction, resprouting after fire and the seedling establishment phase which is assumed to be limiting in savannas (Higgins *et al.* 2000). We simulate reproduction by assuming that a proportion of a plant's carbon gain is allocated to seed production. Seeds can germinate and grow if soil moisture and light availability are favorable. Unfavorable conditions increase the likelihood that seedlings die. Similarly, an unfavorable carbon balance increases the mortality risk of established trees.

Phenology. In tropical and sub-tropical ecosystems the length of the growing season is an important determinant of primary production. The seasonally dry environment of savannas selects for deciduous strategies, while the less seasonal, tropical environment selects for evergreen strategies (Givnish 2002). Our phenology sub-model uses a plant's carbon status, which is a function of local environmental conditions to drive transitions between dormant and active states. Hence, our phenology sub-model assumes that all plants are facultatively deciduous, although in reality both facultatively and obligately deciduous species occur (Ng 1984; Bowman and Prior 2005).

The phenology model builds on the concepts of Lüdeke *et al.* (1994) and Givnish (2002) and assumes that the switch between the active and dormant metabolic states is determined by photosynthetic carbon gain and the respirative costs of carbon gain. This cost-benefit is indexed as

$$A_{index} = A_0 \left(G_i + T_i\right) - R, \tag{5.1}$$

where A_0 is the site specific leaf level photosynthetic rate, R is the site specific leaf level respiration rate (both A_0 and R are influenced by temperature), G_i describes the soil moisture available to the plant and T_i is a temperature index that mimics a slowing of physiological growth processes at temperatures below 15°C (see Chapter 4 for the calculation of A_0 and R and for definitions of G_i and T_i). When A_{index} is positive then conditions for leaf activity are favorable. For example, should a plant be in the dormant phase and A_{index} is positive for d_{pos} successive days, then it is assumed that the plant will move from the dormant to the active state. Similarly, a plant in the active state will move back to the dormant state after d_{neg} successive days of negative A_{index} (Table 5.1).

The model integrates aspects of phenology models based on temperature (via A_0,

R and T_i, Chuine 2000), rainfall (via G_i, Jolly and Running 2004) and the cost-benefit of photosynthesis, leaf construction cost and leaf maintenance cost (via A_{index}, d_{pos} and d_{neg}, Kikuzawa 1991). Hence, the model describes phenology from a whole plant perspective (Williams *et al.* 1997; Givnish 2002), and does this using a generic parametrization, rather than using a species or functional type based parametrization (e.g. Chuine 2000; Chuine and Beaubien 2001). Hence, the phenology model differs from existing DGVMs which assume that phenology is driven by soil moisture ("rain-green" plants) or by temperature ("summergreen" plants) thresholds that are specific to different species or functional types.

Carbon allocation. The site specific leaf-level photosynthetic and respiration rates, plant size, water and light availability define the daily carbon gain (C_Δ) of each individual plant. This carbon gain is allocated to different plant compartments (root, stem and leaf) using an allocation model based on the assumption that carbon is allocated to the compartment that most limits the plant's growth (Tilman 1988; Friedlingstein *et al.* 1999; Arora and Boer 2005). For instance, when light is limiting, as it is the case for small trees which are shaded by taller trees and grasses, then carbon is preferentially allocated to the stem to create the infrastructure to efficiently capture light. When water is limiting, then carbon is preferentially allocated to roots to enable higher water uptake. When photosynthesis is limiting, for instance after a plant has moved from the dormant to the active state, carbon is preferentially allocated to leaves to increase photosynthesis and carbon gain. Hence, the allocation model allows allocation to be influenced by environmental conditions. The realized proportions of carbon gain C_Δ allocated to roots, stems and leaves, a_R, a_S and a_L are defined as

$$a_R = \frac{1 + a_{0R} - G_i}{3 + a_{0R} + a_{0S} - Q_i - G_i - C_i}, \tag{5.2}$$

$$a_S = \frac{1 + a_{0S} - Q_i}{3 + a_{0R} + a_{0S} - Q_i - G_i - C_i}, \tag{5.3}$$

$$a_L = \frac{1 - C_i}{3 + a_{0R} + a_{0S} - Q_i - G_i - C_i}. \tag{5.4}$$

The parameters a_{0R}, a_{0S} and a_{0L} (Table 5.1) describe the fractions of carbon allocated to roots, stems and leaves when resources are not limiting, Q_i and G_i (see Chapter 4

for definitions of Q_i and G_i) describe light and water availability of the plant and

$$C_i = \frac{B_L}{a_{0L}(B_R + B_S + B_L)} \tag{5.5}$$

describes the deviance of leaf biomass from the fraction of leaf biomass in the non-limiting case, a_{0L}. The parameters B_R, B_S and B_L describe living root, stem and leaf biomass of the individual.

Fire model. We use the semi-empirical fire model proposed by Higgins *et al.* (2008). For a fire to spread, two conditions must be fulfilled: there must be an ignition source (we assume that the number of ignitions per year is given by a random variable) and the potential fire intensity I must exceed a threshold of 300 kJ s^{-1} m^{-1} (van Wilgen and Scholes 1997). The potential fire intensity I is given as

$$I(B_F, \theta_F) = hB_F \frac{c \arctan(u)\ f(B_F, a_w)}{Q_m\theta_F + Q_v(1 - \theta_F)} \tag{5.6}$$

where B_F is the fuel biomass, θ_F is the fuel moisture, u is the windspeed, Q_m and Q_v are heats of preignition, c is a constant estimated from data and h is the heat yield of fuel consumed (Table 5.1). Further,

$$f(B_F, a_w) = \frac{B_F}{B_F + a_w} \tag{5.7}$$

is a sigmoidal function of fuel biomass where a_w is a parameter estimated from data (Table 5.1). Fire consumes the total aboveground grass biomass, litter and potentially the aboveground tree biomass (topkill). The probability of an individual tree suffering topkill is an empirically derived function of fire intensity I and tree height H (Higgins *et al.* 2000),

$$P_{topkill}(H, I) = \frac{\exp(4.3 - 5.0\ln(H) + 0.0044\sqrt{I})}{1 + \exp(4.3 - 5.0\ln(H) + 0.0044\sqrt{I})}. \tag{5.8}$$

In our model, fire shapes the size structure of the tree population by decreasing establishment rates and indirectly by increasing mortality of trees. Small trees (<2m) have a high topkill probability, which means that they are often drawn back to resprouts by fires until a favorable sequence of events (e.g. several years without fire) allows them to grow tall enough to escape the fire trap (Bond and Midgley 2001). Topkill does not

directly influence the tree mortality rates. Rather, repeated topkill compromises the plant's carbon balance which increases its chances of mortality. Hence, the fire model modifies the total biomass, the size and structure of the tree population.

5.2.2 Simulations

We conducted simulations of the vegetation of Africa in the period between 1850 and 2100 with a spin-up of 100 years before 1850 at pre-industrial values of CO_2 and temperature. This spin-up phase is necessary and sufficient for the model to reach an equilibrium state. The spin-up phase is ignored in the analyzes. We forced the model with measured and projected CO_2, temperature and rainfall given by the Max Planck Institute for Meteorology's (Hamburg) ECHAM5 IPCC (2007) SRES A1B projections (Roeckner 2005, Table 5.2). We simulated the vegetation of Africa on a 20 minute grid. At each grid coordinate defined by latitude and longitude, we simulated a one hectare stand. As the IPCC (2007) climate projections were given on a coarser grid than our simulations, we used for each study site the climate data of the nearest point in the climate grid. We did not use the monthly data given by the IPCC (2007) climate projections, we rather estimated the trends from the monthly climate projections relative to the period between 1961 and 1990 and used these trends to scale CO_2, temperature and rainfall as defined by New *et al.* (2002). We simulated vegetation in the presence and absence of changes in rainfall and in the presence and absence of fire. Simulation results include the projected rainfall changes, unless it is stated that rainfall was held at ambient levels. The output variables we used for our analyzes are grass and tree biomass, tree cover and the frequency and intensity of fire.

The aDGVM simulates a savanna tree type that is relatively fire resistant and the fire model assumes that the fire intensity must exceed 300 kJ s^{-1} m^{-1} such that a fire can spread. Yet, it has been observed, that in tropical rainforests fires with relatively low intensities (50-100 kJ s^{-1} m^{-1}) might kill forest trees that are poorly adapted to fire (Cochrane *et al.* 1999; Cochrane 2003). To explore the sensitivity of the model to our assumptions of fire resistance and forest fire, we conducted additional simulations for Africa with two additional tree types. These additional simulations include the standard fire-resistant savanna tree, a fire-sensitive savanna tree and a highly fire-sensitive forest tree. We assumed that all tree types are initially equally abundant at a study site. For the two additional tree types we follow Hoffmann and Solbrig (2003) and Hoffmann *et al.* (2003) who defined topkill probabilities as a function of bark thickness (t_b). We

Table 5.2: Datasets used for the climate change scenarios and model validation.

Description	Source
CO_2, temperature and rainfall from 1850 to 2100	IPCC (2007) SRES Scenario A1B, Roeckner (2005)
Tree cover	Defries *et al.* (2000)
Herb cover	Defries *et al.* (2000)
Vegetation maps	
1. EROS Data Center Global Land Cover Classifications, IGBP classification	Loveland *et al.* (2000)
2. ISLSCP Global Vegetation Land Cover Map at 1×1 resolution	Meeson *et al.* (1995)
3. Global distribution of vegetation at 1×1 resolution	Matthews (1983, 1984)
4. EROS Data Center Global Land Cover Classifications, SiB classification	Loveland *et al.* (2000)
5. Global SYNMAP land cover product at 30" resolution	Jung *et al.* (2006)
6. Vegetation type classification of potential natural vegetation	Hickler *et al.* (2006), based on Haxeltine and Prentice (1996)
7. Vegetation type classification of potential natural vegetation	White (1983)
Consensus vegetation map obtained from vegetation maps 1 to 7	
Vegetation from DGVM simulations (HYBRID, IBIS, LPJ, SDGVM, TRIFFID, VECODE)	Cramer *et al.* (2001)
Fire frequency: ATSR-2 World Fire Atlas (European Space Agency)	http://dup.esrin.esa.int/ionia/wfa
Burned area: Global Fire Emissions Database, Version 2 (GFEDv2.1)	Randerson *et al.* (2007)

assume that bark thickness is 28.5% of the stem radius for the fire-sensitive savanna tree and 10.1% of the stem radius for the highly fire-sensitive forest tree. Using data from Hoffmann and Solbrig (2003) and Hoffmann *et al.* (2003)'s studies we propose the following parametrizations of the topkill functions for the fire-sensitive savanna tree and the highly fire-sensitive forest tree,

$$P_{topkill}(t_b, I) = \frac{\exp(3.79 - 3.25\ln(t_b) + 0.005\sqrt{I})}{1 + \exp(3.79 - 3.25\ln(t_b) + 0.005\sqrt{I})} \tag{5.9}$$

and

$$P_{topkill}(t_b, I) = \frac{\exp(5.19 - 3.01\ln(t_b) + 0.005\sqrt{I})}{1 + \exp(5.19 - 3.01\ln(t_b) + 0.005\sqrt{I})}. \tag{5.10}$$

In these simulations, we additionally decrease the minimum fire intensity I (Equation 5.6) required for fire ignition from 300 kJ s^{-1} m^{-1} to 5 kJ s^{-1} m^{-1}. This allows low intensity fires to spread. These low intensity fires are sufficient to damage the two additional tree types. We modified the seed production rules for the two additional tree types. Following Hoffmann and Solbrig (2003) and Hoffmann *et al.* (2003) we assumed that the fire-sensitive savanna tree can produce seeds when it is taller than 3.6 m while the highly fire-sensitive forest tree can reproduce when it is taller than 8 m.

For the simulations described in the previous paragraphs we analyze snapshots of the vegetation state in 2008 and 2100. To illustrate how vegetation changes over time we present timeseries for selected study sites for the period between 1850 and 2100. These simulations serve to illustrate some of the inner-working of the aDGVM and are not necessarily representative for all African savannas. We conducted simulations at two sites. One site is south of Pretoriuskop in the Kruger National Park, South Africa with the coordinates 25°10' S and 31°16' E and 650 mm MAP. This study site is located in what is locally called sour-veld (high C:N ratio in vegetation) and is classified as Pretoriuskop sourveld or Malelane mountain bushveld (Gertenbach 1983). The other site is close to Satara in the Kruger National Park with the coordinates 24°23' S and 31°46‘ E and 437 mm MAP. This study site is located in what is locally called sweet-veld (low C:N ratio in vegetation) and is classified as Knob Thorn or Marula Veld on Basalt (Gertenbach 1983). For these simulations we used site-specific parameters to improve the model parameterization. We used C:N ratios of 300 and 90 for tree stems and roots at Pretoriuskop while we use the aDGVM standard values of 150 and 60 at Satara, based on Scholes and Walker (1993)'s estimates from nutrient poor and nutrient rich savannas. Wilting point and field capacity were set to 0.11 and 0.22 for Pretoriuskop

and to 0.2 and 0.43 for Satara. The canopy extinction coefficient (parameter symbol k in Chapter 4) was set to 0.4 for Pretoriuskop and to 0.45 for Satara. We simulate two scenarios. In the first scenario, fire suppression is introduced in 1954, in the second scenario there is no fire suppression. These simulations imitate the fire suppression experiments conducted in the Kruger National Park (Higgins *et al.* 2007a). The effects of grazing were simulated by reducing aboveground grass biomass by a constant grazing rate Z, where Z is simply the proportion of the standing biomass removed in each time step. We further assume that continuous grazing reduces the regrowth rates of grasses. We simulated this effect by reducing the maximum leaf level photosynthetic rate A_{max} by a factor of $1 - 0.01Z$ for each time step in the metabolic phase. Grazing levels were assumed to be low ($Z = 0.01$) before 1954 but higher ($Z = 0.02$) after 1950 (du Toit *et al.* 2003). We compared the output from these simulations to the aboveground tree biomass data provided by Higgins *et al.* (2007a).

5.2.3 Data analysis

To evaluate the model we compared simulation results for Africa to empirical data and to simulation results obtained from alternative models. We used empirical datasets that estimate the distribution of functional types, grass and tree cover and fire (Table 5.2). The models we compared our results to were published in Cramer *et al.* (2001) (Table 5.2).

Biome types. To analyze the distribution of vegetation simulated by the aDGVM, we follow Cramer *et al.* (2001)'s definition of simplified biome types. Specifically, we distinguish between five different biomes: desert, grassland, savanna, deciduous woodland and evergreen forest. For the classification of our simulation output into one of these biomes we use a mixture of Whittaker and Likens (1975)'s and the IGBP (Loveland *et al.* 2000) classification schemes for biospheres. Specifically, simulated vegetation in a cell is classified as a desert when the tree cover is less than 10% and the living grass biomass is less than 3 t/ha. A cell is classified as a grassland when the simulated treecover is less than 10% and grass biomass is greater than 3 t/ha. In a savanna, grasses and trees coexist, and we classify simulated vegetation as a savanna if the grass biomass exceeds 3 t/ha and the treecover is between 10% and 60%. When the treecover exceeds 60%, then vegetation is classified as a woodland. We classify woodlands where trees move between dormant and active state regularly (on average more than twice in three years) as deciduous woodlands while woodlands where trees move between dormant and

active state infrequently (on average less than twice in three years) as evergreen forest. Note that this classification scheme for deciduous and evergreen vegetation differs from commonly used definitions. For instance, Bowman and Prior (2005) define vegetation as deciduous when it looses leaves for at least one month a year and the IGBP classification scheme (Loveland *et al.* 2000) defines evergreen as "almost all trees remain green all year" and deciduous as trees with "an annual cycle of leaf-on and leaf-off periods". However, aDGVM simulations show that if trees switch from the metabolic to the dormant state, then they generally remain in the dormant state longer than a month, which agrees with Bowman and Prior (2005)'s definition.

To enable comparisons between empirical vegetation maps (Table 5.2) and simulation results, we re-classified the different vegetation maps into the five simplified biomes (desert, grassland, savanna, deciduous woodland and evergreen forest). The scheme for the re-classification is provided in Table 5.3. As the available vegetation maps differ, we used them to create a "consensus" map by using simple vote-counting to assign cells to biome types.

Relative cover, correctly classified cells and κ-statistics. We calculated the relative cover of different biome types (desert, grassland, deciduous woodland, evergreen forest, savanna) for the different scenarios simulated with the aDGVM, for the six models used by Cramer *et al.* (2001) and for the different vegetation maps (Table 5.2). We compared simulation results and vegetation maps by counting the cells where the biome type simulated by a model agrees with the biome type given by a vegetation map. The fraction of correctly classified cells is denoted as a. Further, we used κ-statistics (Monserud and Leemans 1992; Prentice *et al.* 1992) to quantify agreement between simulated and observed vegetation patterns. The comparison between our model results and vegetation maps was conducted on a 1° grid, the comparison with the model results from Cramer *et al.* (2001) was conducted on the 3.75°×2.5° grid used in the Cramer *et al.* (2001) study. To produce coarser scaled maps necessary for these comparisons, we re-sampled the fine scale aDGVM simulation results at the resolution of the coarser scaled grids.

Transitions between biomes. To describe the effects of fire and climate change at the biome level, we generated transition matrices M that count how many cells of the simulated vegetation maps were transformed from one vegetation state t to another vegetation state t' as influenced by fire and as influenced by climate change between 2008 and 2100. For instance in the case of fire, the matrix element $M_{tt'}$ indicates that $M_{tt'}$ cells were in the vegetation state t in absence of fire but moved to the vegetation

state t' in presence of fire. These transition matrices are depicted as graphs, where boxes represent the different biome types and arrows of variable width between boxes represent transitions between biome types under the influence of fire or climate change.

Table 5.3: Scheme for the re-classification of the vegetation maps used in the main text into the five simplified biome types desert (Des), grassland (grl), deciduous woodland (Wol), evergreen forest (Evf) and savanna (Sav). See Table 5.2 for details on the datasets. The numbers given in this table agree with the indices of different functional types used in the vegetation maps.

Product	Wtr	Des	Grl	Wol	Evf	Sav
IGBP	0	16	7, 10	4, 5, 6, 11, 14	2	8, 9, 12
Islscp	0	3	1	12	8	4, 6, 7, 14
Matthews	0	30	19, 21, 25, 26, 27, 28, 29	5, 6, 9, 12, 13, 15, 17, 18	1, 2	23, 24
SiB	0	11	7, 9	8, 13	1, 6	12
SYNMAP	0	45	27, 38, 40, 41, 42, 43	5, 6, 11, 15, 22, 24, 31, 32, 33, 36	4, 13	1, 14, 17, 18, 23, 35, 37, 39
Hickler	0	17	13, 14, 15, 16	10, 11	8, 9	12
White	0, 81	67, 68, 69, 71, 72, 73, 74	17, 18, 19, 20, 47, 48, 49, 50, 51, 52, 53, 54, 55, 56, 57, 58, 59, 60, 61, 62, 63, 75, 76, 78, 79, 80	10, 11, 12, 13, 14, 15, 16, 21, 25, 26, 27, 29, 30, 77	1, 2, 3, 4, 5, 6, 7, 8, 9	22, 23, 24, 28, 31, 32, 33, 34, 35, 36, 37, 38, 39, 40, 41, 42, 43, 44, 45, 46

5.3 Results

5.3.1 The current vegetation of Africa

The model simulates evergreen forests in central Africa (Figure 5.1). In the north of these evergreen forests, the model predicts a gradient from evergreen forests to deciduous woodlands, savannas, grasslands and to deserts, that is, woody biomass decreases while grass biomass increases. Finally, in the arid north of the Sahel, woody biomass disappears and grass biomass decreases until conditions do not allow any vegetation at all. At the horn of Africa, the model simulates bare soil, grasslands and low fractions of savannas. In southern Africa, the model simulates a mixture of savannas, deciduous woodlands and grasslands and a gradient from woody dominance to grass dominance from the north-east to the south-west.

The modelled distribution of major vegetation formations across Africa agrees well with the broad patterns of vegetation distribution given by different vegetation maps (Figure 5.1). However, agreement is strongly dependent on which vegetation map one uses. The best agreement between simulations and vegetation maps is obtained when comparing the model results to the consensus vegetation map (Table 5.4). For this dataset, the model correctly predicts the vegetation in 64% of the simulated cells and the κ-value is 0.54. For all biome types, the percentage of correctly classified cells exceeds 43% and κ is between 0.28 and 0.83, with the lowest agreement for deciduous woodlands (Table 5.5).

The modelled distribution of tree and grass biomass agrees well with the observed tree and grass cover (Figure 5.1). The model simulates highest tree biomasses in the regions of the evergreen forests of central Africa and decreasing biomasses in the north and the south of the evergreen forests. In these regions of decreasing tree biomass, grass biomass is relatively high, which means grass-tree coexistence or grass dominance.

The simulation results summarized in the previous paragraphs assume that vegetation is affected by natural fire. Our model can qualitatively simulate the broad patterns of fire activity observed in Africa (Figure 5.1). That is, the model predicts no fire or only very low fire activity in central Africa but that fire influence increases to the north and the south of the central African evergreen forests where grass biomass is high. The highest fire activity indices can be observed in the Sahel regions and in southern Africa.

The aDGVM provides better agreement with the consensus vegetation map obtained from all vegetation maps than the models analyzed by Cramer *et al.* (2001) do. While κ is 0.61 for the aDGVM, κ ranges between 0.50 for the SDGVM and 0.32 for TRIFFID

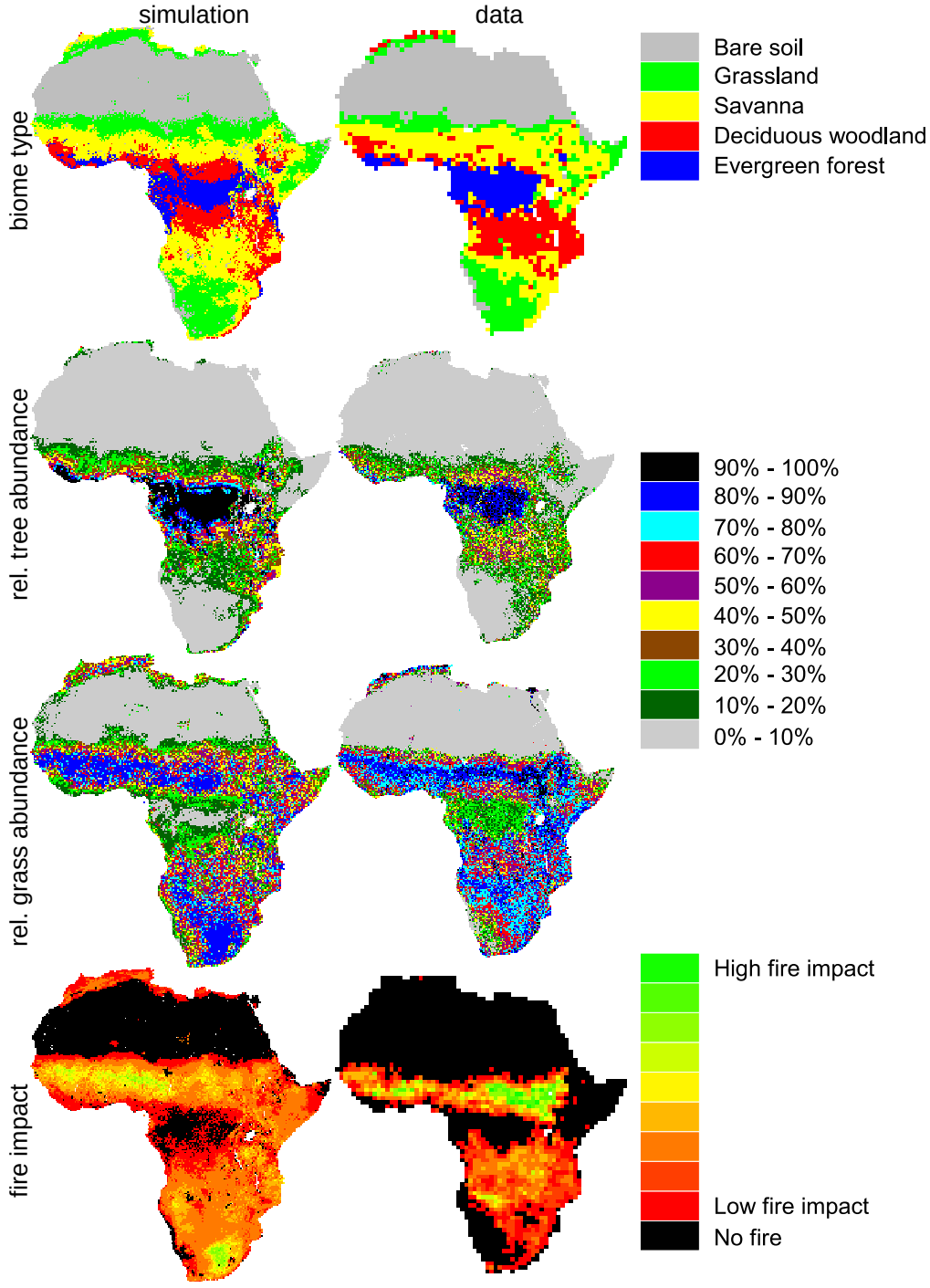

Figure 5.1: Comparison of aDGVM results for 2008 and observed data: biome type (we used a consensus vegetation map for the comparison), relative abundance of trees and grasses (scaled biomass for simulation results and treecover/herbcover for remote sensing data) and fire impact (product of mean fire intensity and fire frequency for simulation results and burned area for remote sensing data). The sources of empirical data are listed in Table 5.2.

Table 5.4: The table gives the relative cover of deserts (Des), grasslands (Grl), deciduous woodlands (Wol), evergreen forests (Evf) and savannas (Sav) given by different vegetation maps (Table 5.2) and simulated by the aDGVM for 2008. Further, the table gives the proportion of correctly classified cells a and the κ-value for the aDGVM results when compared to the different vegetation maps. Analyzes were conducted on a 1° grid.

Vegetation map	Biome type					Statistics	
	Des	Grl	Wol	Evf	Sav	a	κ
SiB	34.3	11.3	1.1	7.0	46.2	0.62	0.50
IGBP	34.2	14.5	7.3	12.9	31.0	0.61	0.49
SYNMAP	35.5	21.8	10.7	9.9	22.0	0.60	0.49
Islscp	34.6	7.7	23.1	7.2	27.4	0.60	0.48
Hickler	29.0	18.4	29.1	9.6	13.8	0.52	0.40
Matthews	29.2	27.4	17.1	9.9	16.5	0.52	0.39
White	26.8	18.4	29.2	8.7	16.7	0.47	0.34
Consensus	33.9	16.2	15.3	8.8	25.6	0.64	0.54
aDGVM	32.8	19.9	13.7	7.8	25.8		

(Table 5.6). Recent studies conducted with the LPJ on a 1×1° grid report κ of 0.63 for a transect from the evergreen forests northwards to savannas and deserts (Hély *et al.* 2006) and 0.42 on a global scale (Hickler *et al.* 2006). Further, Hickler *et al.* (2006) found the greatest disagreements between simulations and vegetation maps in so-called transitional zones such as tropical savannas. Thus, Hickler *et al.* (2006) report κ-values of 0.05 (0.14) and 0.08 (0.12) for moist savannas and dry savannas on a 0.5°(2.5°) grid.

However, the intercomparison between different vegetation maps is difficult for several reasons. First, each vegetation map uses different schemes to classify vegetation into different biome types and in particular in the case of remote sensing data it is not clear to which degree these maps represent the real vegetation (Blasco *et al.* 2000; Jepson and Whittaker 2002; Jung *et al.* 2006). For instance, an intercomparison of three global vegetation maps showed that the agreement between maps is only 41%, with the highest disagreement being reported in transitional zones such as tropical savannas (Jung *et al.* 2006). Hence, there is a need to generate objective vegetation maps (e.g. Blasco *et al.* 2000; Jung *et al.* 2006). Second, we re-classified the functional types defined by different vegetation maps (Table 5.2) into five simplified biome types used in this study, and other authors might have chosen to do this classification differently. Third, remote sensing

Biome type	Statistics	
	a	κ
Desert	0.91	0.83
Evergreen forest	0.57	0.51
Grassland	0.54	0.51
Savanna	0.57	0.42
Woodland	0.43	0.28

Table 5.5: Proportion of correctly classified cells a and the κ-value for the different biomes on a 1° grid. Here, the aDGVM simulation results were compared to the consensus vegetation map.

datasets define vegetation as cropland whereas we do not account for landuse, thus the IGBP dataset (Loveland *et al.* 2000) defines about 9% of the African land surface as cropland. Croplands are masked in our analyses and because croplands are limited to specific environmental conditions, this may hide a systematic bias.

The aDGVM biomass predictions were not sensitive to the definition of the number of tree functional responses to fire. Figure 5.2A shows that there are negligible differences in biomass between simulations with one and simulations with three functional responses of trees to fire. In the situation with three functional responses of trees to fire and in absence of fire, the analysis shows that vegetation is a mixture of the standard tree, the fire-sensitive savanna tree and the highly fire-sensitive forest tree (Figure 5.2B). Fire potentially kills the forest trees such that their abundance tends to zero. In such a situation savanna trees manage to establish and to replace the forest trees. Hence, the predicted carbon storage potential is not modified by the inclusion of a fire-sensitive functional type.

5.3.2 The vegetation of Africa without fire

It is established that fire may strongly influence vegetation by shifting biomes towards grass dominance and may even be a necessary prerequisite for grass-tree coexistence (Higgins *et al.* 2000; Sankaran *et al.* 2005; Bond *et al.* 2005; Higgins *et al.* 2007a, Chapter 2). We found that in large parts of Africa, fire reduces tree biomass (Figure 5.3) as well as dead biomass and thereby allows grasses to grow under reduced competitive pressure. Thus, in regions with high fire activity, grass biomass might be strongly reduced by fire suppression (Figure 5.3), while the carbon stored in trees increases from 74.9 Pg to 84.3 Pg by fire suppression (Table 5.7). The simulations predict that total biomass in vegetation of Africa is increased by fire suppression (80.1 Pg with fire and 90.6 Pg without fire, Table 5.7). The simulated total biomass agrees with the review

Table 5.6: Comparison between simulation results of the aDGVM and the models given by Cramer *et al.* (2001) on the 3.75°×2.5° grid used in the Cramer *et al.* (2001) study. The table gives the relative cover of different biomes as well as the proportion of correctly classified cells a and the κ-value for different models when compared to the consensus vegetation map. To reduce the resolution of simulation results, we re-sampled the fine scale maps at the resolution of the coarser scaled grid. See Table 5.4 for the relative cover of different biome types in empirical vegetation maps.

Model	Biome type					Statistics	
	Des	Grl	Wol	Evf	Sav	a	κ
aDGVM	30.0	20.0	14.3	7.3	28.3	0.70	0.61
SDGVM	29.5	32.6	6.8	12.1	18.9	0.61	0.50
VECODE	29.5	34.1	13.6	6.1	16.7	0.58	0.47
LPJ	30.3	27.3	13.6	16.3	12.5	0.56	0.45
IBIS	34.5	29.5	6.1	18.2	11.7	0.56	0.43
HYBRID	38.3	34.5	0.4	22.7	4.2	0.48	0.33
TRIFFID	48.5	20.5	0.8	23.1	7.2	0.48	0.32
Consensus vegetation map	34.4	16.0	13.5	10.3	25.9		

of Williams *et al.* (2007) who estimated that the total biomass stored in vegetation in Africa is 80±28 PgC.

Nonetheless, it is not clear if the model under- or overestimates the effects of fire on carbon stored in vegetation. For instance, should we assume that only the 15×10^6 km^2 of Africa that Grace *et al.* (2006) classified as savanna are influenced by fire and that 50 years of fire suppression could, on average increase the total carbon in trees by circa 6 t/ha (Higgins *et al.* 2007a) we would expect fire suppression in Africa to allow an additional carbon storage of about 9 Pg which is less than simulated by the model. San José *et al.* (1998b, a) and Grace *et al.* (2006) suggest that fire suppression in savannas could increase carbon storage by almost 1 t/ha/year which would translate into an increase of 67.5 PgC in 50 years for Africa. Scholes (2004) estimates that values between 0.3 and 0.6 t/ha/year would be more appropriate for savannas which would translate into an increase between 14 and 27 PgC in for Africa, assuming that biomass accumulation can only occur for 30 years.

Fire suppression had a more dramatic effect on grass-tree dominance at the regional scale (Figure 5.3). Fire suppression led to substantial increases in tree and total biomass

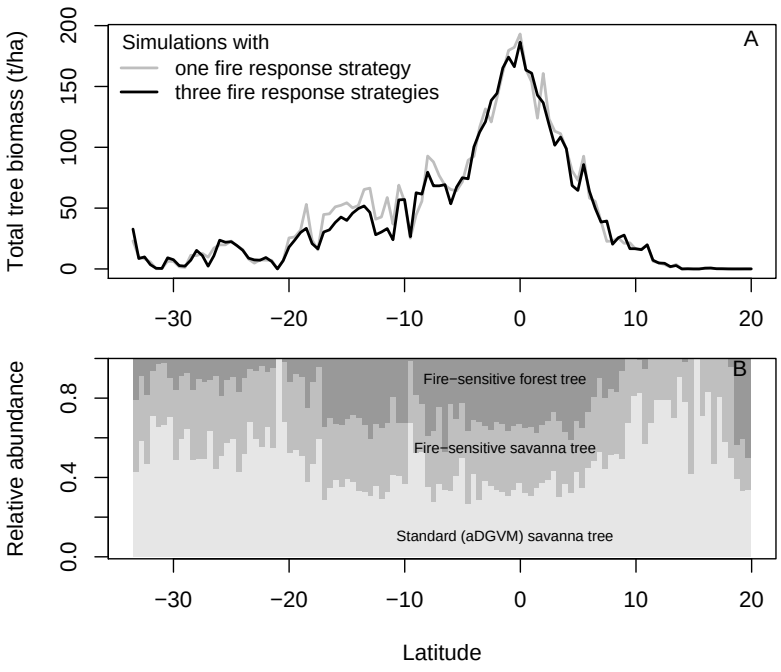

Figure 5.2: (A) Simulated tree biomass on a half-degree gradient between 20° N and -33.5° S and 25° E. Simulations were conducted once with only the standard savanna tree type used in the aDGVM and once with three tree types (the standard savanna tree, a fire-sensitive savanna tree and a highly fire-sensitive forest tree). (B) Relative abundances of the three tree types in absence of fire on the half-degree gradient between 20° N and -33.5° S and 25° E.

in southern Africa and in the northern Sahel. The relative effect of fire on trees is severe in these more arid systems and tree biomass in absence of fire can be more than twice the tree biomass in presence of fire. In the more humid, southern parts of the Sahel and in the south of the central African forests, fire consumes smaller proportions of tree biomass as most tree biomass is stored in large trees that due to their size are fire resistant. Yet, this small reduction in tree biomass is sufficient to reduce the light competition exerted by trees on grasses and this effect is often strong enough to cause an increase in grass growth.

Fire shifts the biomes of Africa towards more grass dominated states, that is, in presence of fire 39.9% of deciduous woodlands move into a savanna state, 31.3% of savannas move into a grassland state and 16.1% of the grasslands move into a desert state (Figure 5.4). Overall, fire leads to an increase in the fractional cover of grasslands of 4%, while the fractional cover of deciduous woodlands decreases by 11.5%. The fractional cover of savannas slightly increases by 4.2% (Table 5.7). In presence of fire, the biomass stored in savannas increased by 2.7 Pg to 14.2 Pg and the biomass in deciduous woodlands and evergreen forests decreased by 12.8 Pg (Table 5.7).

The tree size distribution in savannas is severely modified by fire suppression. Thus, in presence of fire only few trees manage to escape the fire trap and to reach adult

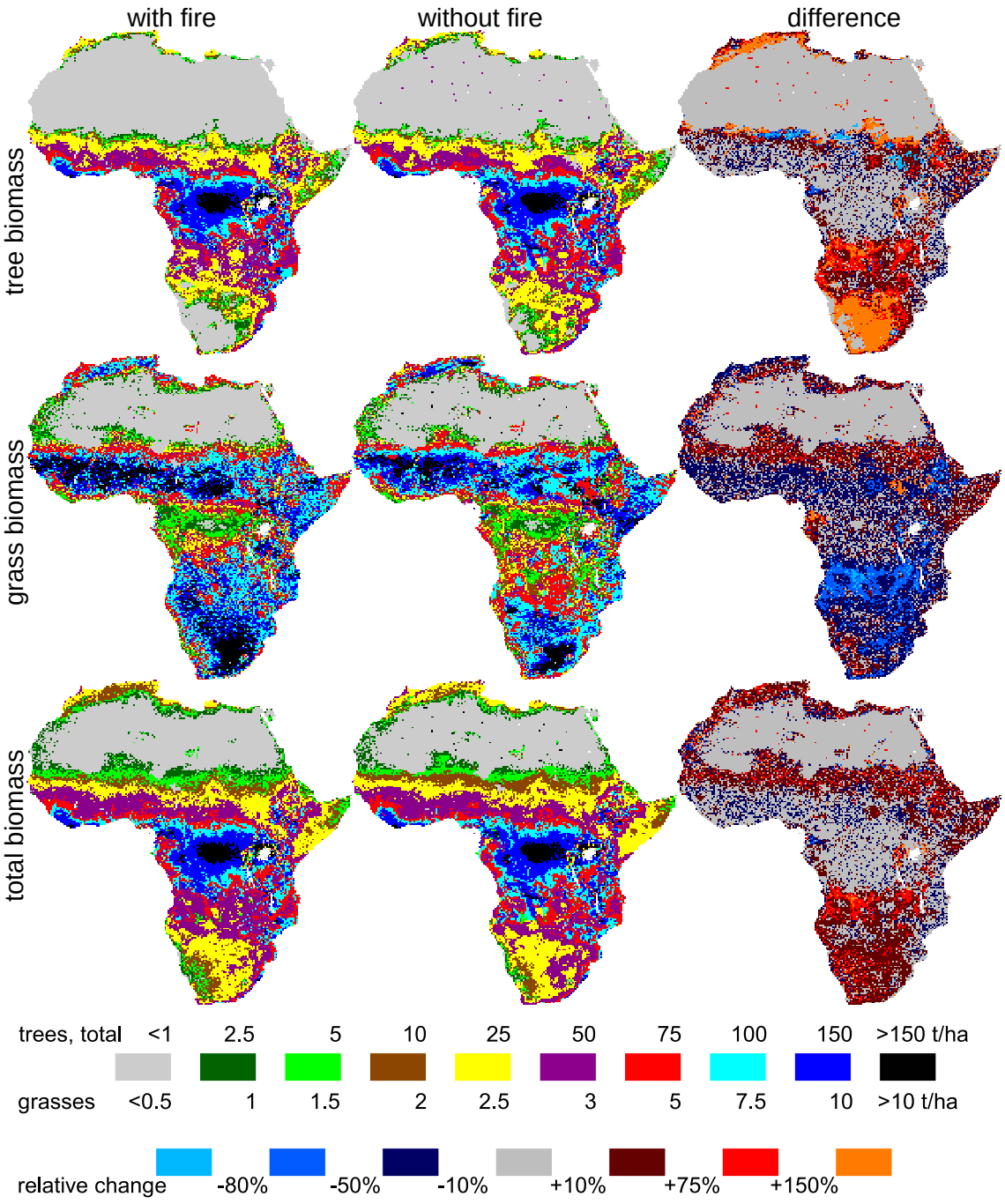

Figure 5.3: Simulated tree, grass and total biomass (aboveground and belowground in t/ha) for 2008 in presence and absence of fire and the relative change between simulations in presence and absence of fire.

Table 5.7: Results of aDGVM simulations with and without fire and aDGVM projections for 2100. The first part of the table gives the simulated relative cover of different biomes. The second part of the table gives the aboveground biomass (in Pg) stored in different biomes, grasses and trees in Africa. The column "Fire" indicates whether the simulations were conducted in presence or absence of fire, the column "Rain" indicates if simulations were conducted in presence or absence of the IPCC (2007) SRES A1B rainfall scenario.

Scenario			Cover by biome (%)				
Year	Fire	Rain	Des	Grl	Wol	Evf	Sav
2008	Yes		32.8	19.9	13.7	7.8	25.8
2008	No		30.9	15.9	25.2	6.5	21.6
2100	Yes	Yes	27.1	18.7	26.9	7.7	19.7
2100	Yes	No	26.9	16.3	27.2	6.8	22.8

Scenario			Biomass by biome (Pg)					Biomass by continent (Pg)		
Year	Fire	Rain	Des	Grl	Wol	Evf	Sav	Trees	Grasses	Total
2008	Yes		0.4	2.5	34.9	28.1	14.2	74.9	5.2	80.1
2008	No		0.7	2.6	52.1	23.7	11.5	84.3	6.3	90.6
2100	Yes	Yes	1.2	6.4	62.3	52.5	34.3	151.7	5.0	156.7
2100	Yes	No	1.2	8.8	50.7	62.4	40.3	158.3	5.1	163.4

tree size classes. Most trees remain in small size classes (Figure 5.5A). Fire suppression allows more trees to reach higher size classes (Figure 5.5B). At forest sites, the model predicts a multi-layer size structure of trees. That is, the model coarsely simulates an immature/sapling layer, a sub-canopy layer, a canopy layer and it simulates single individuals in the emergent layer (Figure 5.5D). At the forest site, fire suppression slightly modifies the abundance of trees in small size classes while individuals in the tall size classes are hardly affected by fire suppression (Figure 5.5E).

5.3.3 Climate change and the vegetation of Africa

Forward simulations to the year 2100 show how the vegetation of Africa changes in response to changes in CO_2, rainfall and temperature. Because C_4-photosynthesis is carbon saturated and C_3-photosynthesis is not carbon saturated at the ambient CO_2, the model simulates a change in the relative performance of grasses and trees and a substantial increase in tree dominance (Figure 5.6). The model predicts that large

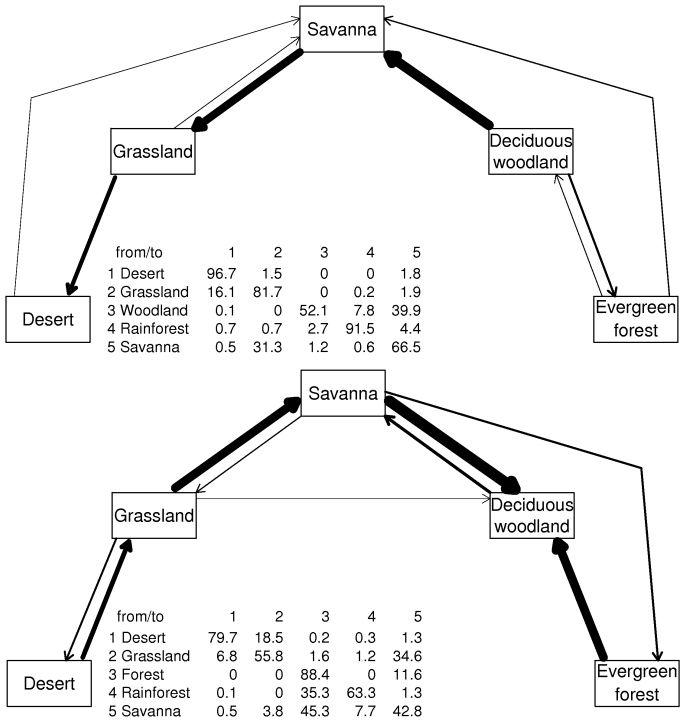

Figure 5.4: Graphs illustrating the transitions in vegetation states induced by fire under ambient conditions (upper panel) and the transitions induced by climate change (2008 to 2100, lower panel). Future vegetation projections use the IPCC (2007) SRES scenario A1B with changes in CO_2, temperature and rainfall.

parts of today's savannas will be replaced by deciduous woodlands under elevated atmospheric conditions. It is predicted that 34.6% of today's grasslands are transformed into savannas and 45.3% of today's savannas are transformed into deciduous woodlands (Figure 5.4). The fraction of deciduous woodlands is predicted to increase by 13.2% to 26.9% while the savanna biome is predicted to decrease by 6.1% to 19.7% (Table 5.7). The total biomass stored in each of the biomes increases, with high relative changes in grasslands and savannas (by 256% and 241% respectively). The absolute changes are more than 20 Pg for savannas, deciduous woodlands and evergreen forests (Table 5.7). These changes together imply that the total carbon stored in trees in Africa increases from 74.9 Pg in 2008 to 151.7 Pg in 2100 (Table 5.7), a difference of 76.8 Pg which is approximately equal to the estimates of Scholes and Hall (1996), who used a different approach to estimate that the conversion of nonwoody savannas to closed woodlands could generate an additional carbon sink of 94.3 Pg. Grace (2004) estimates that if as much carbon as possible is sequestered for instance by afforestation, an amount of 0.2 to 4 PgC/year could be sequestered. Grace (2004)'s estimates imply that Africa has a potential additional carbon sink of 3.68 to 73.6 PgC until 2100.

Although today's grasslands shift towards tree dominance, the relative area covered by grasslands only decreases by 1.2% (Table 5.7). This is because the model predicts

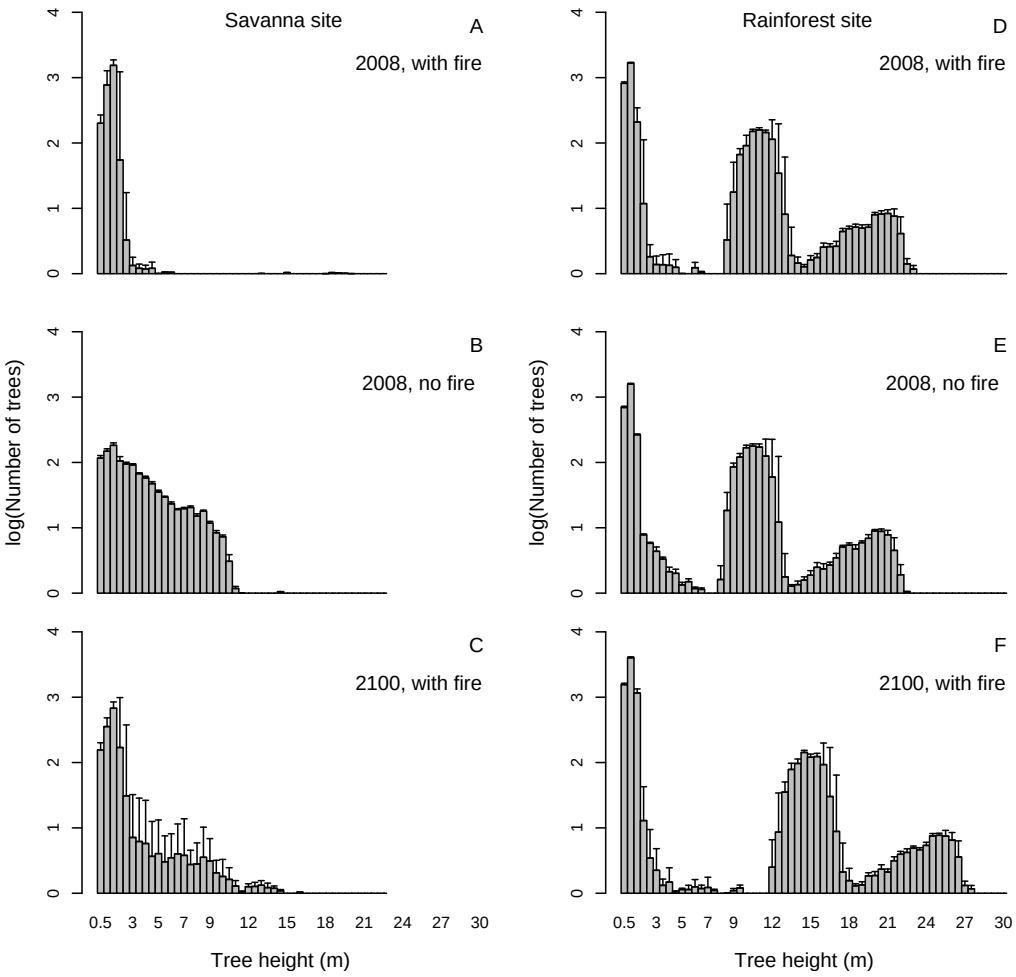

Figure 5.5: Number of trees in height classes for 2008 with fire (panels A and D), without fire (panels B and E) and for 2100 with fire (panels C and F). Panels A, B and C describe the height structure at a savanna site (25°10' S and 31°16' E), panels D, E and F show the height structure at a rainforest site (0° latitude and 25° E). Simulations were conducted using the IPCC (2007) SRES scenario A1B with changes in CO_2, temperature and rainfall.

that grasslands will spread into the Sahara and into the horn of Africa, such that the total area covered by deserts or bare soil decreases by 5.7%. Grasslands replacing deserts have also been predicted by Cramer *et al.* (2001), Lucht *et al.* (2006) and Fischlin *et al.* (2007). The spread of grasses into deserts implies that the effects of increasing CO_2 and temperature have a net effect of improving the water use efficiency allowing plant growth in these arid regions. In the simulations the spread of grasses into deserts cannot be attributed to rainfall changes as this effect is observed in both scenarios with and without rainfall changes.

A comparison of the simulation results for 2100 in presence of the IPCC (2007) rainfall scenario with the scenario in absence of rainfall changes shows that without rainfall changes and in presence of fire, the carbon in vegetation is 6.7 Pg higher than in the case with rainfall changes (Table 5.7). Hence, the projected changes in rainfall patterns are projected to reduce the carbon storage potential in Africa.

The model predicts that climate change induces changes in the size structure of the tree population. Thus, both at savanna and forest sites, the total number of trees and the number of trees in larger size classes increased (Figures 5.5C and 5.5F).

Figure 5.7 depicts timeseries for aboveground tree biomass at the two savanna study sites in the Kruger National Park in the period between 1850 and 2100 as well as empirically observed aboveground tree biomasses (Higgins *et al.* 2007a). The simulated tree biomasses at these sites agree reasonably well with field data in 1954 and 1996. The simulations were conducted with low grazing rates (1%) before 1954 and with slightly higher grazing rates (2%) after 1954. Increasing grazing rates agree with animal census data that show that animal numbers in the Kruger Park increased during the recent decades (du Toit *et al.* 2003).

5.4 Discussion

In this paper, we have presented a vegetation model, the aDGVM, that combines novel mechanistic sub-models for fire, phenology and allometry with established sub-models for photosynthesis, respiration, canopy scaling, allometry and water balance within an individual-based framework. The model was specifically developed for tropical grass-tree systems as called for by House *et al.* (2003) and Sankaran *et al.* (2004) and it can predict current vegetation patterns in Africa better than the available alternative models can (Cramer *et al.* 2001; Bond *et al.* 2005; Hickler *et al.* 2006; Sato *et al.* 2007). We attribute the model's better performance to the fact that it uses more mechanistic rep-

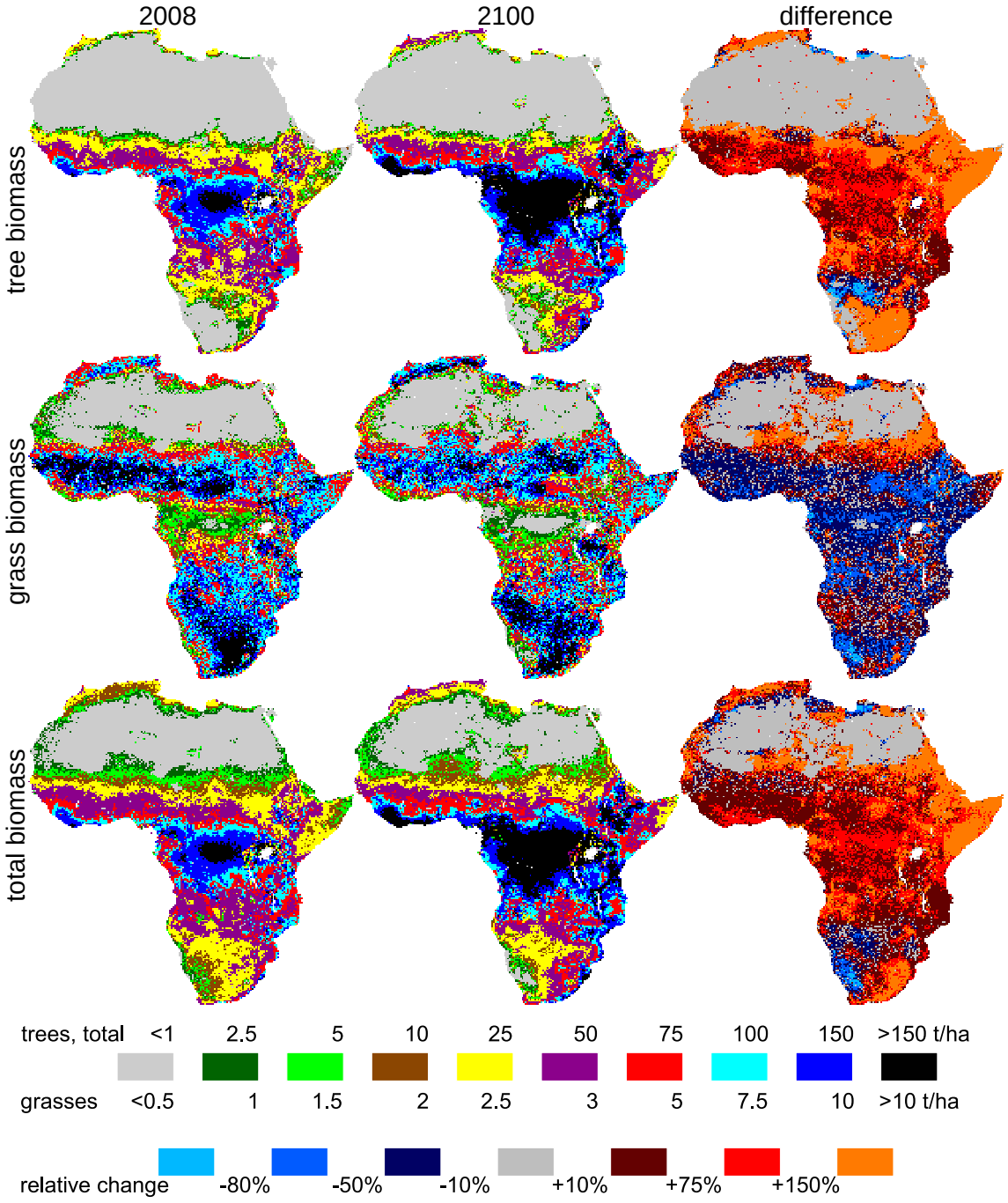

Figure 5.6: Simulated total tree and grass biomass and total biomass (aboveground and belowground, in t/ha) for 2008 and 2100 and the relative change within this time period. These simulations are based on the IPCC (2007) SRES scenario A1B with changes in CO_2, temperature and rainfall. See Table 5.7 for projected biomasses when not using the IPCC (2007) rainfall scenario.

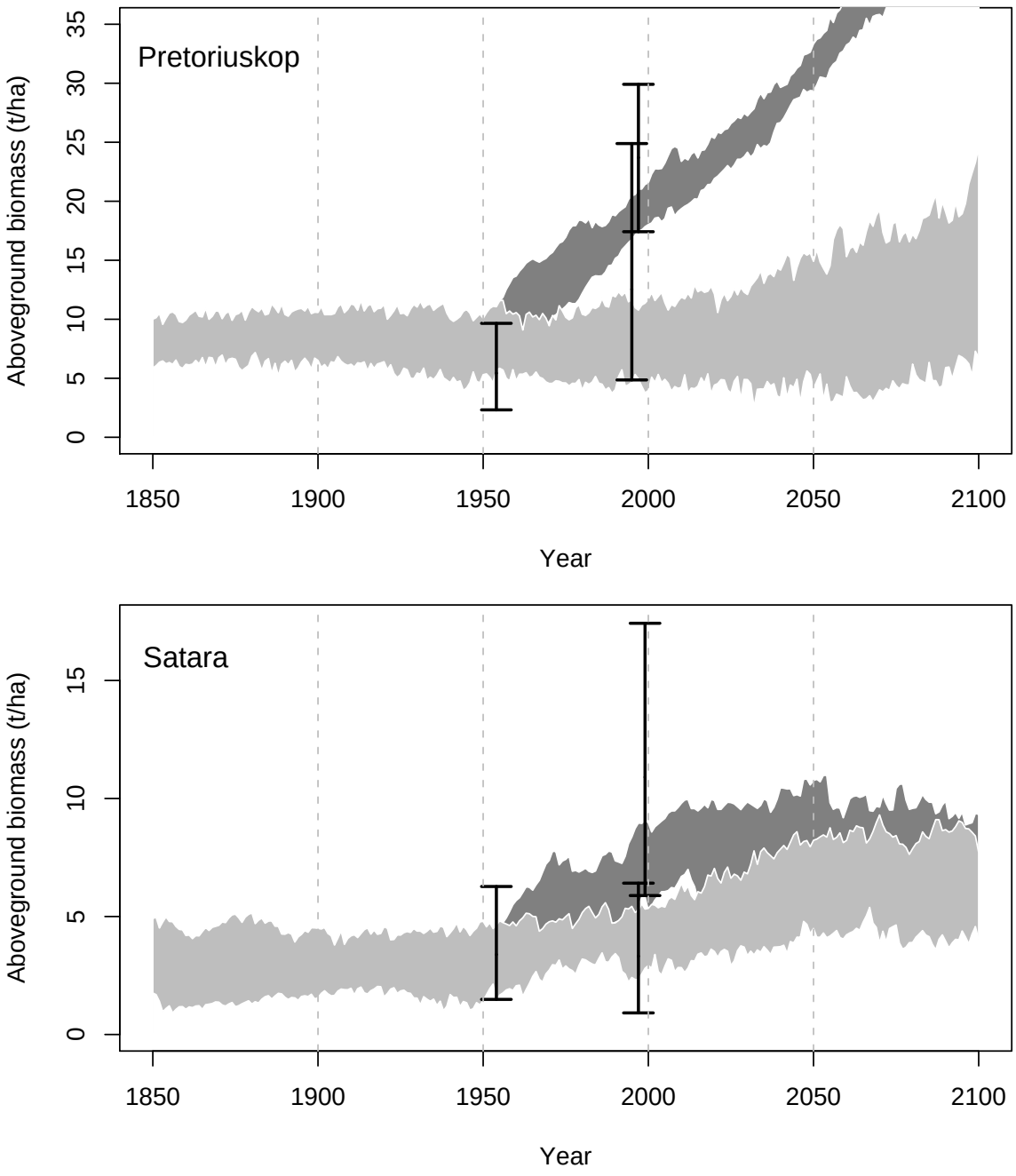

Figure 5.7: Time series of aboveground tree biomass (t/ha) at Pretoriuskop (25°10' S and 31°16' E, upper panel) and Satara (24°23.4' S and 31°46.2' E, lower panel) in the Kruger National Park between 1850 and 2100. Simulations were conducted using the IPCC (2007) SRES scenario A1B with changes in CO_2, temperature and rainfall. In the simulations grass biomass was reduced by grazing. Light grey shaded areas indicate the 10% and 90% quantiles of 20 simulations in presence of fire. Dark grey shaded areas indicate simulations with fire supression after 1954. Error bars indicate the 10% and 90% quantiles of tree biomass estimated by Higgins *et al.* (2007a).

resentations of key ecological processes and to the individual-based modelling approach. Specifically, the model includes mechanistic analogies of leaf phenology and carbon allocation, which allows for more adaptive responses of individual plants to changing environmental conditions, something which most existing DGVMs do not allow.

The aDGVM simulates the physiological feedbacks between phenology and allocation under increasing CO_2 and temperature. The aDGVM predicts extended growing season length for grasses and single trees due to increasing leaf level photosynthesis under elevated CO_2 and temperature (Taylor *et al.* 2008). Hence, the annual net carbon gain per individual increases. This higher carbon gain influences the modelled vegetation dynamics in two ways. First, individual plants can accumulate more biomass and second, tree reproduction rates increase which means that the number of trees increases. For trees, both processes can occur simultaneously but they are independent of each other. A consequence of the increased biomass is a reduction in the water available to individual plants, which in turn stimulates plants to allocate more biomass to roots. Eventually, plant available moisture limits growth and a new equilibrium between the elevated climate and vegetation is reached. Such mechanistic chains articulate hypotheses of how climate change influences ecosystems and the carbon cycle. This model therefore is a useful tool for exploring the consequences of such mechanistic chains (Chuine and Beaubien 2001; McGill *et al.* 2006).

The model can simulate tree-tree interactions as well as how fire mediates these interactions, which have been shown to be necessary for understanding savannas (Liedloff and Cook 2007). One particular aspect of tree-tree interactions is a density dependent self-thinning effect that potentially allows trees to become taller in presence of fire than in absence of fire due to fire induced reductions in tree-tree and grass-tree competition. This finding allows a new interpretation of the effects of fire on vegetation. Fire acts as a bottleneck for tree establishment (Higgins *et al.* 2000) but individual trees that successfully escape the fire trap might benefit from fire because fire reduces the size of their competitors and thereby the asymmetry in competitive interactions. Although density dependent self-thinning effects have been observed in forest systems (Niklas *et al.* 2003; Bagchi 2007; McCarthy and Weetman 2007; Zhang *et al.* 2007), they have only rarely been investigated in savannas (MacGregor and O'Connor 2002) and seldom in the context of fire.

Hély *et al.* (2006) and Hickler *et al.* (2006) report that the fire sub-models of DGVMs (Thonicke *et al.* 2001; Sitch *et al.* 2003) are major sources of uncertainty. We use a novel fire model where fire intensity and frequency are determined by fuel biomass and fuel

moisture and where each tree has an individual response to fire. The model simulates broad patterns of fire activity observed in Africa. However, it is generally difficult to compare fire models to data. Fire regimes predicted by a model are a function of both the simulated vegetation and fire sub-models (Keane *et al.* 2004). Furthermore, fire data obtained from remote-sensing are uncertain due to difficulties separating between fire, bright clouds and hot surfaces (Morisette *et al.* 2005). Hence, the disagreement between fire simulations and empirical data could be a failure of the vegetation sub-model to produce the correct fuel loads, due to errors in the fire sub-models or due to systematic errors in the empirical data. However, what we can learn from our fire simulations is that fire effects need to be explored both on local and on continental scales. At the local scale, fire suppression is important and can increase the carbon stored in vegetation by more than 100%. At the continental scale, fire suppression leads to a more modest 13% increase in the carbon stored in vegetation. Our results suggest that fire shifts the borders between grasslands, savannas and deciduous woodlands. Bond *et al.* (2005) in contrast predicted that fire suppression could induce a dramatic increase in tree cover and argued that almost all grasslands have the potential to form woodlands in absence of fire. Higgins *et al.* (2007a) shows that in the Kruger National Park, 50 years of fire suppression could not transfrom savannas into woodlands. Nonetheless, a simulation experiment conducted with the aDGVM in absence of fire and grasses, which allows trees to grow in absence of any inter-specific competition (results not shown) shows that large parts of savannas and grasslands have the potential to form a forest as predicted by Bond *et al.* (2005). Hence, the differences between our findings and those of Bond *et al.* (2005) could be attributed to differences in how grass-tree competition is modelled.

The simulated response of vegetation to climate change increases the carbon storage potential of savannas. Our simulations project the greatest change in carbon storage potential in the woody savannas that surround the central African evergreen forests and in parts of southern Africa. The model suggests accelerating effects of CO_2-fertilization and carbon sequestration under future CO_2. In contrast, Bond *et al.* (2003) observed the strongest response to CO_2 between pre-industrial and ambient CO_2, which implies that C_3-plants are CO_2-saturated under ambient conditions. Bond *et al.* (2003) argued that changes from woodiness to herbaceousness of C_3-vegetation play a major role under elevated CO_2 while leaf physiology only plays a minor role. Our results imply that these leaf level effects do scale through changes in growing season length and allocation to cause system level carbon allocation.

Although our model simulates how carbon storage in living vegetation is influenced

by elevated climates, the model does not simulate soil carbon, which is a major carbon pool in the global carbon cycle. Thus, Cao *et al.* (2001) showed that in evergreen forests soil can store up to 200 tC/ha and Williams *et al.* (2007) found that in Africa a total amount of 200±50 PgC can be stored in soils while vegetation only stores 80±28 PgC. Robinson (2007) argues that soils may store even more carbon than Grace (2004) and Williams *et al.* (2007) report. Soil carbon pools are temperature-driven (Moorcroft 2006) which means that soils have high potential to store or to release carbon in response to environmental changes. Hence, increasing respiration rates of the soil might compensate the additional carbon storage of vegetation as predicted in this study. Future studies with the aDGVM should investigate how the temperature dependencies of soil carbon decomposition and soil respiration (Giardina and Ryan 2000; Davidson and Janssens 2006) act in concert with vegetation dynamics to define ecosystem carbon storage.

A related point is the dynamics of soil nitrogen pools. Soil and leaf nitrogen are major determinants of the maximum rate of photosynthesis (Woodward *et al.* 1995; Wright *et al.* 2004) and several lines of evidence suggest that reduced nitrogen availability might lead to a down-regulation of photosynthesis as climate change progresses (Sellers *et al.* 1996; Moorcroft 2006). To investigate whether soil nitrogen reduction modifies the ecosystem performance, we conducted a sensitivity analysis that mimicked a soil-nitrogen induced down-regulation of photosynthesis between 1900 and 2100. This sensitivity analysis showed that down-regulation would not significantly influence the carbon storage the model predicts (see Figure 5.8). This result suggests that vegetation and carbon accumulation are only weakly determined by maximum photosynthetic rates. This finding agrees with studies that attribute empirically observed down-regulation to shifts in carbon allocation patterns (Moorcroft 2006) and studies that argue that CO_2 and temperature stimulated increases in biomass are not of a magnitude that would lead to nitrogen limitation (Lucht *et al.* 2006). However, it is clear that a full accounting of carbon and nitrogen pools using a soil CN model (e.g. Parton *et al.* 1987; Liski *et al.* 2005) would provide more clarity.

This study considers the influence of climate on vegetation while it does not account for the fact that vegetation modifies the climate. It is known that the feedbacks between climate and vegetation might significantly influence vegetation (Foley *et al.* 2000; Bonan *et al.* 2003; Scheffer *et al.* 2005; Meir *et al.* 2006). For instance, Claussen and Gayler (1997) and Brovkin *et al.* (1998) observed positive feedbacks between rainfall and vegetation in the Sahel/Sahara regions and Schaphoff *et al.* (2006) found substan-

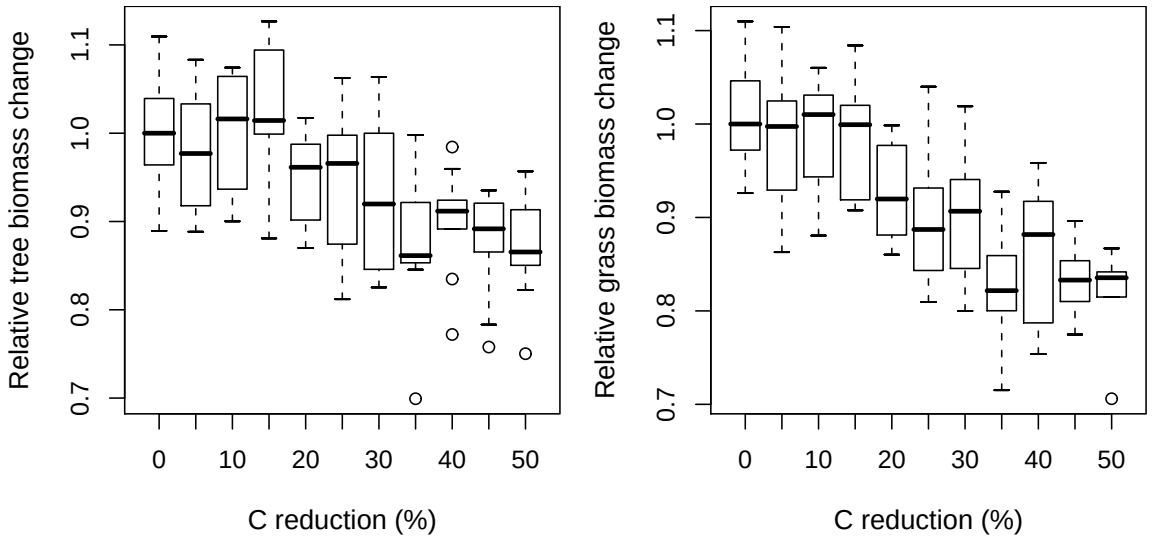

Figure 5.8: Relative change in tree and grass biomass in 2100 when soil carbon is reduced at different rates between 1900 and 2100. Depicted are the results from 30 simulation runs.

tial differences in the terrestrial carbon storage when a vegetation model was coupled to alternative general circulation models. Hence, although valuable progress can be made with offline studies, additional insights would be gained by coupling the aDGVM to a general circulation model.

Vegetation in Africa faces increasing pressure by human landuse, such as livestock production, deforestation and crop production (Williams *et al.* 2007) all of which have large socio-economic consequences (Scholes and Archer 1997). Landuse can significantly modify the grass-tree dynamics and cause regime shifts. This effect might be amplified or accelerated by the tension between observed and potential biomass found in grass-tree systems (Sankaran *et al.* 2005). For instance, grazing might lead to decreases in the grass biomass such that trees might benefit from reduced grass-tree competition and fire activity. The tree biomass in heavily grazed systems can exceed the tree biomass observed in absence of grazers (Smit *et al.* 1999; Bond and Keeley 2005; Higgins *et al.* 2007b) and such tree dominated systems are often, from the perspective of livestock production, degraded (Vetter 2005). Landuse also influences the carbon cycle and the potential of vegetation to store carbon (Williams *et al.* 2007). The aDGVM is, due to its process-based design, suited to explore quantitatively how landuse and climate change interact to modify grass-tree dynamics. This potential was illustrated in our simulations of vegetation development in the Kruger National Park, which showed that

the empirically observed tree biomasses (Higgins *et al.* 2007a) could only be explained by invoking grazing.

Projections of vegetation models are influenced many sources of uncertainty. There is uncertainty in the representation of ecological processes in equations and there is uncertainty in the data used for parametrization and validation (Clark *et al.* 2001). One major uncertainty in the projections of the aDGVM is the parametrization of vegetation. Thus, a sensitivity analysis (not shown) indicates that allometric parameters such as the ratios between biomass and height or height and canopy radius strongly influence the simulation results. These parameters are, as it is typically the case in vegetation models, fixed such that vegetation cannot adapt the allometry to environmental gradients or climate change and poorly chosen parameters may bias the simulation results. Hence, one way to further improve vegetation models would be to allow the dynamic adaption of plant allometry to climatic conditions, analogously to the adaption mechanisms for phenology and allocation used in the aDGVM. Another major source of uncertainty in the model is given by the input soil and climate data (Global Soil Data Task Group 2000; New *et al.* 2002). Our sensitivity analysis (not shown) revealed that the model was sensitive to many of these forcing variables.

Despite various uncertainties, the model we present articulates hypotheses about the functioning of African vegetation. Thus, the model predicts that CO_2 effects on trees are not saturated at ambient CO_2 and together with other atmospheric changes, cause a substantial shift of biomes towards tree dominance. The model is the first vegetation model that allows individual trees to adopt evergreen or deciduous phenology without explicitly pre-defining one of these strategies. Hence, in a more general sense the model is a step away from hard-wired functional types and a step towards the adaptive and individual-based vegetation modelling.

6 Discussion and conclusions

This thesis focuses on two central questions in the context of savanna research, namely (1) can we explain how grass-tree coexistence in savannas occurs under such a broad range of environmental conditions and (2) can we project how grass-tree ratios, carbon storage and fire regimes in African savannas behave under anticipated global climate changes. To contribute to these questions, we have developed two models that greatly differ in their structure and complexity. The model used to explore grass-tree coexistence is a system of differential (or difference) equations, giving a very heuristic and aggregated representation of the study system (Chapters 2 and 3). The second model, the aDGVM, is a process-based and mechanistic vegetation simulation model that imitates ecological processes observed in empirical studies (Chapters 4 and 5).

The savanna models presented in this thesis contribute to the integration of resource- or competition-based explanations of savannas and disturbance- or demography-based aspects of savannas as called for by Sankaran *et al.* (2004). Thus, the models implement the effects of water and light competition, induced by limited resource availability, as well as effects of disturbances such as fire or herbivory on vegetation. In addition, the aDGVM simulates demographic processes (reproduction, mortality and fire response) of the tree population on an individual-based level.

The following paragraphs summarize the main results of the different Chapters, describe the role of fire within the different models and discuss general aspects of model selection, parametrization and validation in the context of the presented models. Further, we outline future applications and perspectives for the presented models.

6.1 Summary of the main results

The grass-tree coexistence model in Chapter 2 predicts that grasses and trees can coexist in a stable equilibrium when inter-specific competition is relatively weak and balanced, that is, when competition exerted by grasses on trees is similar to competition exerted by trees on grasses. In this situation, fire imposes periodicity on the system and modifies the mean grass and tree biomasses but it does not influence the fact that

the system is stable. At high levels of light and root competition, trees can exclude grasses. In this situation the model predicts that fire can reduce competitive effects exerted by trees on grasses sufficiently to allow grass-tree coexistence. These results are fundamentally different to what we find in the literature (Jeltsch *et al.* 1996, 1998; van Langevelde *et al.* 2003; Sankaran *et al.* 2004) and we attribute these differences to the partitioning of biomass into aboveground and belowground compartments. This partitioning allows us to separate between aboveground and belowground competition and to simulate the fact that herbivory and fire only reduce aboveground biomass while belowground biomass potentially supports shoot regrowth and thereby buffers vegetation against disturbances. This modeling approach integrates resource based and disturbance based aspects of savannas within a simple and deterministic framework, as called for by Sankaran *et al.* (2004)

In Chapter 3 the model presented in Chapter 2 is used to show that grass-tree coexistence can be considered as being stable on a rainfall gradient from 200 mm to 1200 mm mean annual precipitation (MAP). This analysis furthermore shows that there is no fundamental difference in the stability of arid and mesic savannas as suggested by Sankaran *et al.* (2005). That is, it is shown that fire is not required for coexistence at sites that receive less that 1200 mm and that it is only a modifier of grass-tree dynamics. However, fire determines whether the system converges towards an asymptotically stable equilibrium (in the absence of fire) or towards a stable limit-cycle (in the presence of fire). Furthermore, we illustrate that the relative ability of fire to draw tree biomass away from the rainfall defined tree biomass does not change with rainfall.

Chapter 4 motivates the development of a new dynamic vegetation model, that focuses on grass-tree dynamics in tropical ecosystems. Then our implementation of a dynamic vegetation model, the aDGVM, is presented in detail. A novel aspect of the aDGVM is, that it simulates phenology and carbon allocation in response to the environmental conditions by using simple mechanisms that control the beginning and the end of the growing season and how the plant's carbon gain is allocated to different plant biomass pools. The aDGVM implements an individual-based approach and a novel fire model which allows us to simulate fire-vegetation interactions on a plant level, which is not possible in most DGVMs (e.g. Sitch *et al.* 2003; Woodward *et al.* 2004). We conducted a sensitivity analysis to investigate how parameters and constants used in the model influence the model results and to explore uncertainties in the model. In Chapter 4 we also claim that vegetation models should allow vegetation to adapt to environmental conditions, instead of using fixed and predefined plant traits. The

importance of such adaptive processes is supported by the sensitivity analysis.

In Chapter 5, the aDGVM was used to simulate the current and future vegetation of Africa. The study shows that the model can simulate current vegetation patterns of Africa in excellent agreement with empirically observed vegetation patterns, in particular, the model simulates the extent of savannas better than previous models do (Cramer *et al.* 2001; Bonan *et al.* 2003; Bond *et al.* 2005; Hickler *et al.* 2006; Schaphoff *et al.* 2006; Sato *et al.* 2007). The resource-based phenology sub-model of the aDGVM allows the simulation of the extent of evergreen and deciduous vegetation in response to the environment and without predefining evergreen or deciduous functional types. Fire suppression experiments conducted with the aDGVM show that fire suppression strongly influences tree dominance at the regional scale, and at a continental scale the aDGVM predicts that fire suppression would increase biomass in vegetation by about 13%. Under changing [CO_2], precipitation and temperature, defined by the IPCC (2007) SRES scenario A1B, the model predicted longer growing periods, higher allocation to roots, higher fecundity, more biomass and a dramatic shift towards tree dominated biomes. The analyses suggest that the [CO_2] fertilisation effect is not saturated at ambient conditions and will strongly increase at future [CO_2] levels.

6.2 Fire effects

The effects of fire on vegetation in savannas have been intensively investigated, both in field studies and in modeling studies (Scholes and Walker 1993; Higgins *et al.* 2000; Sankaran *et al.* 2005; Higgins *et al.* 2007a). However, this study contributes to our understanding of fire as it provides some specific aspects of how fire shapes vegetation. These results can be attributed to the way fire is simulated. Most savanna models and DGVMs assume that fires spread regularly with a fixed frequency or in response to litter moisture and that fire consumes a pre-defined fraction of grass and tree biomass (Thonicke *et al.* 2001). Models using differential equations often assume that fire permanently consumes a small proportion of biomass which means that in these models, fire can be interpreted as non-selective herbivory (van Langevelde *et al.* 2003). Thus, fire models used in previous savanna models do not adequately describe how fire influences vegetation and several authors argue that the implementation of fire sub-models is a major source of uncertainty in vegetation models (Hickler *et al.* 2006; Schaphoff *et al.* 2006).

The fire models used in this thesis assume that fire is a sudden event that consumes

biomass within one single time step. Biomass consumption is assumed to be a function of the fire intensity, which is in turn a function of fuel biomass and fuel moisture (Higgins *et al.* 2008). By the separation of aboveground and belowground biomass, we can simulate the fact that fire only consumes aboveground biomass while belowground biomass buffers vegetation against fire (Crider 1955; Wolfson 1999; Bond and Midgley 2001). In the aDGVM, fire effects are simulated for single trees using a semi-empirical fire model, such that fire influences the demography of the tree population (Higgins *et al.* 2000). The following summarizes three major results of this thesis concerning the effects of fire on vegetation.

(1) The results suggests that below 1200 mm MAP, fire only modifies the system dynamics from a stable equilibrium in absence of fire to stable limit-cycles in presence of fire but it is not necessary to establish grass-tree coexistence. This observation implies that there is no fundamental difference in the stability of arid and mesic savannas. When rainfall is higher than 1200 mm MAP, fire might be necessary for grass-tree coexistence. In this situation, fire reduces the competitive effects that trees exert on grasses and thus prevents grasses from being out-competed. However, we did not have data from savannas that receive more than 1200 mm MAP and therefore cannot identify the threshold with confidence.

(2) When fire is suppressed, the total biomass stored in the vegetation of Africa would increase by 13% while at a local scale, regular fire potentially reduces the aboveground tree biomass by more than 50%, depending on the site characteristics. This effect can be explained by the demographic effect of fire. At arid sites, most trees are in small size classes which means that fire potentially consumes all aboveground tree biomass. At mesic sites, most biomass is stored in tall trees that due to their size are not affected by fire. Hence, at mesic sites fire only removes a relatively small proportion of the total biomass.

(3) The study shows that fire is a demographic bottleneck for single trees (Higgins *et al.* 2000) as it holds trees in small size classes by repeatedly removing aboveground biomass. However, individual trees that successfully escape the fire trap might benefit from fire. Fire reduces the size of competitor trees and thereby inter- and intra-specific competition exerted on the target tree. Hence, in presence of fire, trees might become even larger than in situations without fire. Individual trees that successfully escape the fire trap might benefit from fire due to a reduction of density dependent self-thinning effects to the detriment of the majority of individuals.

6.3 Model selection

The first steps in modelling studies are (1) to identify the question and (2) to select the appropriate model to answer the question. That is the modeller needs to identify the properties that a model must have in order to answer the question. In the context of this thesis, the questions were (1) is it possible to develop a model that explains grass-tree coexistence without invoking rooting niche separation or stochastic mechanisms and (2) how will savannas respond to global climate changes? The model to answer the second question should further be able to simulate grass and tree biomass in savannas under current and future climate conditions from a small number of environmental input data.

Once the decision to develop a new model has been made, it is necessary to specify which model is adequate to describe the target system. For instance, the investigation of how vegetation responds to climate change requires a process-based model that can simulate ecological processes such as photosynthesis or respiration in response to environmental conditions. A simple and heuristic model such as the model presented in Chapter 2 is not appropriate to explore such questions as all model parameters are constants that do not respond to the environment. Nonetheless, examples of how such heuristic models could be extended to allow the simulation of ecosystem responses to the environment are given in Chapters 3 and in Higgins *et al.* (2007b), where the growth rates are defined as a function of precipitation. In contrast, to explore the nature of grass-tree coexistence, a heuristic and mathematically tractable model might be the better choice. Heuristic models focus on few key assumptions such as the partitioning of roots and shoots and allow to test whether these assumptions can explain the observed system dynamics. Such heuristic models are minimalistic in the sense that they neglect all processes that might complicate the analysis while they hopefully include the most important processes and therefore potentially yield elegant theoretical explanations for the questions being examined.

Models are a powerfull tool that have been successfully employed in many fields and disciplines of ecology. However, a model always represents a trade-off between maximizing the realism of simulated ecosystem processes and minimizing the model complexity. Models that minimize the complexity might be over-simplified which means that they potentially neglect key processes of the target system and hence do not appropriately capture the system dynamics. This might yield to bias in the model predictions (Burnham and Anderson 2001). Models that maximize the realism of ecosystem processes might be inaccessible for mathematical analyzes or alternative methods used to explore

the model. Finally, complex models might be over-parametrized. Over-parametrized models have excessive degrees of freedom and their behavior is not necessarily well-defined by a unique sub-set of parameters. Hence, variance in the model predictions might be high (Burnham and Anderson 2001). Despite the intuitive attraction of realistic models, the inclusions of more realism into a model might also yield to a what has been denoted as the "complexity paradoxon" (Oreskes 2003). The inclusion of more and more mechanisms into the model provides a more realistic representation of ecosystem dynamics. More realism in the model suggests that the simulation results are more precise and reliable. However, the inclusion of more and more processes generates more "hidden" interactions which are difficult to identify. It is possible that these hidden interactions are not found in the real ecosystem. A consequence of these interactions might be that in more realistic models, the uncertainty of the predictions might even increase, compared to simpler models that focus on the fundamental processes. Thus, the "truer" the model, the more difficult to show that it is true. Therefore, it has been repeatedly claimed that if possible, simple models should be used instead of larger and larger models. Model complexity should be reduced to the minimum which is necessary to explore the question (Burnham and Anderson 2001; Clark and Gelfand 2006; Aumann 2007). "Everything should be made as simple as possible, but no simpler" (Albert Einstein).

6.4 Model parametrization and validation

Some of the most important, yet most challenging tasks in ecological modelling are the processes of model parametrization and validation. Parametrization is the specification of the model parameters and constants by using empirical data. Validation is the process of illustrating that the model correctly represents and reproduces the required aspects of the real world system dynamics. Validation essentially shows that the appropriate model was developed for a specific question or application (Rykiel 1996; Aumann 2007). Without knowledge of the intended model applications, validation has no end (Overton 1977).

For both parametrization and validation, there exists a large number of techniques and philosophies. However, while there is consensus how parametrization should be conducted, validation is highly debated in the literature (Rykiel 1996). The literature on validation ranges from technical descriptions of how models should be validated over philosophical discussions to papers that argue that validation is not possible or not

essential as the usefullness and scientific value of a model are more important than a validity statement (Mankin *et al.* 1977; Rykiel 1996; Oreskes 2003; Aumann 2007). Models in ecology are considered as tools to investigate ecosystems while the time-consuming processes of model design, verification, validation and documentation do, in general, not contribute to a progress in ecology (here, progress is defined as a result significant enough to warrant publication) and are hence only of minor interest. Yet, these procedures are standard in software engineering and Aumann (2007) claims that ecologists should spend more time on these stages of the modelling process to facilitate the understanding of alternative models and to allow an exploration of uncertainties of different models. However, a rigorous validation of ecological models is difficult and most attempts of validation are therefore best described as rudimentary.

There are generally two options for the parametrization of a model, namely direct and indirect methods. Direct methods assume that parameters and processes in the ecological model represent parameters and processes of the real system. Hence, empirical data obtained in field studies can be directly used to parametrize the model. Generally, direct parametrization is possible in simulation models such as DGVMs which try to mimic real processes. For example we can directly estimate the seed production or the specific leaf area of modelled species. By contrast, in abstract and heuristic models, parameters often describe ecological processes in a highly aggregated and compact form such that direct parametrization is not possible and indirect methods are required. For instance a growth rate parameter for a plant is a function of photosynthesis and respiration. Indirect methods include fitting model parameters to field data by using classical gradient methods, bootstap methods, nonlinear regression techniques, maximum likelihood techniques or Bayesian approaches such as Monte Carlo Markov chain methods (Law and Watkinson 1987; Rees and Bergelson 1997; Freckleton and Watkinson 2000; Wiegand *et al.* 2003; Nelson *et al.* 2004). Studies that use indirect parameter fitting for Volterra-Lotka-type models are rare (Pascual and Kareiva 1996; Freckleton and Watkinson 2000) although it has been shown that indirect techniques might even provide better results than direct methods despite the intuitive appeal of direct methods (Freckleton and Watkinson 2000, 2001).

Validation techniques generally used in ecology are the comparison of model results to (historical) field data, the intercomparison of alternative models and "predictive" validation, that is, field studies are conducted to verify or refute model projections, and hence, the model assumptions (Sargent 2007). Such validation techniques can show whether the simulated processes are general enough to describe all systems included

in the model's domain and to predict independent data or whether the model only reproduces the empirical data used for parametrization. The intercomparison of different models shows whether the selected model can predict field data better and with lower bias than alternative models can. Much of the model validation work is conducted within the model development phase by running test simulations and by evaluating simulation results. Such evaluations include to test whether the model can predict independent field data and whether the model can predict these field data better than alternative models do.

The development of two different models in this thesis implies that the application of different methods for parametrization and validation were necessary. In the heuristic savanna model described in Chapter 2, growth, decomposition and competition parameters cannot be estimated by direct methods such that we had to use indirect methods for model parametrization and validation. In Chapter 3, these parameters were estimated by indirectly fitting the model to a tree abundance data set from Africa (Sankaran *et al.* 2005) using Markov chain Monte Carlo methods. This fitting procedure yields a validation statement for the model as it shows that the model's representation of grass-tree interactions is good enough to simulate the observed tree biomass on a rainfall gradient from 200 mm to 1200 mm MAP.

By contrast, processes and output variables of the aDGVM presented in Chapter 4 imitate processes and variables in the real system, such that model parametrization and validation with field data could be conducted by using direct techniques. However, in this situation, parametrization and validation turn out to be constrained by field data. The aDGVM uses about 150 parameters and constants which were taken from many different sources. Many of the parameters are averages of a set of studies and/or do not come from savanna sites as the required field data are often unavailable for savanna sites or not available at the required scale or resolution. Field data are mostly collected for purposes other than model parametrization (Clark and Gelfand 2006). Further, available datasets might significantly differ as different authors use different methods and techniques for data collection and analysis. Thus, it is difficult to judge whether empirical data are appropriate for model parametrization and validation (Sargent 2007). For instance, an intercomparison of three different global vegetation maps, which are generally used to validate global vegetation models, showed that the vegetation maps only agree on 41% of the grid cells (Jung *et al.* 2006). We faced a similar problem while comparing the biome distribution simulated by the aDGVM with field data such that we decided to use a consensus map of seven different vegetation maps for the model val-

idation (Chapter 5). Thus, our experience supports Jung *et al.* (2006)'s claim that new methods and standards are needed for a robust and unbiased model comparison and validation. Another example where parametrization is critical is the parametrization of vegetation in the aDGVM. The parameters that descibe vegetation attributes must be selected from a trait databases consisting of many values. However, because the data in the trait databases are based on the literature, the data have high taxonomic and regional biases. It is not clear whether one should use the mean, modal or some other attribute of the parameter's distribution in the model. Our sensitivity analysis shows that the choice of parameters describing plant attributes does strongly influence the simulation results.

One general concept to validate models might be to develop benchmarks, that is normed tests to measure performance and to allow the intercomparison of different models. Therefore, different models are used with the same objective parameter set and they simulate pre-defined scenarios. Standard methods could be used to quantify the model performance such that the tests would allow an objective evaluation and validation of alternative models.

6.5 Model uniqueness

Assume that a model perfectly simulates empirically observed patterns on a certain system level. This does not necessarily mean that the model assumptions are reasonable and that the model captures the underlying ecosystem dynamics (Oreskes and Belitz 2001). In fact, the mapping from input data, e.g. environmental data, to output data, e.g. grass and tree biomass is not unique which means that there exists a large number of different models that correctly reproduce empirical data, given a set of input data. These different models might even be based on contradicting assumptions. It is therefore necessary to analyze principal and auxiliary model assumptions as well as model predictions on different process levels included in the model as well as on different spatial and temporal scales.

For instance, in Chapter 5 the aDGVM was compared to different vegetation maps which were mainly obtained by remote sensing. To learn more about the model and to test the model assumptions, it would be necessary to analyze the model on process levels other than the ecosystem level, for instance on a plant physiological level and to study the model at a scale and resolution other than the continental scale. For instance, the model can be further validated by conducting simulations at the regional scale, such

as the Kruger National Park or at single study sites in Africa. Another alternative to test the model is to conduct simulations on other continents. This thesis only provides results where the models have been used to simulate vegetation in Africa although we claim that the models are general enough to simulate the world's tropical vegetation. For this reason, we intend to use the models for simulations of Australian and South-American savannas. On the one hand, such simulations would increase confidence into the models and serve as model validation and on the other hand, such simulations allow us to compare the nature of grass-tree interactions in different savanna environments.

6.6 Land use

Most of the sub-Saharan Africa is savanna and the highest human densities are found in the savanna regions. It follows that savannas are of great socio-economic importance (Scholes and Archer 1997). Increasing population densities and the increasing demands of rural populations ensure that savannas are subjet to increasing rates of livestock production, deforestation or conversion to crop. The consequences of these changes for the carbon cycle are immense (Williams *et al.* 2007). For instance, grass biomass removal by grazing causes shifts to tree dominance (Smit *et al.* 1999; Bond and Keeley 2005). Such tree dominated (or "bush-encroached") systems are, from the perspective of livestock production, degraded which reduces the economic return of savannas (Vetter 2005). Further, studies suggest that under elevated [CO_2], trees have increasing potential to store carbon due to a CO_2-induced fertilization effect of C_3-photosynthesis (Drake *et al.* 1997; Ehleringer *et al.* 1997, Chapter 5). Hence, increasing amounts of anthropogenic CO_2 emissions might potentially be sequestered by the woody vegetation of savannas. While additional carbon sequestration in savanna trees might be assessed positive in the context of the global carbon balance, additional carbon sequestration in trees amplifies bush-encroachment and, from the perspective of lifestock production, degradation.

The complexity of how grass-tree systems respond to climate change, fire and grazing shows that it is necessary to explore sustainable management strategies for savannas. From the perspective of lifestock production, sustainability means that the savanna is managed in a way such that the economic utility does not decline over time (Perman *et al.* 2003). However, sustainability should not only be interpreted from the perspective of livestock production, rather, management should also consider the ecological services of savannas, that is, management should preserve the characteristic structure and biodiversity of savannas over time (Higgins *et al.* 2007b).

Higgins *et al.* (2007b) and Boerner *et al.* (2007) used a modified version of the heuristic grass-tree model (Chapters 2 and 3) to investigate optimal and sustainable management strategies for savannas. Higgins *et al.* (2007b) explores sustainable management strategies of agents motivated by economic, productivity and ecological factors under deterministic and stochastic conditions. The analysis shows that both under deterministic and stochastic conditions, more conservative management strategies are more sustainable compared to more opportunistic management strategies. Boerner *et al.* (2007) found that price and rainfall variability should be considered in the calculation of optimal management strategies and showed that the cost of fire management limit the manager's options for sustainable landuse. The analysis suggests that a reduction of fire management costs could increase livestock production and the sustainability of livestock production.

However, such analyzes have not been conducted using the aDGVM, although the model can accommodate the inclusion of management sub-models. In contrast to the heuristic grass-tree model, the aDGVM would allow a quantitative analysis of land use strategies in terms of grass and tree biomass or cover. Tree size structure and tree density can further be used to describe visibility range and the accessibility of the site, which might be important for livestock production but also for game viewing. Further, the aDGVM could serve to explore how climate change modifies the conditions for optimal and sustainable landuse as it simulates the response of vegetation to environmental variables. Hence, the model could serve as a tool to improve the link between modelling, monitoring and management.

6.7 Coupling of vegetation and climate models

It is known that the feedbacks between climate and vegetation can modify rates of global climate and vegetation change (Foley *et al.* 2000; Bonan *et al.* 2003; Scheffer *et al.* 2005; Meir *et al.* 2006). Thus, vegetation is strongly influenced by climate variables such as $[CO_2]$, temperature, precipitation or radiation. However, vegetation also modifies the climate system. For instance, vegetation cover defines the surface albedo and the surface roughness which in turn influence the surface energy balance and convective precipitation. Using coupled climate-vegetation models, Claussen and Gayler (1997), Brovkin *et al.* (1998) and Liu *et al.* (2006) observed positive feedbacks between precipitation and vegetation in the Sahel/Sahara regions. Schaphoff *et al.* (2006) found substantial differences in the terrestrial carbon storage when a vegetation model was

coupled to different general circulation models. Raddatz *et al.* (2007) observed positive feedbacks in the climate-carbon cycle by comparing coupled and uncoupled climate-carbon cycle simulations. The analysis suggests that the carbon storage potential under elevated CO_2 is lower in the case of coupled simulations than in the case of uncoupled simulations and that vegetation-carbon coupling accelerates the rate of global climate change.

The sensitivity analysis conducted in section 4.8 also showed the high sensitivity of the aDGVM to variations in climate variables, with particularly strong responses to the atmospheric CO_2 concentration, temperature and precipitation (Figure 4.16). This means that the input data taken from the global data bases (Global Soil Data Task Group 2000; New *et al.* 2002) are a major source of uncertainty in our simulation results and that the coupling with a climate model may allow a more objective assessment of the different sources of uncertainty in the model. Thus, coupling the aDGVM with a climate model will improve the quality of aDGVM projections by reducing uncertainty.

However, not only the aDGVM has the potential to be coupled with climate models, it is also possible to couple the heuristic grass-tree coexistence model with climate models. For such an extension, the model parameters must be calculated as a function of environmental conditions. For instance the Farquhar *et al.* (1980) photosynthesis model and precipitation could be used to calculate the growth rate and the decomposition rates could be simulated as a function of temperature (Tjoelker *et al.* 2001; Arora 2003). Such a model would provide a simple and computationally efficient mean to simulate grass-tree dynamics within a coupled climate-vegetation model.

6.8 Conclusions

This thesis contributes to the current savanna and climate change research, as it (1) presents the first deterministic savanna model that can explain coexistence on a wide gradient of environmental conditions without invoking stochastic mechanisms or the rooting niche separation mechanism, (2) shows that savannas can be considered as being stable on a gradient from 200 mm to 1200 mm MAP, while Sankaran *et al.* (2005) argued, that savannas that receive less than 650 mm MAP are stable and savannas that receive more than 650 mm MAP are unstable and (3) provides a process- and individual-based vegetation model specifically for tropical grass-tree systems that can predict the distribution of African savannas and fire regimes in response to climate and soil conditions. This model allows the investigation of the effects of climate change on

a plant physiological level. More specifically, this model predicts that the vegetation in Africa will significantly shift towards tree dominance by CO_2-induced fertilization of C_3-photosynthesis and that CO_2 effects do not saturate at $[CO_2]$ levels below 800ppm.

Based on the models developed in this thesis, we claim that future research should concentrate on (1) including adaptive modeling concepts and community assembly into vegetation models (see Section 4.9), (2) coupling climate and vegetation models and (3) using the aDGVM to explore sustainable landuse strategies for savannas.

Zusammenfassung

Als tropische Savannen bezeichnet man im Allgemeinen Ökosysteme die durch eine gleichmäßige C_4-Grasschicht und eine unregelmäßige Baumschicht charakterisiert sind, d.h., durch die Kodominanz von C_4-Gräsern und Bäumen (Huntley and Walker 1982; Scholes and Walker 1993). Savannen haben einen großen Anteil am globalen Kohlenstoffkreislauf und sind von großer sozio-ökonomischer Bedeutung. Savannen werden in erster Linie durch Störungen, Trocken- und Regenzeiten sowie durch Ressourcenkonkurrenz kontrolliert (Sankaran *et al.* 2004). Eine wichtige Rolle spielt dabei Feuer (Scholes and Walker 1993). Feuer reduziert die Biomasse und die Etablierungsrate von Bäumen, d.h. Feuer verhindert, dass die Baumbiomasse erreicht wird, die aufgrund der Umweltbedingungen zu erwarten wäre (Sankaran *et al.* 2005). Trocken- und Regenzeiten bestimmen die Länge der Wachstumsperiode und damit die Biomasse von Pflanzen (Jolly *et al.* 2005). Das Verhältnis zwischen Gras- und Baumbiomasse kann in Savannen stark variieren. Feuchtsavannen werden meist durch Bäume dominiert, so dass Lichtkonkurrenz eine wichtige Rolle spielt (Scholes and Walker 1993). Trockensavannen sind oft grasdominiert und die Baumbiomasse ist aufgrund starker Wasserkonkurrenz gering. Trockensavannen werden auch als stabil bezeichnet, weil Feuer die Biomasse, nicht aber die Gras-Baum-Koexistenz beeinflusst. Dagegen werden Feuchtsavannen als instabil bezeichnet, weil Gras-Baum-Koexistenz eventuell durch Feuer ermöglicht wird (Sankaran *et al.* 2005).

Obwohl Savannen während der letzten Jahrzehnte intensiv untersucht wurden, ist unser Verständnis der Funktionsweise von Savannen noch vergleichsweise gering (Sankaran *et al.* 2004) und wichtige Aspekte der Savannendynamik konnten noch nicht endgültig geklärt werden. Zwei spezielle Fragen sind (1) wie können Gräser und Bäume in Savannen koexistieren, während sie sich in Grasländern und Regenwäldern gegenseitig auskonkurrieren (Sarmiento 1984) und (2) wie beeinflusst der Klimawandel die Gras-Baum-Dynamik in Savannen (Bond and Keeley 2005). Die Frage der Gras-Baum-Koexistenz ist ein klassisches Problem der Populationsökologie und verschiedene Modelle wurden entwickelt, um diese Frage zu untersuchen. Allerdings können existierende Modelle die Gras-Baum-Koexistenz nicht auf dem gesamten Umweltgradienten erklären,

auf dem Savannen empirisch beobachtet wurden. Weiterhin beruhen die Modelle oft auf speziellen Details der Savannendynamik, die zum Teil noch nicht empirisch belegt werden konnten (Jeltsch *et al.* 1996, 1998; Higgins *et al.* 2000; Gardner 2006).

Aktuelle Klimaprojektionen zeigen, dass Afrika durch den Klimawandel besonders stark betroffen ist (IPCC 2007). Allerdings wurde der Einfluss des Klimawandels auf den Kohlenstoffkreislauf in Afrika nur selten explizit untersucht, da sich die meisten Studien auf den globalen Kohlenstoffkreislauf konzentrieren (Williams *et al.* 2007). Außerdem simulieren existierende Vegetationsmodelle Savannen oft als Regenwald oder Grasland, da die komplexen Gras-Baum-Interaktionen sowie Feuereffekte nicht hinlänglich modelliert werden. Dies bedeutet, dass die klimabedingten Veränderungen des Grasland-Savanne-Regenwald-Komplexes in Afrika einen großen Unsicherheitsfaktor in aktuellen Projektionen des Kohlenstoffkreislaufs darstellen (IPCC 2007).

In dieser Dissertation werden verschiedene Modelle entwickelt und verwendet, um die Gras-Baum-Koexistenz und die Auswirkungen des Klimawandels auf Savannen zu untersuchen. Die Modelle führen Theorien, die auf demographischen Prozessen oder Störungen basieren mit Theorien, die auf Konkurrenz oder Ressourcenverfügbarkeit beruhen zusammen und verwenden neue Methoden, um die Interaktionen zwischen Feuer und Vegetation zu simulieren. In den Modellen ist Feuer ein diskretes Ereignis, das die oberirdische Biomasse in einem Zeitschritt konsumiert, während die unterirdische Biomasse nicht beeinflusst wird und so die Vegetationsdynamik puffert.

Das Modell in Kapitel 2 zur Untersuchung der Gras-Baum Koexistenz ist ein heuristisches Modell. Das Modell trennt zwischen oberirdischer und unterirdischer Gras- und Baumbiomasse. Feuer und Beweidung reduzieren nur die oberirdische Biomasse. Die Modellanalyse zeigt, dass Gräser und Bäume in einem stabilen Gleichgewicht koexistieren können, wenn die inter-spezifische Konkurrenz schwach ist. In diesem Fall erzeugt Feuer lediglich periodische Trajektorien und das System ist nach wie vor stabil. Wenn die Lichtkonkurrenz stark ist, können Gräser von Bäumen verdrängt werden. In diesem Fall kann Feuer die Lichtkonkurrenz reduzieren und dadurch die Gras-Baum Koexistenz ermöglichen.

In Kapitel 3 wird das Gras-Baum-Modell aus Kapitel 2 unter Verwendung von Monte Carlo Markov Chain Methoden indirekt mit empirischen Daten parametrisiert. Das parametrisierte Modell kann Gras-Baum-Koexistenz über einen Regengradienten von 200 mm bis 1200 mm vorhersagen. Weiterhin zeigt die Analyse, dass die Gras-Baum-Koexistenz auf diesem Regengradienten stabil ist und Feuer nicht für Koexistenz notwendig ist. Es besteht also kein grundsätzlicher Unterschied zwischen der Dynamik von

Trocken- und Feuchtsavannen (Sankaran *et al.* 2005). Die Studie lässt jedoch offen, bei welchem Niederschlag Savannen instabil werden, da die notwendigen Daten nicht verfügbar waren.

Das zweite Modell (das adaptive dynamische globale Vegetationsmodell, aDGVM, Kapitel 4) ist ein prozess- und individuenbasiertes Simulationsmodell, das biophysikalische, physiologische und ökologische Mechanismen imitiert, die in Savannen empirisch beobachtet wurden. Das Modell kombiniert etablierte Module für Blattphysiologie, Skalierung auf Baumkronenniveau, Reproduktion und Mortalität mit neuen Konzepten für Phänologie, Kohlenstoffallokation und Feuer in einem individuenbasierten Modell. Das Modell wurde speziell für tropische Ökosysteme entwickelt und es kombiniert Konkurrenzmechanismen zwischen Gräsern und Bäumen mit demographischen Prozessen, die die Struktur der Baumpopulation beeinflussen. Mit diesem Modell lassen sich Gras- und Baumbiomasse, die Struktur der Baumpopulation und Feuerregime in Abhängigkeit von wenigen Boden- und Klimavariablen simulieren. Aufgrund der flexiblen biophysikalischen, physiologischen und ökologischen Prozesse kann man mit dem Modell die Auswirkungen von Feuer und Klimawandel auf die Vegetation simulieren. Kapitel 4 beinhaltet eine detaillierte Beschreibung des aDGVM und eine Sensitivitätsanalyse. Die Sensitivitätsanalyse zeigt, dass Parameter die die Vegetation charakterisieren, vor allem allometrische Parameter, die Simulationsergebnisse stark beeinflussen. Dies zeigt, dass es notwendig ist, adaptive Vegetationsmodelle zu entwickeln, d.h. Modelle, bei denen sich die Vegetation flexibel an die Klimabedingungen anpassen kann, z.B. durch Anpassung der Allometrie.

In Kapitel 5 wird das aDGVM benutzt, um die aktuelle und die zukünftige Vegetation von Afrika zu simulieren. Die Ergebnisse zeigen, dass das Modell die aktuelle Verbreitung von Biomen in hoher Übereinstimmung mit der tatsächlich beobachteten Verbreitung simulieren kann. Des Weiteren kann das Phänologiemodell die Verbreitung von immergrüner und wechselgrüner Vegetation simulieren. Simulationsexperimente zeigen, dass Feuer die Vegetation auf regionaler Ebene stark reduziert und dass Feuerunterdrückung die Biomasse in Afrika um ca. 13% erhöhen würde. Unter Verwendung des IPCC (2007) SRES Klimawandelszenarios A1B simuliert das Modell eine dramatische Verschiebung zu baumdominierten Biomen. Die Simulationsergebnisse zeigen, dass der CO_2-Fertilisationseffekt in Savannen bei den gegenwärtigen Klimabedingungen nicht gesättigt ist und auch bei CO_2-Konzentrationen über 500 ppm noch zunehmen wird.

Diese Dissertation trägt zur aktuellen Forschung zu Savannen und Klimawandel bei, denn (1) sie präsentiert das erste heuristische Savannenmodell, das Gras-Baum-

Koexistenz auf einem großen Umweltgradienten erklären kann, ohne dabei auf stochastischen Effekten oder Wurzelnieschentrennung zu beruhen, (2) sie zeigt, dass Savannen auf dem Niederschlagsgradienten zwischen 200 mm und 1200 mm als stabil betrachtet werden können und (3) sie präsentiert ein prozess- und individuenbasiertes Vegetationsmodell speziell für tropische Gras-Baum-Systeme, das die Verbreitung afrikanischer Savannen und Feuerregime in Abhängigkeit von Klima- und Bodenbedingungen simulieren kann. Weiterhin lassen sich mit dem Modell Effekte von Klimawandel auf die Vegetation untersuchen. Perspektiven für die Weiterentwicklung der vorgestellten Modelle sind (1) die Verwendung von adaptiven Mechanismen in Vegetationsmodellen, (2) die Kopplung von Klima- und Vegetationsmodellen und (3) die Verwendung des aDGVM zur Untersuchung von nachhaltigen Landnutzungsstrategien.

Acknowledgements

First, I want to thank Steven Higgins. He was a very motivating supervisor who always had enough time for inspiring discussions about my work but also for assistance and support with other problems. He gave me the freedom to develop my ideas and his critical feedback helped to improve my work. It was a great time to work with him.
I want to thank Jörg Pfadenhauer for his interest in my work and for hosting the "African Savannas" project at the Chair of Vegetation Ecology in Freising. He supported me throughout the whole project, both with ideas and formalities.
Thanks to William Bond for pointing out several weaknesses of the models and the simulation results. His comments helped to improve the models. Thanks to Mahesh Sankaran for his contribution to Chapter 3.
I want to thank the the Leibnitz Rechenzentrum (LRZ) in Garching/Munich for providing the computer systems and support necessary to conduct the simulations presented in this thesis. In particular, I want to thank Iris Cristadler for helping us to profile, optimize and parallelize the source code of the aDGVM.
I want to thank the working groups both in Freising and in Frankfurt for the friendly and open working atmosphere, in particular Maria who shared the office with me. Thanks to my friends in Olching, Munich and Frankfurt.
This project was financed by the Robert Bosch Foundation and I am grateful to their support.
Finally, I am grateful to my parants and my sister for encouraging and supporting me at any times.

Bibliography

Allen, R. G., Pereira, L. S., Raes, D., and Smith, M. (1998). *Crop evapotranspiration: Guidelines for computing crop water requirements*. Irrigation & Drainage, Paper 56, FAO, Rome, Italy.

Anderies, J. M., Janssen, M. A., and Walker, B. H. (2002). Grazing management, resilience, and the dynamics of a fire driven rangeland system. *Ecosystems*, **5**, 23–44.

Arora, V. K. (2002). Modeling vegetation as a dynamic component in soil-vegetation-atmosphere transfer schemes and hydrological models. *Reviews of Geophysics*, **40**(2), 1006.

Arora, V. K. (2003). Simulating energy and carbon fluxes over winter wheat using coupled land surface and terrestrial ecosystem models. *Agricultural and Forest Meteorology*, **118**, 21–47.

Arora, V. K. and Boer, G. J. (2005). A parameterization of leaf phenology for the terrestrial ecosystem component of climate models. *Global Change Biology*, **11**, 39–59.

Aumann, C. A. (2007). A methodology for developing simulation models of complex systems. *Ecological Modelling*, **202**(3-4), 385–396.

Bagchi, S. (2007). Relationship between size hierarchy and density of trees in a tropical dry deciduous forest of western India. *Journal of Vegetation Science*, **18**(3), 389–394.

Ball, J. T., Woodrow, I. E., and Berry, J. A. (1987). *Progress in Photosynthesis Research*, chapter A model predicting stomatal conductance and its contribution to the control of photosynthesis under different environmental conditions, pages 221–224. Nijhoff, Dordrecht.

Ballinger, G. and Liu, X. (1997). Permanence of population growth models with impulsive effects. *Mathematical and Computer Modelling*, **26**(12), 59–72.

Blasco, F., Whitmore, T. C., and Gers, C. (2000). A framework for the worldwide comparison of tropical woody vegetation types. *Biological Conservation*, **95**(2), 175–189.

Boerner, J., Higgins, S. I., Kantelhardt, J., and Scheiter, S. (2007). Rainfall or price variability: what determines rangeland management decisions? A simulation-optimization approach to South African savannas. *Agricultural Economics*, **37**(2-3), 189–200.

Bonan, G. B., Levis, S., Sitch, S., Vertenstein, M., and Oleson, K. W. (2003). A dynamic global vegetation model for use with climate models: concepts and description of simulated vegetation dynamics. *Global Change Biology*, **9**(11), 1543–1566.

Bond, W. J. and Keeley, J. E. (2005). Fire as a global 'herbivore': the ecology and evolution of flammable ecosystems. *Trends in Ecology & Evolution*, **20**, 387–393.

Bond, W. J. and Midgley, J. J. (2001). Ecology of sprouting in woody plants: the persistence niche. *Trends in Ecology & Evolution*, **16**(1), 45–51.

Bond, W. J., Maze, K., and Desmet, P. (1995). Fire life-histories and the seeds of chaos. *Ecoscience*, **2**(3), 252–260.

Bond, W. J., Midgley, G. F., and Woodward, F. I. (2003). The importance of low atmospheric CO_2 and fire in promoting the spread of grasslands and savannas. *Global Change Biology*, **9**(7), 973–982.

Bond, W. J., Woodward, F. I., and Midgley, G. F. (2005). The global distribution of ecosystems in a world without fire. *New Phytologist*, **165**(2), 525–537.

Bowman, D. M. J. S. and Prior, L. D. (2005). Why do evergreen trees dominate the australian seasonal tropics? *Australian Journal of Botany*, **53**(5), 379–399.

Brovkin, V., Claussen, M., Petoukhov, V., and Ganopolski, A. (1998). On the stability of the atmosphere-vegetation system in the Sahara/Sahel region. *Journal of Geophysical Research-Atmospheres*, **103**(D24), 31613–31624.

Burnham, K. P. and Anderson, D. R. (2001). Kullback-leibler information as a basis for strong inference in ecological studies. *Wildlife Research*, **28**(2), 111–119.

Cahill, J. F. and Casper, B. B. (2000). Investigating the relationship between neighbor root biomass and belowground competition: field evidence for symmetric competition belowground. *Oikos*, **90**(2), 311–320.

Cao, M. K., Zhang, Q. F., and Shugart, H. H. (2001). Dynamic responses of African ecosystem carbon cycling to climate change. *Climate Research*, **17**(2), 183–193.

Case, T. J. (2000). *An Illustrated Guide to Theoretical Ecology*. Oxford University Press.

Chave, J. (1999). Study of structural, successional and spatial patterns in tropical rain forests using TROLL, a spatially explicit forest model. *Ecological Modelling*, **124**(2-3), 233–254.

Cheney, P. and Sullivan, A. (1997). *Grassfires: Fuel, Weather and Fire Behaviour*. CSIRO Publishing, Collingwood, Australia.

Chesson, P. L. and Warner, R. R. (1981). Environmental variability promotes coexistence in lottery competitive systems. *American Naturalist*, **117**, 923–943.

Chuine, I. (2000). A unified model for budburst of trees. *Journal of Theoretical Biology*, **207**(3), 337–347.

Chuine, I. and Beaubien, E. G. (2001). Phenology is a major determinant of tree species range. *Ecology Letters*, **4**(5), 500–510.

Clark, J. S. and Gelfand, A. E. (2006). A future for models and data in environmental science. *Trends in Ecology & Evolution*, **21**(7), 375–380.

Clark, J. S., Carpenter, S. R., Barber, M., Collins, S., Dobson, A., Foley, J. A., Lodge, D. M., Pascual, M., Pielke, R., Pizer, W., Pringle, C., Reid, W. V., Rose, K. A., Sala, O., Schlesinger, W. H., Wall, D. H., and Wear, D. (2001). Ecological forecasts: An emerging imperative. *Science*, **293**(5530), 657–660.

Claussen, M. and Gayler, V. (1997). The greening of the Sahara during the mid-Holocene: results of an interactive atmosphere-biome model. *Global Ecology and Biogeography Letters*, **6**(5), 369–377.

Cochrane, M. A. (2003). Fire science for rainforests. *Nature*, **421**(6926), 913–919.

Cochrane, M. A., Alencar, A., Schulze, M. D., Souza, C. M., Nepstad, D. C., Lefebvre, P., and Davidson, E. A. (1999). Positive feedbacks in the fire dynamic of closed canopy tropical forests. *Science*, **284**(5421), 1832–1835.

Collatz, G. J., Ball, J. T., Grivet, C., and Berry, J. A. (1991). Physiological and environmental regulation of stomatal conductance, photosynthesis and transpiration: a model that includes a laminar boundary layer. *Agriculture and Forest Meteorology*, **54**, 107–136.

Collatz, G. J., Ribas-Carbo, M., and Berry, J. A. (1992). Coupled photosynthesis-stomatal conductance model for leaves of C_4 plants. *Australian Journal of Plant Physiology*, **19**, 519–538.

Connell, J. H. (1983). On the prevalence and relative importance of interspecific competition evidence from field experiments. *American Naturalist*, **122**(5), 661–696.

Cramer, W., Bondeau, A., Woodward, F. I., Prentice, I. C., Betts, R. A., Brovkin, V., Cox, P. M., Fisher, V., Foley, J. A., Friend, A. D., Kucharik, C., Lomas, M. R., Ramankutty, N., Sitch, S., Smith, B., White, A., and Young-Molling, C. (2001). Global response of terrestrial ecosystem structure and function to CO_2 and climate change: results from six dynamic global vegetation models. *Global Change Biology*, **7**(4), 357–373.

Crider, F. J. (1955). Root growth stoppage resulting from defoilation of grass. *USDA Technical Bulletins*, **1102**, 2–23.

Cushing, J. M. (1980). Two species competition in a periodic environment. *Journal of Mathematical Biology*, **10**(4), 385–400.

Davidson, E. A. and Janssens, I. A. (2006). Temperature sensitivity of soil carbon decomposition and feedbacks to climate change. *Nature*, **440**(7081), 165–173.

de Kroon, H., van Groenendael, J., and Ehrlen, J. (2000). Elasticities: A review of methods and model limitations. *Ecology*, **81**(3), 607–618.

de Kroon, H., Mommer, L., and Nishiwaki, A. (2003). *Root Ecology*, chapter Root Competition: towards a mechanistic understanding, pages 215–234. Springer, Berlin.

Defries, R. S., Hansen, M. C., Townshend, J. R. G., Janetos, A. C., and Loveland, T. R. (2000). A new global 1-km dataset of percentage tree cover derived from remote sensing. *Global Change Biology*, **6**(2), 247–254.

DeLucia, E. H., Drake, J. E., Thomas, R. B., and Gonzalez-Meler, M. (2007). Forest carbon use efficiency: is respiration a constant fraction of gross primary production? *Global Change Biology*, **13**(6), 1157–1167.

Dercole, F. and Maggi, S. (2005). Detection and continuation of a border collision bifurcation in a forest fire model. *Applied Mathematics and Computation*, **168**, 623–635.

D'Odorico, P., Laio, F., and Ridolfi, L. (2006). A probabilistic analysis of fire-induced tree-grass coexistence in savannas. *The American Naturalist*, **167(3)**, E–Article.

Drake, B. G., Gonzàlez-Meler, M. A., and Long, S. P. (1997). More efficient plants: A consequence of rising atmospheric CO_2? *Annual Review of Plant Physiology and Plant Molecular Biology*, **48**, 609–639.

du Toit, J. T., Rogers, K. H., and Biggs, H. C. (2003). *The Kruger Experience: Ecology And Management Of Savanna Heterogeneity*. Island Press, Washington.

Ehleringer, J. R., Cerling, T. E., and Helliker, B. R. (1997). C_4 photosynthesis, atmospheric CO_2 and climate. *Oecologia*, **112**(3), 285–299.

Farquhar, G. D., Caemmerer, S. V., and Berry, J. A. (1980). A biochemical-model of photosynthetic CO_2 assimilation in leaves of C_3 species. *Planta*, **149**(1), 78–90.

Fischlin, A., Midgley, G. F., Price, J. T., Leemans, R., Gopal, B., Turley, C., Rounsevell, M. D. A., Dube, O. P., Tarazona, J., and Velichko, A. A. (2007). *Climate Change 2007: Impacts, Adaptation and Vulnerability. Contribution of Working Group II to the Fourth Assessment Report of the Intergovernmental Panel on Climate Change*, chapter Ecosystems, their properties, goods, and services, pages 211–272. Cambridge University Press, Cambridge.

Foley, J. A., Levis, S., Costa, M. H., Cramer, W., and Pollard, D. (2000). Incorporating dynamic vegetation cover within global climate models. *Ecological Applications*, **10**(6), 1620–1632.

Freckleton, R. P. and Watkinson, A. R. (2000). On detecting and measuring competition in spatially structured plant communities. *Ecology Letters*, **3**(5), 423–432.

Freckleton, R. P. and Watkinson, A. R. (2001). Predicting competition coefficients for plant mixtures: reciprocity, transitivity and correlations with life-history traits. *Ecology Letters*, **4**(4), 348–357.

Friedlingstein, P., Joel, G., Field, C. B., and Fung, I. Y. (1999). Toward an allocation scheme for global terrestrial carbon models. *Global Change Biology*, **5**(7), 755–770.

Friend, A. D., Stevens, A. K., Knox, R. G., and Cannell, M. G. R. (1997). A process-based, terrestrial biosphere model of ecosystem dynamics (Hybrid v3.0). *Ecological Modelling*, **95**(2-3), 249–287.

Frost, P. G. H., Menaut, J. C., Walker, B. H., Medina, E., Solbrig, O. T., and Swift, M. (1986). *Responses of savannas to stress and disturbance*. Biology International Special Issue 10.

Gardner, T. A. (2006). Tree-grass coexistence in the Brazilian cerrado: demographic consequences of environmental instability. *Journal of Biogeography*, **33**, 448–463.

Gause, G. F. (1934). *The struggle for existence*. Williams & Wilkins, Baltimore, MD.

Gertenbach, W. P. D. (1983). Landscapes of the Kruger National Park. *Koedoe*, **26**, 9–121.

Geyer, C. (1992). Practical Markov chain Monte Carlo. *Statistical Science*, **7**, 473–511.

Giardina, C. P. and Ryan, M. G. (2000). Evidence that decomposition rates of organic carbon in mineral soil do not vary with temperature. *Nature*, **404**(6780), 858–861.

Gill, R. A. and Jackson, R. B. (2000). Global patterns of root turnover for terrestrial ecosystems. *New Phytologist*, **147**(1), 13–31. 2056.

Givnish, T. J. (2002). Adaptive significance of evergreen vs. deciduous leaves: Solving the triple paradox. *Silva Fennica*, **36**(3), 703–743.

Global Soil Data Task Group (2000). *Global Gridded Surfaces of Selected Soil Characteristics (International Geosphere-Biosphere Programme - Data and Information System).* Data set. Available on-line [http://www.daac.ornl.gov] from Oak Ridge

National Laboratory Distributed Active Archive Center, Oak Ridge, Tennessee, U.S.A.

Goedecker, S. and Hoisie, A. (2001). *Performance Optimization of Numerically Intensive Codes*. SIAM publishing company, Philadelphia, USA.

Grace, J. (2004). Understanding and managing the global carbon cycle. *Journal of Ecology*, **92**(2), 189–202.

Grace, J., San Jose, J., Meir, P., Miranda, H. S., and Montes, R. A. (2006). Productivity and carbon fluxes of tropical savannas. *Journal of Biogeography*, **33**(3), 387–400.

Gragnani, A. and Rinaldi, S. (1995). A universal bifurcation diagram for seasonally perturbed predator-prey models. *Bulletin of Mathematical Biology*, **57**(5), 701–712.

Gurevitch, J., Morrow, L. L., Wallace, A., and Walsh, J. S. (1992). A metaanalysis of competition in field experiments. *American Naturalist*, **140**(4), 539–572.

Haario, H., Laine, M., Mira, A., and Saksman, E. (2006). DRAM: Efficient adaptive MCMC. *Statistics and Computing*, **16**(4), 339–354.

Haxeltine, A. and Prentice, I. C. (1996). Biome3: An equilibrium terrestrial biosphere model based on ecophysiological constraints, resource availability, and competition among plant functional types. *Global Biogeochemical Cycles*, **10**(4), 693–709.

Hély, C., Bremond, L., Alleaume, S., Smith, B., Sykes, M. T., and Guiot, J. (2006). Sensitivity of African biomes to changes in the precipitation regime. *Global Ecology and Biogeography*, **15**(3), 258–270.

Hickler, T., Prentice, I. C., Smith, B., Sykes, M. T., and Zaehle, S. (2006). Implementing plant hydraulic architecture within the LPJ dynamic global vegetation model. *Global Ecology and Biogeography*, **15**(6), 567–577.

Higgins, S. I., Shackleton, C. M., and Robinson, E. R. (1999). Changes in woody community structure and composition under constrasting landuse systems in a semi-arid savanna, South Africa. *Journal of Biogeography*, **26**(3), 619–627.

Higgins, S. I., Bond, W. J., and Trollope, W. S. (2000). Fire, resprouting and variability: a recipe for grass-tree coexistence in savanna. *Journal of Ecology*, **88**, 213–229.

Higgins, S. I., Bond, W. J., February, E. C., Bronn, A., Euston-Brown, D. I. W., Enslin, B., Govender, N., Rademan, L., O'Regan, S., Potgieter, A. L. F., Scheiter, S., Sowry, R., Trollope, L., and Trollope, W. S. W. (2007a). Effects of four decades of fire manipulation on woody vegetation structure in savanna. *Ecology*, **88**(5), 1119–1125.

Higgins, S. I., Kantelhardt, J., Scheiter, S., and Boerner, J. (2007b). Sustainable management of extensively managed savanna rangelands. *Ecological Economics*, **62**, 102–114.

Higgins, S. I., Bond, W. J., Trollope, W. S. W., and Williams, R. J. (2008). Physically motivated empirical models for the spread and intensity of grass fires. *International Journal of Wildland Fire*, **17**, 595–601.

Hoffmann, W. A. and Solbrig, O. T. (2003). The role of topkill in the differential response of savanna woody species to fire. *Forest Ecology and Management*, **180**, 273–286.

Hoffmann, W. A., Orthen, B., and Do Nascimento, P. K. V. (2003). Comparative fire ecology of tropical savanna and forest trees. *Functional Ecology*, **17**(6), 720–726.

House, J. I., Archer, S., Breshears, D. D., and NCEAS-Tree-Grass-Interaction-Participants (2003). Conundrums in mixed woody-herbaceous plant systems. *Journal of Biogeography,*, **30**, 1763–1777.

Hovestadt, T., Yao, P., and Linsenmair, E. (1999). Seed dispersal mechanisms and the vegetation of forest islands in a West African forest-savanna mosaic (Comoé National Park, Ivory Coast). *Plant Ecology*, **144**, 1–25.

Huntley, B. J. and Walker, B. H. (1982). *Ecology of Tropical Savannas*. Springer-Verlag Berlin.

Hutchinson, G. E. (1961). The paradox of the plankton. *American Naturalist*, **95**, 137–145.

IPCC (2007). *Climate Change 2007: The Physical Science Basis. Contribution of Working Group I to the Fourth Assessment Report of the Intergovernmental Panel on Climate Change*. Cambridge University Press, Cambridge, United Kingdom and New York, NY, USA.

Ives, A. R., Gross, K., and Jansen, V. A. A. (2000). Periodic mortality events in predator-prey systems. *Ecology*, **81**(12), 3330–3340.

Jeltsch, F., Milton, S. J., Dean, W. R. J., and van Rooyen, N. (1996). Tree spacing and coexistence in semi-arid savannas. *Journal of Ecology*, **84**, 583–595.

Jeltsch, F., Milton, S. J., Dean, W. R. J., van Rooyen, N., and Moloney, K. A. (1998). Modelling the impact of small-scale heterogeneities on tree-grass coexistence in semi-arid savannas. *Journal of Ecology*, **86**, 780–793.

Jeltsch, F., Weber, G. E., and Grimm, V. (2000). Ecological buffering mechanisms in savannas: A unifying theory of long-term tree-grass coexistence. *Plant Ecology*, **161**, 161–171.

Jepson, P. and Whittaker, R. J. (2002). Ecoregions in context: a critique with special reference to indonesia. *Conservation Biology*, **16**(1), 42–57.

Jolly, W. M. and Running, S. W. (2004). Effects of precipitation and soil water potential on drought deciduous phenology in the Kalahari. *Global Change Biology*, **10**(3), 303–308.

Jolly, W. M., Nemani, R., and Running, S. W. (2005). A generalized, bioclimatic index to predict foliar phenology in response to climate. *Global Change Biology*, **11**(4), 619–632.

Jones, H. G. (1992). *Plants and microclimate: a quantitative approach to environmental plant physiology*. 2nd edn. Cambridge University Press.

Jung, M., Henkel, K., Herold, M., and Churkina, G. (2006). Exploiting synergies of global land cover products for carbon cycle modeling. *Remote Sensing of Environment*, **101**(4), 534–553.

Keane, R. E., Cary, G. J., Davies, I. D., Flannigan, M. D., Gardner, R. H., Lavorel, S., Lenihan, J. M., Li, C., and Rupp, T. S. (2004). A classification of landscape fire succession models: spatial simulations of fire and vegetation dynamics. *Ecological Modelling*, **179**(1), 3–27.

Keddy, P. A. (1992). Assembly and response rules: two goals for predictive community ecology. *Journal of Vegetation Science*, **3**(2), 157–164.

Kernighan, B. W. and Ritchie, D. M. (1990). *Programmieren in C*. Hanser, 2 edition.

Kikuzawa, K. (1991). A cost-benefit-analysis of leaf habit and leaf longevity of trees and their geographical pattern. *American Naturalist*, **138**(5), 1250–1263.

Koch, A. L. (1974). Competitive coexistence of two predators utilizing the same prey under constant environmental conditions. *Journal of theoretical Biology*, **44**, 387–395.

Law, B. E., Ryan, M. G., and Anthoni, P. M. (1999). Seasonal and annual respiration of a ponderosa pine ecosystem. *Global Change Biology*, **5**(2), 169–182.

Law, R. and Watkinson, A. R. (1987). Response-surface analysis of 2-species competition experiment on *Phleum-arenarium* and *Vulpia-fasciculata* . *Journal of Ecology*, **75**(3), 871–886.

Liedloff, A. C. and Cook, G. D. (2007). Modelling the effects of rainfall variability and fire on tree populations in an Australian tropical savanna with the FLAMES simulation model. *Ecological Modelling*, **201**(3-4), 269–282.

Liski, J., Palosuo, T., Peltoniemi, M., and Sievanen, R. (2005). Carbon and decomposition model Yasso for forest soils. *Ecological Modelling*, **189**(1-2), 168–182.

Liu, Z. Y., Wang, Y., Gallimore, R., Notaro, M., and Prentice, I. C. (2006). On the cause of abrupt vegetation collapse in north africa during the holocene: Climate variability vs. vegetation feedback. *Geophysical Research Letters*, **33**(22), L22709.

Loveland, T. R., Reed, B. C., Brown, J. F., Ohlen, D. O., Zhu, Z., Yang, L., and Merchant, J. W. (2000). Development of a global land cover characteristics database and IGBP DISCover from 1 km AVHRR data. *International Journal of Remote Sensing*, **21**(6-7), 1303–1330.

Lowes, M. and Paulik, A. (1995). *Programmieren mit C: Ansi Standard*. Teubner, Stuttgart, 3 edition.

Lucht, W., Schaphoff, S., Erbrecht, T., Heyder, U., and Cramer, W. (2006). Terrestrial vegetation redistribution and carbon balance under climate change. *Carbon Balance and Management*, **1**(6), doi:10.1186/1750–0680–1–6.

Lüdeke, M. K. B., Badeck, F. W., Otto, R. D., Hager, C., Dönges, S., Kindermann, J., Würth, G., Lang, T., Jäkel, U., Klaudius, A., Ramge, P., Habermehl, S., and Kohlmaier, G. H. (1994). The Frankfurt Biosphere Model. A global process oriented model for the seasonal and longterm CO_2 exchange between terrestrial ecosystems and the atmosphere. Part 1: Model description and illustrating results for the vegetation types cold deciduous and boreal forests. *Climate Research*, **4**, 143–166.

MacGregor, S. D. and O'Connor, T. G. (2002). Patch dieback of *Colophospermum mopane* in a dysfunctional semi-arid African savanna. *Austral Ecology*, **27**(4), 385–395.

Mankin, J., ONeill, R., Shugart, H., and Rust, B. (1977). *New Directions in the Analysis of Ecological Systems, Part 1*, chapter The impartance of validation in ecosystem analysis, pages 63–71. The Society for Computer Simulation, La- Jolla, CA.

Matthews, E. (1983). Global vegetation and land use: New high-resolution data bases for climate studies. *Journal of Climate and Applied Meteorology*, **22**(3), 474–487.

Matthews, E. (1984). Prescription of land-surface boundary conditions in GISS GCM II: a simple method based on high-resolution vegetation data sets. Technical report, NASA Technical Memorandum 86096.

McCarthy, J. W. and Weetman, G. (2007). Self-thinning dynamics in a balsam fir (*Abies balsamea* (L.) Mill.) insect-mediated boreal forest chronosequence. *Forest Ecology and Management*, **241**(1-3), 295–309.

McGill, B. J., Enquist, B. J., Weiher, E., and Westoby, M. (2006). Rebuilding community ecology from functional traits. *Trends in Ecology & Evolution*, **21**(4), 178–185.

McMurtrie, R. and Wolf, L. (1983). A model of competition between trees and grass for radiation, water and nutrients. *Annals Of Botany*, **52**(4), 449–458.

Meeson, B. W., Corprew, F. E., McManus, J. M. P., Myers, D. M., Closs, J. W., Sun, K.-J., Sunday, D. J., and Sellers, P. J. (1995). ISLSCP Initiative I – Global Data Sets for Land-Atmosphere Models, 1987-1988, Volumes 1-5. Technical report, Published on CD by NASA (USA_NASA_GDAAC_ISLSCP_001 - USA_NASA_GDAAC_ISLSCP_005).

Meir, P., Cox, P., and Grace, J. (2006). The influence of terrestrial ecosystems on climate. *Trends in Ecology & Evolution*, **21**(5), 254–260.

Monserud, R. A. and Leemans, R. (1992). Comparing global vegetation maps with the kappa-statistic. *Ecological Modelling*, **62**(4), 275–293.

Moorcroft, P. R. (2006). How close are we to a predictive science of the biosphere? *Trends in Ecology & Evolution*, **21**(7), 400–407.

Moorcroft, P. R., Hurtt, G. C., and Pacala, S. W. (2001). A method for scaling vegetation dynamics: The ecosystem demography model (ED). *Ecological Monographs*, **71**(4), 557–585.

Morisette, J. T., Giglio, L., Csiszar, I., and Justice, C. O. (2005). Validation of the MODIS active fire product over Southern Africa with ASTER data. *International Journal of Remote Sensing*, **26**(19), 4239–4264.

Murray, J. D. (2002). *Mathematical Biology I: An Introduction*. Springer.

Nelson, W. A., McCauley, E., and Wimbert, J. (2004). Capturing dynamics with the correct rates: Inverse problems using semiparametric approaches. *Ecology*, **85**(4), 889–903.

New, M., Lister, D., Hulme, M., and Makin, I. (2002). A high-resolution data set of surface climate over global land areas. *Climate Research*, **21**(1), 1–25.

Ng, F. S. P. (1984). *Plant Phenology in the Humid Tropics*. Research Pamphlet No. 96. Malaysian Forest Department.

Niklas, K. J., Midgley, J. J., and Rand, R. H. (2003). Tree size frequency distributions, plant density, age and community disturbance. *Ecology Letters*, **6**(5), 405–411.

Novoplansky, A. (2002). Developmental plasticity in plants: implications of non-cognitive behavior. *Evolutionary Ecology*, **16**(3), 177–188.

Noy-Meir, I. (1978). Stability in Simple Grazing Models: Effects of Explicit Functions. *Journal of theoretical Biology*, **71**, 347–380.

Oreskes, N. (2003). *Models in Ecosystem Science*, chapter The role of quantitative models in science, pages 13–31. Princeton: Princeton University Press.

Oreskes, N. and Belitz, K. (2001). *Model Validation: Perspectives in Hydrological Science*, chapter Philosophical issues in model assessment, pages 23–41. John Wiley & Sons, New York.

Overton, S. (1977). *Ecosystem Modeling in Theory and Practice: An Introduction with Case Histories*, chapter A strategy of model construction, pages 49–73. John Wiley & Sons, New York, Reprinted 1990, University Press of Colorado 1.

Parton, W. J., Schimel, D. S., Cole, C. V., and Ojima, D. S. (1987). Analysis of factors controlling soil organic-matter levels in great-plains grasslands. *Soil Science Society of America Journal*, **51**(5), 1173–1179.

Pascual, M. A. and Kareiva, P. M. (1996). Predicting the outcome of competition using experimental data: Maximum likelihood and bayesian approaches. *Ecology*, **77**(6), 1887–1887.

Perman, R., Common, J., and Ma, Y. (2003). *Natural Resource and Environmental Economics*. Prentice Hall, New York.

Perry, G. L. W. and Enright, N. J. (2002). Spatial modelling of landscape composition and pattern in a maquis-forest complex, Mont Do, New Caledonia. *Ecological Modelling*, **152**(2-3), 279–302.

Poorter, H., Remkes, C., and Lambers, H. (1990). Carbon and nitrogen economy of 24 wild-species differing in relative growth-rate. *Plant Physiology*, **94**(2), 621–627.

Popp, A., Schwager, M., Blaum, N., and Jeltsch, F. (2007). Simulating the impacts of vegetation structure on the occurrence of a small mammalian carnivore in semi-arid savanna rangelands. *Ecological Modelling*, **209**(2-4), 136–148.

Prentice, I. C., Cramer, W., Harrison, S. P., Leemans, R., Monserud, R. A., and Solomon, A. M. (1992). A global biome model based on plant physiology and dominance, soil properties and climate. *Journal of Biogeography*, **19**(2), 117–134.

Prins, H. H. T. and Van der Jeugd, H. P. (1993). Herbivore population crashes and woodland structure in east Africa. *Journal of Ecology*, **81**, 305–314.

R Development Core Team (2005). *R: A language and environment for statistical computing*. R Foundation for Statistical Computing, Vienna, Austria. ISBN 3-900051-07-0.

Raddatz, T. J., Reick, C. H., Knorr, W., Kattge, J., Roeckner, E., Schnur, R., Schnitzler, K. G., Wetzel, P., and Jungclaus, J. (2007). Will the tropical land biosphere dominate the climate-carbon cycle feedback during the twenty-first century? *Climate Dynamics*, **29**(6), 565–574.

Randerson, J. T., van der Werf, G., Giglio, L., Collatz, G., and Kasibhatla, P. (2007). Global Fire Emissions Database, Version 2 (GFEDv2.1). Data set. Technical report, Available on-line [http://daac.ornl.gov/] from Oak Ridge National Laboratory Distributed Active Archive Center, Oak Ridge, Tennessee, U.S.A.

Rees, M. and Bergelson, J. (1997). Asymmetric light competition and founder control in plant communities. *Journal of Theoretical Biology*, **184**(3), 353–358.

Rinaldi, S., Muratori, S., and Kuznetsov, Y. (1993). Multiple attractors, catastrophes and chaos in seasonally perturbed predator prey communities. *Bulletin of Mathematical Biology*, **55**(1), 15–35.

Robinson, D. (2007). Implications of a large global root biomass for carbon sink estimates and for soil carbon dynamics. *Proceedings of the Royal Society B-Biological Sciences*, **274**(1626), 2753–2759.

Rodriguez-Iturbe, I., Porporato, A., Ridolfi, L., Isham, V., and Cox, D. R. (1999). Probabilistic modelling of water balance at a point: the role of climate, soil and vegetation. *Proceedings of the Royal Society of London Series A-Mathematical Physical and Engineering Sciences*, **455**(1990), 3789–3805.

Rodriguez-Iturbe, I., Porporato, A., Laio, F., and Ridolfi, L. (2001). Plants in water-controlled ecosystems: active role in hydrologic processes and response to water stress. I. Scope and general outline. *Advances in Water Resources*, **24**(7), 695–705.

Roeckner, E. (2005). IPCC DDC AR4 ECHAM5/MPI-OM SRESA1B run1. World Data Center for Climate. CERA-DB "EH5_MPI_OM_SRESA1B_1" http://cera-www.dkrz.de/WDCC/ui/Compact.jsp?acronym=EH5_MPI_OM_SRESA1B_1.

Ronda, R. J., de Bruin, H. A. R., and Holtslag, A. A. M. (2001). Representation of the canopy conductance in modeling the surface energy budget for low vegetation. *Journal of Applied Meteorology*, **40**(8), 1431–1444.

Roques, K., O'Connor, T., and Watkinson, A. (2001). Dynamics of shrub encroachment in an African savanna: relative influences of fire, herbivory, rainfall and density dependence. *Journal of Applied Ecology*, **38**, 268–280.

Rykiel, E. J. (1996). Testing ecological models: The meaning of validation. *Ecological Modelling*, **90**(3), 229–244.

San José, J. J., Montes, R. A., and Farinas, M. R. (1998a). Carbon stocks and fluxes in a temporal scaling from a savanna to a semi-deciduous forest. *Forest Ecology and Management*, **105**(1-3), 251–262.

San José, J. J., Montes, R., and Mazorra, M. (1998b). The nature of savanna heterogeneity in the Orinoco Basin. *Global Ecology and Biogeography*, **7**(6), 441–455.

Sankaran, M., Jayashree, R., and Hanan, N. P. (2004). Tree-grass coexistence in savannas revisited - insights from an examination of assumptions and mechanisms invoked in existing models. *Ecology Letters*, **7**, 480–490.

Sankaran, M., Hanan, N. P., Scholes, R. J., Ratnam, J., Augustine, D. J., Cade, B. S., Gignoux, J., Higgins, S. I., Roux, X. L., Ludwig, F., Ardo, J., Banyikwa, F., Bronn, A., Bucini, G., Caylor, K. K., Coughenour, M. B., Diouf, A., Ekaya, W., Feral, C. J., February, E. C., Frost, P. G. H., Hiernaux, P., Hrabar, H., Metzger, K. L., Prins, H. H. T., Ringrose, S., Sea, W., Tews, J., Worden, J., and Zambatis, N. (2005). Determinants of woody cover in African savannas. *Nature*, **438**(7069), 846–849.

Sargent, R. G. (2007). Verification and validation of simulation models. In S. Henderson, M. H. Biller, B. Hsieh, J. Shortle, J. D. Tew, and R. Barton, editors, *Proceedings of the 2007 Winter Simulation Conference*, pages 124–137. Piscataway, New Jersey: IEEE.

Sarmiento, G. (1984). *The Ecology of Neotropical Savannas*. Havard University Press, Cambridge, MA.

Sato, H., Itoh, A., and Kohyama, T. (2007). SEIB-DGVM: A new dynamic global vegetation model using a spatially explicit individual-based approach. *Ecological Modelling*, **200**(3-4), 279–307.

Schaphoff, S., Lucht, W., Gerten, D., Sitch, S., Cramer, W., and Prentice, I. C. (2006). Terrestrial biosphere carbon storage under alternative climate projections. *Climatic Change*, **74**(1-3), 97–122.

Scheffer, M., Baveco, J. M., DeAngelis, D. L., Rose, K. A., and van Nes, E. H. (1995). Super-individuals a simple solution for modelling large populations on an individual basis. *Ecological Modelling*, **80**(2-3), 161–170.

Scheffer, M., Holmgren, M., Brovkin, V., and Claussen, M. (2005). Synergy between small- and large-scale feedbacks of vegetation on the water cycle. *Global Change Biology*, **11**(7), 1003–1012.

Schmaranz, K. (2001). *Softwareentwicklung in C*. Springer, Heidelberg.

Schmaranz, K. (2003). *Softwareentwicklung in C++*. Springer, Heidelberg.

Scholes, R. J. (2004). *Indigenous Forests and Woodlands in South Africa. Policy, People and Practice*, chapter Carbon storage in southern African woodlands, pages 797–813. University of KwaZulu-Natal Press.

Scholes, R. J. and Archer, S. R. (1997). Tree-grass interactions in Savannas. *Annual Review of Ecology, Evolution, and Systematics*, **28**, 517–544.

Scholes, R. J. and Hall, D. O. (1996). *Global Change: Effects on Coniferous Forests and Grasslands*, volume SCOPE 56, chapter The carbon budget of tropical savannas, woodlands and grasslands, pages 69–100. John Wiley, Chichester.

Scholes, R. J. and Walker, B. H. (1993). *An African Savanna-Synthesis of the Nylsvley study*. Cambridge University Press.

Schulze, E. D., Kelliher, F. M., Körner, C., Lloyd, J., and Leuning, R. (1994). Relationships among maximum stomatal conductance, ecosystem surface conductance, carbon assimilation rate, and plant nitrogen nutrition: A global ecology scaling exercise. *Annual Review of Ecology and Systematics*, **25**, 629–662.

Scott, L. (1999). Vegetation history and climate in the savanna biome South Africa since 190,000 ka: a comparison of pollen data from the Tswaing Crater (the Pretoria Saltpan) and Wonderkrater. *Quaternary International*, **57-8**, 215–223.

Sellers, P. J., Berry, J. A., Collatz, G. J., Field, C. B., and Hall, F. G. (1992). Canopy reflectance, photosynthesis, and transpiration. III. A reanalysis using improved leaf models and a new canopy integration scheme. *Remote Sensing of Environment*, **42**, 187–216.

Sellers, P. J., Bounoua, L., Collatz, G. J., Randall, D. A., Dazlich, D. A., Los, S. O., Berry, J. A., Fung, I., Tucker, C. J., Field, C. B., and Jensen, T. G. (1996). Comparison of radiative and physiological effects of doubled atmospheric CO_2 on climate. *Science*, **271**(5254), 1402–1406.

Shabanov, N. V., Knyazikhin, Y., Baret, F., and Myneni, R. B. (2000). Stochastic modeling of radiation regime in discontinuous vegetation canopies. *Remote Sensing of Environment*, **74**(1), 125–144.

Shipley, B. (2006). Net assimilation rate, specific leaf area and leaf mass ratio: which is most closely correlated with relative growth rate? A meta-analysis. *Functional Ecology*, **20**(4), 565–574.

Sitch, S., Smith, B., Prentice, I. C., Arneth, A., Bondeau, A., Cramer, W., Kaplan, J. O., Levis, S., Lucht, W., Sykes, M. T., Thonicke, K., and Venevsky, S. (2003). Evaluation of ecosystem dynamics, plant geography and terrestrial carbon cycling in the LPJ dynamic global vegetation model. *Global Change Biology*, **9**(2), 161–185.

Smit, G. N., Richter, C. G. F., and Aucamp, A. J. (1999). *Veld management in South Africa*, chapter Bush encroachment: An approach to understanding and managing the problem, pages 246–260. University of Natal, Scottsville.

Stigter, J. D. and van Langevelde, F. (2004). Optimal harvesting in a two-species model under critical depensation - the case of optimal harvesting in semi-arid grazing systems. *Ecological Modelling*, **179**(2), 153–161.

Taylor, G., Tallis, M. J., Giardina, C. P., Percy, K. E., Miglietta, F., Gupta, P. S., Gioli, B., Calfapietra, C., Gielen, B., Kubiske, M. E., Scarascia-Mugnozza, G. E., Kets, K., Long, S. P., and Karnosky, D. F. (2008). Future atmospheric CO_2 leads to delayed autumnal senescence. *Global Change Biology*, **14**(2), 264–275.

Thonicke, K., Venevsky, S., Sitch, S., and Cramer, W. (2001). The role of fire disturbance for global vegetation dynamics: coupling fire into a dynamic global vegetation model. *Global Ecology and Biogeography*, **10**(6), 661–677.

Thornley, J. H. M. and Cannell, M. G. R. (2000). Modelling the components of plant respiration: Representation and realism. *Annals of Botany*, **85**(1), 55–67.

Tilman, D. (1988). *Plant Strategies and the Dynamics and Structure of Plant Communities*. Princeton University Press.

Tjoelker, M. G., Oleksyn, J., and Reich, P. B. (2001). Modelling respiration of vegetation: evidence for a general temperature-dependent Q_{10}. *Global Change Biology*, **7**(2), 223–230.

van Langevelde, F., van de Vijver, C. A. D. M., Kumar, L., van de Koppel, J., de Ridder, N., van Andel, J., Skidmore, A. K., Hearne, J. W., Stroosnijder, L., Bond, W. J., Prins, H. H., and Rietkerk, M. M. (2003). Effects of fire and herbivory on the stability of savanna ecosystems. *Ecology*, **84**(2), 337–350.

van Wilgen, B. W. and Scholes, R. J. (1997). *Fire in Southern African Savannas*, chapter The vegetation and fire regimes of southern hemisphere Africa, pages 27–46. Witwatersrand University Press, Johannesburg, South Africa.

Venevsky, S., Thonicke, K., Sitch, S., and Cramer, W. (2002). Simulating fire regimes in human-dominated ecosystems: Iberian peninsula case study. *Global Change Biology*, **8**(10), 984–998.

Vetter, S. (2005). Rangelands at equilibrium and non-equilibrium: recent developments in the debate. *Journal of Arid Environments*, **62**, 321–341.

Walker, B. H. and Noy-Meir, I. (1982). *Tropical Savannas*, chapter Aspects of stability and resilience in savanna ecosystems, pages 556–590. Springer-Verlag, Berlin, Germany.

Walter, H. (1971). *Ecology of Tropical and Subtropical Vegetation*. Oliver and Boyd, Edinburgh.

White, F. (1983). Vegetation of Africa - a descriptive memoir to accompany the Unesco/AETFAT/UNSO vegetation map of Africa. Natural Resources Research Report XX; U. N. Educational, Scientific and Cultural Organization; 7 Place de Fontenoy, 75700 Paris, France.

Whittaker, R. H. and Likens, G. (1975). *Primary productivity of the Biosphere*, volume 14 of *Ecological Studies and Synthesis*, chapter The biosphere and man, pages 305–328. Springer Verlag Berlin, Heidelberg, New York.

Wiegand, T., Jeltsch, F., Hanski, I., and Grimm, V. (2003). Using pattern-oriented modeling for revealing hidden information: a key for reconciling ecological theory and application. *OIKOS*, **100**(2), 209–222.

Williams, C. A., Hanan, N. P., Neff, J. C., Scholes, R. J., Berry, J. A., Denning, A. S., and Baker, D. F. (2007). Africa and the global carbon cycle. *Carbon Balance and Management*, **2**(1), 3.

Williams, R. J., Myers, B. A., Muller, W. J., Duff, G. A., and Eamus, D. (1997). Leaf phenology of woody species in a North Australian tropical savanna. *Ecology*, **78**(8), 2542–2558.

Wolfson, M. M. (1999). *Veld management in South Africa*, chapter The response of forage plants to defoliation: Grasses, pages 91–103. University of Natal, Scottsville.

Woodward, F. I. and Lomas, M. R. (2004). Vegetation dynamics – simulating responses to climatic change. *Biological Reviews*, **79**(3), 643–670.

Woodward, F. I. and Smith, T. M. (1994a). *Ecophysiology of Photosynthesis*, chapter Predictions and measurements of the maximum photosynthetic rate, A_{max}, at the global scale, pages 491–509. Springer, Berlin.

Woodward, F. I. and Smith, T. M. (1994b). Global Photosynthesis and Stomatal Conductance: Modelling the Controls by Soil and Climate. *Advances in Botanical Research*, **20**, 1–41.

Woodward, F. I., Smith, T. M., and Emanuel, W. R. (1995). A global land primary productivity and phytogeography model. *Global Biogeochemical Cycles*, **9**(4), 471–490.

Woodward, F. I., Lomas, M. R., and Kelly, C. K. (2004). Global climate and the distribution of plant biomes. *Philosophical Transactions of the Royal Society of London, Series B-Biological Sciences*, **359**(1450), 1465–1476. 2058.

Woodward, S. J. R. (1997). *Agricultural Systems Modeling and Simulation*, chapter Dynamical systems models and their application to optimising grazing management, pages 419–474. Marcel Dekker, New York.

Wright, I. J., Reich, P. B., Westoby, M., Ackerly, D. D., Baruch, Z., Bongers, F., Cavender-Bares, J., Chapin, T., Cornelissen, J. H. C., Diemer, M., Flexas, J., Garnier, E., Groom, P. K., Gulias, J., Hikosaka, K., Lamont, B. B., Lee, T., Lee, W., Lusk, C., Midgley, J. J., Navas, M. L., Niinemets, U., Oleksyn, J., Osada, N., Poorter, H., Poot, P., Prior, L., Pyankov, V. I., Roumet, C., Thomas, S. C., Tjoelker, M. G., Veneklaas, E. J., and Villar, R. (2004). The worldwide leaf economics spectrum. *Nature*, **428**(6985), 821–827.

Xu, X., Boyce, M. S., and Daley, D. J. (2005). Harvesting in seasonal environments. *Mathematical Biology*, **50**, 663–682.

Zhang, J., Oliver, W. W., and Ritchie, M. W. (2007). Effect of stand densities on stand dynamics in white fir (*Abies concolor*) forests in northeast California, USA. *Forest Ecology and Management*, **244**(1-3), 50–59.

Electronic Appendix: Source code of the aDGVM

The thesis includes a CD-ROM with the source code of the aDGVM and input data for one study site. Please read the README file for further details or contact the authors (scheiter@em.uni-frankfurt.de, higgins@em.uni-frankfurt.de).